Fluorescent Assay Technologies for G-protein Interactions

Tamara Cooper

Discipline of Biochemistry,

School of Molecular and Biomedical Sciences,

The University of Adelaide, South Australia

&

CSIRO Molecular and Health Technologies

Contents

List of Figures and Tables

Declaration

This work contains no material which has been accepted for the award of any other degree or diploma in any university or other tertiary institution and, to the best of my knowledge and belief, contains no material previously published or written by another person, except where due reference has been made in the text.

I give consent to this copy of my thesis, when deposited in the University Library, being made available for loan and photocopying, subject to the provisions of the Copyright Act 1968.

…….

Tamara Cooper

Abstract

Assay technologies for GPCRs and their associated G-proteins are in demand for drug screening and other biotechnology applications such as biosensors for diagnostic purposes or odorant/flavour assessment as well as for elucidating the remaining controversial mechanisms in G-protein mediated signalling. This study aims to make progress towards developing a TR-FRET assay for G-protein interactions that could be used as a generic assay platform for GPCR signalling that would be fluorescent, homogeneous and amenable to miniaturization. The first chapter of this study investigates the use of small molecule labels, CS124-DTPA-EMCH:Tb and Alexa546 in a TR-FRET assay. This TR-FRET pair had previously been applied to Gα, Gβγ and RGS4 proteins and during the characterization of this assay, the protein CrV2 was observed to interact with the G-protein. Using TR-FRET, it was demonstrated that a high affinity interaction appears to occur between $G\alpha_{i1}$ and CrV2 (Apparent *K*d 6.2 nM). CrV2 is encoded by a polydnavirus from endoparasitoid wasps, which is thought to mediate immune suppression, and the interaction with Gα could have important implications in the regulation of the immune system of invertebrates. Improvements to the labelling strategy used in this assay are then attempted through the creation of various G-protein subunit fusions with small, genetically encoded lanthanide binding tags (LBTs) or tetracysteine motifs (TCMs) for site-specific labelling with terbium or FlAsH, respectively. The consequence of the fusions on maintaining G-protein subunit integrity and on the affinity of the tags for their labels is characterized, and then the utility of these constructs as TR-FRET partners is demonstrated. TCM:FlAsH complexes could successfully be used as TR-FRET acceptors for CS124-DTPA-EMCH:Tb labelled binding partners. The interaction between $G\beta\gamma_2$-TCM:FlAsH and Gα:Tb could be measured using TR-FRET and generated an apparent *K*d of 3.6 nM. Likewise, LBT:Tb complexes could be used as TR-FRET donors to Alexa546 labelled binding partners which was demonstrated using the chimeric, promiscuous Gα subunit, LBT2:Tb-$G\alpha_{S25}$ and Gβγ:Alexa. Furthermore, the two site-specific

labelling strategies can be used together in TR-FRET studies and an interaction between LBT2:Tb-$G\alpha_{S25}$ and $G\beta\gamma_2$-TCM:FlAsH was shown to have an apparent *K*d of 2.3 nM. The TR-FRET assays were further validated using protease treatments and the addition of unlabelled binding partners reduced the TR-FRET signal. Finally, the feasibility of fusing lanthanide binding tags to GPCRs for alternate assay platforms or other applications was investigated. The β_2-adrenergic and M_2-muscarinic receptors were fused to LBTs and the integrity of the receptors determined using ligand binding and [^{35}S]GTPγS signalling assays. Terbium binding to the LBT was then demonstrated. The utility of these constructs in alternative TR-FRET platforms with G-proteins was then explored.

Acknowledgements

I would firstly like to thank my supervisors for their support and guidance over the period of my PhD. My principle CSIRO supervisors Assoc. Prof. Ted McMurchie and Dr. Wayne Leifert continued their support and encouragement through major upheavals and the closure of the laboratory in which this project started. Without their continued interest, the completion of this thesis would not have been achieved. Many thanks also go to Dr. Richard Glatz who provided much technical support at the beginning of the project and was later a welcome addition to my supervisory panel when his role with CSIRO ended. I look forward to continuing to work with him in the future. Thanks also to the final member of my supervisory panel, Prof. John Wallace who expanded my PhD experience from CSIRO to within the university community.

My thanks also go to the other scientists who have contributed to the completion of this study. Prof. Richard Neubig, Dr. Sassan Asgari, Prof. James Garrison, Dr. Andrejs Krumins, Prof. Alfred Gilman, Dr. Roger Sunahara and Prof. Yung-Hou Wong generously provided various constructs used in this study. Dr. Jack Ryan and Megan Kruger kindly synthesized the FlAsH used in this study and Prof. John Carver and Dr. Leah Cosgrove provided access to the Cary Eclipse fluorospectrophotometer and the Victor3 multilabel plate reader, respectively.

I would also like to thank other past and present members of our laboratory including Kelly Bailey, Amanda Aloia, Janelle Williams and Sharon Burnard. Their friendship, discussions, advice and support made the period of my PhD a very enjoyable time.

Finally, thank you to my family, friends and partner, Stevan, who have endured with me through what must seem like a never-ending period of study. Your encouragement and faith saw me through it.

Abbreviations

[^{35}S]GTPγS	^{35}S radiolabelled guanosine 5'-O-(3-thiotriphosphate)
a.u.	arbitrary units
ACP	acyl carrier protein
Alexa	Alexa fluor 546 C_5 maleimide
AlF_4^-	aluminium fluoride
AMP-PNP	adenosine 5'-(β,γ-imido)triphosphate
B2AR	β_2-adrenergic receptor
BCIP	5-Bromo-4-Chloro-3'-Indolyphosphate p-Toluidine salt
BirA	*E. coli* biotin ligase
Bp	base pairs
BSA	bovine serum albumin
cAMP	cyclic adenosine monophosphate
cDNA	complementary deoxyribonucleic acid
CFP	cyan fluorescent protein
CNS	central nervous system
CSIRO	Commonwealth Scientific and Industrial Research Organization
Da	daltons
DHFR	dihydrofolate reductase
DMSO	dimethyl sulfoxide
DNA	deoxyribonucleic acid
DTPA	diethylene triamine pentaacetic acid
DTT	dithiothreitol
EC_{50}	effective concentration
EDT	1,2-ethanedithiol
EDTA	ethylenediaminetetraacetic acid
FBS	foetal bovine serum
FlAsH	4',5'-bis(1,3,2-dithioarsolan-2-yl)fluorescein-(1,2-ethanedithiol)$_2$
FRET	Förster Resonance Energy Transfer
GDP	guanosine diphosphate
GFC	glass microfiber 1 µM filter papers
GFP	Green fluorescent protein
GPCR	G-protein coupled receptor
G-protein	heterotrimeric guanine nucleotide binding protein
GTP	guanosine triphosphate
GTPγS	guanosine 5'-O-(3-thiotriphosphate)
Gα	Gα-subunit
Gβ	G-protein β subunit
Gγ	G-protein α subunit
hAGT	human O^6-alkylguanine-DNA alkyltransferase
HEPES	4-(2-hydroxyethyl)-1-piperazineethanesulfonic acid
His-tag	6 histidine tag
hr	hours
IC_{50}	inhibitory concentration
IMAC	immobilized metal affinity chromatography
IMVS	Institute of Medical and Veterinary Science
IPTG	isopropyl-β-D-thiogalactopyranoside
Kd	dissociation constant
LBT	lanthanide binding tag

LBT1	lanthanide binding tag of the amino acid sequence: Tyr Ile Asp Thr Asn Asn Asp Gly Trp Tyr Glu Gly Asp Glu Leu Leu Ala
LBT2	Lanthanide binding tag of the amino acid sequence: Ala Cys Val Asp Trp Asn Asn Asp Gly Trp Tyr Glu Gly Asp Glu Cys Ala
M2R	M_2-muscarinic receptor
min	minutes
MOI	multiplicity of infection
MW	molecular weight
NBT	nitro-blue tetrazolium chloride
Ni-NTA	nickel-nitriloacetic acid
OD	optical density
PBS	phosphate buffered saline
PCP	peptide carrier protein
PCR	polymerase Chain Reaction
PMSF	phenylmethanesulphonylfluoride
PPtase	phosphopantetheinyl transferase
RGS	regulator of G-protein signalling
*R*luc	*Renilla* luciferase
SARDI	South Australian Research and Development Institute
s	seconds
SDS-PAGE	sodium dodecyl sulphate- polyacrylamide gel electrophoresis
TCEP	tris(2-carboxyethyl)phosphine
TCM	tetracysteine motif
TR-FRET	Time resolved - Förster Resonance Energy Transfer
UK	UK 14304, synthetic adrenalin analogue
UV	ultra violet
YFP	yellow fluorescent protein

Academic Prizes and Awards

2008	Lorne Protein Conference Committee travel grant $100
2005-2008	School of Molecular Biosciences travel awards 4 x $500
2007	Doreen McCarthy bursary: The Australian Federation of University Women – South Australian Inc. Trust fund $3000
2007	Informa Life Sciences: 5th Annual Congress: GPCRs in Drug Discovery Poster Prize. "Time-resolved fluorescent technologies for GPCRs, G-protein and Regulator of G-protein signalling interactions".
2006	ARC/NHMRC Research Network: Fluorescence Applications in Biotechnology and Life Sciences (FABLS) $400 to attend Fluoro2006
2005	The Biochemical Journal Poster Prize for biochemistry and molecular biology (Presented at ComBio2005, Adelaide)
2005-2008	Australian Postgraduate Award ~ $19 000 p.a.
2005-2008	CSIRO Postgraduate Studentship $7000 p.a. + $6000 travel
2004	Commonwealth Accommodation Scholarship $4000
2004	Chancellors Letter of Commendation in recognition of outstanding results towards B.Biotechnology (Hons)
2002	Admission into the Advanced Entry Program in 2002 allowing completion of the Bachelor of Biotechnology (Hons) in 3 years rather than 4.

Publications arising from this thesis

2008 **Tamara Cooper** and Wayne R. Leifert (accepted for publication date 2009). [^{35}S]GTPγS binding in G-protein coupled receptor assays. *In Methods in Molecular Biology: G-protein Coupled Receptors in Drug Discovery*. Editor, Wayne R. Leifert. Humana Press, Totowa, New Jersey.

Tamara Cooper, Wayne R. Leifert, Richard V. Glatz and Edward J. McMurchie. (2008). Expression and characterisation of functional lanthanide-binding tags fused to a Gα-protein and muscarinic (M2) receptor. *J. Bionanoscience*. (In press).

Wayne Leifert, **Tamara Cooper** and Kelly Bailey. (2008). G-protein Coupled Receptors: Progress in Surface Display and Biosensor Technology. *Springer Handbook of Nanotechnology, 3rd Edition*. (In press)

Wayne Leifert, **Tamara Cooper**, Kelly Bailey, Richard Glatz, Marta Bally, Brigette Stadler, Eric Reimhult and Joe Shapter. (2008). Biosensors and Biochips. *Annual Reviews in Nanotechnology*. (In preparation)

2007 Glatz, R. V., Leifert, W. R., **Cooper, T. H.,** Bailey, K., Barton, C. S., Martin, A. S., Aloia, A., Bucco, O., Waniganayake, L., Wei, G., Raguse, B., Weiczorek, L. & McMurchie, E. J. (2007). Cell-free assaying of G-protein Coupled Receptors and G-proteins. *Aust. J. Chem*. Research Front "Bionanochemistry". 60, pp.309–313. (Invited Rapid Communication)

2006 Wayne R. Leifert, Kelly Bailey, **Tamara H. Cooper**, Amanda L. Aloia, Richard V. Glatz , Edward J. McMurchie (2006). Measurement of heterotrimeric G-protein and regulators of G-protein signalling interactions by time-resolved fluorescence resonance energy transfer. *Analytical Biochemistry,* 355, pp.201–212.

Abstracts arising from this thesis

2008 **T. Cooper**, R. Glatz, W. Leifert, E. McMurchie (2008). The use of Lanthanide Binding Tags (LBTs) in the development of TR-FRET assay technologies for G-protein coupled receptors (GPCRs). *Lorne Protein Conference*, Lorne, Victoria.

2007 **T. Cooper**, K. Bailey, R. Glatz, W. Leifert, J. Wallace, E. McMurchie (2007). Time-resolved fluorescent technologies for GPCRs, G-protein and Regulator of G-protein signalling interactions. Informa Life Sciences - 5th annual congress: GPCRs in Drug Discovery, Lisbon, Portugal. **Winner of the Poster Prize – Oral presentation**

T. Cooper, K. Bailey, R. Glatz, A. Aloia, W. Leifert, J. Wallace, E. McMurchie (2007). Time-resolved FRET assay development for GPCRs, G-protein and Regulator of G-protein signalling interactions. *Molecular Pharmacology of G-Protein-Coupled Receptors. Proceedings of The Australasian Society of Clinical*

and Experimental Pharmacologists and Toxicologists (ASCEPT). **Invited talk – student oral prize session**

2006 **T. Cooper**, R. Glatz, W. Leifert, J. Wallace, E. McMurchie (2006). Development of site-specific fluorescent labelling of G-protein subunits using a lanthanide (Tb^{3+}) binding tag and a FlAsH binding tetracysteine motif. *Proceedings of the Australian Society for Medical Research Scientific Meeting*.

Richard V. Glatz, Wayne R. Leifert, Kelly Bailey, **Tamara H. Coope**r, Chris S. Barton, A. Scott Martin, Amanda Aloia, Olgatina Bucco, Lakshmi Waniganayake, Gang Wei, Burkhard Raguse, Lech Wieczorek, and Edward J. McMurchie (2006). Cell-free receptor-based biosensors. *International Conference of Nanoscience and Nanotechnology Proceedings.*

Richard V. Glatz, Wayne R. Leifert, Kelly Bailey, **Tamara H. Cooper**, Chris S. Barton, A.Scott Martin, Amanda L. Aloia, Olgatina Bucco, L. Waniganayake, Gang Wei, Burkhard Raguse, Lech Wieczorek and Edward J. McMurchie. (2006). G-protein Coupled Receptors: towards cell-free environmental biosensing. *Proceedings of the Australian and New Zealand Entomological Society Conference*.

2005 **Tamara Cooper**, Wayne R. Leifert, Kelly Bailey, Richard V. Glatz and Edward J. McMurchie (2005). Time Resolved Fluorescence Resonance Energy Transfer assay for studying RGS4 interactions with G-protein Gα-subunits in varying states of activation. *Proceedings of the Australian Society for Biochemistry and Molecular Biology.* ***Biochemical Journal Poster Prize for Biochemistry and Molecular Biology***

R. Glatz, **T. Cooper**, W. Leifert, C. Barton, L. Wieczorek, E. McMurchie (2005). Engineering of G-proteins for production of cell-free ligand biosensors. *Proceedings of the Australian Society for Biochemistry and Molecular Biology.*

Wayne R. Leifert, Kelly Bailey, **Tamara Cooper**, Amanda Aloia, Richard V. Glatz, Edward J. McMurchie (2005). Measurement of heterotrimeric G-protein and RGS interactions by a novel homogeneous TR-LRET assay. Drug Discovery: From Targets to Candidates. *Proceedings of the Society for Biomolecular Screening*. P04049. Geneva PalExpo, Switzerland, Sept 11-15.

T. Cooper, W. R. Leifert, K. Bailey, R. V. Glatz, E. J. McMurchie (2005). Analysis of RGS4 and Gα_{i1} interactions in different activation states. *Proceedings of the Australian Society for Medical Research Scientific Meeting*.

Tamara Cooper, Wayne R. Leifert, Kelly Bailey, Richard V. Glatz, John Wallace and Edward J. McMurchie (2005). Measurement of RGS4 interactions with G-protein subunits in varying states of activation using time-resolved fluorescence resonance energy transfer. *Molecular Pharmacology of G-Protein-Coupled Receptors. Proceedings of The Australasian Society of Clinical and Experimental Pharmacologists and Toxicologists (ASCEPT)*.

1. Literature Review: Measuring G-Protein Coupled Receptor and G-protein signalling

Image of a GPCR coupled to a heterotrimeric G-protein

Obtained from http://www.cmpharm.ucsf.edu/bourne/lab_science/activation.html

1.1. Introduction

The diversity, physiological importance, cell surface location and ligand specificity of G-protein coupled receptors (GPCRs) makes them ideal drug targets. This has been proven with approximately 50% of all recently released pharmaceutical drugs being targeted at GPCRs and world wide sales that exceed US$30 billion (Klabunde, Hessler 2002). These drugs include analgesics, antihistamines, antidepressants, anti-asthmatics and drugs for cardiovascular disorders among others. However, since the complete sequencing of the human genome, 342 unique, non-olfactory GPCRs have been identified (Fredriksson *et al*. 2003) although more than 140 of these are considered 'orphan' GPCRs since they have no known ligand or function (Lecca, Abbracchio 2008). Of the GPCRs with a characterised ligand, only 30 were the targets of marketed drugs in 2002 (Klabunde, Hessler 2002). The remaining 'orphan' receptors are potentially targets for novel therapeutics if their ligands and/or function can be determined. It should also be noted that the G-proteins and other regulatory proteins of GPCR mediated signalling are increasingly attracting interest as potential drug targets to produce effects that receptor ligands cannot, although no such therapeutics are currently on the market (Freissmuth *et al*. 1999; Neubig & Siderovski 2002; Ja, Roberts 2005). Consequently, assays to identify novel or improved therapeutics and ligands that modulate GPCR mediated signalling are of great value to the pharmaceutical industry. There is also increasing interest from the biotechnology sector with regard to exploiting GPCRs as biosensors for diagnostic purposes or odorant/flavour assessment. The research described in this thesis aimed to generate components of a GPCR signalling system that could have use in assays for any of the discussed applications. The following literature review describes the mechanisms involved with GPCR signalling and how assay technologies can and have been designed to measure various aspects of GPCR signalling and the advantages and disadvantages of various approaches. This will lead to a rationale for the approach taken in this research and how this research will build on that done by others.

1.2. G-protein coupled receptors

GPCRs are intrinsic membrane proteins that contain seven transmembrane regions linked by helical loops that extend outside of the cell or into the cytoplasm. The amino terminus is extracellular and the carboxyl terminus intracellular. GPCRs share the greatest amount of homology within the transmembrane segments, and the most variable regions are the C-terminus, the 3rd intracellular loop and the amino terminus (Kobilka 2007). Despite substantial efforts, until recently the only atomic resolution crystal structure of a GPCR available was that of rhodopsin (Palczewski *et al*. 2000), a rather unique GPCR in that it is naturally highly expressed in the retina (Sarramegn *et al*. 2006). In 1972, the Lefkowitz research group reported the purification of the β_2-adrenergic receptor (Lefkowitz, Haber & O'Hara 1972). However, it was not until 2007 that the β_2-adrenergic receptor became the second GPCR structure to be solved (Cherezov *et al*. 2007; Rasmussen *et al*. 2007; Rosenbaum *et al*. 2007) which was closely followed by the β_1-adrenergic receptor (Warne *et al*. 2008) and the opsin receptor (Park *et al*. 2008). This stands as testament to the difficulties in working with GPCRs, their complex hydrophobic structure and structural flexibility presenting major challenges in their recombinant expression, purification and crystallization.

Residing on the cell surface, these receptors receive signals from the extracellular environment in the form of ligands, which are exceptionally diverse both in their physical properties and in their chemical composition including neurotransmitters, hormones, photons and olfactants (**Figure 1.1**). The variety of ligands to which GPCRs bind, involves them in many fundamental physiological processes such as metabolism, reproduction, and the regulation of hormonal and neuronal activity (Luttrell 2008). Consequently, failures in the signalling systems initiated by GPCRs have been indicated in various disease states including neurological and neurodegenerative diseases, cardiovascular disorders, metabolic diseases and cancer

(Lundstrom 2005). Ligands can interact with GPCRs to produce different outcomes. Agonist binding activates downstream signalling and these can be either full agonists or partial agonists. Inverse agonists have an effect on the basal or constitutive activity of the receptor. Antagonists bind to the same site of the receptor as agonists but have no signalling activity and block the access of other ligands to the binding site. Allosteric modulators can also bind to receptors but at a location that is distinct from the orthosteric binding site at which agonists and antagonists bind. Allosteric modulators will usually have an effect on the activity of the endogenous ligand (Reviewed in (Jensen, Spalding 2004; Milligan, Smith 2007)).

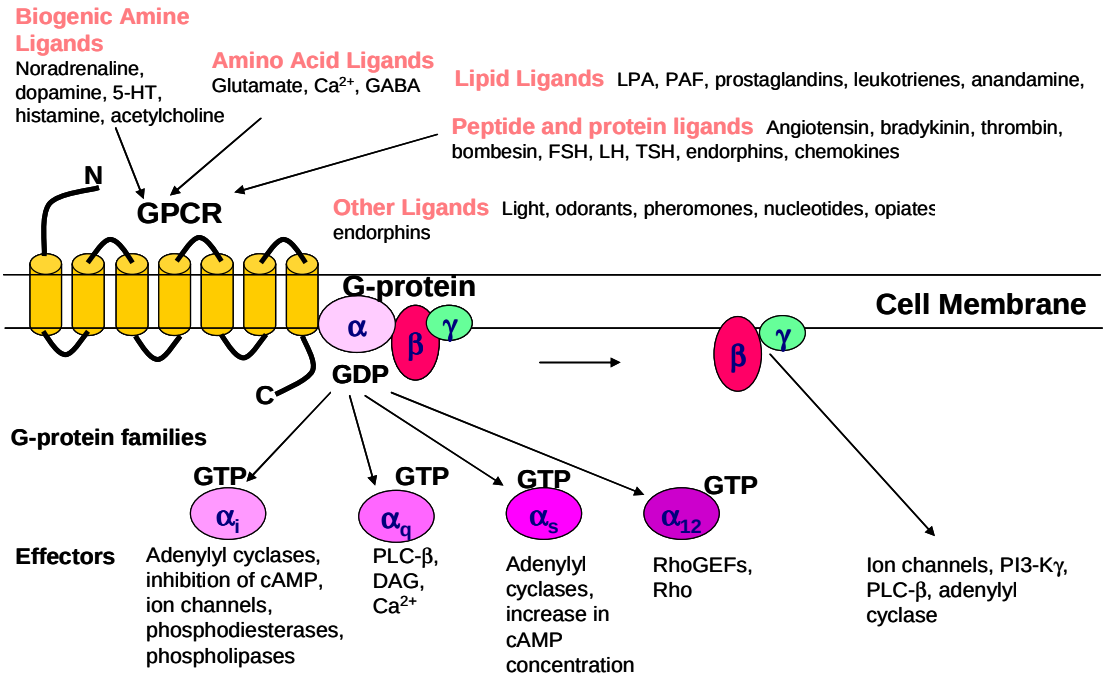

Figure 1.1: The family of GPCRs bind ligands with a high degree of chemical diversity and couple to different families of G-proteins to modulate an array of down stream effectors. Adapted from (Marinissen, Gutkind 2001).

GPCRs are subject to numerous post-translational modifications including palmitoylation, phosphorylation and glycosylation all of which have been reviewed extensively (Duvernay, Filipeanu & Wu 2005, Escriba *et al*. 2007; Qanbar, Bouvier 2003; Torrecilla, Tobin 2006). Briefly, as a general rule, GPCRs are phosphorylated at multiple sites after agonist stimulation and this is thought to be involved with receptor desensitization and internalization. The covalent attachment

of lipid moieties such as palmitate near the C-terminus can be a result of agonist binding. This is thought to induce structural changes that could influence receptor function and the reversible nature of palmitoylation could indicate a mechanism that regulates membrane association or sorting and assembly and may also be involved with G-protein coupling, desensitization and internalization. GPCRs can also be subject to ubiquitination, which appears to be important in intracellular trafficking and degradation of the receptors. Glycosylation is the most common modification of receptors and this is likely to be important in the intracellular trafficking of the receptors.

GPCRs have been categorized into five families based largely on structural similarities (Oldham, Hamm 2008). The largest family of GPCRs is the rhodopsin-like family, which is characterized by most members containing a Asn-Ser-Xaa-Xaa-Asn-Pro-Xaa-Xaa-Tyr and a Asp-Arg-Tyr (DRY) motif. These receptors tend to bind their small molecule ligands deep within the transmembrane bundle. The secretin family receptors bind large peptides, often hormones, using a leucine-rich repeat domain. The glutamate family receptors are characterized by a 'Venus flytrap' N-terminus that "closes" around the ligand. Adhesion family receptors contain an adhesion-like motif that is thought to be involved with mediating cell-cell adhesion and frizzled family GPCRs tend to have a cysteine-rich domain. As model receptors, this study has utilized rhodopsin-like receptors including the α_{2A}-adrenergic, M_2-muscarinic, H_1-histamine and the β_2-adrenergic receptors.

1.2.1. Adrenergic receptors

Adrenergic receptors (adrenoceptors) mediate the biological effects of the catecholamines epinephrine and norepinephrine (Civantos Calzada, Aleixandre de Artiñano, Amaya 2001) and are among the most extensively studied GPCRs. These receptors are widely expressed in nearly all peripheral tissues and the central nervous system. Adrenergic receptors play an important role in controlling blood pressure, heart contractions, airway reactivity as well as having other

metabolic and nervous system functions. There are nine subtypes of adrenergic receptors divided amongst 3 sub-families with α_1-adrenergic receptors being Gq coupled, α_2-adrenergic receptors being Gi coupled and β-adrenergic receptors being primarily Gs coupled (Philipp, Hein 2004). Specifically, this study makes use of the α_{2A}- and the β_2-adrenergic receptors. α_{2A}-adrenergic receptors are identified as being activated by the compounds B-HT 920, UK-14 304 or α-methylNA and these agonists are competitively inhibited by low concentrations of yohimbine, rauwolscine or idazoxan (Civantos Calzada, Aleixandre de Artiñano 2001). These receptors are involved with regulating norepinephrine release (Philipp, Hein 2004) and agonist induced activation of these receptors has been observed to mediate hypotensive, sedative, analgesic and hypothermic responses through Gi family G-proteins (Civantos Calzada, Aleixandre de Artiñano, Amaya 2001). In contrast to the α_{2A}-adrenergic receptors, β_2-adrenergic receptors generally mediate responses using Gs family G-proteins, can be activated by the synthetic agonist isoproterenol, and are inhibited by the antagonist propranolol (Nakanishi *et al*. 2006) amongst others. These receptors are involved with smooth muscle relaxation in airways as well as that of the vascular and uterine systems. Agonists have been used therapeutically to treat asthma and antagonists have been used as antihypertensives.

1.2.2. M_2-muscarinic receptors

There are five muscarinic (acetylcholine) receptor subtypes that are activated by acetylcholine or muscarine and inhibited by atropine. Muscarinic receptors are expressed throughout the central nervous system and peripheral tissues (Caulfield, Birdsall 1998). Structural features common to muscarinic receptors include a long third intracellular loop and an allosteric binding site and they can be coupled to Gq or Gi pathways (Ishii, Kurachi 2006). The M_2-muscarinic receptor is coupled to Gi and its activation in cardiac tissue leads to hyperpolarization of the heart and a drop in heart rate mediated by G-protein–gated potassium channels (Ishii, Kurachi 2006). In neurons, these receptors control the release of acetylcholine and in smooth muscle, the M_2-muscarinic

receptor counteracts adrenergic responses. Muscarinic receptors have been targeted therapeutically; atropine is used to dilate pupils, reduce bronchial and salivary secretion and to accelerate the heart rate and butylscopolamine can be exploited for its antispasmodic effects (Ishii, Kurachi 2006). Muscarinic receptors have also been implicated in CNS diseases such as Alzheimer's disease, Parkinson's disease, depression and schizophrenia, making them targets of ongoing drug-discovery efforts (Wess, Eglen & Gautam 2007).

1.2.3. H_1-histamine receptors

Histamine binds to four subtypes of GPCRs that mediate important allergic and inflammatory responses in particular. The H_1-histamine receptor is generally Gq-coupled and ubiquitously distributed through the body in nerve cells, airway and vascular smooth muscles, hepatocytes, endothelial cells, epithelial cells and cells of the immune system (Akdis, Simons 2006). The H_1-histamine receptor has been implicated in controlling circadian rhythm, cognition, memory, inflammation and allergies with classical anti-histamines to treat allergies targeted at this receptor (Akdis, Simons 2006; Hill *et al*. 1997).

1.3. GPCR signalling through heterotrimeric G-proteins

To design an effective assay for modulators of GPCR signalling, an understanding of the mechanisms by which a signal is transmitted into the cell is required. The standard model of GPCR signalling is through heterotrimeric guanine nucleotide-binding proteins (G-proteins) which couple to intracellular regions of the receptor (reviewed in (Oldham, Hamm 2008)). These G-proteins consist of three subunits, Gα, Gβ and Gγ. Different subtypes of these subunits exist, providing partial specificity in the cellular response by interacting with different down stream effectors upon extracellular binding of ligand to a coupled GPCR (**Figure 1.1**). While inactive (when an agonist is not bound to the receptor), the Gα-subunit of the G-protein is bound to GDP

and associated with Gβ and Gγ. Gβ and Gγ are tightly associated and can only be separated under denaturing conditions so are generally considered as the Gβγ dimer (Clapham, Neer 1997). Once an agonist binds to the receptor, conformational changes promote the release of GDP from the Gα-subunit and its replacement with GTP, since GTP is present at much higher concentrations in the cell. The conformation of the Gα-subunit subsequently changes upon the binding of GTP, causing further structural changes that allow the Gα-subunit and the Gβγ dimer to interact with downstream effectors such as adenylyl cyclase, various ion channels or phospholipase C to provide transmission of a signal leading to a cellular response. Signal transduction is terminated due to the intrinsic GTPase activity of the Gα-subunit which hydrolyzes the bound GTP back to GDP and inorganic phosphate, promoting the return of the G-protein heterotrimer to the inactive state (McCudden *et al*. 2005) (**Figure 1.2**). This cycle is regulated by various mechanisms that are becoming increasingly characterized including receptor internalization via arrestins, regulators and activators of G-protein signalling (reviewed in (Milligan, White 2001)). While this model is currently widely accepted, much debate continues around receptor homo- and hetero-dimerization, whether the signalling complex exists as an organized scaffolded entity, whether all G-protein subunits are required to dissociate completely to provide transmission of the signal, the occurrence of G-protein independent signalling and receptor independent G-protein modulators.

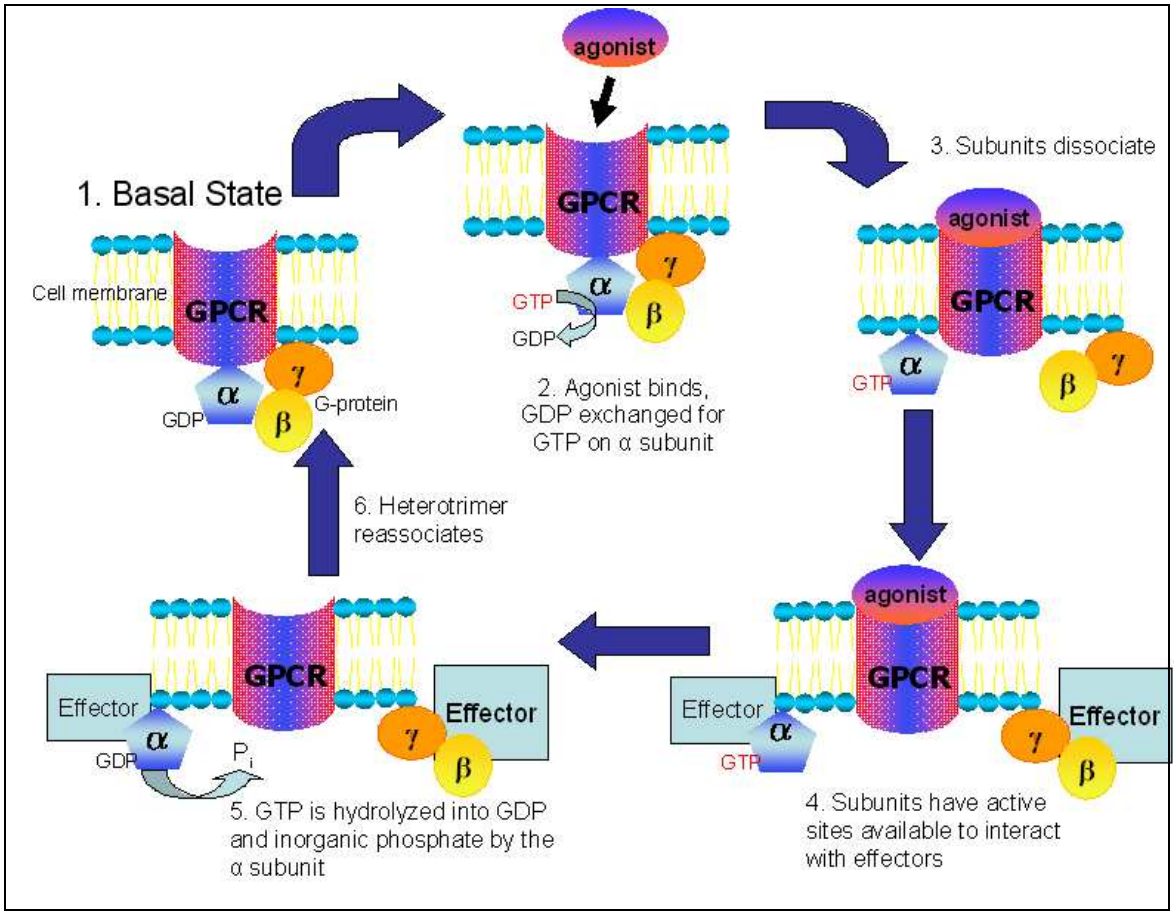

Figure 1.2: Schematic showing the traditional GDP/GTP dependent G-protein mediated signalling cycle. Agonist binding to a GPCR triggers conformational changes that result in the exchange of GDP for GTP on the Gα subunit of the G-protein heterotrimer. GTP binding causes further conformational changes that allow the G-protein subunits to interact with downstream effectors. The intrinsic GTPase activity of the Gα-subunit hydrolyzes GTP back to GDP and inorganic phosphate which promotes the return of the inactive G-protein heterotrimer.

1.4. The G-protein subunits

G-protein heterotrimers are usually an integral part of GPCR signalling with most cells containing many different G-protein subunit subtypes, although agonists will produce highly specific cellular responses by activating defined G-protein signalling pathways. This could be mediated by receptor selectivity for a particular G-protein as well as the formation of G-proteins of a particular subunit composition to produce different efficacies and signalling kinetics. While disease states have long been modulated via drugs targeted at GPCRs, pathological conditions where modulation of the G-protein could be more effective are gaining an increasing amount of attention. A disease state is often produced by multiple receptors that may all converge on a

single G-protein pathway. Such is the case in cardiac hypertrophy, which results in chronic stimulation of the Gq pathway (Akhter *et al*. 1998), and tumour growth is also driven by the activation of several receptors (Prevost *et al*. 2006). Mutations in G-proteins have also been implicated in disease states such as Albright hereditary osteodystrophy, cancer and night blindness (Farfel, Bourne & Iiri 1999) and G_i proteins in particular have been implicated in headaches and fibromialgia (Galeotti *et al*. 2001a; Galeotti *et al*. 2001b). Therapeutics targeting G-proteins could therefore become novel compounds for treating diseases that originate from the signals of many receptors or are caused by mutations in the G-proteins themselves. Assays that screen for G-protein regulators, and that can determine the site of action while excluding an interaction with receptors, are required to identify and develop such compounds. Modulation of the G-protein interaction by a GPCR also provides a generic signalling event that can be measured in functional GPCR signalling assays. The subunits of the G-protein heterotrimer will therefore be discussed in more detail although good reviews on this subject are available (Birnbaumer 2007; Milligan, Kostenis 2006; Offermanns 2003).

1.4.1. Gα-subunits

Twenty Gα subunits are divided into 4 families and define the family to which the heterotrimeric G-protein belongs. This G-protein family is determined by the effector interactions of the Gα-subunits, which can then be further, divided into specific isotypes. In humans, the Gi/o family was originally named as such for its ability to inhibit adenylyl cyclase and the Gs family for the ability to stimulate adenylyl cyclase. Gq family G-proteins activate phospholipase C-β and G12/13 family Gα-subunits affect Rho-GEFs. Each Gα subunit consists of a GTPase domain and an α-helical domain between which lies the guanine nucleotide-binding site. The α-helical domain is thought to sequester the guanine nucleotide at the binding site and must be displaced to allow exchange of the nucleotide (Cherfils, Chabre 2003). The guanine nucleotide binding site and associated "switch regions" of the Gα subunit change conformation depending on the identity of the bound

nucleotide and are also involved with mediating Gβγ binding (Wall, Posner & Sprang 1998). The Gα subunit also contains a binding site for magnesium, a co-factor for GTP hydrolysis (Higashijima *et al*. 1987). The ras-like GTPase domain catalyses GTP hydrolysis to terminate signalling and the C- and N-termini of the subunit also have important functions in determining the specificity of receptor coupling to a particular G-protein (Mody *et al*. 2000), controlling nucleotide dissociation (Denker, Schmidt & Neer 1992), and membrane binding. Gα-subunits are all modified by the reversible attachment of palmitate (a 16-carbon saturated fatty acid) to a cysteine residue near the N-terminus of the subunit (Wedegaertner, Wilson & Bourne 1995). In addition to this modification, Gα-subunits of the G_i family contain an additional N-myristoylation modification where myristate (a 14-carbon saturated fatty acid) is irreversibly attached to a glycine residue present at the N-terminus, after removal of the initial methionine residue by methionine amino-peptidase (Wedegaertner, Wilson & Bourne 1995). These hydrophobic fatty acid modifications promote association of the G-protein with the cell membrane.

1.4.2. The Gβγ dimer

In humans there are six types of Gβ subunits which have a molecular weight of approximately 36 kDa and contain a β-propeller structure around which the C-terminus of Gγ wraps. The N-terminal helix also forms a coiled-coil with the N-terminus of Gγ (Cherfils, Chabre 2003). The Gβ subunits share a high degree of sequence similarity with the exception of $G\beta_5$ which also displays a higher degree of Gα selectivity than the other Gβ subunits (reviewed in (Smrcka 2008)). To date, no post-translational modifications have been identified on the Gβ-subunit.

There are twelve different Gγ subunits of 7-8 kDa in size in humans, among which the amino acid sequence similarity ranges between 10-70%. The central region of the subunit is involved with Gβ binding and the termini are involved with receptor and effector interactions and show a higher level of variability. Gγ subunits are also modified by prenylation with isoprenoids including

geranylgeranyl and farsenyl which are attached to a cysteine residue of the C-terminal Cys-Ala-Ala-Xaa box and involves proteolytic removal of the three C-terminal amino acids and carboxymethylation of the new terminus (reviewed in (Escriba *et al*. 2007)). While prenylation has been found to be necessary for normal function of the Gβγ dimer it is not required for dimer formation. These lipid modifications are thought to be primarily involved with membrane interactions although speculation exists that other functions may be to direct interactions with hydrophobic regions of other proteins.

The Gβγ dimer is required for interactions between the receptor and Gα, aiding in anchoring Gα subunits to the plasma membrane (Myung *et al*. 2006). The binding of the Gβγ dimer to Gα is thought to stabilize the receptor/G-protein complex in the high affinity state for receptor-ligand binding. Downstream interactions involving Gα-subunits were recognized prior to the elucidation of similar interactions between the Gβγ dimer and cellular effectors. However, it is now acknowledged that effectors such as PLC-β, ion channels, phosphatidylinositol-3-kinases and guanine nucleotide exchangers for small GTP-binding proteins, are amongst the effectors regulated by Gβγ and these features of the Gβγ dimer have been thoroughly reviewed (Clapham, Neer 1997; Gautam *et al*. 1998; Smrcka 2008).

1.5. Expression systems

The first step in developing an assay system is to select a suitable expression system from which the proteins of interest can be acquired in a functional form. GPCRs, with the exception of rhodopsin, are present in low levels within their native tissues and have been notoriously difficult to express at high levels in a functional form. This has been in part responsible for hampering efforts to obtain GPCR crystal structures. Recombinant proteins can be tagged to aid with purification or the generation of fluorescent signals using molecular biology techniques that allow manipulation of DNA constructs. Important factors when choosing an expression system include

the need for correct post-translational processing, the lipid composition of membranes for membrane proteins as well as logistical issues regarding the yield, subsequent purification method, convenience, cost, time and labour involved.

1.5.1. Bacterial expression systems

Bacterial expression, commonly using but not limited to *Escherichia coli* is convenient, low in cost, technically simple and can be up-scaled easily. Bacteria do no express endogenous GPCRs or interacting proteins and the genetic manipulation required to produce a heterologous protein is established and has been used to express large amounts of many proteins. Indeed, GPCRs have been expressed in *E. coli* although production of functional receptors required expression to be controlled at a lower level (often by lowering the incubation temperature). Furthermore, a fusion tag such as maltose binding protein to target the receptor to the periplasmic membrane was often useful (McCusker *et al*. 2007; Sarramegna *et al*. 2003). Larger amounts of receptor can be expressed such that the protein is present within inclusion bodies. However, this requires subsequent refolding of the protein to produce a functioning receptor and with few GPCRs successfully re-folded in recent years there are obviously challenges to overcome in terms of understanding the cellular mechanisms involved in the formation of mature GPCRs (McCusker *et al*. 2007). Post-translational modifications are also lacking in prokaryotes and the lipid composition of bacteria is quite different from the native eukaryotic environment of GPCR signalling components. This can be problematic since some GPCRs require glycosylation or other post-translational modifications for ligand binding or interaction with G-proteins. The lipid composition of membranes is also considered an important factor affecting GPCR activity. Gα-subunits have also been expressed in *E. coli* although some Gα subtypes could not be expressed and often refolding was necessary (Di Cesare Mannelli *et al*. 2006; McCusker, Robinson 2008). However, bacterially expressed G-proteins have not been widely used in reconstituted systems with receptors, possibly due to the lack of post-translational modifications leading to a loss of

function. Our laboratory's experience with expressing $G\alpha_{i1}$ in *E. coli* produced a GTP binding protein that was unable to receive signals from receptors.

1.5.2. Yeast expression systems

As unicellular eukaryotes, yeasts such as *Saccharomyces cerevisiae* share many features with higher eukaryotes and are able to perform most post-translational modifications. Yeast can easily be genetically manipulated, cultured on a large scale rapidly and with a low cost. However, the N- and O-linked oligosaccharide structures are different in yeast and often GPCRs have required a signal sequence for membrane targeting. Some mammalian GPCRs have also proven to be toxic to yeast or have failed to be expressed or trafficked appropriately. Again, the difference in lipid composition has also been blamed for reduced functionality of receptors expressed in yeast (McCusker *et al*. 2007; Sarramegna *et al*. 2003).

1.5.3. Mammalian cell expression systems

Mammalian cells can produce recombinant proteins stably or transiently and provide an environment most similar to the native environment of GPCRs with regard to lipid composition and post-translational processing (Sarramegna *et al*. 2003). Furthermore, GPCRs that have been difficult to express in alternate systems have been successful using mammalian cells. However, there is a high cost involved with mammalian cell culture and yields of protein are typically lower. Cultures are also difficult to upscale and proteins expressed in this manner have generally found more use in small-scale biophysical studies.

1.5.4. Baculovirus / Insect cell expression

GPCR expression in insect cells has been very successful, with receptors and G-proteins expressed in this system being almost always functional (Graber, Figler & Garrison 1992; Kozasa *et al*. 1993; McCusker *et al*. 2007; McCusker, Robinson 2008; Sarramegna *et al*. 2003). Whilst insect cells do have some endogenous G-proteins (Knight, Grigliatti 2004) they have a lower

background of endogenous GPCRs compared to mammalian cells. Insect cells are also able to fold, modify and traffic proteins although the N-glycosylation pathway is only similar to that of mammalian cells and sialyation does not occur in insect cells (Kost, Condreay & Jarvis 2005). Although many GPCRs have been functionally expressed using insect cells, the lipid composition of insect cell membranes contains higher amounts of unsaturated lipids and lower amounts of cholesterol compared to mammalian cells. However, compared to mammalian cell culture, the growth of cells is faster and more easily up-scaled since cells can be grown in suspension. Since this expression system is used in this study it will be discussed in more detail.

Baculoviruses such as the *Autographa california* multiple nuclear polyhedrosis virus (AcMNPV) commonly used for heterologous protein expression, normally infect Lepidopteran insects. In a natural infection (**Figure 1.3**), insect larvae will ingest food contaminated with baculoviral polyhedra-derived virions that mediate a primary infection of gut cells. Infected cells then produce budded virions which mediate the secondary infection, spreading the virus through the insect. It is also this virus type that infects cells in culture. Entry of budded virus occurs via adsorptive endocytosis and once in the cell the nucleocapsids move toward the nucleus where the virus DNA is released and expressed, also resulting in further budded virus being released by infected cells. Infected insects will also produce further polyhedra derived virions which are released when the insect dies since the infection cycle is lytic and the virus produces proteins that actively degrade the insect's body (Ghosh *et al*. 2002). For *in vitro* cultures, insect cells are generally transfected with recombinant baculovirus DNA which then produce budded virions that mediate the secondary infection of other cells. Recombinant baculoviruses are generally constructed such that the polyhedron gene is replaced with a gene of interest so that expression of the recombinant protein is driven by the strong polyhedron promoter, leading to high expression levels. Therefore,

in most laboratory cell cultures, polyhedra-derived virions are not produced which removes the need for strict quarantine requirements.

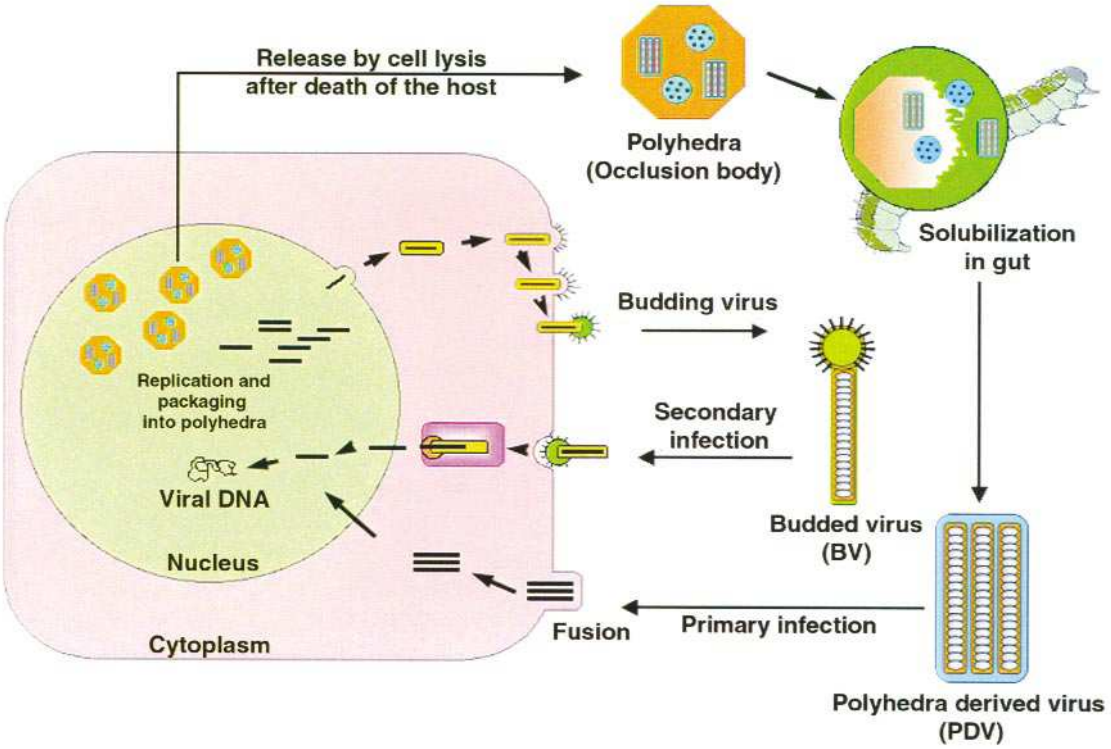

Figure 1.3. Generic infection cycle of pathogenic baculoviruses. Lepidoptera larvae ingest food contaminated with polyhedra-derived virions which mediate a primary infection of the gut cells of the insect. Infected cells then produce budded virions which mediate the secondary infection that spreads the virus through the insect which ultimately results in the death of the insect and release of further polyhedra-derived virions into the environment. Obtained from (Ghosh *et al*. 2002).

Widely used insect cell lines such as *Sf*9 and *Sf*21 were originally established from ovaries of *Spodoptera frugiperda* (fall armyworm) as a tool to study pathogenic insect viruses because they are highly susceptible to infection by baculovirus. Historically, recombinant baculovirus production required for protein expression in insect cells was tedious and time consuming (McCusker *et al*. 2007). However, commercial systems such as the Bac-to-Bac™ baculovirus expression system from Invitrogen have simplified recombinant baculovirus production by using a bacterial transposition method (Luckow *et al*. 1993). This involves cloning the foreign gene into a donor

plasmid (pFastBac™1) that in part facilitates the site-specific transposition of the gene into baculoviral DNA or 'bacmid' present in DH10Bac™ *E. coli* which can be selected for using blue/white screening and antibiotic resistance. The viral DNA can be amplified in the bacteria, isolated and used to transfect the insect cells with a lipid transfection reagent. Once transfected, the cells produce recombinant budded virus which can be used for subsequent infections of cells for recombinant protein production. Although the cells must be newly infected each time since cell lysis eventuates, the infection process offers the possibility of expressing a combination of recombinant proteins simultaneously, which is exploited in this study. Expression vectors utilizing baculovirus promoters are also available for stable heterologous expression in insect cells.

1.6. Assay technologies for GPCRs

Due to the biological and hence commercial importance of GPCRs, many pharmaceutical and biotechnology companies involved with drug discovery are competing to develop advanced assay technologies to identify novel therapeutics targeted at GPCRs and associated signalling proteins. This process often begins by screening many compounds against the desired drug target. To determine if a desirable response has been made, a robust, rapid and cost-effective assay must exist. This assay could be cell-based or cell-free. While both platforms offer different advantages depending on what information is being sought, cell-based assays tend to have higher initial hit rates with much more labour involved with validating the interaction proposed to be occurring between target and compound and in identifying false positives. Other logistical issues also exist with a significant amount of infrastructure required and less convenience since large stocks of reagents cannot be stored for 'screen on demand' purposes as for when cell-free screening is being performed. The other advantages of cell-free screening include offering a higher throughput with an output of specific pharmacological information and basic hit validation (Moore, Rees 2001). A desirable cell-free assay will have a high degree of sensitivity, be amenable to miniaturization for high throughput screening, homogeneous (since washing increases process

steps), while also being generic in nature to offer flexibility (Leifert *et al*. 2005). Assays for GPCRs have exploited different events in GPCR mediated signalling and have used many different technologies to generate signals some of which will be discussed.

1.6.1. Ligand binding assays

Ligand binding to the receptor initiates GPCR signalling and this binding event can be exploited to determine receptor expression, verify receptor subtype by determining affinities for various ligands and as an initial step in confirming receptor functionality. Ligand binding assays involve the use of a labelled ligand and receptors are often in crude membrane preparations. Historically, ligands have usually been radiolabelled; however, an increasing number of fluorescent examples are becoming available. Most often, the labelled ligand is added to a receptor preparation until saturation is achieved. Unlabelled ligands can be added to determine the degree of non-specific binding or to generate competition curves. Saturation binding curves indicate the level of expression of the receptor (mol/mg) and the apparent dissociation constant for the labelled ligand (**Figure 1.4**).

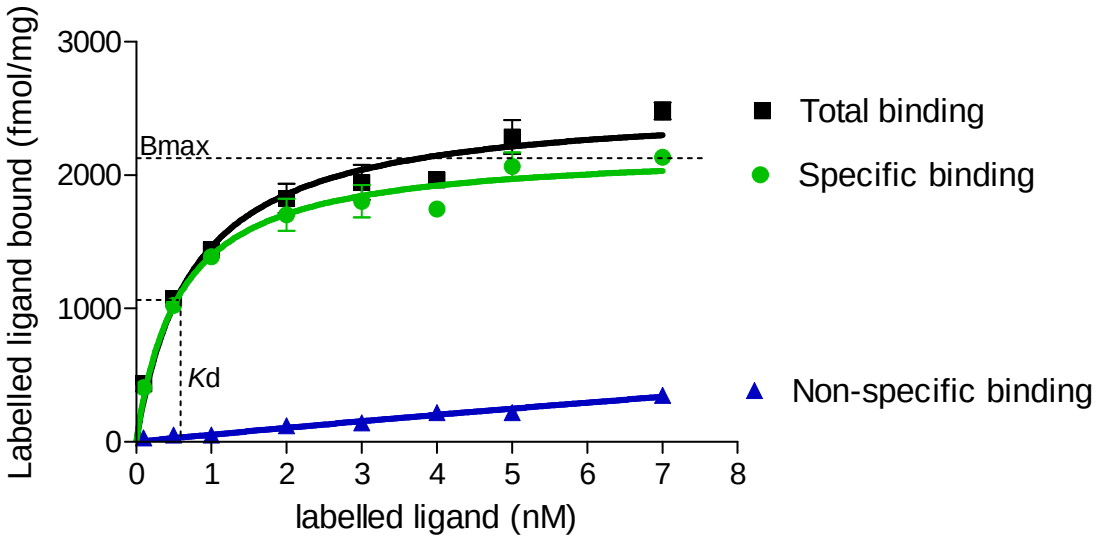

Figure 1.4: Representative example of a ligand-binding curve. Total binding of labelled ligand is measured and non-specific binding is determined by including an excess of a competitive unlabelled ligand. The difference provides specific binding from which Bmax indicates the level of

receptor expression and an apparent *K*d (concentration of ligand at which half the maximal binding is obtained) affinity measurement can also be obtained.

However, the use of these assays in high throughput screening has been limited because of a washing step required to remove unbound ligand that hampers throughput. To overcome this limitation, the principle of fluorescence polarization has been applied to GPCRs to detect ligand binding in a homogeneous (mix and read) assay. Fluorescence polarization assays apply the principle that the binding of a small, fluorescently labelled ligand to a receptor will increase the polarization of emitted fluorescence following illumination with plane-polarized light. The polarization increases since the now larger molecule (receptor bound to fluorescent ligand) rotates more slowly in solution compared to unbound fluorescent ligand (reviewed in (Bylund, Toews 1993; Daly, McGrath 2003; de Jong *et al*. 2005; Lee, Bevis 2000)). This technique has been applied to the melanocortin-4 receptor using a fluorescein-labelled peptide ligand to detect other ligands which compete for binding to the receptor. This assay was high-throughput and homogeneous compared to the traditional ligand-binding assay although membrane preparations caused light scatter and autofluorescence that decreased the signal:noise ratio (Lee, Bevis 2000). To improve this, a chemokine receptor (CXCR4) within virus-like particles was used to increase the amount of receptor present but not the amount of other proteins and membranes. The binding of a fluoresecently labelled-peptide to the receptor was then demonstrated using fluorescence polarization (Jones *et al*. 2008). While this increased the signal to noise ratio, the technique remains limited by the difficulty of chemically modifying ligands with appropriate fluorophores (Banks, Harvey 2002). It also remains that ligand-binding assays are unable to confer information regarding the signalling activity of the bound ligand and assays able to do this will now be discussed.

1.6.2. [^{35}S]GTPγS signalling assays

When characterizing receptors such as GPCRs it is also important that the assay is functional, being able to detect the difference between agonists, partial agonists and antagonists rather than merely showing that compounds can compete for binding at the receptor. To do this, the assay must generally measure changes downstream of receptor activation. Radiolabelled GTPγS binding assays have been considered the best method to distinguish between full and partial agonists. The level of G-protein activation following receptor activation in a reconstituted system can be measured by monitoring the nucleotide exchange event using [^{35}S]guanosine-5'-O-(3-thio)triphosphate ([^{35}S]GTPγS) to replace GTP normally present. Upon activation of the receptor by an agonist, the G-protein is stimulated to bind [^{35}S]GTPγS (**Figure 1.5**) which is not hydrolysable allowing [^{35}S]GTPγS labelled Gα-subunits to accumulate and be measured using scintillation counting (Ferrer *et al*. 2003; Harrison, Traynor 2003). Using a read out as close as possible to receptor activation, such as the nucleotide exchange event in this assay, is often regarded highly because events further downstream can be regulated independently of the GPCR generating false positives or negatives. Since by definition all GPCRs interact with G-proteins, nucleotide exchange provides the most upstream generic event that can be used to measure ligand-mediated signalling (Milligan 2003; Niedernberg *et al*. 2003). However, while this method provides traditional pharmacologic parameters of potency and efficacy, a number of limitations exist. Firstly, this assay is not homogeneous with washing steps required to remove unbound [^{35}S]GTPγS. Attempts at applying this method to high throughput screening practices have been unsuccessful generating poor signal to noise ratios and Z factors that are common parameters used to assess the viability of high throughput assays (Milligan 2003).

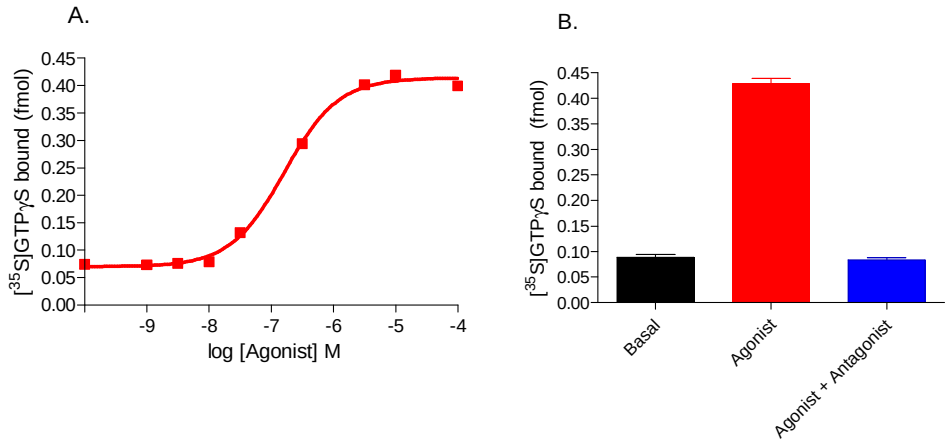

Figure 1.5: Representative examples of data from [^{35}S]GTPγS signalling assays. GPCRs expressed in membrane preparations are reconstituted with G-proteins and [^{35}S]GTPγS. Agonists and antagonists are added as appropriate and the basal level of [^{35}S]GTPγS binding is measured in the absence of agonist. After the desired incubation time, unbound [^{35}S]GTPγS is removed and the accumulated [^{35}S]GTPγS bound to Gα is measured using scintillation counting. (A) An agonist dose-response curve provides a measure of efficacy as an EC_{50} value and can determine whether a ligand is a full or partial agonist. (B) Agonist-induced receptor stimulation compared to basal conditions and when an antagonist is present. The reduction in [^{35}S]GTPγS binding shows that the agonist-induced response was ligand specific.

To overcome the limitations of the traditional [^{35}S]GTPγS binding assay, a scintillation proximity assay (SPA) has been developed using beads or micro plates containing scintillant to which preparations of GPCRs and G-proteins are immobilized. [^{35}S]GTPγS binding, stimulated by an agonist excites the scintillant generating a light signal. Unbound [^{35}S]GTPγS generates no signal since a low energy emitting isotope is used which requires the isotope to be in close proximity to the scintillant (Ferrer *et al*. 2003). However, considerable safety and waste concerns exist around the use of radioactive materials which has generated much interest in applying fluorescent technologies with rapid read times to assays for GPCRs.

1.6.3. Signalling assays using fluorescent GTP analogues

Functional fluorescent assays have been developed using fluorescently labelled GTP analogues. Europium-labelled GTP has proved useful in functional assays due to the long-lived emission lifetime of the lanthanide europium allowing measurements to be delayed until background

fluorescence has decayed (Frang *et al*. 2003). This assay produces similar results to the [^{35}S]GTPγS binding assay while using a preferable fluorescent GTP analogue. However, the assay remains non-homogeneous requiring washing steps to remove unbound europium-labelled GTP. Other fluorescent GTP analogues including MANT-GTP and BODIPY-GTP are able to bind to Gα-subunits and increase in fluorescence upon binding to provide a mechanism for a homogeneous assay (McEwen *et al*. 2001; Remmers 1998). However, studies with these analogues to investigate receptor induced GTP binding are lacking, suggesting that high background signals, poor signal to noise ratios and difficulty in achieving purified receptor preparations to reduce this, probably prevents their utility in functional GPCR assays.

1.6.4. Second messenger assays

GPCR activation can also be measured using cell-based functional assays that determine changes in concentration of secondary messengers such as cyclic AMP (cAMP), Ca^{2+} or inositol phosphates and are particularly useful for Gs- and Gq-coupled receptors that perform poorly in GTP binding assays. Alternatively, effects even further downstream that occur as a consequence of changes to secondary messengers such as altered gene expression, ERK1/2 phosphorylation (Osmond *et al*. 2005) or even changes in cell morphology (Yu *et al*. 2006) can be measured. Measurements are usually taken from treated whole-cells that have been lysed and reviews on many of these technologies are available (Eglen 2005; Thomsen, Frazer & Unett 2005). However, second messenger levels can be mediated independently of a GPCR and thorough controls are necessary to avoid false positives the chances of which increase the more distal the event being measured is to GPCR activation (Thomsen, Frazer & Unett 2005).

1.6.5. Use of “promiscuous” G-protein subunits

Assays that detect changes in second messenger levels such as calcium usually require whole cell assay platforms and can be restricted to receptors that couple to a specific G-protein pathway

that must be known. To increase the generic application of these assays, second messenger assays that use "promiscuous" G-proteins (so named because they are capable of interacting with many GPCRs) to force signalling through a common effector pathway have been designed (Milligan, Rees 1999). This approach could be applied to *in vitro* applications to increase the generic property of the assay in being applied to a wider range of GPCRs. G-proteins $G\alpha_{15}$ and $G\alpha_{16}$ (from the Gq family) are currently the most promiscuous G-proteins identified to date, recognizing many receptors including those that would normally signal through $G\alpha_i$ or $G\alpha_s$. Attempts at further increasing this promiscuity have been made by constructing chimeric G-proteins. Two chimeras termed $G\alpha_{Z25}$ and $G\alpha_{Z44}$ have been constructed by replacing the last 25 or 44 C-terminal residues of $G\alpha_{16}$ with the corresponding amino acids from $G\alpha_z$ (Liu *et al*. 2003). These chimeras were then shown to be superior in promiscuity and sensitivity compared to $G\alpha_{16}$ in functional cell-based assays. Likewise, a chimera of $G\alpha_{16}$ and $G\alpha_s$ ($G\alpha_{S25}$) has been constructed with the C-terminal 25 amino acids of $G\alpha_s$ replacing those of $G\alpha_{16}$. Of the receptors tested with $G\alpha_{S25}$, only the V2-receptor was found to couple less efficiently than with $G\alpha_{16}$ although $G\alpha_{S25}$ did signal through the glucagon receptor that did not couple to the $G\alpha_{16}$ receptor under the same conditions (Hazari *et al*. 2004).

The interactions discussed above, have so far been the most widely used to generate signals in GPCR assays. However, platforms measuring receptor dimerization and internalization are among others that are becoming better established with the increasing amount of understanding of the molecular mechanisms involved in GPCR signalling.

1.6.6. Förster resonance energy transfer platforms

Milligan (2000) proposed that an ideal assay for monitoring GPCR activation would use a change in spectral properties of either the GPCR or associated proteins such as the G-protein heterotrimer. Förster resonance energy transfer (FRET) technologies are available that can

provide such measurements. FRET applies Förster's principles of resonance energy transfer (reviewed in (Selvin 1995)) which states that the efficiency of energy transfer from donor fluorophores to acceptor fluorophores is dependent on both the orientation of the energy transfer partners and the distance between suitable donor and acceptor partners. A suitable donor and acceptor pair will have an overlap between the emission spectrum of the donor and the excitation spectrum of the acceptor. Generally, these moieties must be within 100 angstroms (10 nm) of each other for FRET to occur. FRET can be measured as a decrease in donor emission or lifetime, an increase in acceptor emission or a ratio between donor emission and acceptor emission (**Figure 1.6**).

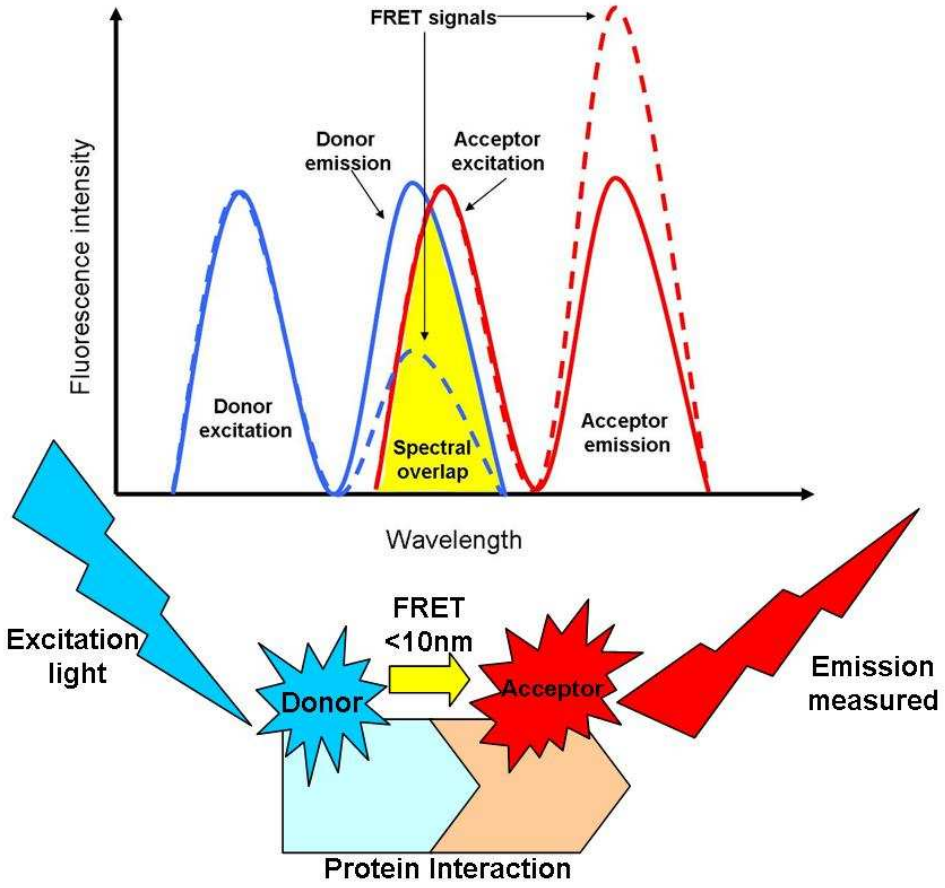

Figure 1.6: Schematic of Förster resonance energy transfer (FRET). FRET requires a donor and acceptor molecule to be brought into close proximity, in this case due to an interaction between labelled proteins. The emission spectrum of the donor overlaps with the excitation spectrum of the acceptor and upon excitation of the donor, FRET can be observed as a decrease in donor emission and increase in acceptor emission, occurring at different wavelengths.

GPCRs have been successfully tagged with appropriate donor and acceptor molecules for FRET to measure changes in the oligomerization state of the GPCR upon binding of a ligand. However, studies have indicated that the oligomerization state does not change in all GPCRs so such assays do not offer a generic approach for GPCR ligand screening (Milligan 2000). In addition, the mechanisms and biological/metabolic effects of oligomerization are still being established. Attention has now turned to approaches that monitor changes in the G-protein that occur upon activation of the receptor. Cyan fluorescent protein (CFP) and yellow fluorescent protein (YFP), two variants of Green fluorescent protein (GFP), have been used as a FRET pair to show conformational changes in GPCRs and G-protein activation (Janetopoulos, Jin & Devreotes 2001; Krasel *et al*. 2004). The G-protein subunits Gα2 and Gβ from *Dictyostelim discoideum* have been fused with CFP and YFP respectively. Using a cell-based assay, it was observed that the addition of cAMP as an agonist to cells transformed with both fusion proteins caused a rapid 70% decrease in FRET suggesting receptor-mediated activation of the G-protein and subsequent dissociation of the subunits (Janetopoulos, Jin & Devreotes 2001). A similar approach has also been used with $G\alpha_{i1}$ and $G\beta_1\gamma_2$ subunits where the Gα subunit was fused to YFP and the Gβ subunit to CFP (Bunemann, Frank & Lohse 2003). However, an increase in FRET was observed when mammalian cells expressing the α_{2A}-adrenergic receptor were stimulated, fuelling debate as to whether G-protein subunits dissociate or rather undergo changes in conformation upon activation in cells. Studies using fluorescent proteins for FRET have shown that a number of factors including the direct excitation of the acceptor, varying expression levels of each FRET partner, assay components and the detection system used, can generate background signals. Therefore, appropriate controls must be included so as to not mistakenly interpret this background as a FRET signal (Milligan, Bouvier 2005). The low sensitivity in these systems has also prevented their use in high throughput screening programs (Selvin 2000).

1.6.7. Bioluminescence resonance energy transfer (BRET) assay platforms

An alternative to FRET is Bioluminescence Resonance Energy Transfer (BRET) which is conceptually similar to FRET and can also share similar limitations. A protein of interest is fused to *Renilla* luciferase (*R*luc) which oxidizes a substrate such as h-coelenterazine or DeepBlueC. The oxidization of h-coelenterazine or DeepBlueC produces light that can excite YFP or GFP, respectively when in close proximity. The fluorescent proteins are fused to a protein brought into close proximity to the luciferase fusion protein due to an interaction occurring. The primary advantage of BRET is that no light source is required to excite the donor, thus no direct excitation of the acceptor can occur and autofluorescence is reduced. However, the BRET pair of h-coelenterazine being oxidized to excite YFP generates a high background signal due to the emission of the acceptor overlapping significantly with the emission produced by the oxidation of h-coelenterazine (Milligan, Bouvier 2005). To improve this, DeepBlueC was introduced to produce light accepted by GFP. However, oxidation of DeepBlueC has a poor quantum efficiency resulting in a lower signal making the system too insensitive to be amenable to high content platforms (Milligan 2004). While this technique has been used to examine various aspects of receptor pharmacology and extensively for monitoring GPCR oligomerization (Angers *et al*. 2000; Mercier *et al*. 2002; Ramsay *et al*. 2002) drawbacks of steric hindrance caused by tagging with such large polypeptides can exist for both FRET and BRET platforms. The exploitation of FRET and BRET technologies in studies using GPCRs or G-proteins have been thoroughly reviewed (Milligan 2004; Pfleger, Eidne 2005)

1.6.8. Time resolved-FRET

To overcome the limitations of traditional FRET, time resolved-FRET (TR-FRET) techniques using lanthanide donors such as terbium or europium have been developed, particularly for *in vitro* applications (Selvin, Hearst 1994). The advantages of TR-FRET include greater distances

over which FRET will occur and desirable donor fluorescent properties including a high quantum yield and non-polarised emission reducing the orientation dependence of FRET (Selvin 1996; Selvin 2002). Lanthanides also display a large Stokes shift resulting in hundreds of nanometers between the excitation spectra and emission spectra, which produces better signal resolution since scattering of the excitation light and direct excitation of the acceptor is not likely to cause background signals. Most importantly, luminescence generated from lanthanides has a relatively long (millisecond) lifetime compared to the nanosecond lifetime of fluorescence and this property can be exploited by using a delay after excitation before measuring the emission (time-gating). This greatly improves the signal to noise ratio by temporally eliminating background fluorescence and scatter (**Figure 1.7**).

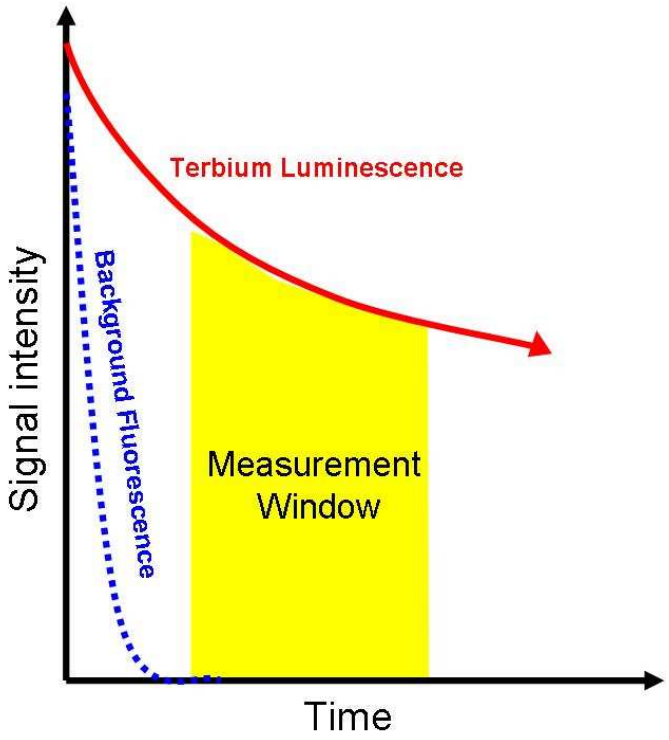

Figure 1.7: Gated measurement of terbium emission. As a lanthanide, terbium can exhibit long- lived luminescence that remains after background fluorescence has decayed. A delay after the excitation of terbium allows background fluorescence to decay before acceptor fluorescence generated by TR-FRET from terbium is measured. This increases the signal to noise ratio of the assay compared to traditional FRET.

TR-FRET studies involving GPCRs have generally demonstrated dimerization on the surface of cells using europium labelled antibodies with another acceptor labelled antibody. GPCRs modified with different tags that are exposed on the surface of the cell are recognized by the antibodies and TR-FRET indicated that dimerization was occurring (Liu *et al*. 2004; McVey *et al*. 2001; van Rijn *et al*. 2006). Potential problems with this method have been recognized since the antibodies used could act to cluster receptors due to their bivalent nature, the large size of antibodies can also be problematic and in some cases, antibody binding can change the activity of the receptor modulating the system that they are used to observe (Milligan, Bouvier 2005).

We have previously exploited TR-FRET in an assay to measure the interactions between $G\alpha_{i1}$ with Gβγ and RGS4 (Leifert *et al*. 2006). Purified proteins were labelled with terbium or Alexa546 as the donor or acceptor, respectively and TR-FRET was used to measure apparent dissociation constants, demonstrate competitive binding and modulators of the interactions (**Figure 1.8**).

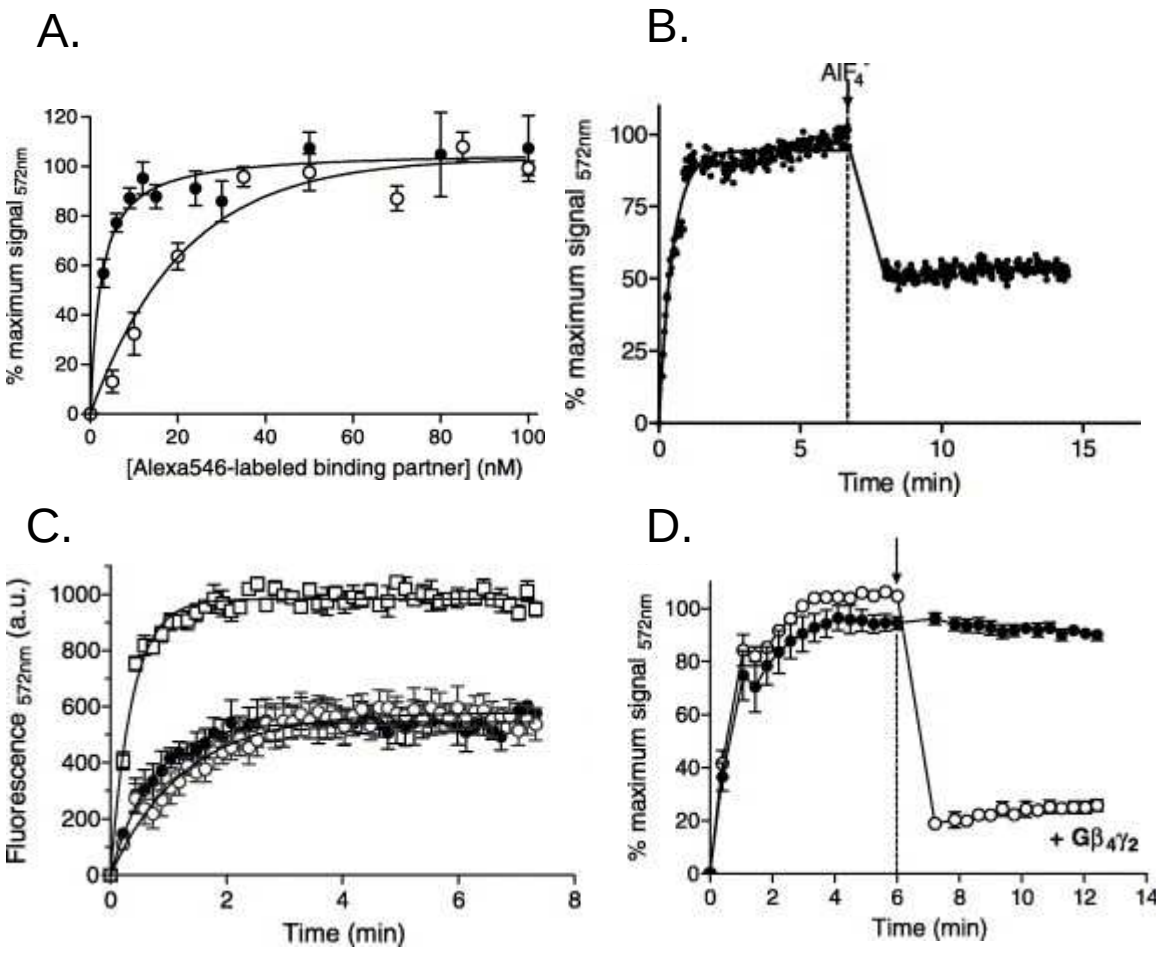

Figure 1.8: Measurement of heterotrimeric G-protein and regulators of G-protein signalling interactions by time-resolved fluorescence resonance energy transfer (Leifert *et al*. 2006)**.** (A) $G\beta_4\gamma_2$ has a higher affinity for $G\alpha_{i1}$ than RGS4. TR-FRET between 5 nM $G\alpha_{i1}$:Tb and various concentrations of $G\beta_4\gamma_2$:Alexa546 (•) in TMND buffer (50 mM Tris, pH 8.0, 100 mM NaCl, 1 mM $MgCl_2$, and 1 mM DTT) generated an apparent *K*d of 2.4 nM. TR-FRET between 50 nM $G\alpha_{i1}$:Tb and various concentrations of RGS4:Alexa546 (○) produced an apparent *K*d of 14.6 nM. All data shown are mean ± SEM (*n* = 3). (B) Addition of aluminium fluoride caused a reduction in TR-FRET between $G\alpha_{i1}$:Tb and $G\beta_4\gamma_2$:Alexa. TR-FRET between 15 nM $G\alpha_{i1}$:Tb + 15 nM $G\beta_4\gamma_2$:Alexa546 in TMND buffer was rapidly decreased upon the addition of aluminium fluoride (10 mM NaF followed by 30 µM $AlCl_3$) (representative data). (C) Activation state of Gα alters interaction with RGS4. (A) TR-FRET between 40 nM inactive (+GDP) (•), active (+GTPγS) (○), or transitional state (+aluminium fluoride) (□) $G\alpha_{i1}$:Tb with 70 nM RGS4:Alexa546 in TMND buffer. All data shown are mean ± SEM (*n* = 3). (D) Steady state TR-FRET between 50 nM $G\alpha_{i1}$:Tb + 150 nM RGS4:Alexa546 in TMND buffer was rapidly decreased (75%) upon the addition of excess unlabelled $G\beta_4\gamma_2$ subunits (at the indicated time) to a final concentration of 900 nM. All data shown are mean ± SEM (*n* = 3).

1.7. Fluorescent labelling technologies for TR-FRET applications

While fluorescent assays are becoming increasingly popular and sophisticated, the crucial and often most labour intensive step remains achieving labelled protein samples (Heyduk 2002). A good fluorescent labelling strategy must uphold the integrity of the labelled protein by not interfering with its function. The fluorophores must also have good fluorescent properties to obtain high signal to noise ratios. Important fluorescent properties include a high extinction coefficient at the excitation wavelength as well as a high quantum yield (Waggoner 1995). Traditionally, the attachment of fluorescent probes to proteins has been accomplished by chemical modification after protein purification. This process often involves exploiting the reactive amino, sulfhydryl or hydroxyl groups contained in the side chains of amino acids such as lysine, cysteine, serine or threonine. Many reactive fluorescent dyes with succinimidyl ester, isothiocyanate, sulfonyl chloride, or maleimide groups are commercially available. These dyes are small so that the possibility of steric hindrance interfering with protein functionality is minimal. However, there are often multiple potential sites for labelling on a given protein giving rise to variability of the labelling site (potentially reducing signal resolution) and labelling efficiency.

While this strategy of protein labelling has been widely utilized, advances in molecular biology have made site-specific strategies for labelling of proteins far more viable. Methods that can site-specifically label proteins provide control over where fluorescent labels are incorporated to achieve the best chance of producing a protein whose function remains unchanged, while also offering improvements to consistency between labelled protein samples and enabling the optimization of signals. When small proteins are under study it may be possible to use mutagenesis so that only a single reactive residue is available for labelling. However, this is time consuming, may alter protein function and for larger proteins (with more potential labelling sites) this strategy may not be viable. A number of alternate site-specific labelling strategies have

emerged for both *in vitro* and *in vivo* studies and these approaches have been reviewed in recent years (Chen, Ting 2005; Heyduk 2002; Miyawaki, Sawano & Kogure 2003).

1.7.1. Donor labelling strategies

TR-FRET requires a lanthanide donor with long-lived fluorescence and such lanthanide probes have previously been used in immunoassays, molecular diagnostics as well as drug discovery applications (reviewed in (Hemmila, Laitala 2005)). The lanthanides europium (Eu), terbium (Tb) and gadolinium (Gd) are the only lanthanides that have emission lifetimes that remain in excess of 0.1 ms in aqueous solutions (Parker, Williams 1996). However, gadolinium emits in the UV range leaving europium and terbium being the labels of choice for most labelling strategies. As well as having millisecond lifetimes, lanthanides have unusual spectral characteristics in their narrow and multiple emission bands and large Stokes shift (>150 nm). Both europium and terbium have been exploited in a number of assay platforms such as LANCE® (Perkin Elmer) and LanthaScreen™ (Invitrogen). Europium offers some advantages in that its emissions are red-shifted compared to those of terbium, which emits in the regions of the visible light spectra that biological media components can more readily absorb causing fluorescence which might increase background signals. However, the multiple emission peaks of terbium offer more flexibility in choosing an appropriate acceptor fluor for TR-FRET applications and the possibility of multiplexing. Terbium also has a larger energy gap between the ground and emissive states resulting in terbium luminescence being quenched by hydroxyl groups to a lesser extent than europium is once chelated (Hemmila, Laitala 2005). These lanthanide ions require an appropriate coordination environment and a sensitizing chromophore to produce their characteristic long-lived luminescent emission (Franz, Nitz & Imperiali 2003). Long-lived luminescence occurs due to forbidden electronic transitions, however, a consequence is that lanthanides have poor light absorption with direct excitation of lanthanide ions yielding only a weak signal that is easily quenched by water molecules (Gomez-Hens, Aguilar-Caballos 2002). To provide conditions

under which lanthanides have improved luminescent properties, lanthanide chelates have been commercially developed which prevent fluorescence quenching by water and contain aromatic moieties that act as antenna molecules by absorbing and transferring the excitation energy to increase the emission of the lanthanide (Handl, Gillies 2005) (**Figure 1.9**). These chelates, although expensive and often difficult to synthesize, will also have a functional group such as a maleimide available to facilitate protein labelling. However, as described previously, these methods of labelling are inherently not site-specific and offer little control over the extent of labelling.

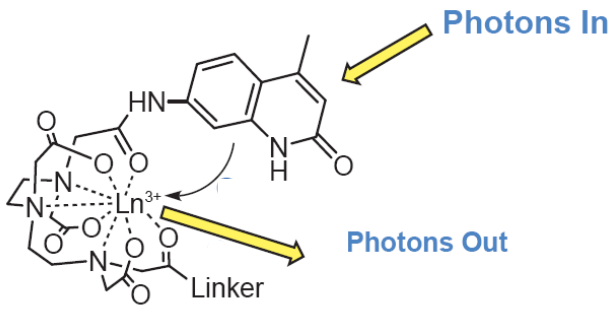

Figure 1.9: Example of a diethylene triamine pentaacetic acid based-chelate for a lanthanide ion available from Molecular Probes (Invitrogen).

An emerging terbium label takes the form of what is termed a terbium doped nanoparticle. These consist of an inorganic matrix that acts as a host crystal for terbium ions and also acts as the antenna molecule for terbium luminescence. These nanoparticles generate strong luminescence and can be excited with infra-red light using the process of up-conversion. This could significantly increase the sensitivity of assays since infra-red light induces less autofluorescence (Wang *et al*. 2006). While terbium doped silica nanoparticles (45 nm in diameter) functionalized with free amino groups, have been conjugated to an antibody and BSA (Ye *et al*. 2005), the nanoparticles are large in size compared to many proteins and the synthesis, surface modification and conjugation methods are still in the early stages of development.

Lanthanide chelates have also been packed inside a nanoscale polystyrene shell to produce a particulate fluorescent label that has been shown to reduce the sensitivity of the luminescence to environmental factors such as pH and the presence of other metal ions (Kokko, Lövgren & Soukka 2008). Similarly to the terbium doped nanoparticles, these are also relatively large in size (92 nm) and conjugation methods are still developing.

Lanthanide binding tags (LBTs) are short peptides (17 amino acids) that bind terbium with a high affinity having a dissociation constant (*K*d) in the nanomolar range. LBTs were derived from the EF-hand motif of calcium binding proteins since for some time lanthanides have been used as probes of calcium binding proteins such as calmodulin and galactose binding protein (Wilkins *et al*. 2002). EF-hand motifs usually bind calcium ions, however, since calcium and terbium ions have similar ionic radii, 1.06 and 0.98 respectively, terbium and other members of the lanthanide series can also occupy EF-hand motifs (Vazquez-Ibar, Weinglass & Kaback 2002). Initially, when the calcium ion binding loops were isolated from their native proteins the affinity for terbium significantly decreased and this lead to a combinatorial library of peptides based on the EF-hand motif of calmodulin being developed and screened for improved terbium binding and luminescence (Nitz *et al*. 2003). This work generated two short peptide sequences, LBT1 and LBT2 that were of particular interest (**Figure 1.10**). Co-ordination of the terbium ion within the LBT occurs due to the presence of negatively charged aspartate and glutamate residues. Hydrophobic residues aid in shielding the terbium from the quenching effects of water and aromatic amino acids tryptophan (and tyrosine residues to a lesser extent) sensitize the terbium for increased luminescence since the excitation spectrum of terbium overlaps with the emission spectrum of these amino acids.

Amino acid sequence of LBT1

Tyr Ile **Asp** Thr Asn Asn **Asp** Gly *Trp* *Tyr* **Glu** Gly **Asp** **Glu** Leu Leu Ala

Amino acid sequence of LBT2

Ala Cys Val **Asp** *Trp* Asn Asn **Asp** Gly *Trp* *Tyr* **Glu** Gly **Asp** **Glu** Cys Ala

Aromatic amino acids
Hydrophobic amino acids
Negatively charged amino acids

Figure 1.10: Amino acid sequence of lanthanide binding tags LBT1 and LBT2. Aromatic amino acids that sensitize the terbium luminescence, hydrophobic amino acids that shield the terbium from quenching and negatively charged amino acids that co-ordinate the terbium ion are indicated.

LBT1 had an apparent *K*d of 57 nM for terbium and LBT2 a higher affinity with a *K*d of 2 nM presumably due to the presence of cysteine residues that can form a disulphide bond to stabilize the peptide (**Figure 1.11**) (Nitz *et al*. 2003). While a high affinity for terbium is desirable, LBT1 achieved a higher maximum fluorescence indicating it may have superior luminescent properties which may also be advantageous.

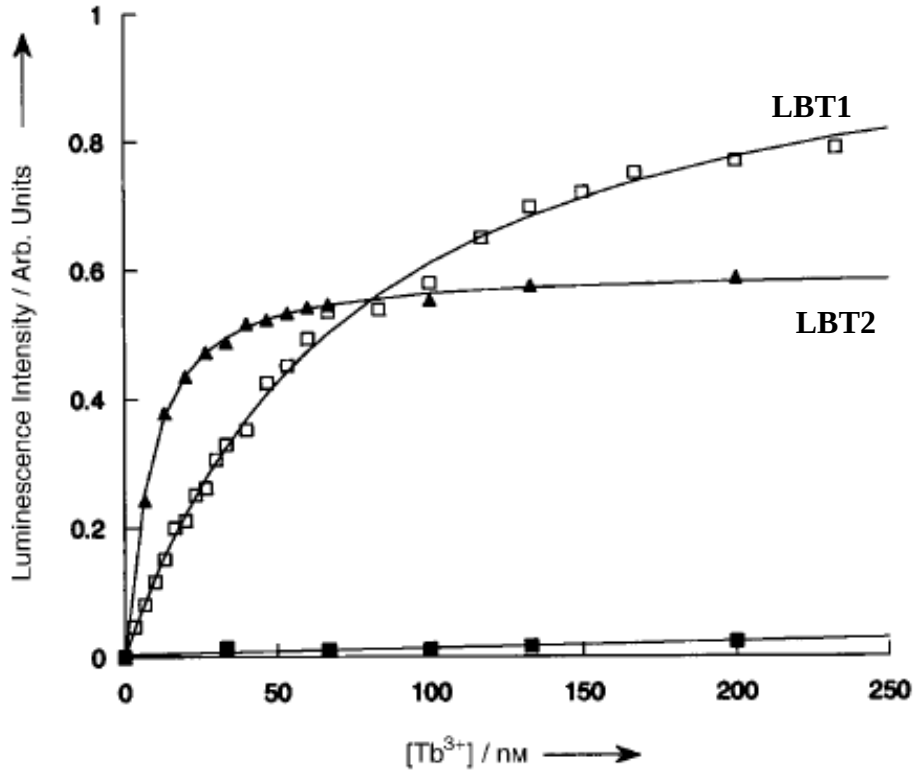

Figure 1.11: Terbium binding to lanthanide binding tags LBT2 and LBT1. Terbium ion titrations against 10 nM of lanthanide binding tag peptides showed LBT 1 (□) had a *K*d of 57 nM and LBT2 (▲) had a *K*d of 2 nM. Figure modified from (Nitz *et al*. 2003).

Lanthanide binding tags are proposed to be suitable fusion partners for labelling a protein of interest with terbium. The lanthanide binding tag should have a high enough affinity for terbium to prevent non-specific lanthanide binding problems and the quenching of terbium luminescence by water can be turned into an advantage as only terbium ions bound within a LBT should display luminescence. While preliminary fusion protein experiments using ubiquitin had been performed (Franz, Nitz & Imperiali 2003), at the commencement of this project, the utility of these LBTs had yet to be shown with more complex proteins under FRET circumstances and the utility of site-specific donor labelling was yet to be exploited with a site-specific acceptor labelling strategy.

1.7.2. Acceptor labelling strategies

An appropriate acceptor fluor for terbium will have an excitation spectrum that overlaps with the emission spectrum of terbium. The emission peak of the acceptor should also occur near a

wavelength where little emission from terbium occurs. Alexa546, a rhodamine derivative, has previously been used successfully as an acceptor for terbium in TR-FRET assays (Blomberg, Hurskainen & Hemmila 1999; Leifert *et al*. 2006). Alexa546 is part of a range of organic dyes that have been improved by the introduction of sulphonic acid groups to give the dye a negative charge that makes it more hydrophilic and therefore, exhibits a lower tendency to aggregate. Alexa dyes also have good fluorescent properties including high molar extinction coefficients, high photo stability and pH insensitivity (Wang *et al*. 2006). Proteins are labelled with Alexa via reactive amino acids presenting similar complications to that already discussed.

Options for site-specific labelling with an appropriate acceptor are more plentiful although each has its own advantages and disadvantages. These site-specific labelling technologies generally involve a fusion protein strategy where the fusion itself is fluorescent or specifically recognizes a fluorophore and binds it through a covalent or non-covalent interaction. A number of these strategies will be discussed.

Green fluorescent protein

Green fluorescent protein was isolated from the jellyfish *Aequorea victoria* and other fluorescent proteins have since been identified and/or engineered including GFP-like proteins and non-fluorescing chromo proteins from anthozoan (Tsien 1998; Verkhusha, Lukyanov 2004; Wolff *et al*. 2006). The discovery of GFP-like proteins expanded the range of colours and mutational and directed evolution methods have been used to improve the properties of these proteins as fluorescent tags. Proteins of interest can be engineered so that they are fused directly to GFP or another genetically encoded fluorescent protein. The cDNA encoding the fluorescent protein is fused in frame with that of the gene encoding the protein of interest. GFP is spontaneously fluorescent so production of the fusion protein is simply a matter of achieving expression of the gene in the desired cell type. This technique has been successfully used to visualize gene

expression, for protein localization studies and FRET or BRET experiments to study protein interactions and conformational changes (reviewed by (Tsien 1998)). CFP and YFP have been often used as a FRET pair to show conformational changes in GPCRs and G-protein activation (Janetopoulos, Devreotes 2002; Janetopoulos, Jin & Devreotes 2001; Krasel *et al*. 2004). A disadvantage of GFP is that it is quite large, containing 238 amino acids (27 kDa) and therefore, has the potential to perturb the function or cellular localization of the protein of interest. Formation of the correct structure of GFP also requires a multi-step folding process, which often results in slow or incomplete maturation and therefore a lack of fluorescence or incorrect fluorescent properties (Miyawaki, Nagai & Mizuno 2003).

Labelling proteins translated *in vitro*

In vitro translation systems can also be exploited to achieve site-specific labelling of proteins in strategies using puromycin-fluorophores to label the C-terminus of proteins (Nemoto, Miyamoto-Sato & Yanagawa 1999) or unnatural amino acids to introduce a reactive group such as a ketone not normally found in proteins at desired sites. These groups can then be specifically labelled by a commercially available hydrazide-functionalized fluorophore (Chin *et al*. 2003; Zhang *et al*. 2003). However, methods associated with *in vitro* translation currently produce low yields of protein, are labour intensive, and subsequent problems with protein folding to produce functional proteins are often encountered.

Quantum dots

Quantum dots are semi-conductor nanocrystals (1-10 nm) consisting of groups II-VI or III-V elements (reviewed in (Hild, Breunig & Goepferich 2008; Jamieson *et al*. 2007)). The elemental composition of the quantum dot core determines the fluorescence maxima and this can be tuned by changing the size of the quantum dot. Quantum dots offer colour variations that cover the visible to near infrared spectrum. The quantum dot cores are then usually capped with another

semiconductor such as ZnS providing a shell to enhance the quantum yield. Quantum dots are presenting themselves as the "gold standard" fluorophores of the future being stable, having customizable emission spectra and broad excitation spectra. Compared to conventional fluorophores, quantum dots have better fluorescence properties with regard to stability, Stokes shift, and fluorescence intensity (one quantum dot can emit the same amount of light as 20 rhodamine molecules (Clapp, Medintz & Mattoussi 2005)). Although the field of quantum dots is rapidly progressing, at the inception of this project, quantum dots were expensive with a low availability and techniques for the conjugation to biomolecules were still at the experimental stages (Michalet *et al*. 2005, Sutherland 2002). Their utility as acceptors has also been questioned, due to their broad excitation range and slightly longer emission lifetime (30-100 ns). Thus, quantum dots may be better donors than acceptors for FRET signals with a high signal to noise ratio. Depending on the emission wavelength required, quantum dots remain relatively large in size in comparison to many proteins to which they could be conjugated.

Strategies for non-covalent labelling of fusion proteins

The extensively characterized interaction between dihydrofolate reductase (DHFR) and methotrexate has been adapted for a fluorescent labelling strategy (Miller *et al*. 2004). Methotrexate can be chemically conjugated to a wide variety of fluorophores without having an effect on binding to DHFR. Fluorescently labelled methotrexate analogues are commercially available and will be recognized by DHFR fused to proteins of interest. DHFR is a monomeric 18 kDa (157 amino acids) protein making it significantly smaller than GFP. However, the non-covalent nature of the interaction between DHFR and methotrexate has proven problematic with dissociation causing signal deterioration (Chen, Ting 2005).

In yet another fusion protein strategy by Marks and colleagues, a mutant FK506-binding protein 12 (F36V) was used as a high affinity binding-partner for a synthetic ligand termed SLF' that can

be conjugated to fluorescein. FK506-binding protein 12 (F36V) contains 108 amino acids and while the potential for conjugation of a wide variety of fluorophores to SLF' exists, problems similar to those with the DHFR strategy regarding ligand dissociation causing signal deterioration over time remain (Marks, Braun & Nolan 2004). Another labelling strategy with problems associated with signal deterioration uses a small hexa-histidine tag often incorporated into proteins for purification purposes (Guignet, Hovius & Vogel 2004; Kapanidis, Ebright & Ebright 2001; Srinivasan, Yao & Yeo 2004). The well known interaction between polyhistidine sequences and Ni^{2+}-NTA (most often utilized for protein purification) can be exploited for fluorescent labelling using readily available and economically produced Ni^{2+}-NTA probes conjugated to organic fluorophores. However, the non-covalent interaction has insufficient affinity to offer a viable labelling strategy for many applications, although improvements using an increased number of NTA moieties or histidine complexes could improve this.

The high affinity between avidin and biotin has often been exploited for protein purification purposes and attempts have been made to use these principles in protein labelling (reviewed in (Zhang *et al*. 2002). One such strategy is to create avidin fusion proteins by using genetic engineering methods similar to those used to create GFP fusion proteins already discussed. Avidin tags are recognized by fluorescent biotin derivatives achieving site-specific labelling of the desired protein. The affinity between biotin and avidin is so high that femtomolar dissociation constants are achieved, however, avidin is a 63 kDa tetramer which significantly increases the probability that protein function will be disrupted. Over expression of avidin is also likely to be toxic to the cells in which it is expressed leading to low protein yields. Another consideration is that the biotinylated probe may need to compete with endogenous biotin for binding to avidin.

Fluorophore dye binding peptides (or fluorettes) are the result of using target phage display and affinity maturation systems to select for peptides capable of selectively binding the fluorophore dyes Texas red, rhodamine red, Oregon green 514 or fluorescein (Rozinov, Nolan 1998). However, *in vitro*, many of the peptides failed to bind to the fluorophores once removed from the phage particles. Only two Texas red binding peptides remained successful. These were further improved, resulting in a 39 residue peptide able to bind Texas red with enough affinity to sustain several washes (Marks, Rosinov & Nolan 2004). However, this dye is not a suitable acceptor for terbium in TR-FRET.

Labelling strategies using specific covalent attachment of fluorophores

Fusion protein strategies exploiting peptide carrier protein (PCP) and acyl carrier protein (ACP) for site-specific labelling offer a number of improvements over those strategies previously discussed. Although the principles are basically similar, with PCP or ACP coding sequences being genetically fused with the gene encoding the protein of interest, these proteins are significantly smaller being 80 or 77 amino acids in length, respectively (George *et al*. 2004; Yin *et al*. 2004). The enzyme phosphopantetheinyl transferase (PPtase) is used to transfer 4'-phosphopantetheine-linked fluorescent probes from coenzyme A to a serine side chain of ACP or PCP to label the protein of interest. The human DNA repair protein O^6-alkylguanine-DNA alkyltransferase (hAGT), truncated to 177 amino acids, can be utilized in a similar approach. Recombinant proteins fused to hAGT are labelled with fluorescent derivatives of the substrate O^6-benzylguanine by irreversible transfer of the alkyl group to a reactive cysteine residue of hAGT (Keppler *et al*. 2004). The specific covalent attachment of fluorophores in these examples overcomes the previously described problems with ligand dissociation although possible problems with the size of these fusion partners still exist.

Another strategy using fluorescent biotin derivatives developed by Chen and colleagues (Chen *et al*. 2005) involves the enzyme biotin ligase (BirA). BirA has a high specificity for a 15 amino acid acceptor peptide sequence (Lys-Lys-Lys-Gly-Pro-Gly-Gly-Leu-Asn-Asp-Ile-Phe-Glu-Ala-Gln-**Lys**-Ile-Glu-Trp-His) to which it ligates biotin. A ketone isostere of biotin was found to also be effectively ligated to a specific lysine residue (shown in bold) of the acceptor peptide. Since ketone groups are absent in natural proteins, carbohydrates and lipids, recombinant proteins containing the acceptor peptide can be tagged by the ketone probe and then fluorescently labelled using commercially available hydrazide or hydroxylamine-functionalized fluorophores. Labelling has been demonstrated on synthetic peptides, purified proteins and mammalian cell surface proteins. The ketone platform promises labelling capabilities for a wide range of fluorophores using a small peptide tag. However labelling must be conducted in two stages and synthesis of the ketone-containing biotin derivative is required.

Biarsenical dyes binding to tetracysteine motifs have shown promise as a means for acceptor labelling in FRET applications for G-proteins (Milligan 2004). Trivalent arsenic compounds are known to bind proteins that contain closely located pairs of cysteine residues, which is the basis for arsenic toxicity (Griffin, Adams & Tsien 1998). This association has been exploited in a labelling strategy using a tetracysteine motif (Cys-Cys-Xaa-Xaa-Cys-Cys) genetically fused with the gene of interest to create a recombinant fusion protein. Two appropriately spaced trivalent arsenics were found to specifically bind the tetracysteine motif with proline and glycine the most effective amino acids between the cysteine residues (Tsien 2005). 4',5'-bis(1,3,2-dithioarsolan-2-yl)fluorescein-(1,2-ethanedithiol)$_2$, a fluorescein arsenical helix binder (FlAsH) was subsequently generated and was found to be essentially non-fluorescent until bound to the tetracysteine motif upon which a very large increase in fluorescence was reported, presumably because the ethanedithiol moiety was displaced. A dissociation constant was found to be less than 10 pM showing that an exceptionally high affinity exists between the tetracysteine motif and FlAsH. The

quantum yield of FlAsH bound to the peptide is 0.49 which is similar to that of GFP. The excitation and emission peaks of FlAsH were 508 nm and 528 nm respectively which are approximately 20 nm longer than free fluorescein making it an appropriate acceptor for terbium emissions (**Figure 1.12**).

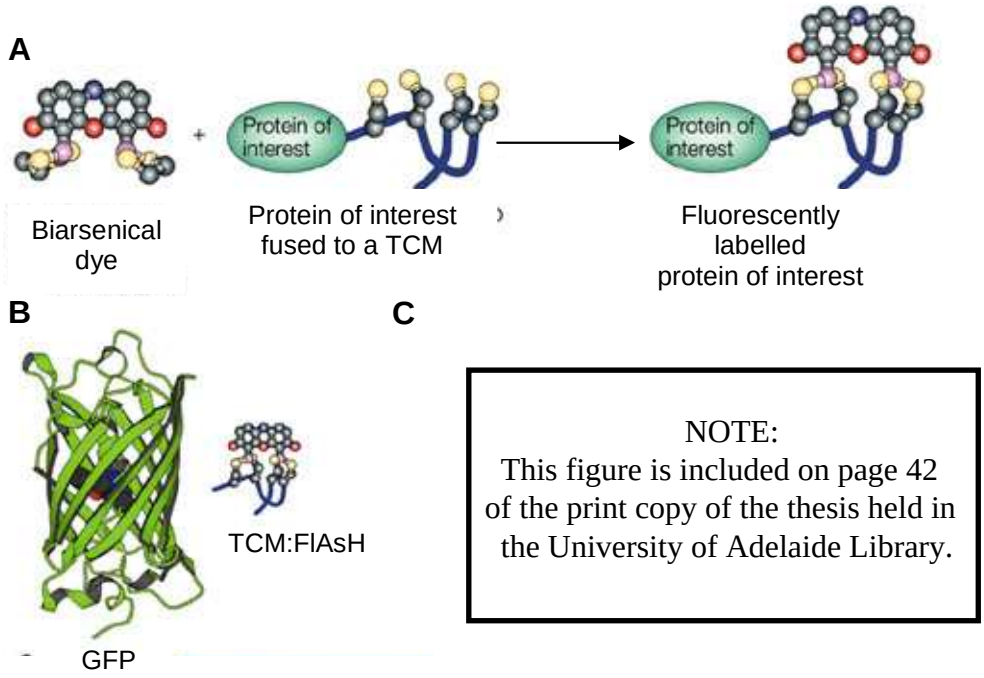

Figure 1.12: Strategy for labelling a tetracysteine motif with 4',5'-bis(1,3,2-dithioarsolan-2-yl)fluorescein-(1,2-ethanedithiol)$_2$ (FlAsH). (A) schematic of labelling strategy, modified from (Zhang *et al*. 2002). (B) Relative size of TCM:FlAsH complex compared to green fluorescent protein (Zhang *et al*. 2002). (C) Excitation and emission spectra of the TCM:FlAsH complex (Griffin, Adams & Tsien 1998).

Labelling of proteins with FlAsH can be achieved both *in vivo* or *in vitro* (Adams *et al*. 2002), however, high background signals have been observed during *in vivo* imaging experiments due to FlAsH binding to endogenous cysteine-containing proteins (Stroffekova, Proenza & Beam 2001). *In vitro* labelling with FlAsH could offer an alternative to fluorescein labelling with iodoacetamide or maleimide reagents without affecting single cysteine residues (Griffin *et al*. 2000). Labelling has been achieved at the N- or C-termini or in an alpha helix when target cysteine residues are fully reduced, as FlAsH does not react with disulfides. The rate of labelling has been found to be

pH sensitive and the presence of β-mercaptoethanol (1 mM) improves the efficiency of labelling. FlAsH (acceptor) and CFP (donor) have been used in a FRET approach to detect changes in receptor conformation upon activation and this was shown to disturb receptor function less than using CFP and YFP as a FRET pair (Hoffmann *et al*. 2005). Thus, it would appear that biarsenical dyes binding to tetracysteine motifs might offer a viable labelling strategy for TR-FRET applications.

1.8. Summary

Assay technologies for GPCRs and their associated G-proteins are in demand for drug screening and other biotechnological applications, as well as for elucidating the remaining controversial mechanisms in G-protein mediated signalling. Such assay technologies are ideally fluorescent, homogeneous and amenable to miniaturization. While both cell-free and cell-based assays have advantages in different circumstances, cell-free assays require less infrastructure and can be available for 'screen on demand' purposes. FRET offers a promising means of achieving such assays with TR-FRET a further improvement over traditional techniques. The success of TR-FRET relies on the generation of an appropriate labelling strategy that can be consistently reproduced. For this purpose, this research proposes that a lanthanide binding tag labelled with terbium and fused to a G-protein subunit in combination with a FlAsH labelled tetracysteine motif fused to the opposing G-protein subunit binding partner as an acceptor, may prove to be an appropriate site-specific labelling strategy for TR-FRET (**Figure 1.13**). This donor and acceptor pair could also be further extended to monitor conformational changes within the same protein such as a GPCR or in the development of alternative assay platforms.

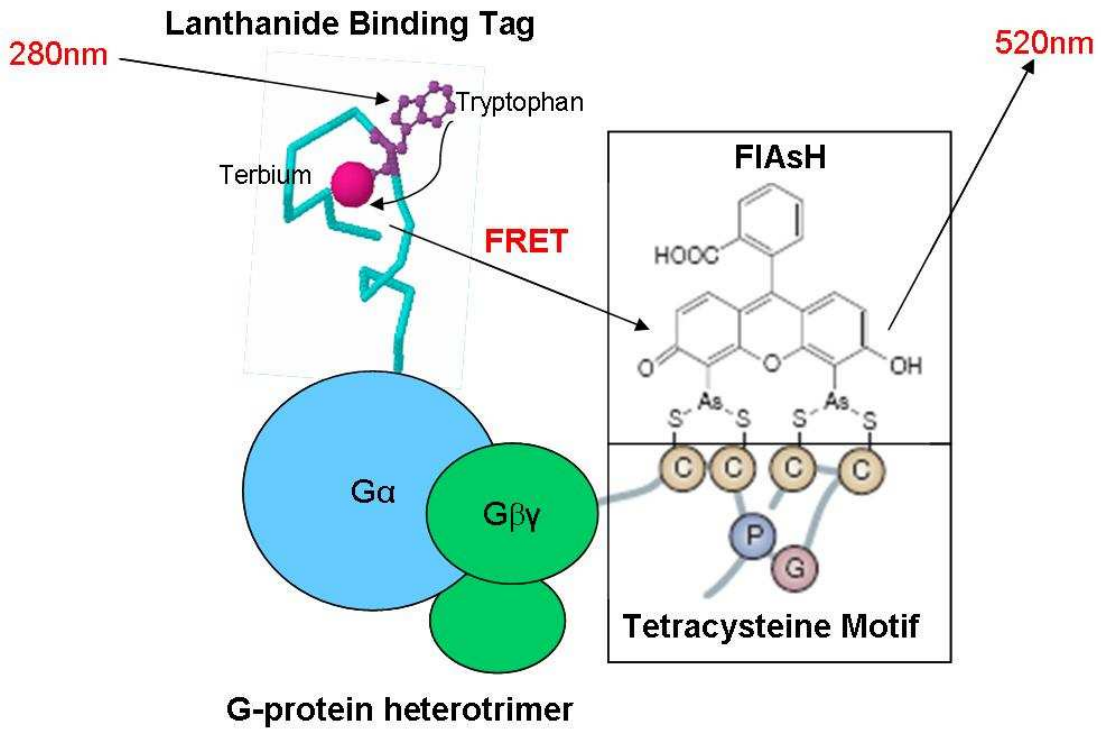

Figure 1.13: Schematic of the proposed TR-FRET platform for G-protein subunit interactions using site-specific labelling. G-protein subunit binding partners are fused to a TCM or LBT and recombinant fusion proteins labelled with FlAsH or terbium, respectively. When the proteins are interacting (the G-protein heterotrimer is inactive) the donor and acceptor labels are brought into close proximity, excitation of the LBT:Tb complex at 280 nm results in resonance energy transfer to the TCM:FlAsH complex, the emission of which is measured at 520 nm after time-gating to remove background fluorescence from the signal.

1.9. Structure and aims of this study

This study aims to make progress towards developing a TR-FRET assay for G-protein interactions which could be used as a generic assay platform for GPCR signalling. The first chapter of this study investigates the use of small molecule labels of CS124-DTPA-EMCH:Tb and Alexa546 in a TR-FRET assay. This TR-FRET pair had previously been applied to Gα, Gβγ and RGS4 proteins and during the characterization of this assay, the protein CrV2 was observed to interact with the G-protein. CrV2 is encoded by a polydnavirus from an endoparasitoid wasp and is thought to be involved with mediating immune suppression within a host insect. The second chapter of this thesis aims to characterize what could be a novel interaction between a Gα-subunit with CrV2. Improvements to the labelling strategy used in this assay are then attempted through the creation of G-protein subunits fused with lanthanide binding tags or tetracysteine motifs. Therefore, the core of this project aims to generate a cell free, homogeneous, potentially arrayable and high throughput fluorescent assay that shows the interaction between site-specifically labelled G-protein subunits Gα and Gβγ using a LBT and a TCM in a TR-FRET assay. The development of this TR-FRET system is broken down into a further three chapters as shown in (**Figure 1.14**) and primarily involves the following steps:

- Creating LBT and TCM fusion constructs with Gα and Gβγ-subunits as recombinant baculovirus.
- Expressing and purifying the fusion proteins in *Sf*9 cells.
- Determining whether the functional integrity of the G-protein subunits is maintained.
- Labelling LBTs and TCMs with terbium and FlAsH, respectively.
- Detecting and characterizing the interaction between terbium-labelled G-protein subunits with their FlAsH labelled G-protein subunit binding partner.

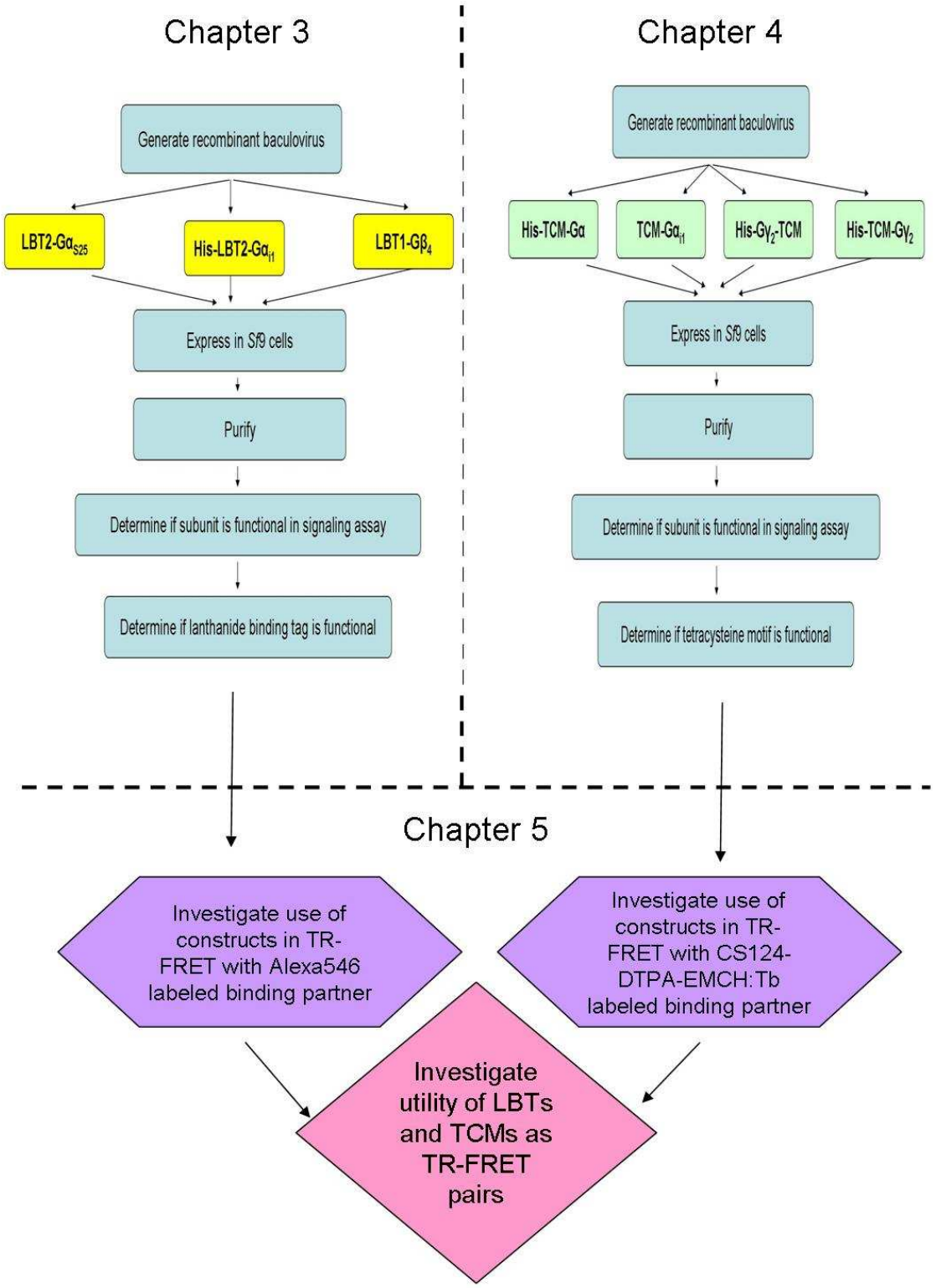

Figure 1.14: Experimental layout for chapters 3-5. These chapters involve a description of the production of TR-FRET assay components, assay production and validation. Chapter 3 describes the construction, labelling and characterization of G-protein subunits fused to LBTs. Chapter 4 describes the construction, labelling and characterization of G-protein subunits fused to TCMs and chapter 5 describes the use of these fusion proteins in TR-FRET assays.

Finally, the utility and feasibility of fusing LBTs to GPCRs for alternate assay platforms or other applications is investigated in chapter 6.

2. TR-FRET assays for G-protein interactions using small molecule labels: Characterization of a novel interaction between Gα-subunits and CrV2

Endoparasitoid wasp *Cotesia rubecula* and butterfly host *Pieris rapae* photos by Mike Keller, University of Adelaide (A and B) and Dr. Sassan Asgari , University of Queensland (C,D,E,F)

2.1. Introduction

Previously, an assay for G-protein subunit association was established and then expanded upon to examine the interaction of the Gα-subunit with RGS4 (Leifert *et al*. 2006). This assay used purified G-protein subunits that had been expressed in *Sf*9 cells and RGS4 that had been expressed in *E. coli*. Proteins were labeled with a small molecule terbium chelate as a donor fluor or Alexa546 as the acceptor, using thiol chemistry. Mixing of binding partners with the appropriate donor/acceptor combination resulted in TR-FRET signals greater than 3-fold above background using nanomolar concentrations of protein. Furthermore, the signal could be decreased upon the addition of an unlabelled binding partner and the presence of aluminium fluoride acted to decrease the signal generated by Gαβγ association while the signal from RGS4 binding to Gα increased. While the assay was originally developed to measure GPCR activation, there was also potential to exploit the assay to identify small molecule regulators of G-protein interactions and other binding partners of the subunits, and rather inadvertently, CrV2 was identified as putatively interacting with G-protein subunits.

CrV2 is a protein encoded by a polydnavirus (*Cotesia rubecula* bracovirus) that is produced endogenously by the endoparasitoid wasp *Cotesia rubecula*, which is crucial for its reproduction (Glatz, Schmidt & Asgari 2004). Polydnavirus particles are injected into a host (generally a lepidoptera species) with the wasp egg and other maternal protein secretions. The virus proteins are then expressed and they function in part to suppress the immune response of the host. Polydnaviruses are unique in that the viral DNA does not encode structural or replicative proteins; these are found in the wasp chromosomal DNA and viruses are not replicated in the parasitized host cells (reviewed in (Beckage, Gelman 2004; Kroemer, Webb 2004)). Initially, 4 proteins (CrV1-4) were associated with parasitisation by *C. rubecula*. The expression of these proteins in the host larvae (*Pieris rapae*) is transient and has been associated with temporary inactivation of

the host immune system (Glatz, Schmidt & Asgari 2004). The CrV2 gene was shown to encode a protein that can form oligomers and contains a signal peptide at the N-terminus. CrV2 is secreted from infected cells into the haemolymph before the signal peptide is cleaved from the mature protein which can then be taken up by haemocytes (Glatz, Schmidt & Asgari 2004). CrV2 has not been found to share significant homology to other proteins and the function of its interaction with haemocytes is unclear but being a protein expressed from a polydnavirus, it is expected to be involved with suppression of the host immune system given that these cells mediate many immune responses (reviewed in (Beckage, Gelman 2004)).

This chapter investigates the possibility of an interaction occurring between CrV2 and G-protein subunit Gα. CrV2 was expressed and purified in *E. coli* and G-protein subunits in *Sf*9 cells. The proteins were labelled with small molecule dyes Alexa546 and CS124-DTPA-EMCH:Tb via thiol-linkages and TR-FRET used to determine if a protein interaction was occurring.

2.2. Methods

2.2.1. General Materials

All chemicals and reagents were of analytical grade and purchased from Sigma Aldrich unless otherwise stated. All buffers were prepared in milli-Q water.

2.2.2. Purification of CrV2 from *E. coli*

CrV2 (without the first 20 N-terminal amino acids of the signal peptide) cloned into pQE30 (Qiagen) and transformed into M15[pREP4] (Qiagen) *E. coli* was obtained from Dr. Richard Glatz (SARDI, formerly CSIRO). Overnight cultures of recombinant M15[pREP4] *E. coli* were used to inoculate 300 mL of YT broth (8 g/L tryptone, 5 g/L yeast extract, 2.5 g/L NaCl, pH 7.0) containing 100 µg/mL of ampicillin and 50 µg/mL of kanamycin. Incubation at 37°C with vigorous shaking was then continued until the OD_{600nm} reached above 0.4. Isopropyl-β-D-thiogalactopyranoside (IPTG) was added to a final concentration of 1 mM to induce expression of CrV2 and then the incubation was continued for 3 hrs. Bacterial cells were then pelleted by centrifugation at 3500 xg in a Beckman J2-21 centrifuge for 10 min. The supernatant was then discarded and the pellets stored at -80°C. Cell pellets were resuspended in 10 mL of TBP buffer (50 mM Tris pH 8, 10 mM β-mercaptoethanol, 0.02 mg/mL phenylmethanesulphonylfluoride (PMSF), 0.03 mg/mL benzamidine). Lysozyme was then added to a final concentration of 0.2 mg/mL and gently mixed at 4°C for 30 min. $MgCl_2$ was then added to a final concentration of 5 mM followed by DNaseI to a concentration of 0.01 mg/mL. Mixing was then continued at 4°C for a further 30 min. 20% (w/v) cholate solution (50 mM NaHEPES pH 8.0, 3 mM $MgCl_2$, 50 mM NaCl and 200 g/L cholic acid (Na^+)) was added to a final cholate concentration of 1% (v/v). The preparation was then allowed to extract at 4°C with gentle stirring for 1 hr before ultra-centrifugation in a Beckman Coulter Optima™ LE-80K ultracentrifuge at 100 000 xg for 40 min. 800 µL of Ni-NTA agarose beads (Qiagen) in TBP (50% (v/v)) were then added to the supernatant and incubated on ice for 30 min

with occasional stirring. Supernatants were then applied to columns and liquid run through by gravity. Columns were then washed with 20 mL of TBP containing 100 mM NaCl followed by washing with 5 mL TBP containing 100 mM NaCl and 10 mM imidazole, pH 8.0. All washing procedures were carried out at 4°C. CrV2 with a 6 histidine tag (His-tag) was then eluted from the column in 400 µL fractions using TBP containing 100 mM NaCl and 250 mM imidazole. Eluted fractions were then analysed by sodium dodecyl sulphate-polyacrylamide gel electrophoresis (SDS-PAGE) and gels stained using the Coomassie blue staining procedure. Elutions containing CrV2 were identified and fractions pooled. Protein concentration was determined using the Bradford assay or laser densitometry before aliquotting and storage at -80°C.

2.2.3. SDS-PAGE and Coomassie blue staining procedure

Samples were mixed 1:1 with Laemmli sample buffer (Bio-rad) and heated for 3 min at 95ºC. Samples (30 µL) and a molecular weight marker were then loaded into 15% Tris-HCl pre-cast polyacrylamide gels (Bio-rad) and electrophoresed at 200 V in running buffer (3 g/L Tris, 1 g/L sodium dodecyl sulphate, 14.5 g/L glycine, pH 8.0) until the dye front reached the bottom of the gel. The gel was then washed 3 times in water for at least 5 min and stained in Coomassie blue stain (0.1% (w/v) Coomassie blue R-250, 40% (v/v) methanol, 10% (v/v) acetic acid) for 30 min. The gel was then washed in several changes of destain (40% (v/v) methanol, 10% (v/v) acetic acid) until background staining was removed. Destain was then removed by washing the gel in milli-Q water. Gel images were then recorded by scanning on a flat bed scanner.

2.2.4. *Sf*9 cell culture and infection with baculovirus

*Sf*9 cell cultures adapted to serum-free media were maintained in Sf-900 II SFM medium (GibcoBRL) at 27ºC with gentle shaking in Schott bottles with lids loosened for adequate oxygenation. When the cell density reached > 2 x10^6 cells/mL, as determined by cell counting on

a haemocytometer, cells were passaged to between 0.3-1 x10^6 cells/mL. Cell viability was determined by staining with Trypan Blue (0.05% (w/v) in PBS, diluted 1:1 with cells).

Baculoviral stocks were amplified by infecting *Sf*9 cells at a density of 2 x10^6 cells/mL with a multiplicity of infection (MOI) of 0.1. Infected cells were cultured for a further 48-72 hrs before the cells were removed by centrifugation. The supernatant (with 3% (v/v) Foetal Bovine Serum (FBS) (GibcoBRL) added) containing the amplified baculovirus stock was then filtered through 0.22 µm pore size stericups (Millipore) and stored in darkness at 4ºC.

To infect cells for protein expression, filtered baculovirus was added to *Sf*9 cells such that a final concentration of ~ 2 x10^6 cells/mL and a MOI of 2 was obtained. Incubation was continued for 48-72 hrs before cells were processed.

2.2.5. Purification of G-protein subunits

1-2 L of *Sf*9 cells were infected with the desired recombinant baculovirus to express G-protein subunits. Mammalian, His-tagged $G\alpha_{i1}$ (His-$G\alpha_{i1}$), His-tagged $G\gamma_2$ (His-$G\gamma_2$), $G\alpha_{i1}$ and $G\gamma_2$ baculovirus were obtained from Prof. Rick Neubig (University of Michigan), $G\beta_4$ and $G\beta_1$ from Prof. James Garrison (University of Virginia) and *Drosophila* $G\alpha_o$ from Dr. Sassan Asgari (University of Queensland). After ~72 hrs incubation, the cells were harvested by centrifugation and washed with PBS (137 mM NaCl, 2.7 mM KCl, 10 mM Na_2HPO_4, 1.8 mM KH_2PO_4, pH 7.4). The cells were then resuspended in 150 mL wash buffer (50 mM NaHEPES pH 8.0, 3 mM $MgCl_2$, 50 mM NaCl, 10 mM β-mercaptoethanol, 10 µM GDP and 0.02-0.03 mg/mL of PMSF, bacitracin, soybean trypsin inhibitor and benzamidine). 20% (w/v) cholate solution (20 mM NaHEPES pH 8.0, 3 mM $MgCl_2$, 50 mM NaCl and 200 g/L cholic acid (Na^+)) was then added to a final concentration of 1% (v/v) cholate. The mixture was then stirred at 4ºC for 1 hr before high speed centrifugation at 100 000 xg for 40 min. The supernatant was then applied to a Ni-NTA column

with a 400-500 µL bed volume. The column was then washed with 150-200 mL of Ni-NTA wash buffer (20 mM NaHEPES pH 8.0, 300 mM NaCl, 1 mM $MgCl_2$, 0.5% (w/v) $C_{12}E_{10}$, 10 mM β-mercaptoethanol, 10 µM GDP and 5 mM imidazole). The non His-tagged subunit or dimer could then be eluted from the column in fractions using an aluminium fluoride solution consisting of buffer E (20 mM NaHEPES pH 8.0, 50 mM NaCl, 10 mM β-mercaptoethanol, 10 µM GDP, 1% cholate, 50 mM $MgCl_2$, 5 mM imidazole) containing 10 mM NaF and 30 µM $AlCl_3$. The remaining His-tagged subunit or dimer could then be eluted using buffer E with 150 mM imidazole pH 8. An aliquot of each fraction was then analysed by SDS-PAGE using a 15% polyacrylamide gel (Bio-rad) which was stained with Coomassie blue. The fractions were assessed for the presence of the desired protein and its purity. Suitable fractions were then pooled and dialysed using Slide-a-lyzers with a 3500 MW cut off (Pierce) with multiple changes of buffer F (20 mM NaHEPES pH 8.0, 3 mM $MgCl_2$, 10 mM NaCl, 0.1% (w/v) cholate, 10 mM β-mercaptoethanol and 1 µM GDP). The purified protein was then aliquotted and stored at -80ºC.

2.2.6. Labelling of CrV2 and G-protein subunits

Purification of the proteins was carried out as has been described until the purified protein remained on the Ni-NTA column. β-mercaptoethanol was removed from the column by washing with buffer A (20 mM NaHEPES pH 8.0, 10 mM NaCl, 1 mM $MgCl_2$, 0.5% (w/v) $C_{12}E_{10}$, 10 mM β-mercaptoethanol, 10 µM GDP) and then cysteine-reactive Alexa Fluor 546 C_5-maleimide (Invitrogen) or CS124-DTPA-EMCH:Tb (Invitrogen) was added at an estimated 4x molar excess. The columns were incubated at room temperature for 3 hrs in darkness before unbound fluors were removed by further washing with buffer A. Fluorescence in the flow-through was monitored in 1 cm path length cuvettes using a Hitachi Fluorescence Spectrophotometer 650-105 using the appropriate excitation and emission wavelengths. Once the fluorescence could not be further reduced in the wash flow-through, proteins were eluted from the column as described earlier.

2.2.7. Determining protein concentration

Total protein concentration was determined using the Bradford method (Bradford 1976) or specifically using laser densitometry which compared protein bands on SDS-PAGE with bovine serum albumin (BSA) standards.

2.2.8. [^{35}S]GTPγS binding to Gα

40 nM of purified Gα-subunit was mixed with 1 nM [^{35}S]GTPγS in a final volume of 100 µL of TMN buffer (50 mM Tris pH 7.6, 100 mM NaCl, 10 mM $MgCl_2$) and incubated in a shaking water bath for 90 min at 27°C. 25 µL (in triplicate) was then filtered through glass microfiber 1 µm filter papers (GFCs) (Filtech) and unbound [^{35}S]GTPγS removed by washing with 3 x 4 mL of TMN buffer (50 mM Tris pH 7.6, 100 mM NaCl, 10 mM $MgCl_2$). The filters were dried and the amount of bound [^{35}S]GTPγS was measured by scintillation counting for 60 s in pico pro vials with 4 mL of Ultima Gold™ scintillation cocktail (Perkin Elmer) using a Wallac 1410 liquid scintillation counter .

2.2.9. TR-FRET Assays

The interaction between Alexa546 (Alexa) and CS124-DTPA-EMCH:Tb (Tb) labelled proteins was measured using TR-FRET in black 96-well plates as described in by Leifert *et al*. 2006. Briefly, 20x working solutions of proteins were made in TMN buffer (50 mM Tris pH 7.6, 100 mM NaCl, 10 mM $MgCl_2$). 5 µL of each was applied to opposite sides of the well such that mixing did not occur. Other indicated components such as proteinase K could also be added in this manner where required. TMN buffer was then added to a final assay volume of 100 µL, which initiated mixing. TR-FRET was then measured using a Victor3 multilabel plate reader (Perkin Elmer) with an excitation wavelength of 340 nm and a delay of 50 µs before measuring the emission at 572 nm for 900 µs. To assess the affect of additional components, measurements could be ceased so that these components could be added and then measurements resumed.

2.2.10. Data analysis

Data was analysed using Prism™ 4.00 (GraphPad software Inc., San Diego CA, USA). Data is presented as mean ± SEM where n ≥ 3. Where n = 2, data is presented as the mean and error bars represent the range of the duplicates. Apparent *K*d values were generated by fitting a one-site binding curve of the equation Y= Bmax . X / (*K*d + X). If error bars are not visible they are hidden by the symbols.

2.3. Results and Discussion

2.3.1. Purification of CrV2 from *E. coli*

CrV2 without the signal peptide (first 20 amino acids), had previously been purified under denaturing conditions from *E. coli*, since it was found to be located largely in the insoluble fraction (Glatz, Schmidt & Asgari 2004). The protein was expressed without the signal sequence since this results in the protein being secreted from infected cells after which it is cleaved off to yield the mature protein. This study utilized the same recombinant bacterial strain with the purification protocol described here. His-tagged CrV2 expression was induced in M15[pREP4] *E. coli* with IPTG as shown by SDS-PAGE analysis (**Figure 2.1**A). CrV2 was subsequently purified using Ni-NTA agarose beads and labelled with Alexa546 (**Figure 2.1**B). The detergent cholate was used to solubilise the protein for purification, as this had also been a successful method for purifying RGS4 from the insoluble fraction of *E. coli*. A number of lower molecular weight bands also seen in the original study in recombinant bacteria and *in vivo* were persistently present even with more stringent washing conditions and these were also recognized by anti-CrV2 antibodies in a western blot (data not shown). Since the His-tag is present on the N-terminus, these are likely to be C-terminal truncations of CrV2. These lower molecular weight bands could be a result of protein degradation although protease inhibitors were used to prevent this. In the future it may prove useful to remove the truncated CrV2 species. Interestingly, when infected host haemolymph, haemocytes and fat bodies were probed for CrV2, a number of truncated versions also appeared indicating the possibility of further processing of CrV2 (Glatz, Schmidt & Asgari 2004). While CrV2 has previously been recombinantly expressed in *E. coli*, the original study used the resulting protein to produce antibodies for further characterization of the expression of CrV2 *in vivo* rather than to investigate the biochemical interactions and functions of the protein (Glatz, Schmidt & Asgari 2004). Since the molecular interactions and functions of CrV2 are

currently unestablished, it is unknown whether this method of recombinant expression will have produced a fully functional protein.

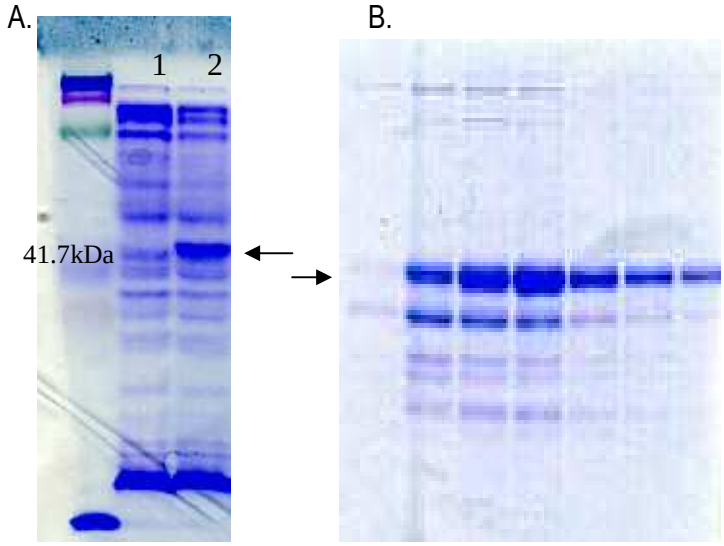

Figure 2.1: Expression and purification of CrV2 from *E. coli*. (A.) *E. coli* lysates showing CrV2 expression is induced with IPTG (lane 2) compared to non-induced lysates (lane 1). **(B.)** Elution profile of Alexa546 labelled CrV2 purified from 200 mL of *E. coli* using Ni-NTA beads.

2.3.2. Purification of G-protein subunits from *Sf*9 cells

G-protein subunits were typically purified from 1-2 L of infected *Sf*9 cells at ~2 x10^6 cells/mL. Either the Gα-subunit or the Gγ-subunit would contain a His-tag, to enable non His-tagged subunits to be eluted separately using aluminium fluoride (AlF_4^-) **(Figure 2.2).** Aluminium fluoride occupies the position normally taken by the γ-phosphate of GTP but the fluorine atoms assume a square planar configuration about the central aluminium atom to reorientate critical residues of the α subunit (Berman, Kozasa & Gilman 1996). This mimics an activated conformation of Gα referred to as the transition state, which is thought to occur in the lead up to GTP hydrolysis and results in the dissociation of the Gα-subunits from Gβγ-dimers. Subunits eluted with aluminium fluoride are always of a highly purified nature while some contamination is often present in the fractions eluted with imidazole due to some non-specific binding of histidine containing proteins. However, a higher yield of His-tagged protein is usually obtained. It was also observed that

fluorescent labelling of the G-protein heterotrimer was more successful in producing G-protein subunits that were functional in subsequent assays, presumably since areas critical for G-protein heterotrimer formation were protected from modification during the labelling process. G-protein subunits were estimated to be labelled on average 20-80% on exposed cysteine residues. These G-protein subunits could be shown to be functional in receiving signals from GPCRs when reconstituted in the [^{35}S]GTPγS signalling assays and could also be used as binding partners in TR-FRET assays (Leifert *et al*. 2006).

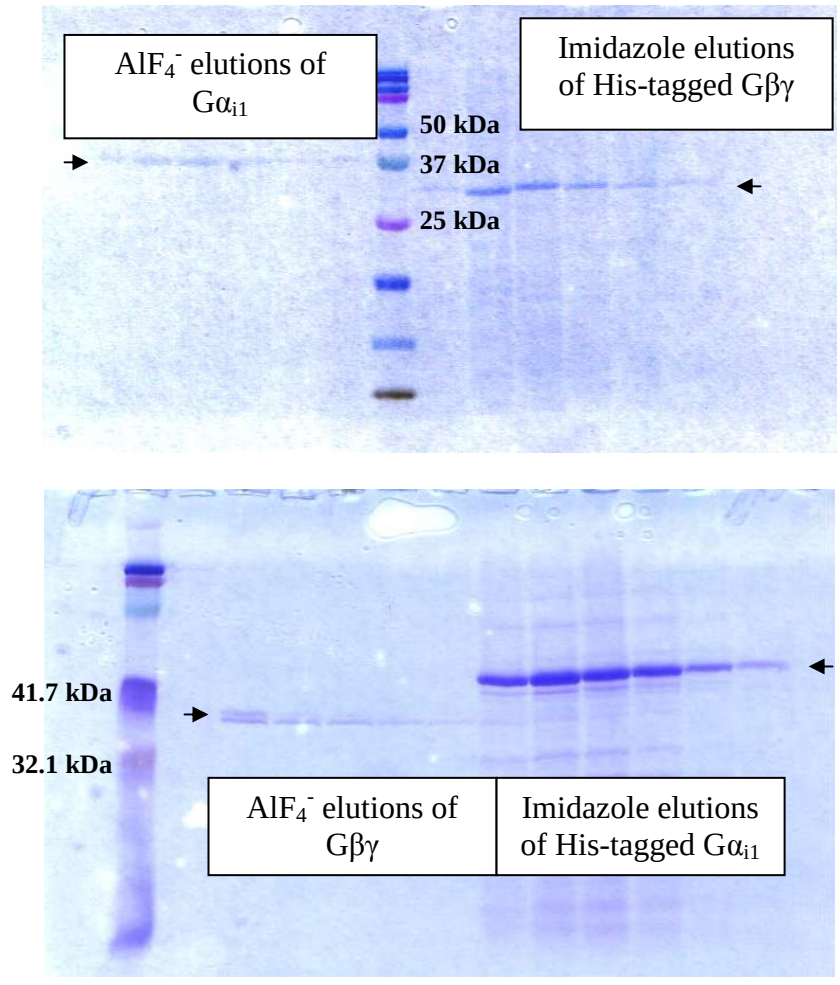

Figure 2.2: Representative SDS-PAGE analyses of purified fractions of G-protein subunits expressed in *Sf*9 cells, eluted from a Ni-NTA column.

2.3.3. Interaction of CrV2 with $G\alpha_{i1}$ measured using TR-FRET

Purified CrV2 labelled with Alexa546 (CrV2:Alexa) was mixed with purified $G\alpha_{i1}$ labelled with CS124-DTPA-EMCH:Tb ($G\alpha_{i1}$:Tb). Mixing of the two proteins caused an increase in Alexa546 (acceptor) fluorescence at 572 nm with time, upon excitation of terbium (donor) at 340 nm. Signals were up to 5-fold greater than background and the signal increased with an increased amount of CrV2:Alexa (**Figure 2.3**). Background fluorescence was generated by $G\alpha_{i1}$:Tb emission in the 572 nm channel while background contributions from Alexa546 and other buffer components were negligible since typical fluorescence had decayed during the 50 µs gating period before the emission was measured. This indicated that an interaction between $G\alpha_{i1}$ and CrV2 was occurring although further experiments were required to confirm this interaction.

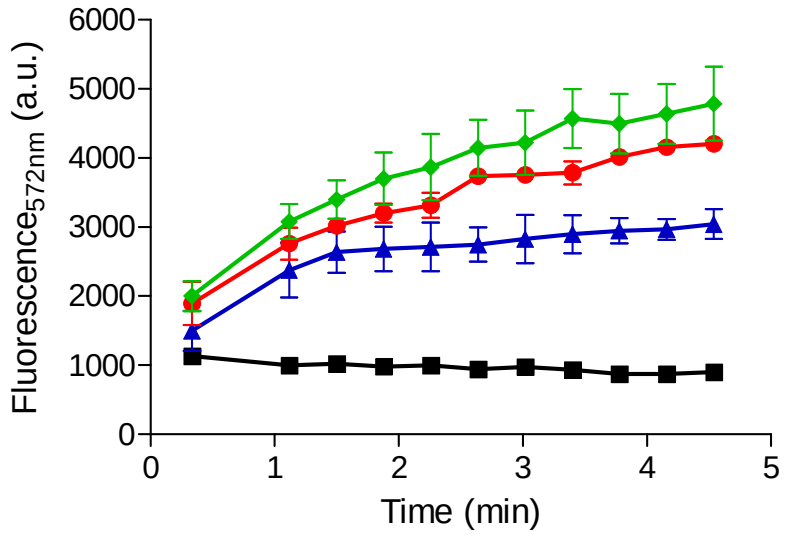

Figure 2.3: CrV2:Alexa association with $G\alpha_{i1}$:Tb. 10 nM $G\alpha_{i1}$:Tb (■) was mixed with 20 nM (▲), 40 nM (●) or 100 nM (◆) CrV2:Alexa. The final volume was made up to 100 µL with TMN buffer and TR-FRET measured using a Victor3 plate reader set for time-resolved fluorescence with the following parameters: λ_{ex} 340 nm, λ_{em} 572 nm, 50 µs delay and 900 µs counting duration over the shown time period. Data shown are mean (n=2).

When increasing concentrations of CrV2:Alexa were added to 10 nM $G\alpha_{i1}$:Tb, saturation was achieved at approximately 25 nM CrV2:Alexa and an apparent dissociation constant (*K*d) of 6.2 nM was calculated (**Figure 2.4**). This indicated that a relatively high affinity interaction was

occurring between CrV2:Alexa and $G\alpha_{i1}$:Tb, albeit lower than the affinity between the Gα subunit and the Gβγ dimer (2 nM) measured using the same technique (Leifert *et al*. 2006).

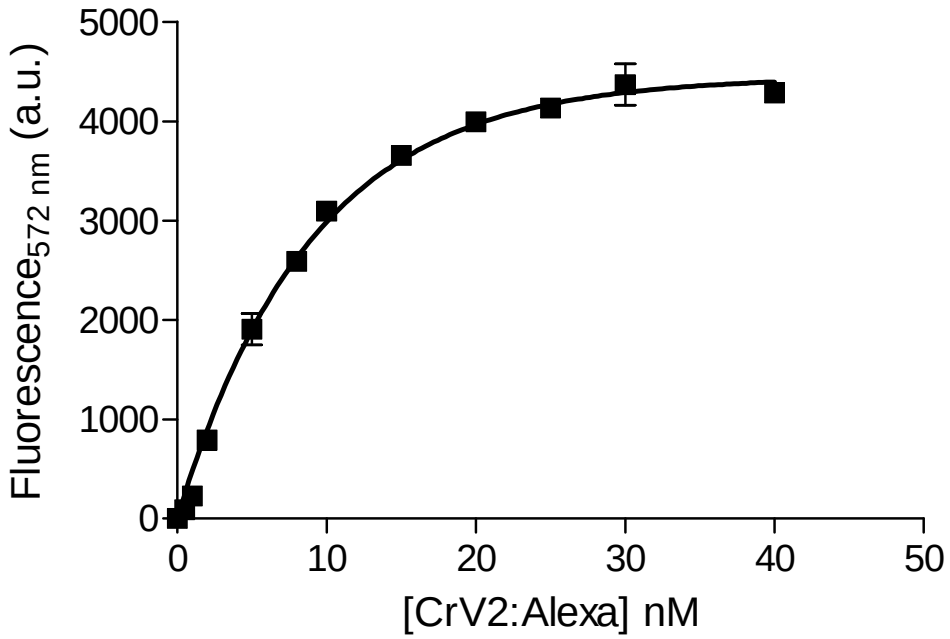

Figure 2.4: Saturation of $G\alpha_{i1}$:Tb with CrV2:Alexa. 10 nM $G\alpha_{i1}$:Tb was mixed with increasing concentrations (0-40 nM) of CrV2:Alexa. After a 10 min incubation, TR-FRET measurements were taken using a Victor3 plate reader set for time-resolved fluorescence with the following parameters: λ_{ex} 340 nm, λ_{em} 572 nm, 50 µs delay and 900 µs counting duration. Background of 10 nM $G\alpha_{i1}$:Tb has been deducted. A *K*d of 6.2 nM was calculated. Data shown are mean ± SEM (n=3).

Proteinase K is a broad spectrum serine protease that cleaves peptide bonds at the carboxylic sides of aliphatic, aromatic or hydrophobic amino acids and was used to digest the proteins to confirm the TR-FRET signal was due to a protein interaction and this treatment successfully reduced the TR-FRET signal (**Figure 2.5**). This suggests that the TR-FRET signal is a specific response to the interaction between CrV2 and $G\alpha_{i1}$ which was destroyed by digestion with proteinase K.

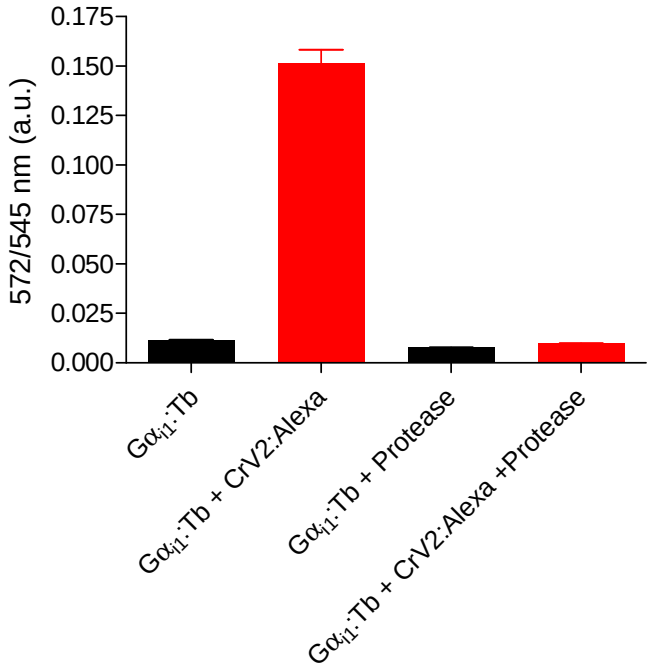

Figure 2.5: Protease treatment reduces the TR-FRET signal from CrV2:Alexa interacting with $G\alpha_{i1}$:Tb. 10 nM $G\alpha_{i1}$:Tb was mixed with 20 nM CrV2:Alexa ± 0.1 mg/mL proteinase K (protease) in a final volume of 100 µL using TMN buffer. After an incubation period of 30 min at 37ºC, TR-FRET measurements were taken with the following parameters: λ_{ex} 340 nm, λ_{em} 572 nm and 545 nm, 50 µs delay and 900 µs counting duration. Data shown are mean ± SEM (n=3).

Further confirmation that TR-FRET was due to a specific protein-protein interaction was that the addition of an excess of unlabelled binding partners including $G\alpha_{i1}$ (**Figure 2.6**), or CrV2 (**Figure 2.7**) rapidly decreased the TR-FRET signal while the addition of buffer had no effect. Gβγ could also inhibit the association of Gα:Tb with CrV2:Alexa (**Figure 2.8**). This indicated that unlabelled proteins were binding to labelled proteins, thereby competing with potentially interacting labelled proteins resulting in a decrease in TR-FRET.

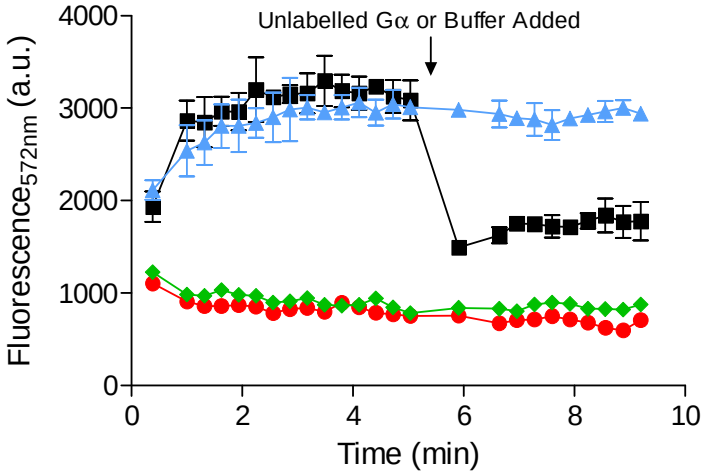

Figure 2.6: Unlabelled $G\alpha_{i1}$ competes with $G\alpha_{i1}$:Tb for binding to CrV2:Alexa. 10 nM $G\alpha_{i1}$:Tb was mixed with 20 nM CrV2:Alexa in 100 µL of TMN buffer. At 5 min, 2 µM of unlabelled $G\alpha_{i1}$ (■) or an equivalent volume of TMN buffer (▲) was added and TR-FRET measurements continued with the following parameters: λ_{ex} 340 nm, λ_{em} 572 nm, 50 µs delay and 900 µs counting duration over the shown time period. Background of 10 nM $G\alpha_{i1}$:Tb (●) and 10 nM $G\alpha_{i1}$:Tb + 2 µM unlabelled $G\alpha_{i1}$ (◆) are shown. Data shown are mean (n=2).

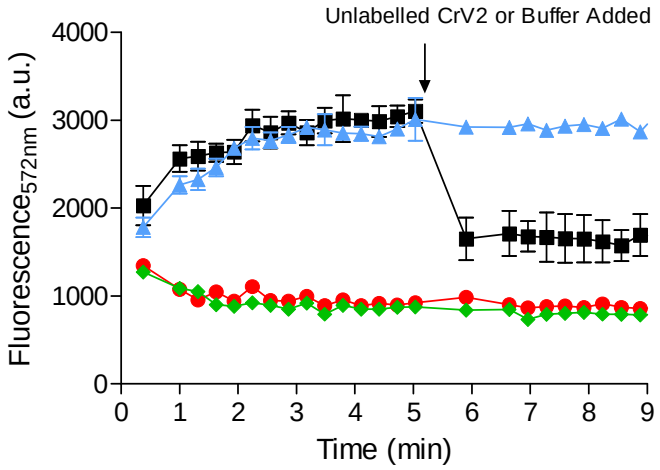

Figure 2.7: Unlabelled CrV2 competes with CrV2:Alexa for binding to $G\alpha_{i1}$:Tb. 10 nM $G\alpha_{i1}$:Tb was mixed with 20 nM CrV2:Alexa in 100 µL of TMN buffer. At 5 min, 70 nM of unlabelled CrV2 (■) or an equivalent volume of TMN buffer (▲) was added and TR-FRET measurements continued with the following parameters: λ_{ex} 340 nm, λ_{em} 572 nm, 50 µs delay and 900 µs counting duration over the shown time period. Background of $G\alpha_{i1}$:Tb (●) and $G\alpha_{i1}$:Tb + unlabelled CrV2 (◆) are shown. Data shown are mean (n=2).

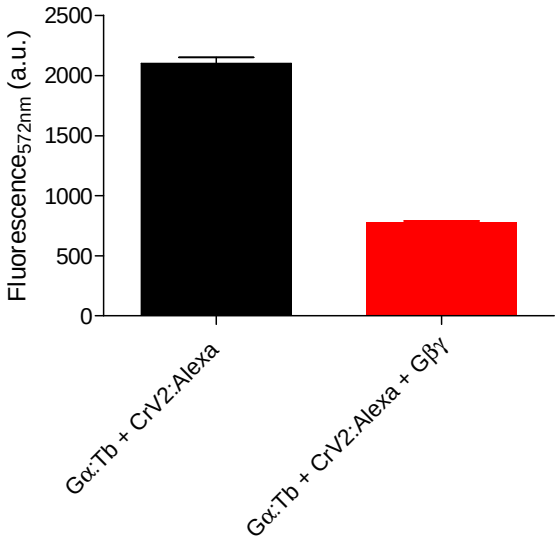

Figure 2.8: $G\beta_4\gamma_2$ inhibits CrV2:Alexa association with $G\alpha_{i1}$:Tb. 10 nM $G\alpha_{i1}$:Tb was mixed with 20 nM CrV2:Alexa with or without 240 nM $G\beta_4\gamma_2$ in 100 µL of TMN buffer. TR-FRET measurements were taken with the following parameters: λ_{ex} 340 nm, λ_{em} 572 nm, 50 µs delay and 900 µs counting duration. Backgrounds of $G\alpha_{i1}$:Tb and $G\alpha_{i1}$:Tb + $G\beta_4\gamma_2$ have been deducted as appropriate. Data shown are mean (n=2).

Interestingly, Gβγ appeared to compete with CrV2 for binding to $G\alpha_{i1}$ and this could suggest that these proteins have overlapping binding sites on the $G\alpha_{i1}$ subunit or otherwise disrupt the binding of the other. To gain an insight into whether the reduction in TR-FRET could be occurring through CrV2 associating with Gβγ, CrV2:Alexa was mixed with Gβγ labelled with terbium (Gβγ:Tb). This failed to produce a substantial TR-FRET signal compared to that generated by CrV2 and $G\alpha_{i1}$ or by $G\alpha_{i1}$ and Gβγ (**Figure 2.9**). Although labelling of the Gβγ subunits with terbium may be of a different efficiency to Gα, the similar level of background terbium luminescence suggested that the amount of terbium present was not significantly less and did not result in the lack of TR-FRET signal. This was further established by the strong TR-FRET signal gained from the interaction of Gβγ:Tb with $G\alpha_{i1}$:Alexa.

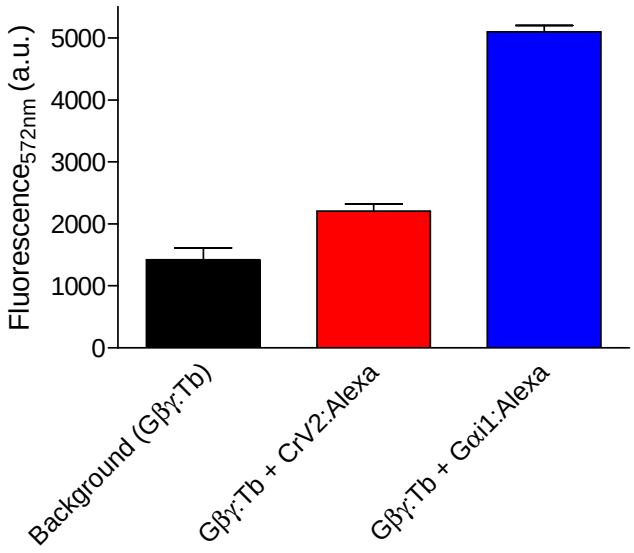

Figure 2.9: CrV2:Alexa interacts minimally with Gβγ:Tb. 10 nM Gβγ:Tb was mixed with 20 nM CrV2:Alexa or 10 nM $G\alpha_{i1}$:Alexa to a final volume of 100 µL with TMN buffer. TR-FRET measurements were taken with the following parameters: λ_{ex} 340 nm, λ_{em} 572 nm, 50 µs delay and 900 µs counting duration after a 10 min incubation period. Data shown are mean (n=2).

Furthermore, the activation state of the Gα subunit appeared to be important in modulating the interaction with CrV2. The addition of excess GDP or GTPγS (not shown) produced similar association curves over time, while the presence of aluminium fluoride (AlF_4^-) (achieved by adding 10 mM NaF and 30 µM $AlCl_3$) appeared to decrease the maximum fluorescence achieved (**Figure 2.10**). This is similar to the association of Gα with Gβγ whereby aluminium fluoride causes dissociation of the subunits and a decrease in TR-FRET signal and is in contrast to RGS4 where an increase in the TR-FRET signal with Gα is achieved (Leifert *et al*. 2006). The decrease in signal in the presence of aluminium fluoride generated by the interaction of Gα with CrV2 could be a result of the inability of CrV2 to bind to Gα subunits in the transition state or a conformational change resulting in the donor and acceptor labels being moved further apart decreasing FRET efficiency. The fact that aluminium fluoride does not return the signal to the background level could indicate that conformational change or a decrease in affinity is occurring. However, results from the purification of G-protein subunits demonstrates that aluminium fluoride does cause the Gα and Gβγ subunits to dissociate although in the TR-FRET assay, aluminium fluoride does not

return the signal to the background level probably due to a new equilibrium being established between labelled binding partners. Furthermore, the purification often shows incomplete dissociation and therefore not all of the Gα subunits may be in the aluminium fluoride-bound transition state. Therefore, it cannot be conclusively stated whether dissociation or a change in conformation is occurring from the TR-FRET data.

To show an interaction between CrV2 and the Gα-subunit, pull down assays using Ni-NTA beads were performed. $G\alpha_{i1}$ was captured using His-tagged CrV2 bound to the Ni-NTA which was detected by SDS-PAGE and western blot (data not shown, experiment conducted by colleague; Kelly Bailey, CSIRO). This method could also be used in the future to confirm the effect of AlF_4^- in possibly dissociating Gα from CrV2. Interestingly, while GTPγS and aluminium fluoride both induce activated conformations of the Gα subunit, in the TR-FRET assay they do not produce similar effects. The results show that GTPγS produces no effect on the TR-FRET signal of interactions between Gα and Gβγ, or CrV2, compared to when GDP is present. Aluminium fluoride however, decreases the TR-FRET signal from Gα interactions with Gβγ and CrV2 while increasing the signal from RGS4 (Leifert *et al*. 2006). Since neither of these conformations induced with GTPγS or aluminium fluoride may occur *in vivo* or be held in Gα subunits for extended periods of time, it is difficult to determine if this is of physiological importance although these are potentially useful biochemical tools.

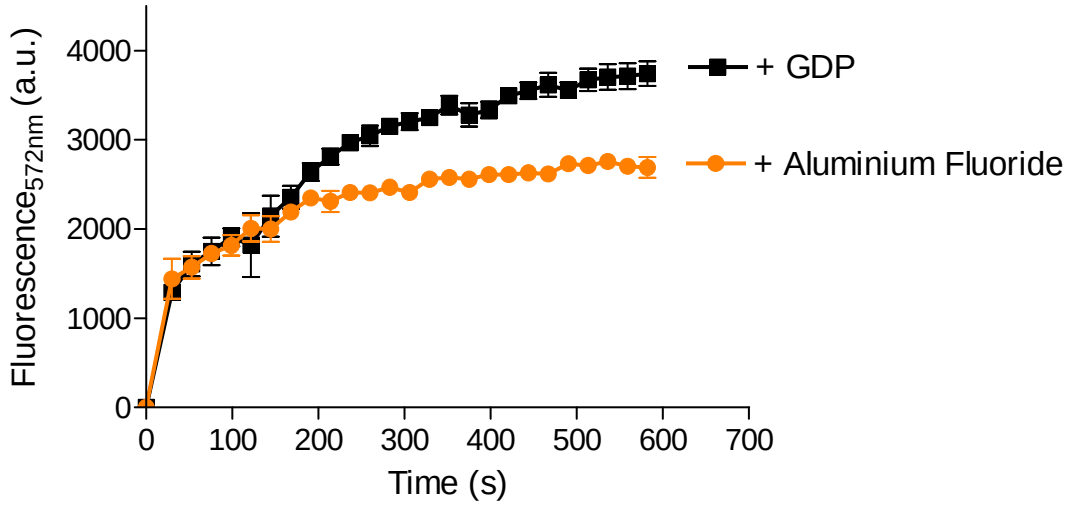

Figure 2.10: Effect of the activation state of $G\alpha_{i1}$ on interacting with CrV2. 10 nM $G\alpha_{i1}$:Tb was mixed with 20 nM CrV2:Alexa with excess amounts of GDP (2.5 µM) or "aluminium fluoride" (produced by the addition of 10 mM NaF and 30 µM $AlCl_3$) for TR-FRET measurements. The following parameters were used: λ_{ex} 340 nm, λ_{em} 572 nm, 50 µs delay and 900 µs counting duration. Background of $G\alpha_{i1}$:Tb with GDP, or aluminium fluoride has been deducted. Data shown are mean ± SEM (n=3).

CrV2 is natively expressed in an invertebrate so it was of interest to see if CrV2 would interact with an invertebrate Gα subunit (since the experiments shown above used a mammalian $G\alpha_{i1}$ from rat). For this purpose, recombinant baculovirus encoding *Drosophila* $G\alpha_o$ was constructed by Dr. Sassan Asgari (University of Queensland) from a *Drosophila* cDNA library. Recombinant *Drosophila* $G\alpha_o$ was successfully purified with a high yield from *Sf*9 cells using Ni-NTA chromatography to exploit the presence of a histidine tag (**Figure 2.11**).

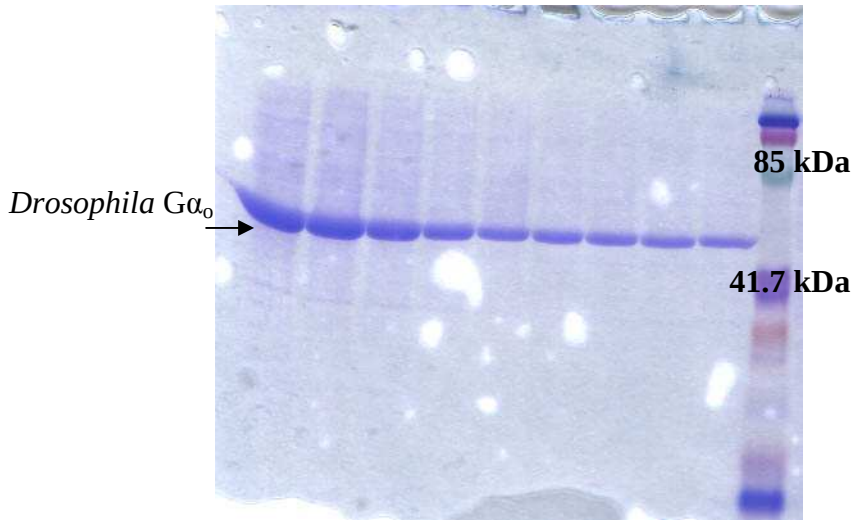

Figure 2.11: Purification of *Drosophila* $G\alpha_o$ from *Sf*9 cells. SDS-PAGE of eluted fractions of His-tagged $G\alpha_o$ from 1.7 L of infected cells purified using Ni-NTA affinity chromatography.

Recombinant *Drosophila* $G\alpha_o$ was shown to bind [^{35}S]GTPγS to a similar level compared with $G\alpha_{i1}$ (**Figure 2.12**). This was in contrast to our previous attempts at purifying a mammalian $G\alpha_o$ protein which was found to bind significantly lower amounts of [^{35}S]GTPγS than $G\alpha_{i1}$ (unpublished data). To our knowledge, the *Drosophila* $G\alpha_o$ subunit has not previously been expressed and purified using *Sf*9 cells. If this subunit was required for more extensive investigations, the functional integrity of the $G\alpha_o$ subunit could be further confirmed both by co-expressing Gβγ subunits to determine if heterotrimer formation can occur, and by reconstituting the $G\alpha_o$ subunit with an appropriate GPCR and Gβγ to determine if GTP binding to $G\alpha_o$ can be stimulated upon agonist activation of the receptor.

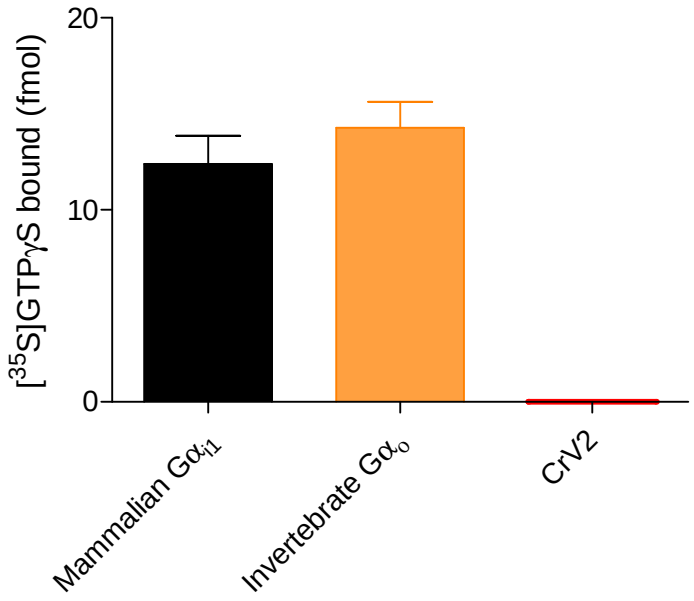

Figure 2.12: Drosophila Gα$_o$ binds to [^{35}S]GTPγS. 40 nM of Gα or CrV2 was mixed with 1 nM [^{35}S]GTPγS in a final volume of 100 µL of TMN buffer and incubated in a shaking water bath for 90 min at 27°C. 25 µL was then filtered through GFC filters and unbound [^{35}S]GTPγS removed by washing with TMN buffer. The amount of bound [^{35}S]GTPγS was then measured by scintillation counting. Data shown are mean ± SEM (n=6) of filter triplicates for 2 experiments.

Our main purpose of purifying Gα$_o$ was to determine if it could compete for binding to CrV2 in TR-FRET assays against mammalian Gα$_{i1}$. The results showed that when increasing concentrations of purified unlabelled Gα-subunits were added to the TR-FRET assay of CrV2 and Gα$_{i1}$, *Drosophila* Gα$_o$ competed for binding to CrV2:Alexa at lower concentrations than unlabelled mammalian Gα$_{i1}$ with an IC$_{50}$ of 41 nM compared to 241 nM (**Figure 2.13**). This indicated *Drosophila* Gα$_o$ had a higher affinity for CrV2 than mammalian Gα$_{i1}$. *Drosophila* Gα$_o$ shares 69.6% amino acid identity with rat Gα$_{i1}$ (**Appendix 8.1**). *Drosophila* Gα$_{i1}$ and rat Gα$_{i1}$ share 77% identity between amino acids and it would be interesting to determine if *Drosophila* Gα$_{i1}$ has a higher affinity for CrV2 than its rat counterpart, however, *Drosophila* Gα$_{i1}$ baculovirus could not be constructed within the timeframe of this study. It would also be of interest to determine what G-protein subunits are expressed in lepidoptera haemocytes. However, this result suggests that there could be physiological importance in the CrV2 interaction with Gα-subunits in insects.

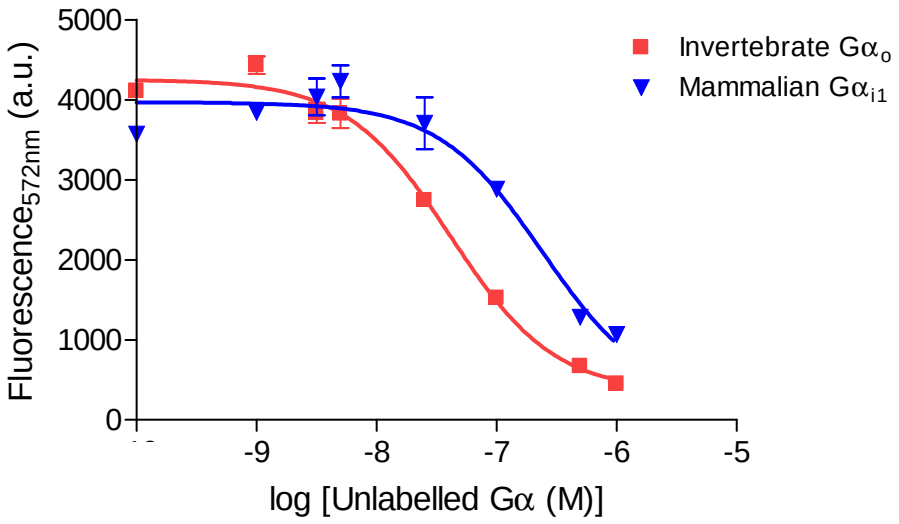

Figure 2.13: CrV2:Alexa binds preferentially to *Drosophila* Gα$_o$. 20 nM CrV2:Alexa was mixed with 20 nM mammalian Gα$_{i1}$:Tb. Doses (0-900 nM) of unlabelled invertebrate (*Drosophila*) Gα$_o$ (■) or mammalian (rat) Gα$_{i1}$ (▼) were then added to compete with labelled proteins. After a 15 min incubation, TR-FRET measurements were taken with the following parameters: λ_{ex} 340 nm, λ_{em} 572 nm, 50 µs delay and 900 µs. Data shown are mean ± SEM (n=3).

To further establish the function of CrV2 in relation to binding Gα-subunits, increasing concentrations of CrV2 were added to Gα$_{i1}$ in the presence of [^{35}S]GTPγS. Gα$_{i1}$ bound [^{35}S]GTPγS to a level that was not significantly affected by the presence of CrV2, which alone did not bind [^{35}S]GTPγS (**Appendix 8.2**). However, a time course of [^{35}S]GTPγS binding would be more appropriate to confirm CrV2 has no effect on the kinetics of [^{35}S]GTPγS binding and any guanine nucleotide exchange factor properties. Studies carried out by a colleague (Genevieve Abbot, CSIRO) also showed that CrV2 did not effect GPCR signalling in a reconstituted system using the α$_{2A}$-adrenergic receptor and Gα$_{i1}$β$_1$γ$_2$ G-protein subunits. CrV2 binding to Gα may only function to compete for a binding site to prevent heterotrimer formation, binding to other regulatory molecules or down stream effectors. However, the binding of CrV2 to the Gα subunit may have effects downstream of G-proteins that cannot be measured in a [^{35}S]GTPγS binding assay. For instance, it would be of interest to investigate the effect of the presence of CrV2 with regard to the activation of downstream effectors such as adenylyl cyclase.

2.4. Further discussion and conclusions

We have now widely exploited the use of the CS124-DTPA-EMCH:Tb donor and Alexa546 acceptor fluor pair for TR-FRET studies of protein interactions. Previously, the interaction between Gα and Gβγ had been characterized as well as that of RGS4 with Gα and now a novel interaction between Gα and CrV2 has been proposed. It has been demonstrated that CrV2 appears to bind to Gα subunits and this interaction can be modulated by aluminium fluoride, which changes the conformation of the Gα subunit. It also appears that the binding site of CrV2 could overlap with that of Gβγ since Gβγ can compete with CrV2 for binding to Gα. This may also in part explain the effect of aluminium fluoride in decreasing the interaction between CrV2 and Gα since it changes the conformation of Gα in switch regions known to be important for Gβγ binding (Wall, Posner & Sprang 1998).

However, the significance of the interaction between CrV2 and Gα subunits requires further investigation. While preliminary experiments have not shown any effects of CrV2 with regard to maximal GTP binding or GPCR signalling, studies directed at the effects on GTPase activity or other interactions of the Gα subunit such as with other modulators or downstream effectors could prove informative. Furthermore, 4 putative N- and 6 putative O-glycosylation sites have also been predicted on CrV2 (Glatz, Schmidt & Asgari 2004), thus a more appropriate expression system for CrV2 may be in insect cells such as *Sf*9 cells where these modifications can take place in an environment which more closely represents that in which CrV2 in its native state is expressed. The lack of these modifications may have an effect on the function of CrV2 and warrants further investigation as does the origin and significance of the truncated CrV2 peptides. The mechanism of CrV2 binding could also be further probed by generating mutants and this may also further validate the TR-FRET assay system used.

Most work on GPCRs, G-proteins and their associated signal transduction pathways have been conducted in vertebrates. However, Gα subunits have been identified in a number of invertebrates including the dipteran species, *Drosophila melanogaster*, *Anopheles gambiae* and lepidopteran species such as the tobacco hornworm, silkworm and cabbage moth (Knight, Grigliatti 2004). Therefore, the lepidopteran host species in which CrV2 is naturally expressed, *Pieris rapae* (cabbage white butterfly) would also express Gα-subunits with which CrV2 could interact. There are also other examples of proteins from invertebrates that interact with G-proteins to modulate immune responses. Tachyplesin is a major granular component of haemocytes of the horseshoe crab and is an antimicrobial peptide with broad spectrum activity against both Gram positive and negative bacteria (Nakamura *et al*. 1988). Moreover, tachyplesin has been found to induce haemocyte exocytosis in a positive feedback mechanism to amplify the immune response to an infection and has been found to interact directly with a bovine G-protein with a *K*d of 0.88 μM using surface plasmon resonance (Kurata, Ariki & Kawabata 2006; Ozaki, Ariki & Kawabata 2005). Tachyplesin shares a number of structural similarities with a wasp venom protein, mastoparan, that has also been found to regulate immune responses by inducing exocytosis of substances from mammalian cells such as histamine from rat mast cells, serotonin from platelets, catecholamines from chromaffin cells and prolactin from the anterior pituitary (Higashijima *et al*. 1988). Mastoparan has been shown to directly interact with bovine G-proteins with a *K*d of 220 nM using surface plasmon resonance (Ozaki, Ariki & Kawabata 2005) and has also been shown to increase the GTPase activity and rate of nucleotide exchange to purified bovine $G\alpha_o$ independently of a GPCR by mimicking an agonist bound GPCR (Higashijima *et al*. 1988). However, these are small peptides, tachyplesin is 17 residues in length (Nakamura *et al*. 1988) and mastoparan 14 residues (Higashijima *et al*. 1988). CrV2 is a larger protein of 319 amino acids (including signal sequence), although there is some evidence that processing of the larger protein may occur. CrV2 is thought to be involved with the suppression of a host immune system.

G-protein interactors such as tachyplesin, have been shown to increase immune responses through a G-protein mediated pathway and the CrV2 interaction with Gα subunits proposed in this study could indicate that the virally expressed CrV2 that is taken up by host haemocytes could function to suppress immune responses through what could be a similar G-protein pathway. Exocytotic responses that release defence-related molecules from the intracellular stores of haemocytes are an important part of the immune response of invertebrates to the detection of pathogens that results in their encapsulation (Raftos, Fabbro & Nair 2004) and the induced release of these molecules has been shown to be mediated by G-proteins in the invertebrate *Styela plicata* (Raftos, Fabbro & Nair 2004). Exocytosis has also been shown to be regulated, particularly by Gβγ subunits, in mammalian cells (Blackmer *et al*. 2005, Pinxteren *et al*. 1998, Zhang, Yasrebi-Nejad & Lang 1998) and also by G_i and G_o (Lang *et al*. 1995). Therefore, it could be proposed that binding of CrV2 to Gα subunits could function to regulate exocytosis to suppress immune responses. *Pieris rapae* is of commercial interest since it is a world-wide pest of cruciferous crops that is endemic to Europe and Northern Asia and has spread to regions including the USA and Australia. *Cotesia rubecula* was introduced into Australia in the 1940's as a biological control agent targeting *P. rapae*. The genes or gene products encoded by the *Cotesia rubecula* bracovirus such as CrV2 could be useful in understanding the molecular mechanisms in invertebrate immunology and in designing effective, environmentally safe control agents for pests.

The use of the terbium chelate CS124-DTPA-EMCH:Tb and Alexa546 fluor pair was advantageous in generating a good signal:noise ratio. This is due in part to the excitation of the donor not resulting in direct excitation of the acceptor due to the large Stokes shift of terbium (this is often a complicating factor in many FRET studies). Time-gating also functioned to eliminate most background fluorescence. Improvements, such as the removal of unlabelled proteins, could further increase the signal and produce less variability between preparations of proteins. Studies

that use the green fluorescent protein variants, cyan fluorescent protein (CFP) and yellow fluorescent protein (YFP) for FRET studies, often present their data as fluorescence ratios due to only slight changes in donor and acceptor emissions. The ratio functions to amplify the signal by taking into account the change in both the acceptor and donor emission. In general, this data manipulation was not required due to improved signal resolution although it could be integrated if required. This method has potential for application in high throughput screening for novel therapeutics. Unfortunately, during the course of this study the supply of the terbium chelate, CS124-DTPA-EMCH:Tb was discontinued by Invitrogen, the sole world-wide distributor. Some of the disadvantages of this particular assay system are that when the terbium chelate was available, it was very expensive partly due to the difficulty in its synthesis. This coupled with the inconsistencies in labelling proteins and the non-specific nature of labelling available cysteine residues leaves room for improvements to the labelling strategy. This led to the investigation of using fusion tags such as lanthanide binding tags and tetracysteine motifs for donor and acceptor labelling, respectively, while maintaining the advantages of the TR-FRET platform.

3. Constructing Lanthanide Binding Tag (LBT) Fusion Proteins and Labelling with Terbium

Schematic representation of a lanthanide binding tag bound to terbium which is being excited via a tryptophan residue
Figure by Ezra Peisach of Karen Allen's group at Boston University and obtained from http://web.mit.edu/imperiali/LBTs.html

3.1. Introduction

As discussed earlier, terbium offers unique luminescent properties that can be exploited in biochemical studies by labelling proteins with terbium. Terbium ions are only weakly luminescent in aqueous solutions due to a low extinction coefficient and significant quenching by water molecules. For these reasons, chelating agents are required for lanthanide ions to improve quantum yields and emission lifetimes (Parker, Williams 1996). Since direct excitation results in weak emissions, the chelate will contain an "antenna" moiety which will absorb light at a suitable wavelength and then transfer its energy to excite the nearby lanthanide (Parker, Williams 1996). Commonly used chelates such as diethylenetriaminepentaacetic acid (DTPA) attached to carbostyril 124 (CS124) as the antenna (Li, Selvin 1997) also contain functional groups so they can be chemically conjugated to reactive amino acids after purification of the desired protein. The utility of this labelling method has been shown in characterizing the interaction between G-protein subunits, with RGS4 and here with CrV2. However, this method provides only a limited amount of control over the placement of fluorescent labels since often more than one reactive amino acid will be present and variation between protein preparations often occurs with increased or decreased amounts of labelling and a heterogeneously labelled protein population.

Lanthanide binding tags (LBTs) were developed from a combinatorial library of peptides based on the EF-hand motif of calmodulin and the peptides were tested for terbium binding indicated by an increase in luminescence (Nitz *et al*. 2003). Optimal peptide sequences for terbium luminescence were found to contain a tryptophan at position 7 as well as other tyrosine residues because the emission spectra of these aromatic amino acids overlaps with the excitation spectra of terbium, sensitizing terbium for better luminescence emissions. Aspartic acid and glutamic acid residues are used to coordinate the terbium ion, and other hydrophobic residues are present to aid in shielding the terbium ion from the quenching effects of water. The best peptide sequences were

short, 17 amino acids in length and had nanomolar affinities for terbium (Nitz *et al*. 2003). The LBT invention has been patented (US patent 7101667) with claims to application in the areas of x-ray crystallography due to the powerful scattering properties of terbium, NMR spectroscopy and imaging to exploit the paramagnetic properties of lanthanides as well as fluorescent imaging technologies.

This chapter characterizes properties of the lanthanide binding tag, LBT2, and investigates the feasibility of fusing LBTs onto G-protein subunits, characterizing the terbium binding properties of the fusion proteins and their ability to remain functional in receiving signals from GPCRs. The process involved with this is outlined in **Figure 3.1**. During the course of this study, five LBT constructs were generated and used to produce recombinant baculoviruses although only three will be discussed in detail. Each construct was ultimately expressed in *Sf*9 cells and purification attempted. The integrity of the tagged G-protein subunits were then assessed with regard to the ability to reconstitute a functionally active complex with a GPCR in [^{35}S]GTPγS signalling assays. The integrity of the fused LBT was also assessed with regard to affinity for terbium and luminescent emissions.

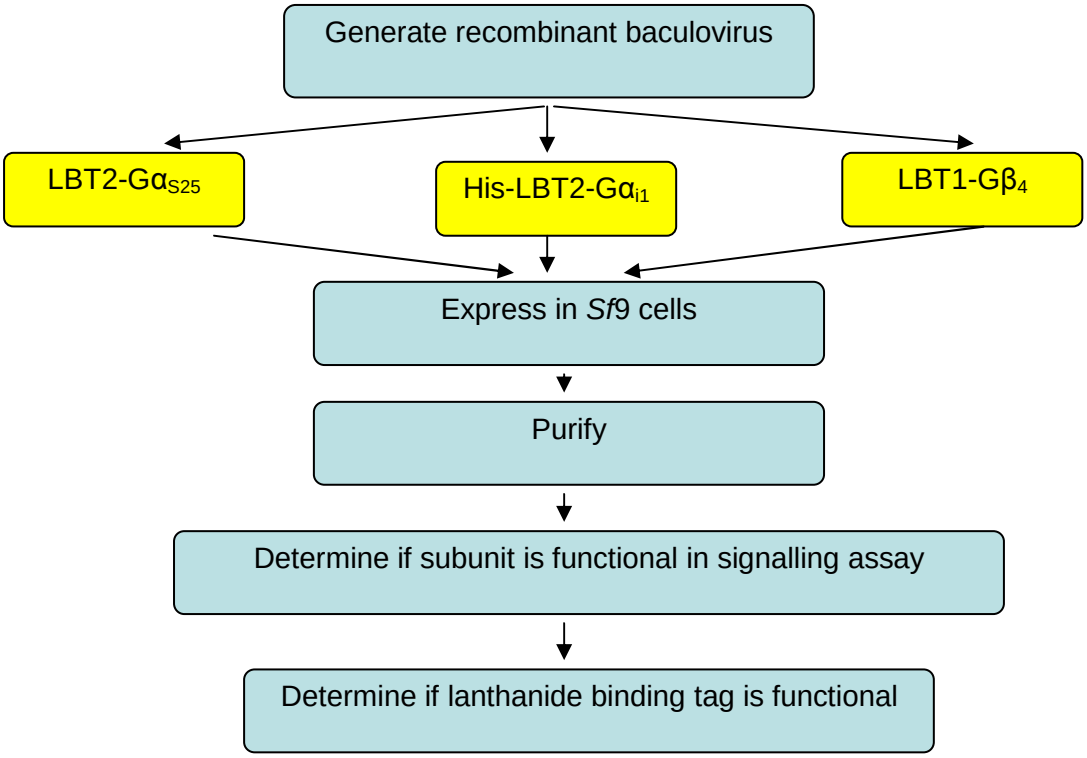

Figure 3.1: Brief experimental procedure for expression and characterization of lanthanide binding tag-G-protein fusion constructs.

3.2. Methods

All chemicals and reagents were of analytical grade and purchased from Sigma Aldrich unless otherwise stated. All primers were synthesized by Geneworks (Hindmarsh, SA, Australia) and restriction enzymes were purchased from New England Biolabs. All buffers were made in milli-Q water.

3.2.1. Lanthanide binding tag (LBT2) peptide assays

The LBT2 peptide was synthesized by Auspep (Parkville, VIC, Australia) with an amino acid sequence of Ala-Cys-Val-Asp-Trp-Asn-Asn-Asp-Gly-Trp-Tyr-Glu-Gly-Asp-Glu-Cys-Ala. The peptide was highly hydrophobic requiring dimethyl sulfoxide (DMSO) for solubilisation in a stock concentration of 1 mM. Assays for terbium binding were conducted in Tb binding buffer (20 mM NaHEPES, 100 mM NaCl, pH 7.0) and dilutions of all stocks were made in this buffer. To generate terbium binding curves, a 100 mM terbium chloride hexahydrate stock solution was made in 1 mM HCl. This stock solution was further diluted into buffer to a concentration 2x that in the assay as required. The LBT2 peptide was diluted to a 20 nM working solution in buffer. Assays were carried out in black 96-well plates with 50 µL of the LBT2 working solution added to appropriate wells followed by the addition of 50 µL of the desired terbium chloride concentration, to make the final assay volume 100 µL. The plate was then shaken at 500 rpm at room temperature for 15 min. A Victor3 multilabel plate counter (Perkin Elmer) fitted with a 1500 V Xenon Flash light source was then used to conduct time-resolved fluorescence measurements using the following instrument settings: excitation at 280 nm, emission at 545 nm, 50 µs delay and 900 µs counting duration.

Stocks of 2 mM gadolinium chloride were made in 1 mM HCl. Gadolinium competition assays were conducted by adding 5 µL of the required gadolinium chloride solution (which was 20x the

final concentration in the assay), 5 µL of a 100 nM working solution of terbium chloride and 5 µL of LBT2 at a working concentration of 200 nM. The final assay volume was taken up to 100 µL with the addition of 85 µL of Tb binding buffer. Plates were shaken at 500 rpm at room temperature for 15 min. In a similar manner, the pH conditions of the assay were varied using Tb binding buffer adjusted to the indicated pH values. Ion concentrations were varied by the addition of 5 µL of 20x stocks being added to wells, and the amount of buffer adjusted so that the final volume remained at 100 µL. Time-resolved measurements were then taken under the same conditions used to determine the terbium binding curve.

3.2.2. Generation of excitation and emission spectra

Excitation and emission scans were conducted on a Cary Eclipse fluorescence spectrophotometer (Varian). A 1 cm path-length quartz cuvette containing 500 µL of 20 µM LBT2 peptide and 2 mM $TbCl_3$ was read in phosphorescence mode using a 100 µs delay and 1 ms count time.

3.2.3. Chimeric Gα / lanthanide binding tag fusion gene construction

The three chimeric Gα subunits $G\alpha_{S25}$, $G\alpha_{Z44}$, and $G\alpha_{Z25}$ were cloned in frame with LBT1 (Tyr-Ile-Asp-Thr-Asn-Asn-Asp-Gly-Trp-Tyr-Glu-Gly-Asp-Glu-Leu-Leu-Ala) or LBT2 (Ala-Cys-Val-Asp-Trp-Asn-Asn-Asp-Gly-Trp-Tyr-Glu-Gly-Asp-Glu-Cys-Ala) coding sequences using PCR such that the LBTs would be attached to the N-terminus of the fusion protein. Template cDNA was generously obtained from Dr. Young-Hou Wong (Hong Kong University of Science and Technology) and recombinant baculoviruses of $G\alpha_{S25}$, $G\alpha_{Z25}$, and $G\alpha_{Z44}$ were constructed by Dr. Richard Glatz (SARDI, formerly CSIRO). Fusions were made using forward primers that encoded the lanthanide binding tag as well as an appropriate restriction enzyme site (*Kpn*I) and the start of the chimeric Gα subunit sequence. All primers were synthesized by Geneworks and the primer sequences were 5' GGT ACC TAT ATT GAT ACT AAT AAT GAC GGT TGG TAC GAA GGT GAC GAA

CTT CTT GCT ATG GCC CGC TCG CTG ACC 3' and 5' GGT ACC GCT TGT GTT GAC TGG AAT AAT GAC GGT TGG TAC GAA GGT GAC GAA TGT GCT ATG GCC CGC TCG CTG ACC 3' to fuse LBT1 and LBT2 to the chimeric Gα subunit, respectively. These were paired with appropriate reverse primers for the chimera to generate a PCR product that encoded the entire fusion protein. The reverse primer for $G\alpha_{S25}$ was 5' GCG CAA GCT TTT AGA GCA GCT CGT ATT GG 3' and the reverse primer sequence for $G\alpha_{Z44}$ and $G\alpha_{Z25}$ was 5' GCG CAA GCT TTC AGC AAA GGC CAA TGT AC 3'. PCR reactions were comprised of the following reagents.

Reagent	volume (µL) (1 reaction)
template	1
10 mM dNTPs (New England Biolabs)	0.7
25 mM $MgCl_2$ (Bioline)	1.5
10X Taq buffer (Bioline)	2.5
0.1 mg/mL forward primer	1.0
0.1 mg/mL reverse primer	0.5
Taq Polymerase (Bioline)	0.15
Sterile water	18.35

Reactions were then placed in a Corbett Research cooled/gradient palm-cycler™ under the following cycling protocol.

initial denaturation	95ºC for 5 min	1 cycle
denature annealing extension	95ºC for 30 s 60ºC for 30 s 72ºC for 90 s	30 cycles
final extension	72ºC for 5 min	1 cycle
cooling	4ºC indefinite	1 cycle

The resulting PCR products were ligated into the vector pGEM®-T Easy (Promega) according to the manufacturer's direction. Competent DH5α *E. coli* (Invitrogen) were transformed with the recombinant vector by heat shock, and recombinant *E. coli* were selected using 100 µg/mL ampicillin and checked by PCR using M13 forward (5' GTT TTC CCA GTC ACG AC 3') and M13 reverse (5' CAG GAA ACA GCT ATG AC 3') primers. Recombinant plasmid was then purified from *E. coli* using a Genelute mini or midi prep kit (Sigma Aldrich) according to the manufacturer's

instructions and digested using *Kpn*I and *Hind*III. Digested plasmid fragments were separated by gel electrophoresis on a 1% (w/v) agarose gel and visualized by ethidium bromide or Gelgreen™ (Biotium) staining. The inserted fragment of ~1200 bp was purified from the gel using an Ultraclean® gel spin DNA purification kit (Mo Bio Laboratories Inc.) according to the manufacturer's directions. This fragment was then ligated into the pQE30 vector (Invitrogen) and then the N-terminally His-tagged construct subcloned into the pFastBac™1 vector (Invitrogen) using the *EcoR*I restriction enzyme site upstream of the start codon and His-tag, and the *Hind*III restriction enzyme site. Recombinant baculovirus was subsequently generated from recombinant pFastBac™1 (refer to section 3.2.14).

3.2.4. Construction of the His-LBT2-$G\alpha_{i1}$ fusion gene

While the same strategy was initially employed for N-terminally tagged $G\alpha_{i1}$ fusion proteins as for the chimeric Gα subunits, this was found to be problematic due to secondary structures forming in the long forward primer. Therefore, a series of three overlapping primers encoding LBT2 were used with $G\alpha_{i1}$ template DNA obtained from recombinant baculovirus generously obtained from Prof. Richard Neubig (University of Michigan). Firstly, forward primer one 5' GG TGAC GAA TGT GCT ATG GGC TGC ACA CTG AGC GC 3' was used to generate a PCR product which was then used as the template for the next PCR using forward primer two 5' GGA ATA ATG ACG GTT GGT ACG AAG GTG ACG AAT GTG C 3'. This PCR product was then used as the template for the final PCR using forward primer three 5' GGT ACC GCT TGT GTT GAC TGG AAT AAT GAC GG 3'. In this way the lanthanide binding tag was gradually added until the full LBT2-$G\alpha_{i1}$ gene had been constructed. These three PCRs used the reverse primer 5' GC AAG CTT TTA GAA GAG ACC ACA GTC TTT TAG 3'. The final PCR product was then ligated into pGEM®-T Easy (Promega), subcloned into the pQE30 vector (Invitrogen) using *Kpn*I and *Hind*III restriction enzyme sites. The N-terminally His-tagged construct was then inserted into the pFastBac™1

vector (Invitrogen) using *EcoR*I and *Hind*III restriction enzyme sites for the construction of a recombinant baculovirus.

3.2.5. Construction of LBT1-Gβ$_4$

Lanthanide binding tag, LBT1, was fused to the 5' end of the Gβ$_4$ subunit coding sequence by PCR using a forward primer containing the LBT and a *Kpn*I restriction enzyme site (5' GGT ACC ATG TAT ATT GAT ACT AAT AAT GAC GGT TGG TAC GAA GGT GAC GAA CTT CTT GCT ATG AGC GAG CTG GAG CAG 3') with a reverse primer containing a *Hind*III restriction enzyme site (5' GC AAG CTT TCA ATT CCA GAT TCT AAG AAA AC 3'). The template Gβ$_4$ DNA was generously obtained from Prof. James Garrison (University of Virginia) as recombinant baculoviurs. As described earlier, PCR products were purified from a 1% agarose gel and ligated into pGEM®-T Easy (Promega) then subcloned into pFastbac™1 (Invitrogen) for subsequent generation of a recombinant baculovirus.

3.2.6. Construction of a LBT2:pQE30 vector and a LBT2:pFB1 vector

Construction of this vector was designed by Dr. Richard Glatz (SARDI, formerly CSIRO). Complimentary oligonucleotides synthesized with 5' phosphates (5' GCA TGC CTC GAG GCT TGT GTT GAC TGG AAT AAT GAC GGT TGG TAC GAA GGT GAC GAA TGT GCT TAG A 3' and 5' A CTA AGC ACA TTC GTC ACC TTC GTA CCA ACC GTC ATT ATT CCA GTC AAC ACA AGC CTC GAG GCA TGC 3') that encoded LBT2 were designed such that *Sph*1 and *Xho*1 restriction enzyme sites were positioned 3' to LBT2. A-overhangs were also included so that once the oligonucleotides had been annealed together, they were ligated into the vector pQE30-UA (Qiagen). DH5α *E. coli* were transformed and transformants selected using 100 µg/mL ampicillin. PCR was used to confirm the presence of a recombinant vector and sequencing of the subsequently purified plasmid used to confirm that the oligonucleotides had annealed correctly and been successfully ligated into the plasmid. LBT2:pQE30 was then digested using *Eco*R1 and

*Hind*III which excised the start codon, the His-tag, LBT2 and the multiple cloning site containing LBT2 of pQE30-UA. This fragment was then ligated into pFastBac™1 to generate LBT2:pFastBac1, which was confirmed by sequencing and is shown as per **Figure 3.2**.

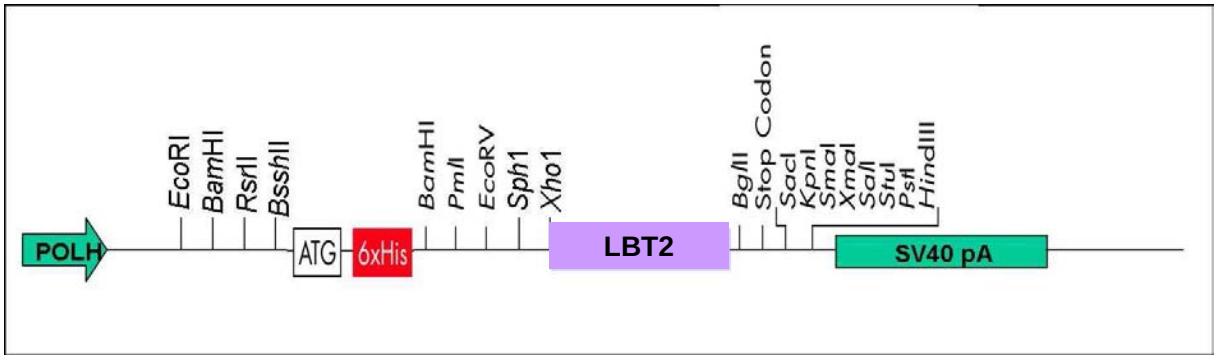

Figure 3.2: Multiple cloning site of the LBT2:pFastBac1 vector. pFastBac™1 flanks the *Eco*R1 and *Hind*III restriction enzyme sites and the sequence between these sites originates from recombinant pQE30-UA.

3.2.7. Construction of $G\alpha_{i1}$-LBT2

$G\alpha_{i1}$ with LBT2 fused to the C-terminus ($G\alpha_{i1}$-LBT2) was constructed using the LBT2:pFastBac1 vector. $G\alpha_{i1}$ was amplified with *Bam*HI and *Xho*I restriction enzyme sites on the forward and reverse primers, respectively. The forward primer also contained a start codon and had the sequence 5' G CGC GGA TCC ATG GGC TGC ACG CTG AGC GC 3' while the reverse primer was 5' GCGC CTC GAG GAA GAG ACC ACA ATC TTT TAG 3' and contained no stop codon. The PCR product was ligated into pGEM®-T Easy (Promega) and then subcloned into LBT2:pFB1. $G\alpha_{i1}$-LBT2 baculovirus was subsequently generated.

3.2.8. Construction of $G\gamma_2$-LBT2

To construct $G\gamma_2$ with LBT2 fused to the C-terminus ($G\gamma_2$-LBT2), $G\gamma_2$ was amplified using the forward and reverse PCR primers 5' GC GCA TGC ATG GCC AGC AAC AAC ACC 3' and 5' GC CTC GAG AAG GAT GGC GCA GAA GAA C 3', respectively. These primers introduced *Sph*I and *Xho*I restriction enzyme sites to 5' and 3' ends of $G\gamma_2$, respectively, which were used to ligate the digested PCR product into LBT2:pFastBac1 from which recombinant baculovirus was produced.

3.2.9. Restriction enzyme digests

All restriction enzymes were purchased from New England Biolabs. The required DNA was digested by mixing with the appropriate enzymes and buffer according to the manufacturer's guidelines and then incubating the samples at 37ºC for 2-15 hrs. Digested DNA was then run on a 1% agarose gel, stained and fragments visualized under UV light. The appropriate digested fragment was then purified from the gel using the Ultraclean® gel spin DNA purification kit (Mo Bio Laboratories Inc) according to the manufacturer's instructions. If required, the DNA was concentrated by precipitating the DNA by the addition of 0.2 M NaCl and a 2x volume of ethanol. The DNA was then pelleted by microcentrifuge at 14 000 xg for 10 min before being washed with 70% (v/v) ethanol and subsequently dried. The DNA was then resuspended to the desired concentration in sterile water.

3.2.10. DNA gel electrophoresis

DNA was separated on 1% (w/v) agarose gels. Agarose was melted in TAE buffer (2 M Tris, 1 M acetic acid, 0.05 M EDTA, pH 7.6-7.8) using a microwave before casting. 5x loading dye (0.1% (w/v) bromophenol blue and 30% (v/v) glycerol) was added to samples before loading. 1 kb or 100 kb molecular weight markers (New England biolabs) were included as appropriate, and the gel was then run in TAE buffer at 120 V until the dye front had travelled the required distance. Gels were then stained with ethidium bromide or alternatively, Gelgreen™ (Biotium) was incorporated into the gel so that DNA could be visualized under UV light.

3.2.11. Ligation reactions

Fusion genes were ligated into the appropriate vectors by mixing DNA at an approximate 3:1 ratio of fragment:vector, 1 µl T4 DNA ligase (New England Biolabs) and ligase buffer was added according to the manufacturer's recommendation. Reactions were incubated at room temperature for 20 min or 4ºC overnight.

3.2.12. Preparation of competent *E. coli* and heat shock transformation

The required bacterial strain was cultured overnight with appropriate antibiotics in 5 mL Luria broth (LB) (10 g/L tryptone, 10 g/L NaCl, 5 g/L yeast extract, pH 7.0) at 37ºC with shaking. The following day, the overnight culture was used to inoculate 100 mL of LB and incubation continued until the OD_{600nm} reached ~0.5. The bacteria were then harvested by centrifugation at 3000 xg for 5 min at 4ºC. The bacterial pellet was then resuspended in 30 mL of transformation buffer 1 (100 mM rubidium chloride, 50 mM manganese chloride, 30 mM potassium acetate, 10 mM calcium chloride and 15% (v/v) glycerol). Centrifugation was then repeated. 4 mL of transformation buffer 2 (10 mM rubidium chloride, 10 mM MOPS, 75 mM calcium chloride and 15% (v/v) glycerol) was then added to the cell pellet. Resuspended bacteria were then separated into 100 µL aliquots, snap frozen in liquid nitrogen and stored at -80ºC.

To transform the cells by heat shock, an aliquot of competent cells was thawed on ice. DNA was gently mixed with the cells and incubation on ice continued for 20 min. Bacteria were then heat shocked by incubation at 42ºC for 90 s and placed back on ice for 2 min. 1 mL of LB was added and the bacteria incubated at 37ºC for 1-4 hr depending on the bacterial strain being used. 600 µL of bacteria was then plated onto LB agar (1% (w/v) tryptone, 0.5% (w/v) yeast extract, 1% (w/v) NaCl, 15 g/L agar, pH 7) containing the appropriate antibiotics and other chemicals for blue-white screening to identify successful transformants as indicated. Plates were incubated overnight at 37ºC and then individual colonies chosen for PCR analysis to confirm the presence of the desired insert.

3.2.13. Sequencing

Correct construction of the fusion proteins was confirmed by sequencing using the Big Dye Terminator V3 system (Applied Biosystems). 20 µL reactions were made as follows:

Reagent	volume (µL) (1 reaction)
Template (plasmid)	2-5
Big dye terminator mix	1
Primer (0.02µg/µL)	3
Sterile Water	To final volume of 20µL

Reactions were then placed in a Corbett Research cooled/gradient palm-cycler™ under the following cycling protocol.

initial denaturation	96ºC for 4 min	1 cycle
denature annealing extension	96ºC for 30 s 56ºC for 45 s 60ºC for 4 min	25 cycles
cooling	4ºC indefinite	1 cycle

At the completion of cycling, samples were cleaned by the addition of 80 µL of 75% (v/v) isopropanol, thorough mixing and incubation for 15 min at room temperature. Samples were then centrifuged at 14 000 xg for 20 min in a microcentrifuge and the supernatant was discarded. The pellet was washed with 50 µL of 75% isopropanol followed by a repeat centrifugation step for 5 min. The resulting supernatant was discarded, the pellet dried and stored in darkness until sent for analysis by the Institute of Medical and Veterinary Science (IMVS, Adelaide, SA, Australia). DNA sequences files were analysed using BioEdit Sequence Alignment Editor and compared to sequences contained in GenBank which were accessed via the National Centre for Biotechnology Information website (http://www.ncbi.nlm.nih.gov/).

3.2.14. Generating recombinant baculovirus and transfection of *Sf*9 cells

Recombinant baculoviruses for protein expression in *Sf*9 cells were produced using the Bac-to-Bac® system (Invitrogen). Competent DH10Bac™ *E. coli* (Invitrogen) were transformed with recombinant pFastBac™1 constructs by heat shock. Transformants containing recombinant bacmid were selected for using antibiotics (10 µg/mL tetracycline, 50 µg/mL kanamycin and 7

µg/mL gentamycin) and blue/white screening (40 µg/mL IPTG and 100 µg/mL X-gal) on 1.5% (w/v) LB agar plates (1% tryptone, 0.5% yeast extract, 1% NaCl, 15 g/L agar, pH 7). The presence of recombinant bacmid in white colonies was confirmed by PCR analysis using M13 primers specific for the bacmid and/or the gene of interest. M13 primer sequences were M13 (-40) forward 5' GTT TTC CCA GTC ACG AC 3' and M13 reverse 5' CAG GAA ACA GCT ATG AC 3'. PCR reactions contained the components shown below.

Reagent	Volume (µL) (1 reaction)
Template	1
dNTPs (10mM) NEB	0.7
$MgCl_2$ (25mM) Bioline	1.5
10X Taq buffer Bioline	2.5
forward primer (0.1 mg/mL)	0.5
reverse primer (0.1 mg/mL)	0.5
Taq polymerase (Bioline)	0.15
Sterile water	18.35

PCR products were amplified using the thermocyler protocol shown below.

initial denaturation	95ºC for 5 min	1 cycle
denature annealing extension	95ºC for 30 s 55ºC for 30 s 72ºC for 3.5 min	30 cycles
final extension	72ºC for 5 min	1 cycle
cooling	4ºC indefinite	1 cycle

Recombinant bacmid was identified as having a PCR product greater than 300 bp and these clones were cultured in LB overnight at 37ºC and the recombinant bacmid was purified by the 3-solution method (refer to section 3.2.15).

*Sf*9 cells were transfected with recombinant bacmid using Cellfectin® (Invitrogen). 20 µL of purified recombinant bacmid was added to 2 mL of Sf-900 II SFM medium and then 15 µL of Cellfectin® reagent was added. The mixture was incubated at room temperature for 15 min. 8 mL

of *Sf*9 cells at a density of between 1 and 3 x10^6 cells/mL were centrifuged to pellet the cells that were subsequently resuspended in the Cellfectin® mixture. Cells were then incubated at 27°C with gentle shaking for 5 hrs before being harvested and resuspended in fresh medium at a concentration of 2 x10^6 cells/mL and incubated for a further 72 hrs. Cells were then removed by centrifugation from the supernatant containing infective budded viruses, which was subsequently filter sterilized. The resulting recombinant baculovirus then underwent at least 3 amplification cycles using an MOI of 0.1 to generate a high-titre baculovirus stock that could be used for subsequent infections of *Sf*9 cells for protein production. After each amplification, cells were spun down by centrifugation, the supernatant collected and filtered with FBS added to 2% (v/v). This was then used as inoculum for subsequent amplification cycles or infections. Bacmid isolated from infected cells could be analysed by PCR to confirm the success of transfection.

3.2.15. 3-Solution method for bacmid purification from recombinant DH10Bac™ *E. coli* or *Sf*9 cells

1.5 mL of recombinant bacterial or infected *Sf*9 cell culture was harvested by centrifugation. Media was removed and the cell pellet resuspended in 300 µL of cold solution 1 (15 mM Tris pH 8.0, 10 mM EDTA, 100 µg/mL RNase A). 300 µL of room temperature solution 2 (0.2 M NaOH, 1% (w/v) SDS) was added before gentle mixing by inversion. After a 2-5 minute incubation at room temperature, 300 µL of cold solution 3 (3 M potassium acetate pH 5.5) was added followed by mixing by inversion. A further 10 min incubation on ice followed and then samples were centrifuged for 10 min to pellet the precipitate. The supernatant was then transferred to tubes containing 800 µL of isopropanol. After gentle mixing, this was incubated on ice for 10 min followed by centrifugation to pellet precipitated bacmid DNA. The pellet was then washed with 500 µL of 70% (v/v) ethanol and then allowed to air dry before gentle resuspending in sterile water to avoid DNA shearing. Bacmid preparations were then stored at 4ºC for use in downstream applications such as cell transfection or diagnostic PCR.

3.2.16. Expression and purification of His-tagged proteins from *E. coli*

Protein expression was induced with 1 mM IPTG and His-tagged proteins purified using Ni-NTA chromatography as described in chapter 2.

3.2.17. *Sf*9 cell culture, infection and amplification of baculovirus

Cell culture, infections and amplifications were carried out as previously described in chapter 2.

3.2.18. Terbium staining of SDS-PAGE gels

Polyacrylamide gels (15%) were run as described in chapter 2. Staining with terbium chloride was carried out by washing gels with milli-Q water and then soaking in Tb binding buffer (20 mM NaHEPES, 100 mM NaCl, pH 7.0). Once the gel had equilibriated for 10 min, $TbCl_3$ was added to the desired concentration and the gel stained overnight. Terbium-stained proteins were visualized on a UV transilluminator.

3.2.19. Western Blotting

Samples were firstly subjected to SDS-PAGE (See chapter 2 methods) and once the dye front reached the end of the gel, gels were equilibriated in transfer buffer (25 mM Tris, 190 mM glycine, 20% (v/v) methanol, pH 8.5). Western blotting apparatus (Bio-rad criterion blotter) was assembled according to the manufacturer's instructions so that proteins from the gel would be transferred onto a nitrocellulose membrane (Bio-Rad). The transfer was carried out at 100 V for approximately 1 hr. The membrane was then washed in TBST buffer (8.8 g/L NaCl, 0.2 g/L KCl, 3 g/L Tris, 500 µL/L Tween-20 detergent, pH 7.4) for 5 min and blocked for over 1 hr in 2-3% (w/v) BSA in PBS (0.137 M NaCl, 2.7 mM KCl, 4.3 M Na_2HPO_4 pH 7.2-7.4). His-tagged proteins were detected using monoclonal anti-poly histidine conjugated to alkaline phosphatase (Sigma) at a ratio of 1:5000, allowed to bind overnight. TBST buffer was then used to wash the membrane 3 x 10 min, before being immersed in 20 mL of development buffer (100 mM Tris, 100 mM NaCl, 50

mM $MgCl_2$, pH 9.5). The membrane was developed by the addition of 330 µL of 10 mg/mL nitro-blue tetrazolium chloride (NBT) and 33 µL of 50 mg/mL 5-bromo-4-chloro-3'-indoyphosphate p-toluidine salt (BCIP). Once the desired level of development was achieved, the membrane was washed thoroughly with water to cease staining. Anti-Gα blots were performed by adding the primary rabbit derived anti-Gα antibody (Calbiochem) at a ratio of 1:5000 and incubating overnight. Membranes were then washed 3 x 5 mins in TBST buffer and then incubated with the secondary antibody (anti-rabbit conjugated to alkaline phosphatase) at a ratio of 1:5000 for at least 2 hrs. The membrane was then developed using NBT and BCIP.

3.2.20. Membrane preparation of $G\alpha_{S25}$ chimeras

1 L of *Sf*9 cells were infected with $G\alpha_{S25}$ or LBT2-$G\alpha_{S25}$ baculovirus at an MOI of 2. Infected cells were incubated at 27ºC with gentle shaking for ~ 72 hrs. At each 24 hr period, 1.5 mL samples were taken and cells harvested by centrifugation. The cell pellet was then frozen for time-course western blot analysis. After 72 hrs, the remaining culture was harvested by centrifugation at 1000 xg for 10 min. Cell pellets were then washed in 400 mL of PBS and centrifugation was repeated. Cells were then resuspended in lysis buffer (50 mM NaHEPES, 0.1 mM EDTA, 3 mM $MgCl_2$, 10 mM β-mercaptoethanol, 0.02 mg/mL PMSF, 10 µM GDP, pH 8.0) and lysed by nitrogen cavitation using a pressurization of 500 psi for up to 15 min. The lysate was then centrifuged at 750 xg for 10 min to remove any remaining whole cells and large particles. Samples then underwent centrifugation at 100 000 xg for 30 min. The pellet (membrane fraction) was then resuspended in incubation buffer (250 mM sucrose, 50 mM Tris, 3 mM $MgCl_2$, 10 µM GDP, pH 8.0). Samples were then aliquotted and frozen in liquid nitrogen before storage at -80°C. Total protein concentration was determined by the Bradford assay.

3.2.21. Purification of G-protein subunits

G-protein subunits were purified using Ni-NTA chromatography as described in chapter 2.

3.2.22. Measurement of terbium binding to fusion LBTs

Terbium labelling of LBTs was carried out in black 96-well plates and measured on a Victor3 multilabel plate reader (Perkin Elmer). Samples were excited at a wavelength of 280 nm and the emission at 545 nm was measured after a 50 µs delay for 900 µs. Working solutions (20x) of proteins, $TbCl_3$ and other indicated components were prepared in Tb binding buffer and 5 µL added to the appropriate wells such that mixing did not occur until the addition of Tb binding buffer to make the final assay volume 100 µL.

3.2.23. Receptor preparations

Recombinant baculovirus for human M_2-muscarinic receptors, pig α_{2A}-adrenergic receptors, human H_1-histamine receptors or human β_2-adrenergic receptors were obtained from Dr. Andrejs Krumins and Prof. Alfred Gilman (University of Texas Southwestern Medical Centre, USA), Prof. Richard Neubig (University of Michigan, USA), Prof. Wim deGripp (Nijmegen Centre for Molecular Life Sciences, Switzerland) and Dr. Roger Sunahara (University of Michigan, USA), respectively. Membrane preparations of *Sf*9 cells infected with recombinant baculovirus were used as the source of receptors in subsequent assays and were produced from 1-2 L of infected *Sf*9 cells. Cells were harvested by centrifugation and washed with PBS. Cells were then resuspended in lysis buffer (50 mM NaHEPES pH 8.0, 0.1 mM EDTA pH 8.0, 3 mM $MgCl_2$, 10 mM β-mercaptoethanol, 0.02-0.03 mg/mL PMSF, Benzamidine, Bacitracin, soy bean trypsin inhibitor) and the cells lysed by nitrogen cavitation at 500 psi for 10-15 min. Intact cells and larger debris were then removed by centrifugation at 750 xg for 10 min. High speed centrifugation at 100 000 xg then followed for 30 min at 4°C. The pelleted membrane fraction was then resuspended in 100 mL of incubation buffer (50 mM Tris pH 8.0, 250 mM sucrose, 3 mM $MgCl_2$) containing 7 M urea and stirred on ice for 30 min. 100 mL of cold incubation buffer was then added and the high speed centrifugation step repeated. The pellet was then washed twice in a further 100 mL of cold incubation buffer. The remaining pellet was then resuspended in 15 mL of incubation buffer, the

total protein concentration was determined by the Bradford assay and small aliquots frozen in liquid N_2 and stored at -80ºC until use.

3.2.24. Testing G-protein functionality through receptor signalling in a [^{35}S]GTPγS binding assay

Membrane preparations of chimeric G-proteins (0.05 mg/mL (total protein)) or 20 nM of purified Gα-subunits, expressed in *Sf*9 cells, were reconstituted with 20-40 nM purified Gβγ-subunits. 10 µM Adenosine 5'-(β,γ-imido)triphosphate (AMP-PNP) and 5 µM GDP were then added to the reconstitution mixture followed by the desired receptor membrane preparation (usually 0.1 mg/mL (total protein)). [^{35}S]GTPγS (Perkin Elmer) was then added to the desired concentration followed by the appropriate agonist, with or without an antagonist as indicated. The final volume was 100 µL and dilutions were made in TMND buffer (50 mM Tris pH 7.6, 100 mM NaCl, 10 mM $MgCl_2$, 1 mM DTT). Basal measurements were determined in the absence of agonist. Assay tubes were incubated at 27ºC, shaking in a water bath. After the desired incubation time, triplicate 25 µL samples were filtered through GFC filters (pre-wet with TMN buffer) (Filtech) on a vacuum manifold. Filters were washed with 3 mL of ice-cold TMN buffer three times to remove unbound [^{35}S]GTPγS, before being dried. A Wallac 1410 liquid scintillation counter was then used to determine the amount of [^{35}S]GTPγS bound by adding 4 mL of Ultima Gold™ scintillation cocktail (Perkin Elmer) to filters in pico pro vials (Perkin Elmer) and were counted for 60 s.

3.2.25. Data analysis

Data was analysed using Prism™ 4.00 (GraphPad software Inc., San Diego CA, USA). Data is presented as mean ± SEM where n is equal or greater than 3. If error bars are not visible they are behind the symbols. Apparent *K*d values were generated by fitting a one-site binding curve of the equation Y= Bmax . X / (*K*d + X).

3.3. Results and Discussion

3.3.1. Characterisation of the LBT2 peptide

Terbium binding to the LBT2 peptide synthesized by Auspep could be determined by measuring the fluorescence emitted by terbium at 545 nm, after excitation at 280 nm, using a Victor3 multilabel plate reader (Perkin Elmer). Unbound terbium was not removed since the low excitation efficiency and high degree of quenching of terbium ions in solution was thought to make this unnecessary, and background luminescence for unbound $TbCl_3$ could be measured. Increasing concentrations of terbium chloride ($TbCl_3$) added to 10 nM of LBT2 peptide increased the fluorescence dose dependently to saturation (**Figure 3.3**). The apparent dissociation constant (*K*d) was 9.3 ± 0.5 nM confirming the peptide does have a high affinity for terbium. $TbCl_3$ alone in solution produced a lower amount (5-fold) of luminescence which was not increased by the presence of purified $G\alpha_{i1}$ (**Figure 3.3**) showing the specificity of terbium for LBT2 and the possibility of conducting assays without the removal of unbound $TbCl_3$.

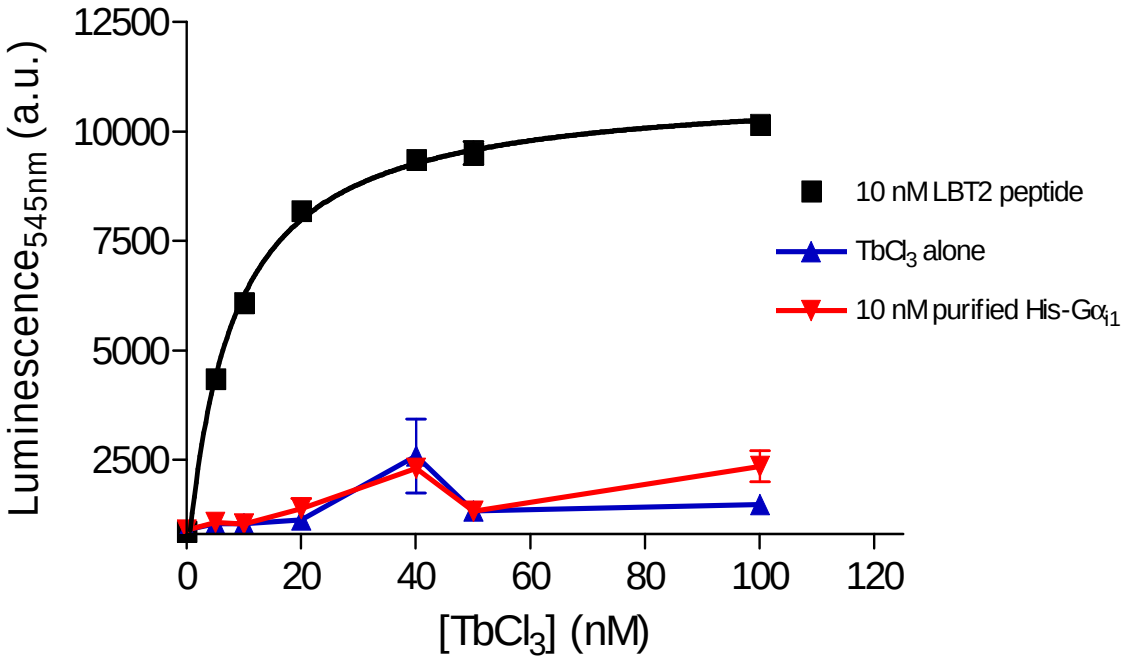

Figure 3.3: Specificity and affinity of terbium for LBT2. 10 nM LBT2 peptide or 10 nM purified His-Gα_{i1} was mixed with the indicated concentrations of $TbCl_3$. The final volume was made up to 100 µL with Tb binding buffer and following a 10 min incubation period, the terbium emission was measured using a Victor3 plate reader set for time-resolved fluorescence with the following parameters: λ_{ex} 280 nm, λ_{em} 545 nm, 50 µs delay and 900 µs counting duration. Data shown are mean ± SEM (n=3).

The addition of gadolinium chloride ($GdCl_3$) was shown to be able to compete with terbium for binding to the LBT as demonstrated by a dose dependent decrease in the luminescence at 545 nm with increasing concentrations of $GdCl_3$ (**Figure 3.4**). $GdCl_3$ was determined to have an inhibitory concentration (IC_{50}) of 24.4 ± 0.1 nM demonstrating that gadolinium also has a high affinity for the LBT. The paramagnetic properties of gadolinium are widely utilized for magnetic resonance imaging and this suggests that LBT:Gd complexes could be used for similar applications.

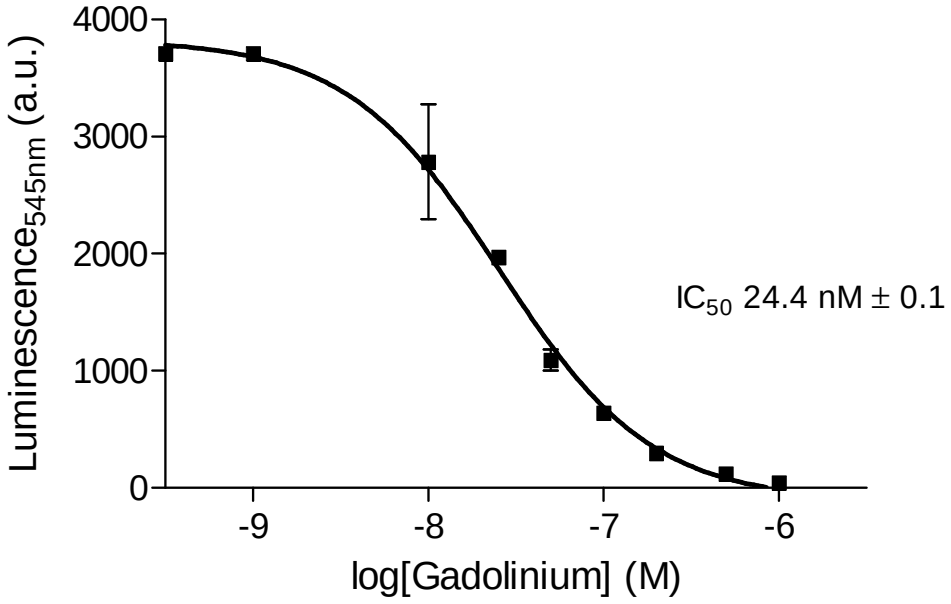

Figure 3.4: Gadolinium competes with terbium for binding to LBT2. An increasing dose of $GdCl_3$ was added to 10 nM LBT2 and 50 nM $TbCl_3$. The final volume was made up to 100 µL with Tb binding buffer and following a 10 min incubation period, the terbium emission was measured using a Victor3 plate reader set for time-resolved fluorescence with the following parameters: λ_{ex} 280 nm, λ_{em} 545 nm, 50 µs delay and 900 µs counting duration. Data shown are mean ± SEM (n=3).

While the lanthanide gadolinium appeared to compete with terbium for binding sites, other common ions did not compete with terbium for binding to the LBT, particularly at biologically relevant concentrations. To determine ion selectivity and specificity of the LBT2:Tb^{3+} complex, other ions were investigated for their potential to compete with Tb^{3+} ions for LBT2-binding, observed as a decrease in Tb^{3+} emission. High concentrations of $CaCl_2$ (100 mM) and $AlCl_3$ (0.2 mM) decreased the LBT2:Tb^{3+} luminescence, but not $NiSO_4$ (1 mM), CsCl (200 mM), KCl (200 mM), $MgCl_2$ (100 mM) nor the detergents cholate (9 mM) or CHAPS (9 mM) (data not shown, experiments carried out by Wayne Leifert, CSIRO). To further characterise the LBT2:Tb^{3+} luminescence in the presence of the competitive ions Al^{3+} and Ca^{2+}, a concentration curve for each was produced and showed the IC_{50} for each of the ions was 19 µM and 16 mM, respectively (Cooper *et al*. 2008).

Terbium binding to the LBT2 peptide could also be observed visually under UV light after staining an SDS-PAGE gel in 1.6 mM $TbCl_3$ for greater than 1 hour (**Figure 3.5**). A small amount of background staining of some markers can be seen and the dye front also seemed to accumulate or increase the fluorescence of $TbCl_3$. With further optimization and validation, this could be a much less time-consuming and inexpensive method of determining recombinant protein expression than using western blot techniques.

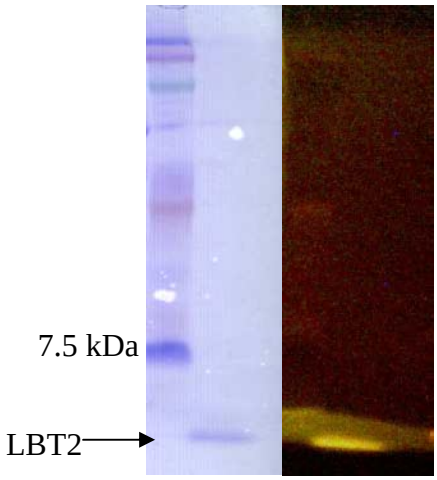

Figure 3.5: LBT2:Tb visualized on SDS-PAGE under UV light. 100 nmoles of LBT2 was run on an SDS-PAGE and stained in 1.6 mM $TbCl_3$. Following visulization under UV light (right), the gel was stained with Coomassie blue (left).

Terbium binding to the LBT2 peptide was also examined at different pH values (4-10). Optimal terbium luminescence occurred at a pH close to neutral, at lower and higher pH values terbium luminescence was decreased (**Figure 3.6**). The theoretical isoelectric point (pI) of the peptide was calculated to be 3.33. The increase in terbium luminescence may therefore be explained by more negative charges being present in the peptide as the pH increases away from the pI. At pH values above 7.5, terbium increasingly forms insoluble aggregates (Harris, Walter 2003), which could explain the decrease in terbium luminescence as the availability of soluble Tb^{3+} decreases. Low pH levels have been reported previously to dissociate lanthanide ions from chelate structures and a high pH was also found to decrease luminescence of a 9-dentate Eu(III) chelate (Kokko, Lovgren & Soukka 2007).

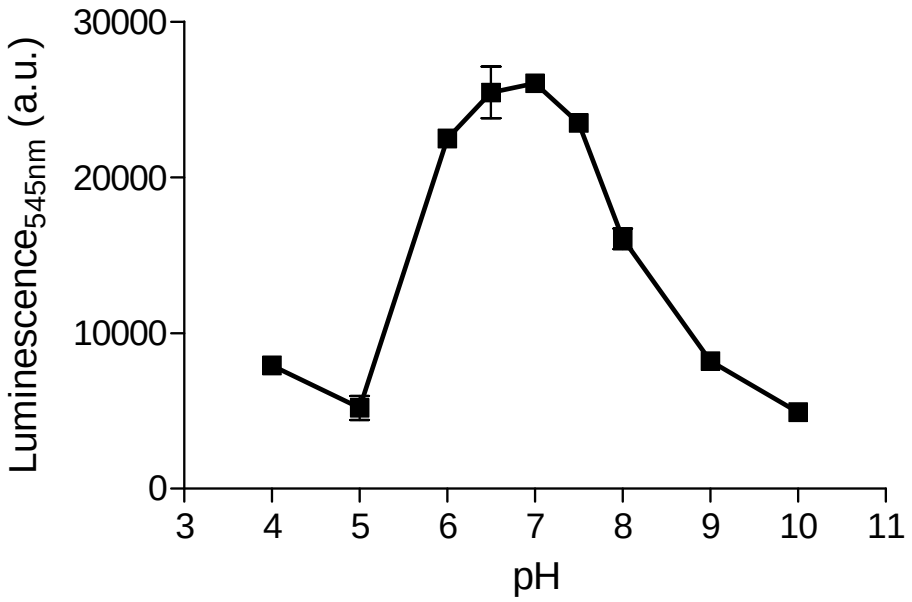

Figure 3.6: Optimal luminescence from LBT2 binding to Tb^{3+} occurred at pH 7. 50 nM LBT2 was added to 200 nM $TbCl_3$ in Tb binding buffer adjusted to the desired pH as shown. Data shown are mean ± SEM (n=3)

The excitation and emission spectra from terbium bound to LBT2 was determined using a Cary Eclipse fluorospectrophotometer (Varian) and shows the excitation maxima to occur at 280 nm as expected, since excitation occurs via aromatic amino acids tryptophan and tyrosine. The four emission peaks characteristic of terbium are also evident at 488 nm, 542 nm, 581 nm, and 616 nm with the first two peaks being the larger of the four (**Figure 3.7**).

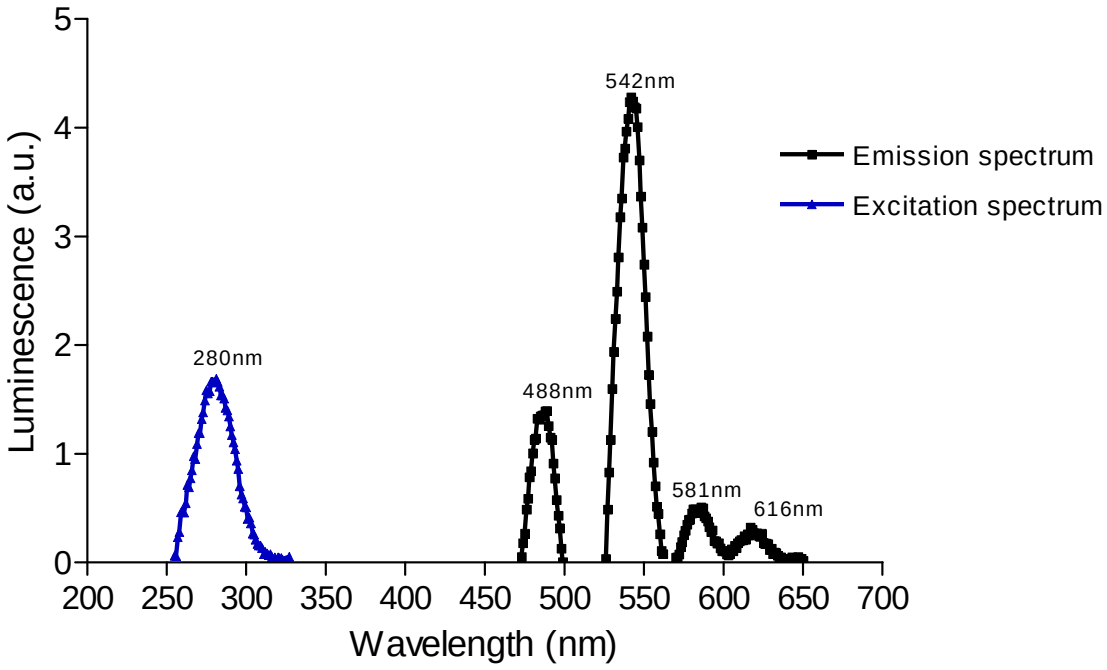

Figure 3.7: Excitation and Emission spectra of LBT2:Tb^{3+}. 20 µM LBT2 was mixed with 2 mM $TbCl_3$ in Tb binding buffer to a final volume of 1 mL. Excitation and emission spectra were scanned for using a Cary Eclipse fluorospectrophotomoter (Varian) set for phosphorescence measurements with the following parameters: 100 µs delay and 1 ms counting duration. Background of 2 mM $TbCl_3$ has been deducted. Data shown is a single representative experiment.

These results confirm that the LBT2 peptide is capable of binding to terbium under biological conditions with a high affinity and this can be readily measured using a Victor3 multilabel plate reader. It has also not been necessary to separate unbound terbium from bound since relatively little luminescence is emitted from Tb^{3+} in solution.

3.3.2. Production of recombinant baculoviruses for lanthanide binding tag fusion protein expression

To generate recombinant baculoviruses the Invitrogen Bac-to-Bac® system was used. Firstly, LBT coding sequences were fused in frame to the gene of interest using PCR. This method had varying degrees of success due to the length of the primers encoding the LBT and the tendency to form secondary structures that resulted in deletions within the PCR product. In some cases, this was relatively easily overcome by increasing the annealing temperature during PCR. However, in other cases this was unsuccessful making an alternate strategy necessary such as adding the LBT in increments. Ultimately, this lead to the design of LBT fusion vectors for recombinant protein expression in *Sf*9 cells or *E. coli*, which was successful in simplifying this procedure. After cloning into a pFastBac™ vector, the recombinant vectors were transformed into DH10Bac™ *E. coli* that contains baculovirus DNA. Isolated colonies containing recombinant baculovirus DNA (bacmid) were selected for using antibiotics and blue/white screening. However, it was necessary to check recombination using PCR as some white colonies could contain non-recombinant bacmid due to the inefficient production of β-galactosidase or a combination of recombinant and non-recombinant bacmid (**Figure 3.8**). This is undesirable since the subsequent transfection of both species into *Sf*9 cells will probably lead to lower expression and eventual loss of expression of the desired protein since the non-recombinant baculovirus is likely to amplify more efficiently.

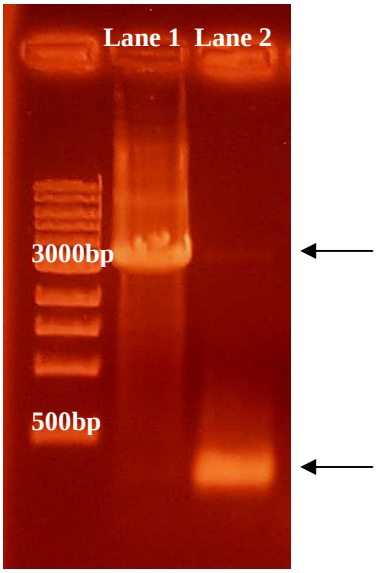

Figure 3.8: Example of a diagnostic PCR to check for recombinant bacmid. Lane 1 shows a PCR product from a colony of DH10Bac™ *E. coli* that contains recombinant bacmid compared to Lane 2 which shows a PCR product generated from non-recombinant bacmid

Sequencing was conducted on all LBT fusion constructs (**Figure 3.9**) and the data can be located in **Appendix 8.3.** By using the bacterial transposition method of the Bac-to-Bac™ system, plaque assays to isolate viruses are not necessary and this is an advantage due to the technical difficulty of such assays (Wong, Ho & Wong 2003). However, although every effort was made to isolate single recombinant colonies, due to the possibility of some contamination with non-recombinant bacmid, plaque assays could have been helpful to further purify recombinant baculoviruses as well as for determining the exact viral titre for expression optimization.

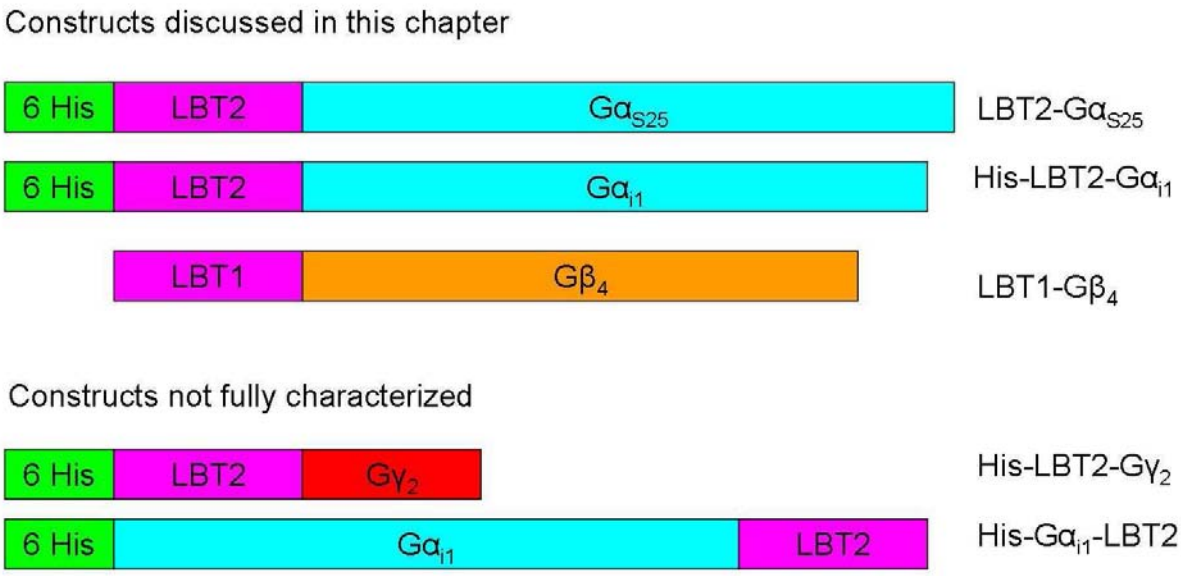

Figure 3.9: Lanthanide binding tag constructs.

3.3.3. Generation and characterization of promiscuous LBT-Gα proteins

With regard to developing a generic assay platform for G-protein coupled receptors, a G-protein that is 'promiscuous' in nature, capable of coupling to a wide range of receptors represents an attractive goal. For this reason, a number of chimeric Gα subunits have been developed by the group of Dr Yung-Hou Wong at the Hong Kong University of Science and Technology. These promiscuous, chimeric Gα subunits are primarily based on the most promiscuous naturally occurring $G\alpha_{16}$ subunit of the Gq family. However, substituting the 25 C-terminal amino acids with the corresponding C-terminal amino acids of $G\alpha_S$ or $G\alpha_Z$ to give rise to $G\alpha_{S25}$ and $G\alpha_{Z25}$, respectively, or the 44 C-terminal amino acids of $G\alpha_Z$ to give rise to $G\alpha_{Z44}$, was found to further increase the promiscuity of $G\alpha_{16}$. These proteins had previously been used in COS-7 cell-based assays and this study aimed to adapt them for use in fluorescent cell-free assays. Three different chimeric Gα-subunits ($G\alpha_{Z25}$, $G\alpha_{Z44}$ and $G\alpha_{S25}$) were fused to 2 different lanthanide binding tags (LBT1 or LBT2) at their N-terminus. A His-tag was also added to the N-terminus via an *E. coli* expression vector (pQE30).

Although chimeric Gα-subunit fusion proteins were shown to be successfully expressed in bacteria (**Appendix 8.4**), repeated attempts at purifying these proteins by exploitation of the His-tag using nickel ion affinity chromatography, failed due to their lack of solubility. This was therefore abandoned since it was unknown if the proteins expressed by bacteria would be functional without post-translational modifications and previous attempts at producing functional $G\alpha_{i1}$ in bacteria had been unsuccessful. Therefore, expression was attempted in *Sf*9 insect cells. Expression of recombinant proteins in *Sf*9 cells detected by a monoclonal poly-histidine antibody was apparent from 48 hrs post infection (**Figure 3.10**A). Attempts were then made to purify $G\alpha_{S25}$ and LBT2-$G\alpha_{S25}$ using nickel ion affinity chromatography. However, as with the bacterial expression, purification attempts failed even with a detergent (cholate) extraction step with the recombinant protein remaining in the insoluble fraction. Therefore, a partial clean up was performed which collected the insoluble membrane fraction which contained the recombinant protein as detected using an anti-Gα subunit antibody (**Figure 3.10**B). However, it remained to be seen whether the insoluble nature of the protein was due to misfolding resulting in a non-functional Gα subunit. While the promiscuous Gα-subunits have not previously been purified, the successful purification of $G\alpha_{16}$ from *Sf*9 cells has been reported (Kozasa *et al*. 1993), which also used cholate extraction but required GTPγS to stabilize the protein, which is undesirable for many downstream applications. Successful purification may have been achieved by using an alternate detergent or by purifying the protein under denaturing conditions and then re-folding the protein, as has been partially achieved for other Gα-subunits expressed in *E. coli* (McCusker, Robinson 2008).

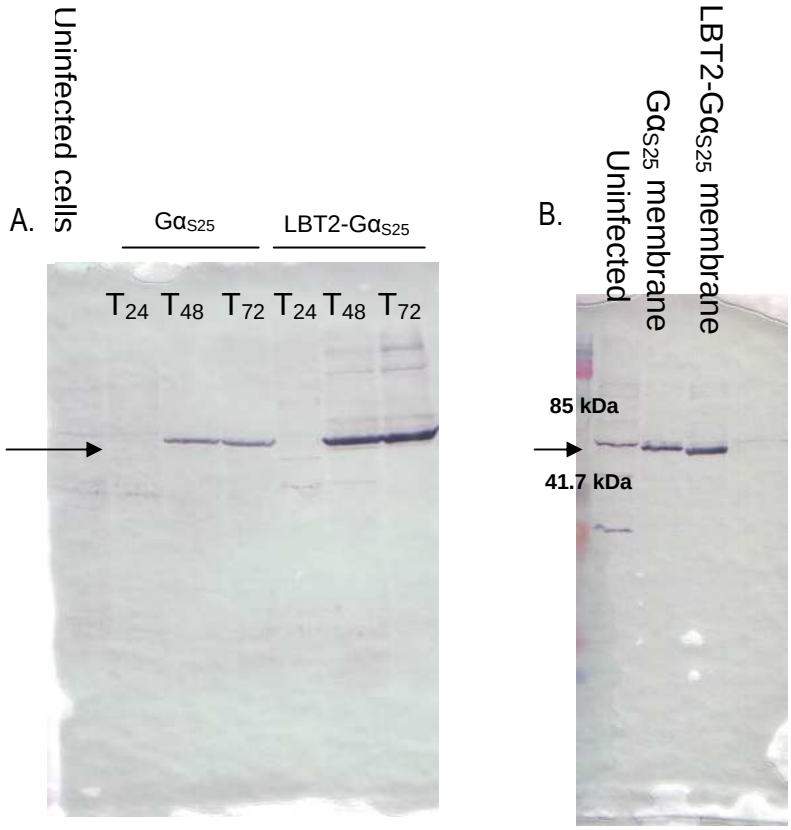

Figure 3.10: Western blots showing expression of chimeric Gα$_{S25}$ subunits in *Sf*9 cells. **(A)** Protein from cells harvested at 24, 48 and 72 hrs after infection ($T_{24,}$ T_{48}, and T_{72}) were separated by SDS-PAGE and then transferred to a nitrocellulose membrane. Monoclonal anti poly-histidine antibody was used to determine the presence of Gα$_{S25}$ and LBT2-Gα$_{S25}$. **(B)** Proteins in membrane preparations from infected cells were separated by SDS-PAGE and western blot using an anti-Gα subunit used to identify Gα$_{S25}$ and LBT2-Gα$_{S25}$.

To determine if recombinant Gα$_{S25}$ and LBT2-Gα$_{S25}$ were functional, the subunits were reconstituted with membrane preparations of the H_1-histamine receptor, the β_2-adrenergic receptor or the α_{2A}-adrenergic receptor that had been expressed in *Sf*9 cells. These receptors are most widely regarded as Gq, Gs and Gi coupled receptors, respectively. Signalling from the receptor was indicated as an increased level of [^{35}S]GTPγS binding in the presence of an agonist compared to when signalling was blocked by the addition of an excess of antagonist. Both Gα$_{S25}$ and LBT2- Gα$_{S25}$ showed signalling activity, more so in receiving signals from the H_1-histamine and β_2-adrenergic receptors than from the α_{2A}-adrenergic receptor (**Figure 3.11**). Of the receptors tested here, only the β_2-adrenergic receptor had been previously shown to couple to Gα$_{S25}$ in

transfected COS-7 cells, where inositol phosphate accumulation was measured (Hazari *et al*. 2004).

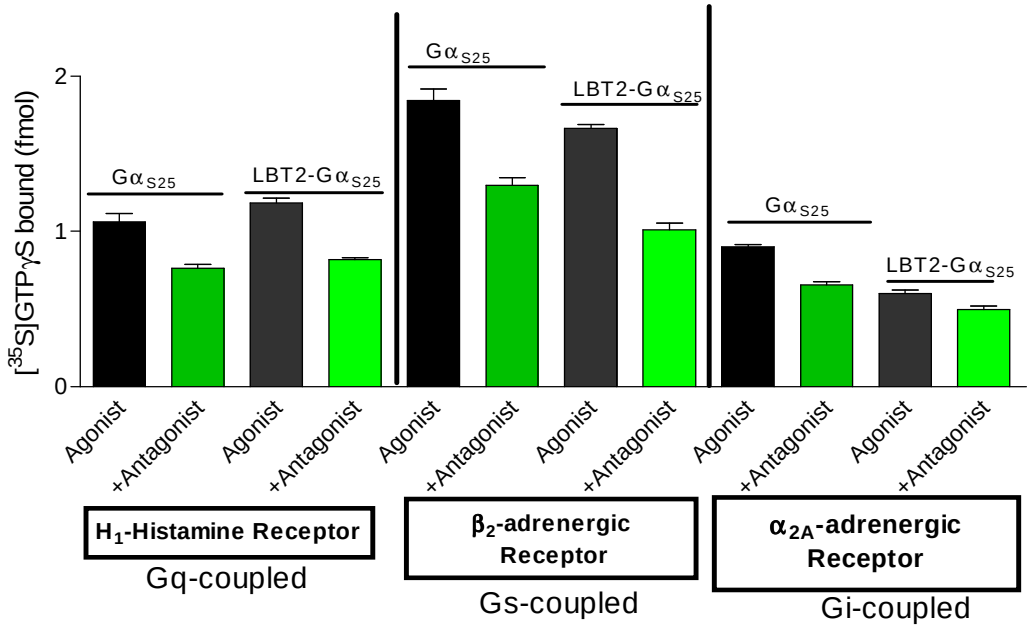

Figure 3.11: Signalling of various receptors through promiscuous $G\alpha_{S25}$. 0.1 mg/mL (total protein) of the indicated receptor preparation was reconstituted with 0.05 mg/mL Gα-subunit preparation and 40 nM purified Gβγ in TMND buffer with 10 µM AMP-PNP, 5 µM GDP and 0.5 nM ^{35}S-GTPγS. 10 µM agonist and 100 µM antagonist were present as indicated. Agonists were histamine, isoproterenol, and UK 14304 and antagonists were pyrilamine, propranolol and yohimbine for the H_1-histamine, β_2-adrenergic and α_{2A}-adrenergic receptors, respectively. The reactions were incubated for 90 min at 27ºC with shaking and 25 µL was filtered through GFC filters in triplicate and washed with 3 x4 mL of cold TMN buffer. Data shown is triplicate samples (mean ± SEM) of a single representative experiment.

The α_{2A}-adrenergic receptor normally couples to G-proteins of the Gi family that function downstream to inactivate adenylyl cyclase. However, Gαs family G-proteins have the opposite effect on adenylyl cyclase, activating it. These opposing functions of the Gα-subunit of these G-proteins could make it challenging to engineer a promiscuous G-protein that can mediate through the selectivity of both kinds of receptor for a universal G-protein and may explain why the signalling from the α_{2A}-adrenergic receptor was less effective in signalling to $G\alpha_{S25}$ than the other receptors. In all receptor reconstitutions, the increase in signal was relatively small, since greater

than 2-fold increases in [^{35}S]GTPγS binding upon agonist stimulation are routinely achieved in our laboratory, particularly when using Gi family G-proteins. Gq and Gs family G-proteins are reported to have a lower rate of GDP/GTP exchange making them less suitable for this type of assay (Milligan 2003). Therefore, the functionality of the $G\alpha_{S25}$ proteins may better be shown in another assay platform, one for example that measures cAMP production after adenylyl cyclase stimulation. The signal to noise ratio may also have been decreased by the extra amount of protein introduced with membrane preparations of the $G\alpha_{S25}$ proteins not present under the usual conditions using purified Gα. It has also been suggested that $G\alpha_{S25}$ may be weakly constitutively active or may promote the formation of constitutively active GPCRs (Hazari *et al*. 2004) which could also decrease the signal to noise ratio by raising the basal level of signalling. With regard to the promiscuous nature of $G\alpha_{S25}$, it should be noted that all the receptors tested showed equal if not higher signalling activity through reconstitution with membrane preparations of $G\alpha_{i1}$ (data not shown). While there is also some evidence for the H_1-histamine and β_2-adrenergic receptors coupling to $G\alpha_{i1}$ in the literature (Kilts *et al*. 2000, Seifert *et al*. 1994), it may also signify that the cell-free nature of this assay reduces the G-protein selectivity of the receptors. However, it appeared that $G\alpha_{S25}$ and LBT2-$G\alpha_{S25}$ had some functionality detected in the [^{35}S]GTPγS binding assay. With this in mind the terbium binding properties of these constructs were investigated next.

Terbium binding was measured by mixing the membrane preparations of LBT2-$G\alpha_{S25}$ and $G\alpha_{S25}$ with terbium chloride, exciting the sample at 280 nm and measuring the emission at 545 nm after a 50 μs delay. The presence of increasing concentrations of protein from the cell membrane preparations increased the luminescence at 545 nm in both LBT2-$G\alpha_{S25}$ and $G\alpha_{S25}$ samples. However, LBT2-$G\alpha_{S25}$ bound significantly higher levels of terbium as evidenced by the 3-fold increase in luminescence at 545 nm compared to membrane preparations containing $G\alpha_{S25}$ (**Figure 3.12**). The increase in terbium luminescence in the absence of a LBT indicated that some

non-specific terbium binding and excitation was occurring. Given the insoluble nature of the membrane preparations and presence of many contaminating proteins, this is not surprising. The amount of non-specific binding could possibly be reduced if required by further efforts at solubilising the recombinant proteins so that contaminating proteins can be removed. Alternatively, a washing step to remove non-specifically bound terbium could be utilized although the nature of the membrane preparations made finding an appropriate method for this difficult.

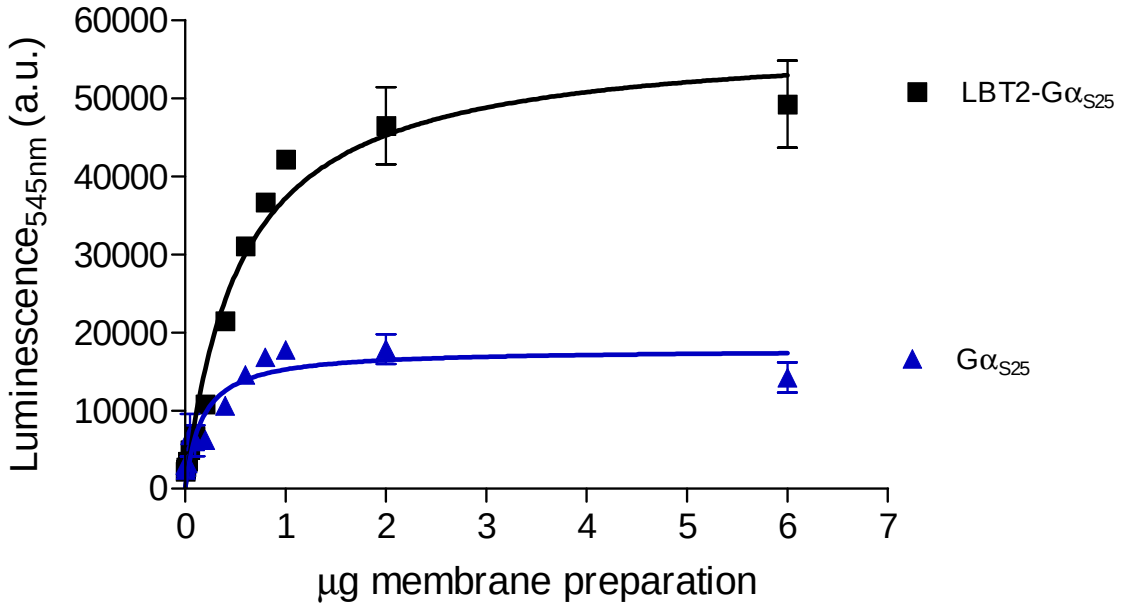

Figure 3.12: Luminescence from Tb^{3+} binding to LBT2-$G\alpha_{S25}$ in *Sf*9 membrane preparations was significantly higher compared to $G\alpha_{S25}$. 1 µM of $TbCl_3$ was added to the indicated amounts of *Sf*9 membrane preparations containing recombinant LBT2-$G\alpha_{S25}$ (■) or $G\alpha_{S25}$ (▲). The final volume was made up to 100 µL with Tb binding buffer and following a 10 min incubation period, the terbium emission was measured using a Victor3 plate reader set for time-resolved fluorescence with the following parameters: λ_{ex} 280 nm, λ_{em} 545 nm, 50 µs delay and 900 µs counting duration. Data shown are mean ± SEM (n=3).

In an attempt to show specific terbium-binding to the LBT, gadolinium was used to compete with terbium for binding sites. The addition of a 100-fold excess of gadolinium reduced the fluorescence of LBT2-$G\alpha_{S25}$ mixed with terbium by 78%. However, the fluorescence of $G\alpha_{S25}$ was also reduced but by a smaller amount of 45% suggesting that gadolinium competes not only for binding to the lanthanide binding tag but also for non-specific binding sites (**Figure 3.13**).

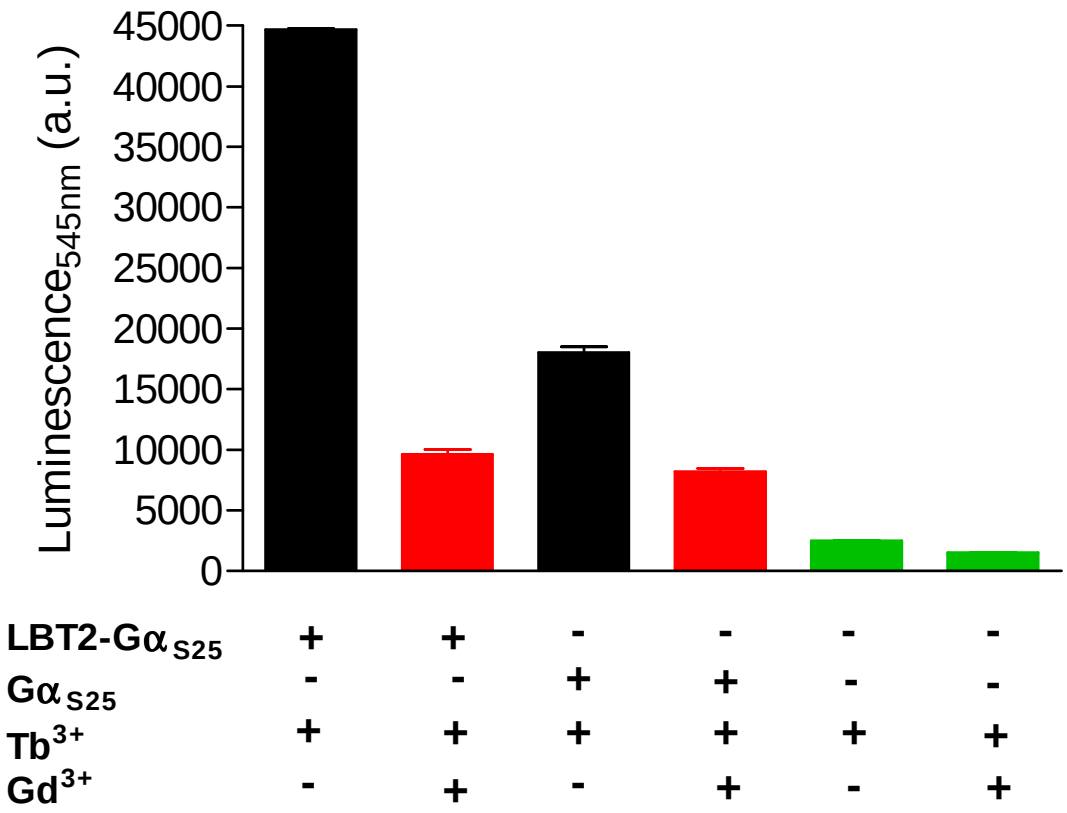

Figure 3.13: Gd^{3+} competes for Tb^{3+} binding sites. 2 µg of membrane preparations containing either LBT2-$G\alpha_{S25}$ or $G\alpha_{S25}$ were mixed with 1 µM of $TbCl_3$ and 100 µM of $GdCl_3$ where indicated. The final volume was made up to 100 µL with Tb binding buffer and following a 10 min incubation period, the Tb emission was measured using a Victor3 plate reader set for time-resolved fluorescence with the following parameters: λex 280 nm, λem 545 nm, 50 µs delay and 900 µs counting duration. Data shown are mean ± SEM (n=3).

However, treatment of the LBT2-$G\alpha_{S25}$ and $G\alpha_{S25}$ preparations with the broad protease, proteinase K (that is predicted to cut the LBT2 at a number of positions) reduced luminescence only in the LBT2-$G\alpha_{S25}$ samples suggesting that this luminescence was not attributable to only non-specific terbium binding but to the presence of a LBT (**Figure 3.14**). These results suggest that the LBT of LBT2-$G\alpha_{S25}$ is capable of binding to terbium although, due to the presence of impurities, the affinity of the terbium for the LBT could not be measured. Non-specific terbium luminescence was also detected and methods to reduce this may have to be further investigated should this produce artefact TR-FRET signals.

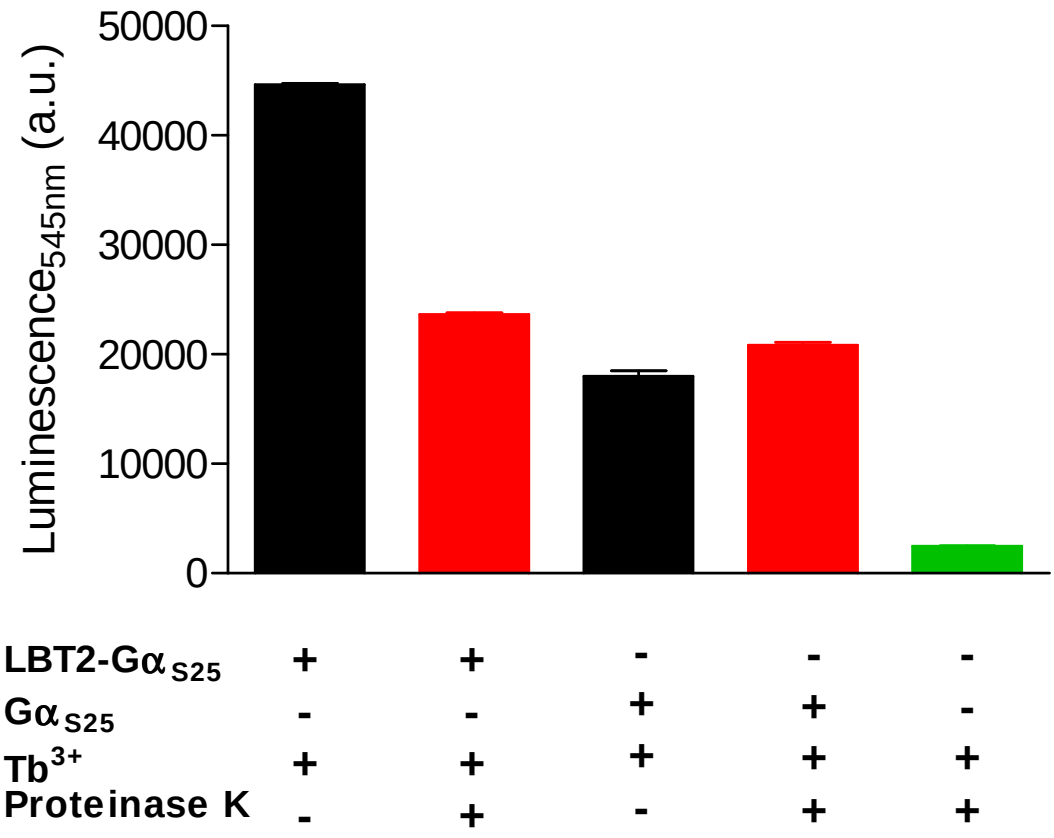

Figure 3.14 Effect of Proteinase K treatment on terbium binding to membrane preparations. 2 µg of membrane preparations containing either LBT2-Gα_{S25} or Gα_{S25}, pre-treated with 0.2 mg/mL proteinase K or an equivalent volume of buffer for 1 hr at 37ºC as indicated, was mixed with 1 µM of $TbCl_3$. The final volume was made up to 100 µL with Tb binding buffer and following a 10 min incubation period, the terbium emission was measured using a Victor3 plate reader set for time-resolved fluorescence with the following parameters: λ_{ex} 280 nm, λ_{em} 545 nm, 50 µs delay and 900 µs counting duration. Data shown are mean ± SEM (n=3).

In summary, Gα_{S25} proteins were difficult to purify both from *E. coli* and *Sf*9 cells. However, membrane preparations containing the recombinant proteins Gα_{S25} and LBT2-Gα_{S25} were shown to be functional in signalling to GPCRs. An increased level of terbium binding to LBT2-Gα_{S25} was observed compared to Gα_{S25}, and protease treatment indicated that at least half of this fluorescence was attributable to terbium binding to the LBT.

3.3.4. Construction, Expression and Characterization of His-LBT2-$G\alpha_{i1}$

His-LBT2-$G\alpha_{i1}$ was constructed using a series of PCR primers and was expressed in *Sf*9 cells and successfully purified using Ni-NTA chromatography (**Figure 3.15**).

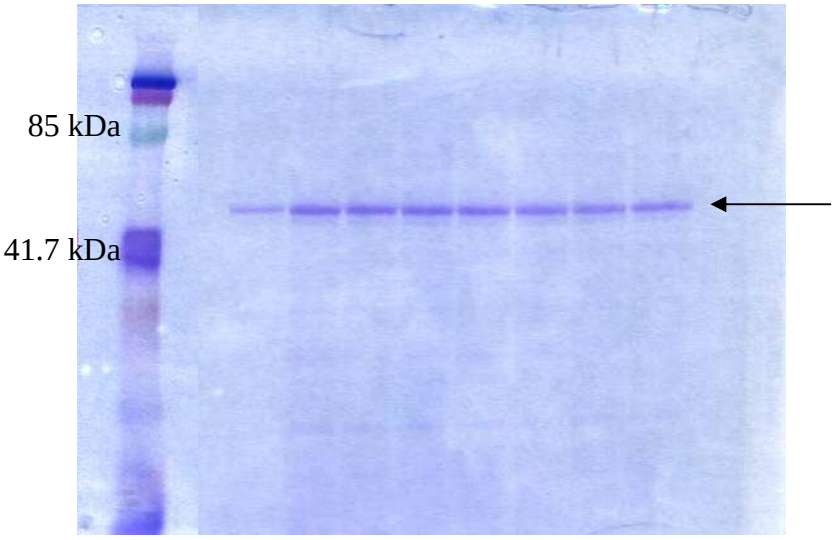

Figure 3.15: Purification of His-LBT2-$G\alpha_{i1}$. 1 L of *Sf*9 cells at 2 x10^6 cells/mL were infected with His-LBT2-$G\alpha_{i1}$ baculovirus at a MOI of 2. His-LBT2-$G\alpha_{i1}$ was purified using Ni-NTA beads and eluted from the column in fractions as shown with an excess of imidazole.

The ability of His-LBT2-$G\alpha_{i1}$ to bind terbium was then tested by adding an increasing concentration of protein to 100 or 50 nM $TbCl_3$ (**Figure 3.16**). As the protein concentration increased, so too did terbium luminescence at 545 nm until a saturating concentration was reached. The affinity of His-LBT2-$G\alpha_{i1}$ for terbium appeared to be well maintained with an apparent *K*d of ~ 3.4 nM at both concentrations of $TbCl_3$, which is comparable to the 2 nM *K*d reported by Nitz *et al*. 2003.

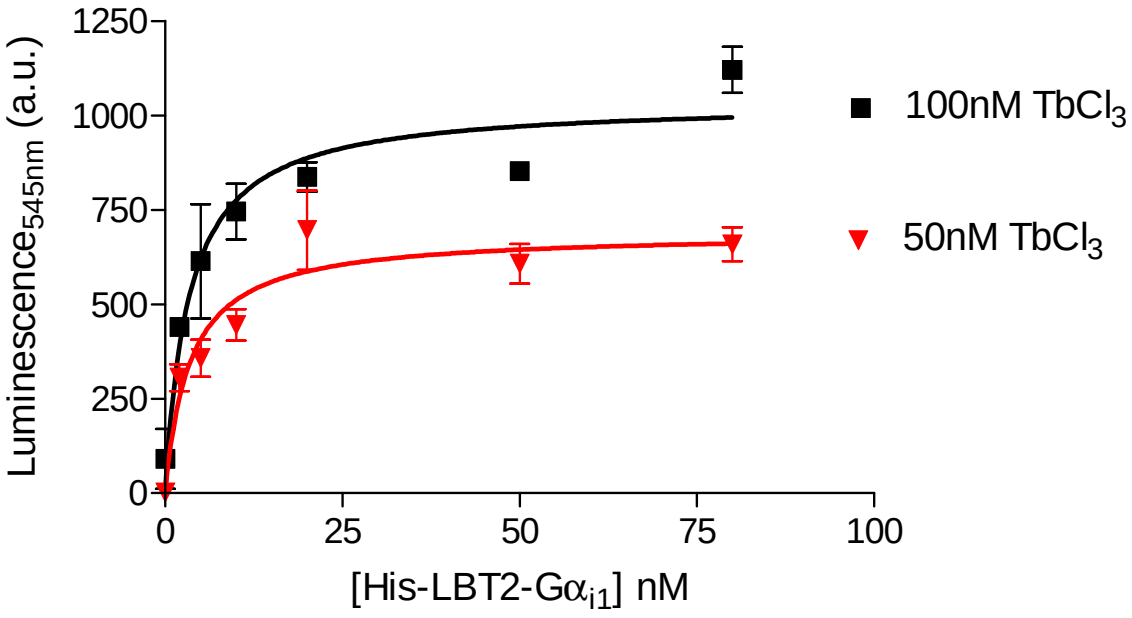

Figure 3.16: Affinity of His-LBT2-Gα$_{i1}$ for Tb^{3+}. Various concentrations of His-LBT2-Gα$_{i1}$ were mixed with 100 nM $TbCl_3$ (■) or 50 nM $TbCl_3$ (▼). The final volume was made up to 100 µL with Tb binding buffer and after a 10 min incubation, the terbium emission was measured using a Victor3 plate reader set for time-resolved fluorescence with the following parameters: λ_{ex} 280 nm, λ_{em} 545 nm, 50 µs delay and 900 µs counting duration. Data shown are mean ± SEM (n=3). Background from 100 nM or 50 nM $TbCl_3$ alone has been deducted as appropriate.

In comparison to Gα$_{i1}$, His-LBT2-Gα$_{i1}$ had increased terbium binding properties (**Figure 3.17**A). However, when compared to the properties of the LBT2 peptide alone, the level of luminescence was much lower (**Figure 3.17**B). This could suggest a change in the structure of the lanthanide binding tag upon fusion to the Gα subunit resulting in less efficient excitation of the terbium or poorer protection of the terbium from the quenching effects of water. Another consequence of fusing the LBT to a protein of interest is that this will most likely introduce amino acids capable of absorbing the excitation light but not specifically resulting in the excitation of terbium, which would decrease the light available to excite aromatic amino acids within the LBT that results in terbium luminescence. Furthermore, the introduction of the fusion protein could increase scattering resulting in less efficient excitation or less luminescence being detected.

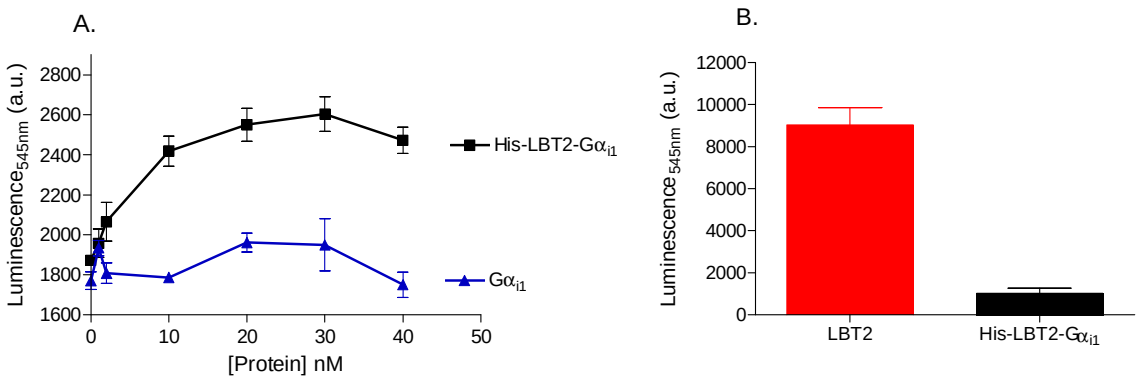

Figure 3.17: Specificity of Tb^{3+} binding to His-LBT2-$G\alpha_{i1}$ and comparison with LBT2. (A) Doses (0-40 nM) of His-LBT2-$G\alpha_{i1}$ (■) or $G\alpha_{i1}$ (▲) were mixed with 100 nM $TbCl_3$. **(B)** 80 nM $TbCl_3$ was added to 20 nM of His-LBT2-$G\alpha_{i1}$ or 20 nM LBT2. The final volume was made up to 100 µL with Tb binding buffer and after a 10 min incubation, the terbium emission was measured using a Victor3 plate reader set for time-resolved fluorescence with the following parameters: λ_{ex} 280 nm, λ_{em} 545 nm, 50 µs delay and 900 µs counting duration. Data shown are mean ± SEM (n=3).

The ability of His-LBT2-$G\alpha_{i1}$ to receive ligand-mediated signals from a GPCR was then investigated using the M_2-muscarinic receptor. The presence of the agonist carbachol, did not increase [^{35}S]GTPγS binding to His-LBT2-$G\alpha_{i1}$ although under the same conditions, the positive control using His-$G\alpha_{i1}$, produced a 3-fold increase in [^{35}S]GTPγS binding in the presence of carbachol, which was blocked when the higher affinity antagonist atropine was present (**Figure 3.18**). Studies using green fluorescent protein variants have found the N-terminus of Gα to be an unsuitable fusion site for a functional protein (Janetopoulos, Devreotes 2002). Gαi family Gα-subunits undergo N-myristoylation on a glycine residue at the extreme N-terminus, which involves the removal of the initiating methionine. N-terminal fusions would prevent this from occurring and as such, has been suggested to inhibit membrane association resulting in non-functional proteins (Wedegaertner, Wilson & Bourne 1995). However, in the case of our [^{35}S]GTPγS binding assay, a His-tag on the N-terminus of the $G\alpha_{i1}$ subunit is readily tolerated suggesting that for our signalling system, myristoylation is not critical for interaction with the receptor, although it would seem only short extensions to this region may be tolerated.

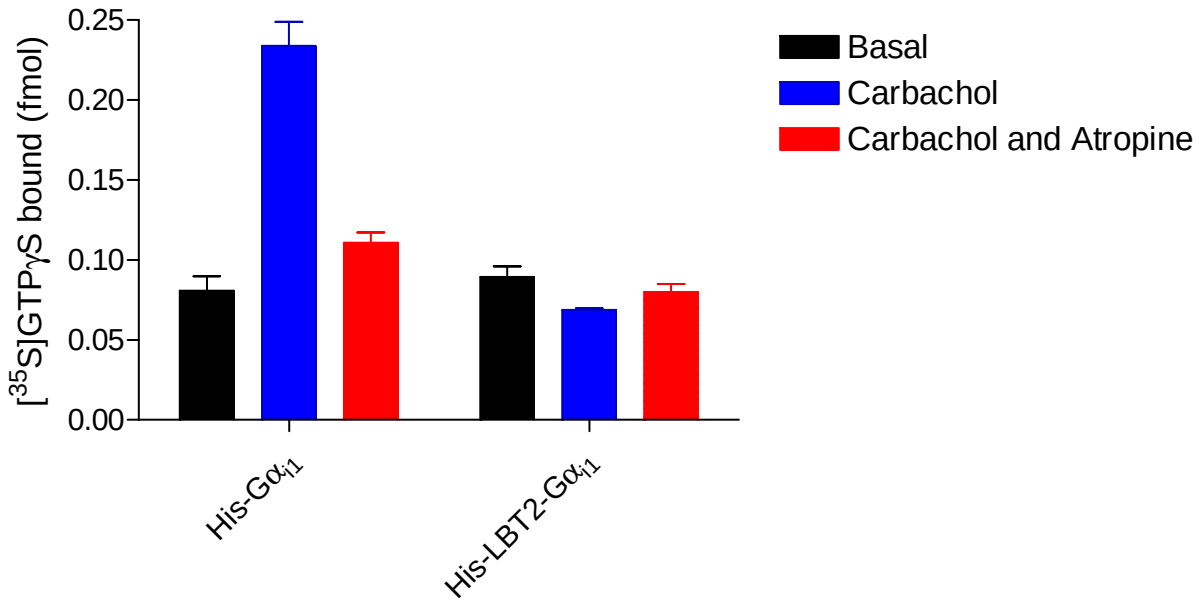

Figure 3.18: His-LBT2-Gα$_{i1}$ failed to receive signals from the M$_2$-muscarinic receptor. 20 nM of His-LBT2-Gα$_{i1}$ or His-Gα$_{i1}$ as a positive control, were reconstituted with 20 nM Gβγ, 0.2 nM [^{35}S]GTPγS, 5 µM GDP, 10 µM AMP-PNP and 0.1 mg/mL (total protein) of M$_2$-muscarinic receptor preparation. The agonist carbachol (120 mM) was added to stimulate [^{35}S]GTPγS binding and the antagonist atropine (100 µM) added to compete with carbachol for binding to the receptor to show signalling specificity. The reactions were incubated for 90 min at 27°C with shaking and triplicate 25 µL samples were filtered through GFC filters and washed with 3 x 4 mL of cold TMN buffer. Data shown are triplicate samples (mean ± SEM) of a single representative experiment.

To investigate the lack of function of His-LBT2-Gα$_{i1}$, the inherent ability of the subunit to bind [^{35}S]GTPγS was investigated. Gα subunits were incubated in the presence of [^{35}S]GTPγS so that, with time, [^{35}S]GTPγS would replace GDP, remain bound, and accumulate since [^{35}S]GTPγS is non-hydrolysable. It was found that this subunit had bound a significantly lower amount of [^{35}S]GTPγS at the end of a 90 min incubation period compared to Gα$_{i1}$ (**Figure 3.19**). The lack of signaling function of this subunit is therefore in part due to poor [^{35}S]GTPγS binding, although receptor and Gβγ interactions may also be affected, resulting in poor signal transmission. Although the 1:1 binding of [^{35}S]GTPγS to Gα$_{i1}$ was also not achieved, this could be accounted for by the lower concentration of [^{35}S]GTPγS used and the decay of the [^{35}S] label during storage.

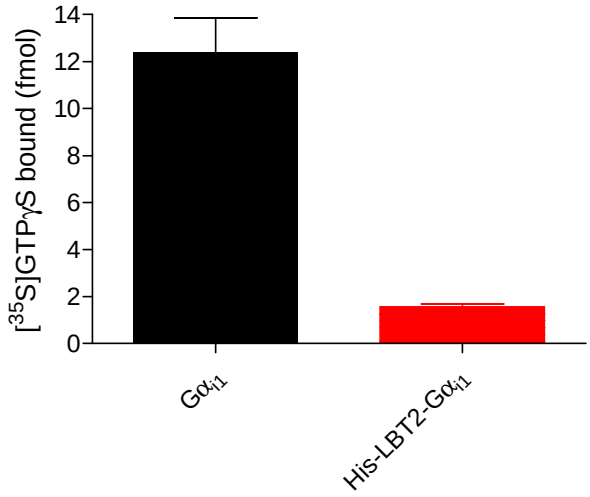

Figure 3.19: His-LBT2-Gα$_{i1}$ binds less [^{35}S]GTPγS than Gα$_{i1}$. 40 nM of Gα was mixed with 1 nM [^{35}S]GTPγS and incubated in a shaking water bath for 90 min at 27ºC. Triplicate 25 µL samples were filtered through GFC filters and washed with 3 x 4 mL of cold TMN buffer. Data shown are triplicate samples (mean ± SEM) of 2 experiments.

In summary, His-LBT2-Gα$_{i1}$ was constructed and expressed in *Sf*9 cells. The recombinant protein was successfully purified using Ni-NTA chromatography and the LBT was found to bind terbium with a high affinity although the luminescent emissions appeared to be decreased compared to an equivalent amount of pure LBT2 peptide. However, in hindsight, it would appear that the indicated *K*d was too low for one-site binding considering the concentrations of terbium used. The Gα subunit contains a magnesium binding site that could potentially bind terbium, although competition with magnesium ions failed to reduce terbium emissions. There is also the potential that the terbium was binding non-specifically to proteins and both these factors could have resulted in an over-estimation of the affinity for terbium and the lower luminescent signal generated. The fusion of the LBT also appeared to have functional consequences on the integrity of the Gα-subunit resulting in poor GTP binding and a lack of response to an activated receptor.

3.3.5. Construction, expression and characterization of LBT1-Gβ$_4$

LBT1 was fused to the N-terminus of Gβ$_4$ using PCR. Fusions of Gβ to larger fluorescent reporter proteins have previously been successfully attached on this terminus without loss of function

(Krasel *et al*. 2004). LBT1-Gβ$_4$ was co-expressed with Gγ$_2$ and His-Gα$_{i1}$ and then purified from *Sf*9 cells. The G-protein heterotrimer was captured onto Ni-NTA beads and then the non His-tagged protein (LBT1-Gβ$_4$γ$_2$) eluted using aluminium fluoride (AlF_4^-) (**Figure 3.20**). In comparison to the His-tagged Gα, a relatively low yield of LBT1-Gβ$_4$ was obtained, however, the sample was highly pure. This also showed that LBT1-Gβ$_4$γ$_2$ was capable of binding to Gα$_{i1}$. Owing to the small size of Gγ$_2$ and the relatively low sensitivity of Coomassie staining, it is often unobservable on the gel unless present at a particularly high concentration. The yield of LBT1-Gβ$_4$ may be increased by further amplification of the virus or purification using His-tagged Gγ$_2$.

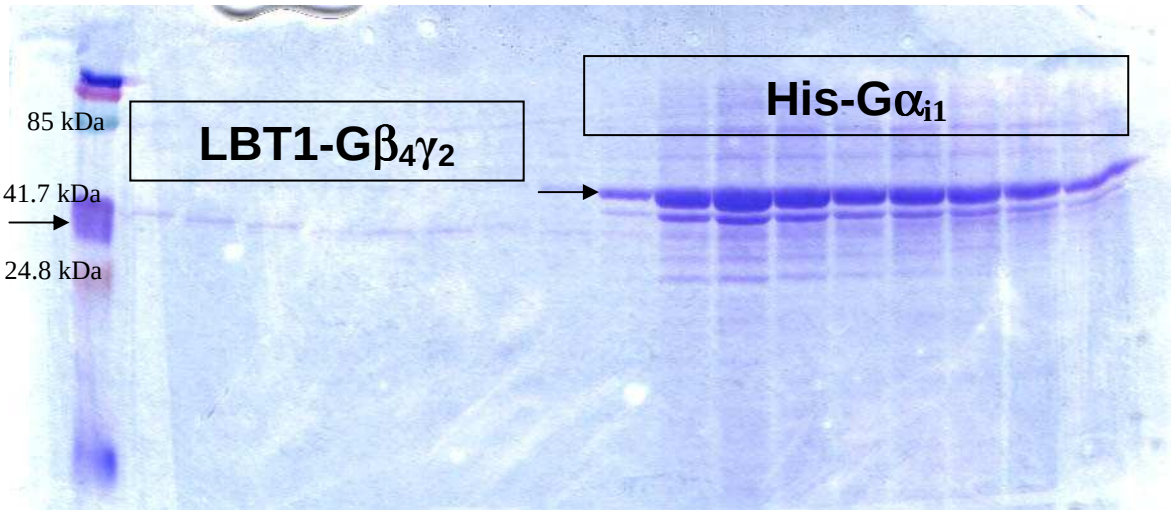

Figure 3.20: SDS-PAGE elution profile from purification of His-Gα$_{i1}$ from LBT1-Gβ$_4$γ$_2$ using Ni-NTA beads. AlF_4^- was used to dissociate the G-protein heterotrimer so that LBT1-Gβ$_4$γ$_2$ was purified separately from His-Gα$_{i1}$. His-Gα$_{i1}$ could then be eluted from the Ni-NTA beads with an excess of imidazole.

Purified LBT1-Gβ$_4$γ$_2$ was then compared to the LBT2 peptide for terbium binding and was found to be significantly inferior in its capability to bind Tb^{3+}. LBT1-Gβ$_4$ produced only a 2-fold increase in Tb^{3+} luminescence compared to the 5-fold increase obtained in the presence of LBT2 (**Figure 3.21**). This is in contrast to results that have suggested that LBT1 has superior luminescence emissions in comparison to LBT2 (Nitz *et al*. 2003). This suggested that a fusion to the C-terminus of the lanthanide binding tag LBT1 might adversely affect the terbium binding properties of the tag. Whether this problem is specific to Gβ$_4$ or applies to all fusions of LBT1 in general is

unknown. In addition to this, the introduction of other aromatic amino acids that can absorb the excitation light may also contribute to reduced terbium excitation compared to the LBT2 peptide per se.

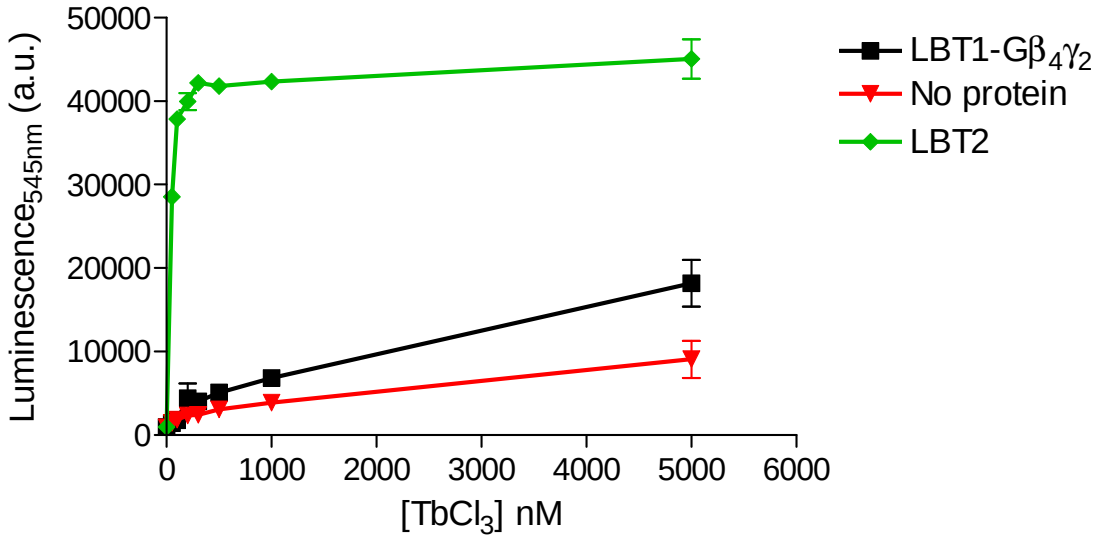

Figure 3.21: Tb^{3+} binding of LBT1-Gβ$_4$γ$_2$ compared to LBT2. 100 nM of protein was mixed with the indicated concentration of $TbCl_3$. The final volume was made up to 100 µL with Tb binding buffer and after 30 min incubation the terbium emission was measured using a Victor3 plate reader set for time-resolved fluorescence with the following parameters: λ_{ex} 280 nm, λ_{em} 545 nm, 50 µs delay and 900 µs counting duration. Data shown are mean ± SEM (n=3).

The affinity of terbium for LBT1-Gβ$_4$ was also much lower than that determined for the LBT2 peptide with an apparent *K*d of 1 ± 0.3 µM generated from a concentration response curve of $TbCl_3$ against 100 nM of LBT1-Gβ$_4$ (**Figure 3.22**). Although LBT1 had been shown to have a lower affinity for terbium than LBT2, this apparent *K*d was also lower than that published for LBT1 (57 nM) (Nitz *et al*. 2003) suggesting that the presence of Gβ$_4$ inhibited terbium binding to LBT1. Fusing the C-terminus of LBT2 to Gα$_{i1}$ did not appear to significantly affect the affinity of the tag for terbium suggesting that the presence of 2 cysteine residues within the tag may be forming a disulphide bond that maintains the integrity of the LBT structure as part of a fusion protein. The

fusion of LBT2 to Gβ$_4$ would be required to confirm this; however, the construction of that protein was not achieved during the course of this study.

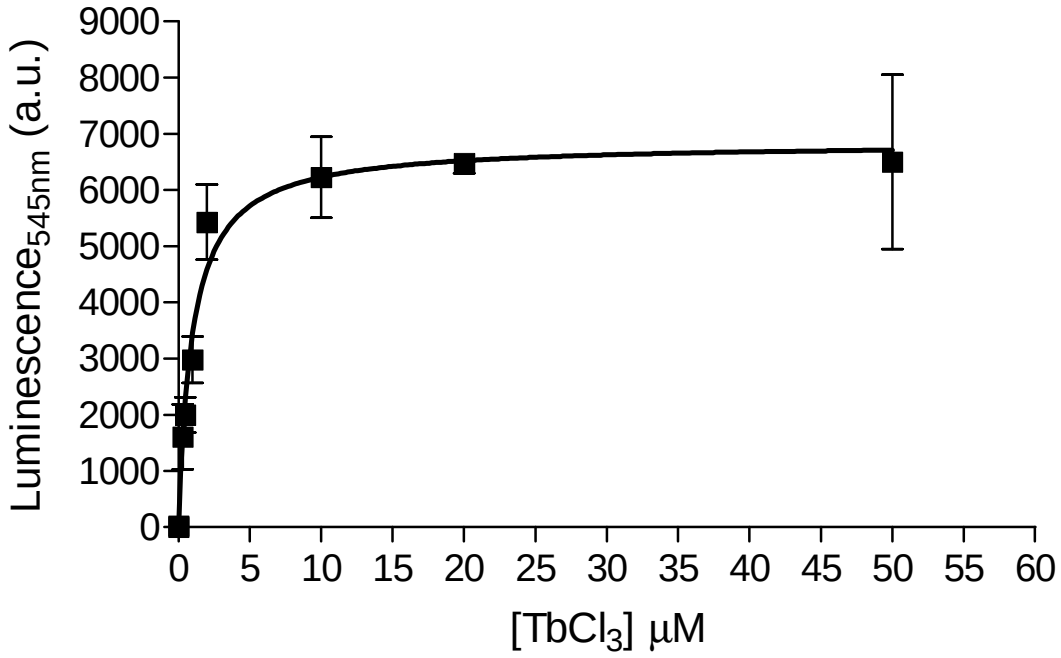

Figure 3.22: Affinity of LBT1-Gβ$_4$ for Tb^{3+}. 100 nM LBT1-Gβ$_4$ was mixed with various concentrations of $TbCl_3$. The final volume was made up to 100 µL with Tb binding buffer and following a 10 min incubation period, the terbium emission was measured using a Victor3 plate reader set for time-resolved fluorescence with the following parameters: λ_{ex} 280 nm, λ_{em} 545 nm, 50 µs delay and 900 µs counting duration. Data shown are mean ± SEM (n=3).

Treatment with Proteinase K successfully resulted in the reduction of Tb^{3+} luminescence suggesting that the increased terbium luminescence was a product of terbium binding to LBT1-Gβ$_4$ (**Figure 3.23**).

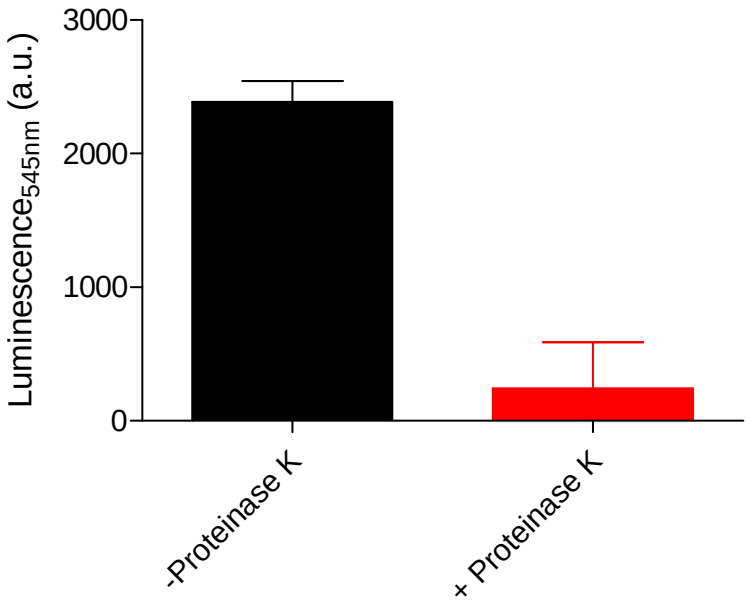

Figure 3.23: Proteinase K treatment reduces terbium binding to LBT1-Gβ4γ2. 1 µM LBT1-Gβ4γ2 was added to 120 nM $TbCl_3$ ± 0.2 mg/mL proteinase K as indicated. The final volume was made up to 100 µL with Tb binding buffer and after 60 min incubation at 37ºC, the terbium emission was measured using a Victor3 plate reader set for time-resolved fluorescence with the following parameters: λ_{ex} 280 nm, λ_{em} 545 nm, 50 µs delay and 900 µs counting duration. Data shown are mean ± SEM (n=3).

The functionality of LBT1-Gβ4γ2 in receiving signals as part of the G-protein heterotrimer was assessed using α_{2A}-adrenergic receptors in membrane preparations from infected *Sf*9 cells. Reconstitution of the signalling system resulted in increased [^{35}S]GTPγS binding in the presence of the agonist (UK 14304) which was blocked by the presence of an excess of antagonist (yohimbine). In the absence of Gβγ, the agonist stimulates only a minimal amount of [^{35}S]GTPγS binding (<2-fold increase) whereas the presence of Gβ4γ2 increases this signal to >4-fold. Likewise, LBT1-Gβ4γ2 restored the signalling potential to almost 5-fold above basal binding (**Figure 3.24**). This indicated that LBT1-Gβ4γ2 was forming a functional G-protein heterotrimer with $G\alpha_{i1}$ (also seen during purification) and could receive signals from a GPCR.

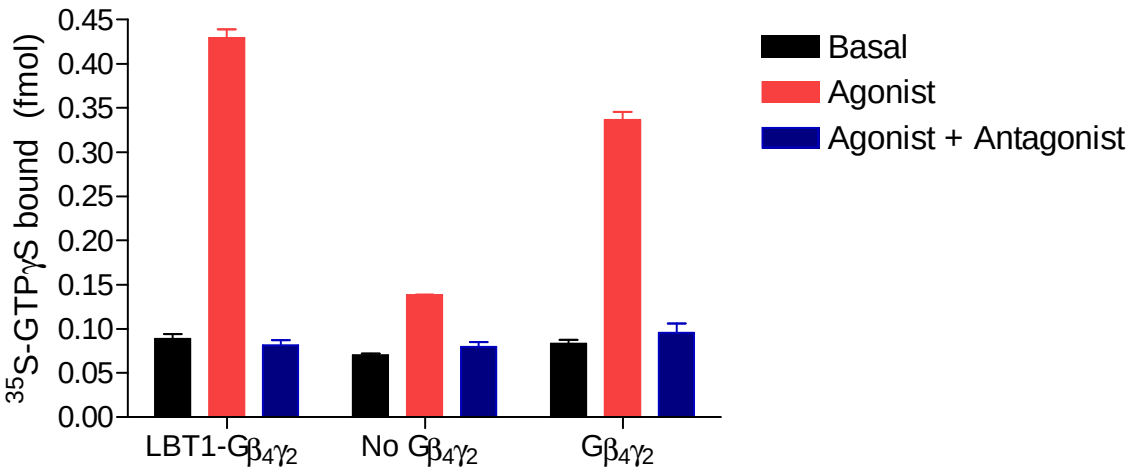

Figure 3.24: LBT1-Gβ$_4$γ$_2$ can reconstitute a functional signalling transductosome. 0.1 mg/mL (total protein) of *Sf*9 membranes containing recombinant α_{2A}-adrenergic receptors was reconstituted with 20 nM purified Gα_{i1} and LBT1-Gβ$_4$γ$_2$. [^{35}S]GTPγS (0.2 nM) binding was stimulated by the agonist UK 14304 (40 µM) and the effect blocked by the antagonist yohimbine (400 µM). The reactions were incubated for 90 min at 27ºC with shaking and triplicate 25 µL samples were filtered through GFC filters that were washed with 3 x 4 mL of cold TMN buffer. Data shown is triplicate samples (mean ± SEM) of a single representative experiment.

In summary, LBT1-Gβ$_4$ was successfully constructed, expressed in *Sf*9 cells and purified. LBT1-Gβ$_4$ was found to bind terbium, albeit with a lower than expected affinity, and the integrity of the subunit appeared maintained with successful reconstitution with a GPCR and subsequent ligand-mediated signalling activity observed.

3.3.6. Other LBT fusion proteins

Recombinant baculoviruses were also later generated for a His-tagged Gγ$_2$ with a lanthanide binding tag at either the N- or C-terminus termed Gγ$_2$-LBT2 and LBT2-Gγ$_2$, respectively. These constructs were attempted due to the success of tagging a binding partner with a tetracysteine motif (discussed in the next chapter). A Gα_{i1} subunit was also tagged at the C-terminus with LBT2 (Gα-LBT2) as an alternative to the non-functional construct produced when the LBT was fused to the N-terminus (His-LBT2-Gα_{i1}). Some of these constructs were expressed in *Sf*9 cells (**Appendix 8.5**) and were non-functional in some aspect or the time constraints of this study intervened in their full investigation.

3.4. Further discussion and conclusions

This chapter has described the construction, expression and purification of various G-protein subunits fused to LBTs. The functional integrity of both the LBT and the G-protein subunit was investigated and these aspects varied in success for each fusion protein as summarised in **Table 3.1**.

Construct	Lanthanide Binding Tag	Protein Function	Purification
LBT2-$G\alpha_{S25}$	Functional	Difficult to determine, but some indications of ligand-mediated signalling	Cannot purify
LBT1-$G\beta_4$	Lower than expected affinity (*K*d 1 µM). Poorer luminescent emissions	Signals from α_{2A}-adrenergic receptor	Purified by Ni-NTA chromatography
His-LBT2-$G\alpha_{i1}$	Affinity for terbium maintained (*K*d 3 nM) Luminescence decreased	No signalling; No GTP binding	Purified by Ni-NTA chromatography
$G\alpha_{i1}$-LBT2	Decreased terbium affinity	Not tested	Purified by Ni-NTA chromatography
$G\gamma_2$-LBT2	No terbium binding detected	Not tested	Purified by Ni-NTA chromatography

Table 3. 1: LBT constructs generated and assessment of binding terbium and signalling.

While LBT2-$G\alpha_{S25}$ was unable to be solubilized for protein purification, terbium binding and some signalling was measurable. Further characterization of the $G\alpha_{S25}$ signalling functionality would be desirable since this subunit is unlikely to be highly suited to [^{35}S]GTPγS binding assays used in this study and, although only a single band was identified in anti-Gα blots of membranes expressing recombinant proteins, endogenous proteins could be present in the membranes resulting in the signalling seen. LBT2-$G\alpha_{S25}$ could be labelled with terbium while present in membrane preparations in contrast to when labelling with CS124-DTPA-EMCH:Tb, the latter of which requires a purified protein preparation to label the protein of interest. The utility of LBTs in

non-purified preparations of proteins could significantly decrease the time, money and labour involved with the preparation of signalling components. However, the presence of a range of contaminants including insoluble proteins and lipids may contribute to background terbium luminescence. This could prove problematic in resolving a true TR-FRET signal from a specific protein interaction. The homogenous nature in which LBTs can be labelled with terbium and terbium binding measured, may also be exploitable in whole-cell assays. LBT1-$G\beta_4$ was shown to have a significantly lower affinity for terbium than anticipated for LBT1. This protein was able to receive signals from a GPCR and was also able to be purified via His-Gα further showing that the LBT fusion did not appear to have an effect on the function of the Gβ subunit. His-LBT2-$G\alpha_{i1}$ was able both to be purified and to bind terbium with a high affinity, although the luminescence generated was much lower than that of the LBT2 peptide. The fusion of the LBT to this site also appeared to have an affect on the signalling abilities of the Gα-subunit which could be at least in part, contributed to the lack of inherent GTPγS binding to this subunit.

For the fusion proteins constructed in this study, it was found that LBT2 which contains 2 cysteine residues possibly linked via a disulphide bridge maintained its affinity for terbium when in the format of a fusion protein. In contrast, LBT1, which would be expected to be more structurally flexible, lost affinity for terbium when fused to a protein. However, it should also be noted that the fusion of LBT2 resulted in a Gα-subunit with reduced function perhaps indicating that the more rigid nature of the tag may be more likely to be detrimental to protein function. However, fusion of the tags to the same proteins would be required for a direct comparison since larger fusions to the N-terminus of $G\alpha_{i1}$ have previously been shown to disrupt protein function (Janetopoulos, Devreotes 2002).

In all cases, the levels of luminescence obtained from the terbium were lower than that obtainable from labelling with the commercially available chelate or that of the LBT2 peptide. This suggests that in the context of a fusion protein, the LBTs were less efficient at binding the terbium, shielding the terbium from water, and/or exciting the terbium. This may prove to be a significant disadvantage in TR-FRET assays using a terbium bound LBT as the donor. To improve the properties of the LBT within a fusion protein, it may be helpful to incorporate glycine linkers. This strategy has previously been used to decrease the impact of the fusion of a calcium binding loop on both the tag and the protein of interest (Ye *et al*. 2001). More appropriate fusion sites could also be investigated. $G\alpha_{i1}$ has successfully been tagged with YFP within the α-helical domain of the subunit (Bunemann, Frank & Lohse 2003) and this may have proved to be a more successful strategy for maintaining the functional integrity of the Gα subunit. However, at the initiation of this study, a terminus of the Gα subunit was chosen both for the technical ease and in keeping with the hypothesis that a significantly smaller fusion than a GFP-like protein may not prove deleterious. There was also no indication as to the functionality of the LBT whilst constrained within a protein. However, recently, LBT1 has been introduced between transmembrane segments of a potassium channel, which showed good protection of the terbium ion from collisional quenching by water although optimal terbium concentrations were relatively high at 2-3 μM (Sandtner, Bezanilla & Correa 2007). These optimal concentrations of terbium were similar to that found for terbium binding to LBT1-$G\beta_4$. This suggests that the LBTs could be successfully incorporated into the α-helical domain of the $G\alpha_{i1}$ subunit; a fusion site which has been a successful site in other studies (Bunemann, Frank & Lohse 2003; Janetopoulos, Devreotes 2002). To some extent, the low luminescence intensity has been acknowledged by other groups and a recent effort to improve this has been to incorporate unnatural amino acids into the LBT that feature a more efficient sensitizer than tryptophan, such as carbostyril 124 (Reynolds, Sculimbrene & Imperiali 2008). However, this required *in vitro* synthesis of the tag and chemical

ligation to the protein of interest making this strategy much more technically demanding than using a fusion protein. Another benefit of this strategy, apart from increasing the luminescence, included decreasing the excitation energy from 280 nm (which is not ideal for studying biological systems) and this also enabled luminescence emissions from europium to be generated. Alternatively, the concatenation of two LBTs to simultaneously bind and excite two terbium ions has also been demonstrated to increase luminescence by up to 3-fold compared to a single LBT (Martin *et al*. 2007).

Despite some reductions in binding and luminescence efficiency, G-protein subunits have been fused to LBTs and some of these subunits were found to be successful in both binding to terbium and in receiving signals from GPCRs. The utility of these fusion proteins as TR-FRET donors was further investigated in chapter 5.

4. Labelling Tetracysteine Motifs (TCMs) with FlAsH

Structures of various fluorescent labels shown to scale.
Figure adapted from (Giepmans *et al*. 2006).

4.1. Introduction

Biarsenical dyes were developed in a labelling strategy that exploited the ability of arsenic compounds to bind paired thiol groups. FlAsH (4',5'-bis(1,3,2-dithioarsolan-2-yl)fluorescein-(1,2-ethanedithiol)$_2$) is a fluorescein derivative containing two As(III) substituents conjugated to ethanedithiol. FlAsH is reported as being almost non-fluorescent until bound to a tetracysteine motif (TCM) such as Cys-Cys-Pro-Gly-Cys-Cys (Adams *et al*. 2002). The interaction between FlAsH and the TCM is covalent with four bonds being formed between the arsenic groups in FlAsH and the thiol groups in the TCM. This covalent linkage should minimize signal deterioration over time (due to dissociation of the label) which has been found problematic in other labelling strategies. TCMs can be attached to C- or N-termini of fusion proteins as well as within alpha helical regions. Recombinant TCM fusion proteins can be labelled either *in vitro* or inside live cells due to the membrane permeability of FlAsH. The TCM rarely exists naturally and these factors should contribute to good signal to noise ratios, reducing the interferences of non-specific fluorescence. Labelling with FlAsH has been exploited for protein localization and trafficking studies in mammalian cells (Andresen, Schmitz-Salue & Jakobs 2004; Griffin, Adams & Tsien 1998) as well as for studying protein interactions or conformational changes using FRET in combination with CFP as the donor (Hoffmann *et al*. 2005; Nakanishi *et al*. 2006).

At the commencement of this project, the advantages of FlAsH in FRET had not yet been fully exploited with an appropriate second small peptide-small molecule pair. FlAsH-TCM used in conjunction with a LBT bound to terbium would achieve a TR-FRET system that uses site-specific labelling with peptide fusions much smaller than the more widely used fluorescent protein alternatives (CFP, YFP etc.). This chapter describes the construction, expression and characterization of TCM fusion proteins with regard to maintaining the functional integrity of the protein and labelling functions with FlAsH (**Figure 4.1**).

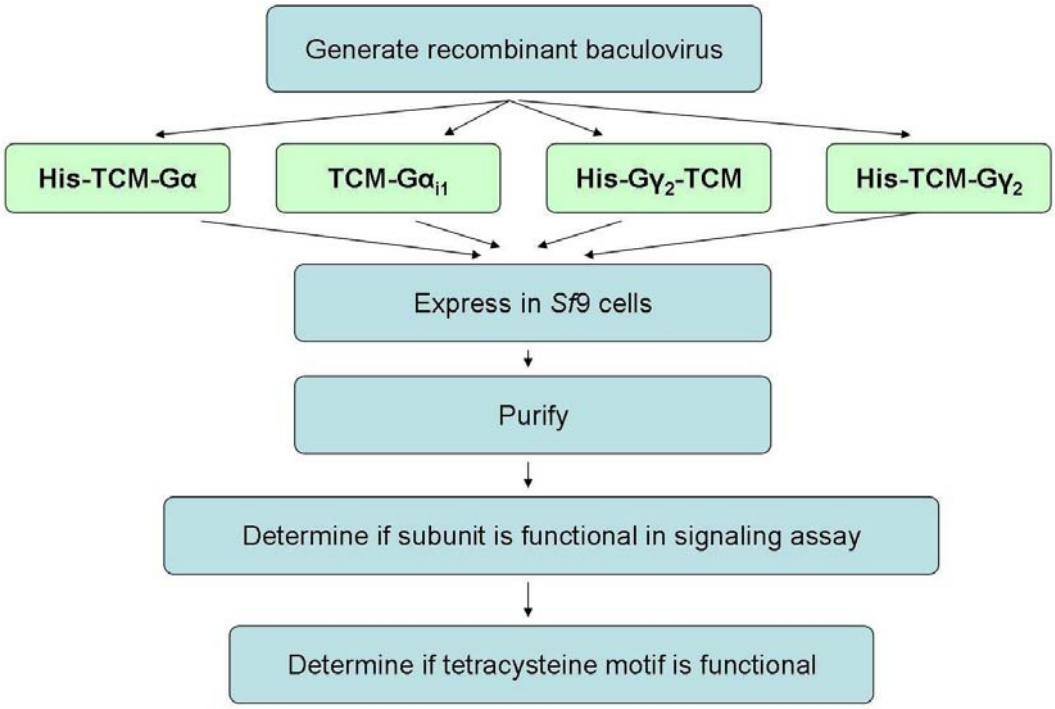

Figure 4.1: Layout of the investigation of tetracystine motif-G-protein fusion constructs.

4.2. Methods

4.2.1. Labelling TCMs with FlAsH and measuring FlAsH fluorescence

To label TCMs with FlAsH, FlAsH (kindly manufactured by Dr. Jack Ryan and Ms. Megan Kruger of CSIRO Molecular and Health Technologies, Clayton, VIC, Australia) and the TCM peptide Gly-Ala-Glu-Gly-**Cys-Cys-Pro-Gly-Cys-Cys**-Gly-Gly-Gly (synthesized by Auspep, Parkville, VIC, Australia) or TCM fusion protein were diluted together in black 96 well plates to the indicated concentrations. In general, 20x working concentrations of assay components were made in PBS or Tb binding buffer and 5 µL added to wells before buffer was added to a final volume of 100 µL. Plates were then incubated for the desired time with shaking. Where a reducing agent was used, 20x working solutions were made fresh containing the desired reducing agent (tris(2-carboxyethyl)phosphine hydrochloride (TCEP), β-mercaptoethanol (BME) or dithiothreitol (DTT)) so that the final concentration of reducing agent in the assay was 1 mM. Prompt fluorescence measurements were taken using a Victor3 multilabel plate reader (Perkin Elmer) with a continuous wave lamp (CW-lamp) and an excitation wavelength of 485 nm. The emission at 520 nm was measured for 0.1 s.

4.2.2. Construction of $G\gamma_2$-TCM and TCM-$G\gamma_2$

$G\gamma_2$-TCM constructs in pQE30 (Qiagen) were generated using PCR primers to attach the tag to the N- or C-terminus of the protein. To construct $G\gamma_2$ with a N-terminal TCM (TCM-$G\gamma_2$) the forward primer (containing the TCM) 5' GGA TCC ATG TGC TGT CCA GGA TGC TGT ATG GCC AGC AAC AAC ACC 3' and reverse primer 5'GC AAG CTT TTA AAG GAT GGC GCA GAA GAA C 3' were used. $G\gamma_2$ with a C-terminal TCM ($G\gamma_2$-TCM) was constructed using the forward primer 5' GC GGA TCC ATG GCC AGC AAC AAC ACC 3' and reverse primer (containing the TCM) 5' AAG CTT TTA ACA GCA TCC TGG ACA GCA AAG GAT GGC GCA GAA GAA C 3'.

Dr. Richard Glatz (SARDI, formerly CSIRO) cloned the resulting PCR products into pQE30 using *Bam*HI and *Hind*III restriction enzyme sites contained in the primers. Using the *EcoRI* and *Hind*III restriction enzyme sites, the TCM constructs with an N-terminal His-tag were then subcloned into pFastBac™1 for subsequent generation of recombinant baculovirus and expression of His and TCM tagged $G\gamma_2$ subunits in *Sf*9 cells as has been previously described (see chapter 3). Sequencing was used to confirm that constructs were correct.

4.2.3. Construction of TCM-$G\alpha_{i1}$ and His-TCM-$G\alpha_{i1}$

$G\alpha_{i1}$ was constructed such that the protein was fused to a TCM at its N-terminus with or without a His-tag at the N-terminus of the TCM. TCM-$G\alpha_{i1}$ was constructed by PCR using the forward primer (containing the TCM) 5' GGT ACC ATG TTT CTT AAT TGT TGT CCT GGT TGT TGT ATG GAA CCT GGT GGT GGT 3' and reverse primer 5' GC AAG CTT TTA GAA GAG ACC ACA GTC TTT TAG 3'. The PCR product was cloned into pFastBac™1 using *Kpn*1 and *Hind*III restriction enzyme sites also containined in the primers. To generate a His-tagged protein (His-TCM-$G\alpha_{i1}$), the PCR product was cloned into pQE30 using *Kpn*1 and *Hind*III restriction enzyme sites before the resulting N-terminally His-tagged construct was excised using *EcoR*1 and *Hind*III and subcloned into pFastBac™1. Clones were sequenced to confirm their correct construction as has been described earlier and then recombinant baculovirus generated.

4.2.4. Expression of TCM fusion proteins in *Sf*9 cells

Recombinant baculovirus was generated using the Bac-to-Bac® system (Invitrogen) as has been described earlier. TCM fusion proteins were then expressed in *Sf*9 cells in the same manner as LBT fusion proteins. Gγ subunits were always co-expressed with Gβ.

4.2.5. Protein purification from insect cells and on-column or solution labelling with FlAsH

TCM-G-protein fusions were purified from *Sf*9 cells in the previously described manner (Chapter 2). The TCM was often labelled on the column using 100 μM FlAsH and incubating overnight at 4°C. The unbound FlAsH was then washed from the column using Ni-NTA wash buffer. Non His-tagged subunits were then eluted from the column using Buffer E containing aluminium fluoride and the His-tagged protein eluted using an excess of imidazole in Buffer E.

Where proteins had been purified and then found to bind FlAsH with low efficiency, labelling with FlAsH was carried out on stock proteins that were of a higher concentration (μM) with an overnight incubation at 4°C. Dialysis or buffer exchange using Bio-spin 6 columns (Bio-rad) according to the manufacturer's direction was used to remove unbound FlAsH.

4.2.6. Western Blot

Western blots were conducted as previously described in chapter 2 using anti poly-histidine antibody conjugated to alkaline phosphatase.

4.2.7. [^{35}S]GTPγS binding assays

Signalling and binding assays using [^{35}S]GTPγS were conducted as has been previously described in chapter 2.

4.3. Results and Discussion

4.3.1. Characterization of the TCM:FlAsH interaction

The TCM peptide synthesized by Auspep was mixed with FlAsH and the fluorescence at 535 nm monitored with time. Upon mixing of the TCM peptide with FlAsH, an increasing amount of fluorescence was detected to saturation with time, indicative of FlAsH binding to the TCM since FlAsH is almost non-fluorescent until bound to a TCM, resulting in the displacement of EDT (Griffin, Adams & Tsien 1998) (**Figure 4.2**). With 2 µM FlAsH and 5 µM TCM, it took ~60 min for the fluorescence to stabilize and the presence of the TCM peptide induced a 33-fold increase in fluorescence (535 nm).

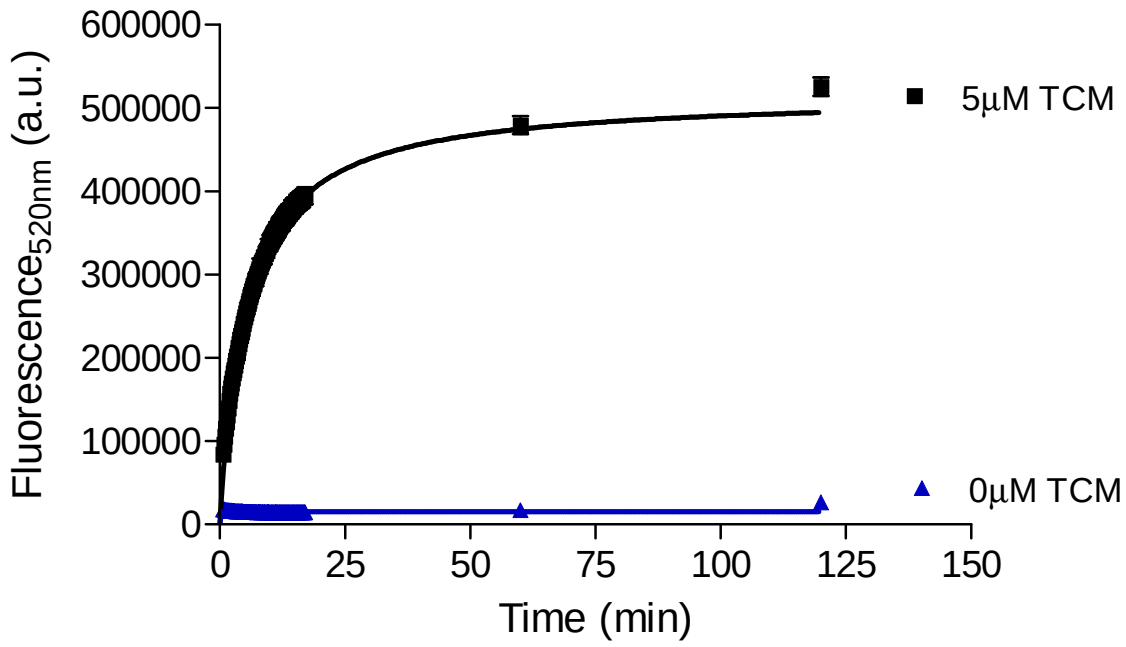

Figure 4.2: Time course of FlAsH binding to the TCM peptide. 2 µM FlAsH was mixed with 5 µM TCM in PBS (pH 7.4) in a 100 µL total volume. FlAsH emission was measured using a Victor3 plate reader set for fluorescence measurements with the following parameters: λ_{ex} 485 nm, λ_{em} 520 nm. Data shown are mean ± SEM (n=3).

The presence of increasing concentrations of the TCM peptide mixed with FlAsH increases the fluorescence until a saturating concentration is reached and likewise, increasing concentrations of FlAsH increased the maximum fluorescence reached (**Figure 4.3**).

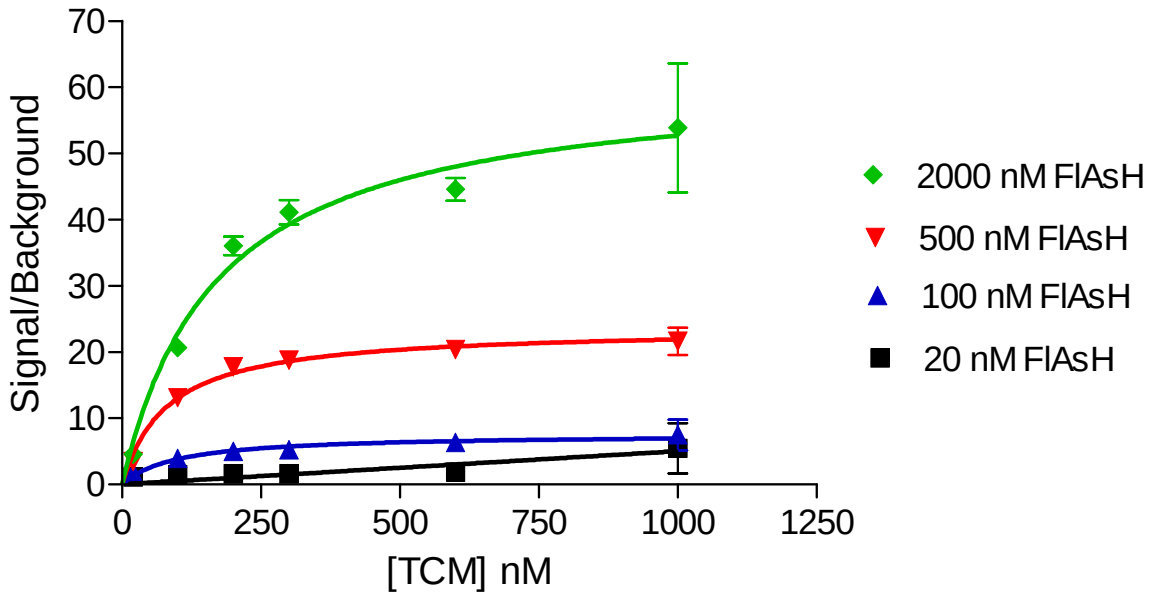

Figure 4.3: Effect of increasing FlAsH and TCM peptide concentrations on FlAsH fluorescence. TCM peptide was mixed with FlAsH in PBS to a final volume of 100 µL. Background FlAsH fluorescence was determined in the absence of TCM peptide. Following overnight incubation, FlAsH emission was measured using the following parameters: λ_{ex} 485 nm, λ_{em} 520 nm. Background fluorescence was determined in the absence of TCM peptide has been deducted. Data shown are mean ± SEM (n=3).

For FlAsH to bind to the TCM, the cysteine residues must be in the reduced state (Griffin *et al*. 2000). This appeared to be evidenced by the introduction of reducing agents such as β-mercaptoethanol, TCEP and DTT which increased the maximum fluorescence compared to that when no reducing agent was present (**Figure 4.4**A). However, some reducing agents, notably those that contain thiol groups such as β-mercaptoethanol and DTT, increased the fluorescence of FlAsH in the absence of a TCM. This has also been observed in previous studies using β-mercaptoethanol and 2-mercaptoethanesulfonic acid (MES) (Adams *et al*. 2002; Griffin *et al*. 2000). This results in the fold increase in FlAsH fluorescence in the presence of TCM being significantly less than when a non-thiol containing reducing reagent such as TCEP is used (**Figure 4.4**B). Interestingly, it has been reported that the presence of small monothiols such as β-mercaptoethanol increase the speed of labelling (Adams *et al*. 2002; Griffin *et al*. 2000) and have

also been used to reduce non-specific FlAsH binding (Hearps *et al*. 2007; Langhorst, Genisyuerek & Stuermer 2006). Fluorescent FlAsH not bound to a TCM in assays would be undesirable since it would be expected that the presence of such a species would increase the probability of bystander FRET occurring from random collisions of labelled molecules. For this reason, the most desirable reducing agent for use in subsequent labelling is TCEP. An alternative approach would be to remove FlAsH not bound to a TCM after labelling. This also raises the question of how specifically the FlAsH binds to the TCM and whether non-specific binding of FlAsH to single or dithiols within proteins could be problematic.

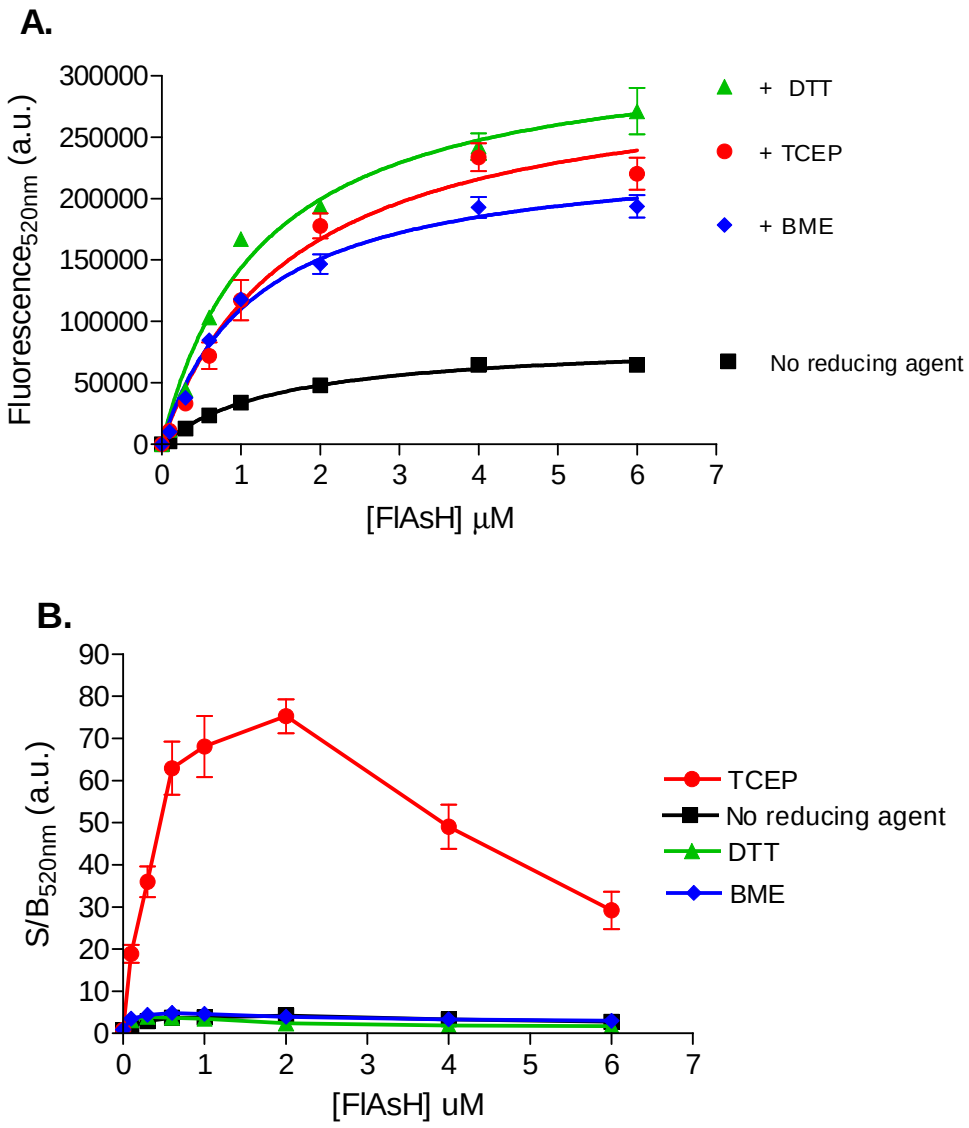

Figure 4.4: Effect of reducing agents on FlAsH binding to the TCM peptide. 1 µM TCM peptide was mixed with doses of FlAsH (0-6 µM) in the absence (■) or presence of 1 mM DTT

(▲), 1 mM TCEP (●) or 1 mM β-mercaptoethanol (BME) (◆). After incubation overnight, FlAsH emission was measured using a Victor3 plate reader set for prompt fluorescence measurements with the following parameters: λ_{ex} 485 nm, λ_{em} 520 nm. Data shown are mean ± SEM (n=3). **(A)** Background fluorescence from the reducing agent and FlAsH alone has been deducted. **(B)** Background signal was measured in the absence of the TCM peptide to determine signal/background (S/B). Data shown are mean ± SEM (n=3).

The excitation and emission spectra of FlAsH were determined using a Cary Eclipse fluorospectrophotometer (Varian). The TCM peptide was mixed with FlAsH in the cuvette, incubated, and the excitation and emission spectra determined with peaks at 508 nm and 528 nm respectively (**Figure 4.5**). These spectral properties were the same as has previously been reported and are approximately 20 nm red-shifted to that of fluorescein (Griffin, Adams & Tsien 1998). Although FlAsH is commercially available and marketed as Lumio™ Green by Invitrogen, for our purposes FlAsH was manufactured by CSIRO and these results confirm its integrity in regards to binding to the TCM and increasing in fluorescence upon binding.

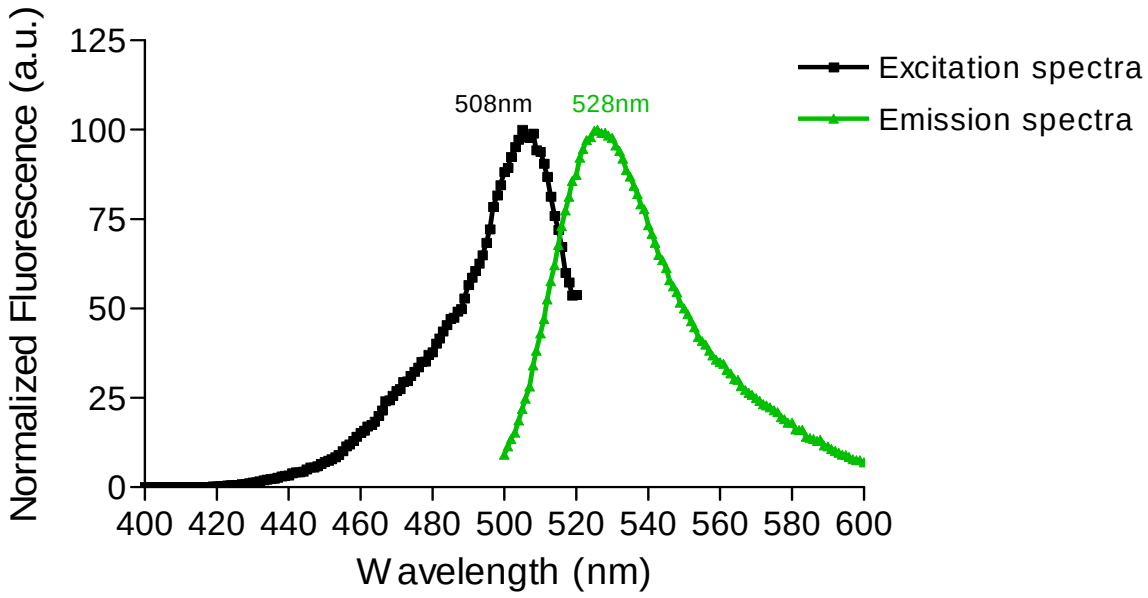

Figure 4.5: Excitation and emission spectra of FlAsH bound to TCM peptide. 200 nM TCM was mixed with 400 nM FlAsH and 1 mM TCEP in Tb binding buffer. Background fluorescence of 400 nM FlAsH in the absence of TCM has been deducted.

4.3.2. Generation of recombinant baculoviruses

This study used PCR to fuse a TCM to the protein of interest, although a Gateway® vector is commercially available for tagging proteins with a TCM from Invitrogen. This method was generally successful due to the short length of the motif. Recombinant baculoviruses were subsequently generated to infect *Sf*9 cells and, as per the baculoviruses constructed for the LBT fusion protein expression, plaque assays may have lead to improved expression levels. Four recombinant baculoviruses were generated for expression of the fusion proteins shown in **Figure 4.6**. The sequencing data for these constructs can be located in **Appendix 8.6**.

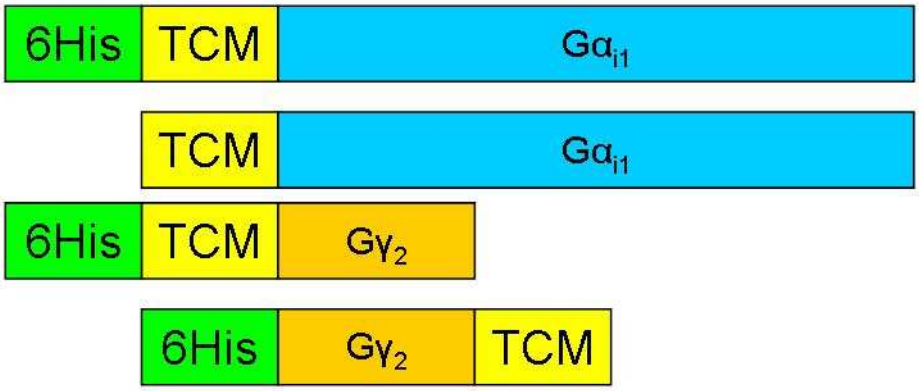

Figure 4.6: Schematic of TCM fusions constructs generated in this study.

4.3.3. Construction and characterization of TCM fusions to $G\gamma_2$

His-tagged $G\gamma_2$ fused to TCM at the C-terminus ($G\gamma_2$-TCM) was co-expressed with $G\beta_4$ in *Sf*9 cells to enable the formation of the $G\beta_4\gamma_2$-TCM dimer since it has previously been reported that co-expression is necessary for Gβγ dimer function (Iniguez-Lluhi *et al*. 1992). The Gβγ dimer was then purified using Ni-NTA beads (**Figure 4.7**A) where the $G\beta_4$ is clearly distinguishable after SDS-PAGE. Although the presence of the small 8 kDa $G\gamma_2$-TCM is not distinguishable using Coomassie staining, it can be inferred by the presence of $G\beta_4$ since this protein could only be captured in the presence of a His-tagged binding partner. Expression of $G\gamma_2$-TCM was confirmed

by western blot using an alkaline phosphatase conjugated monoclonal anti poly-His antibody (**Figure 4.7**B).

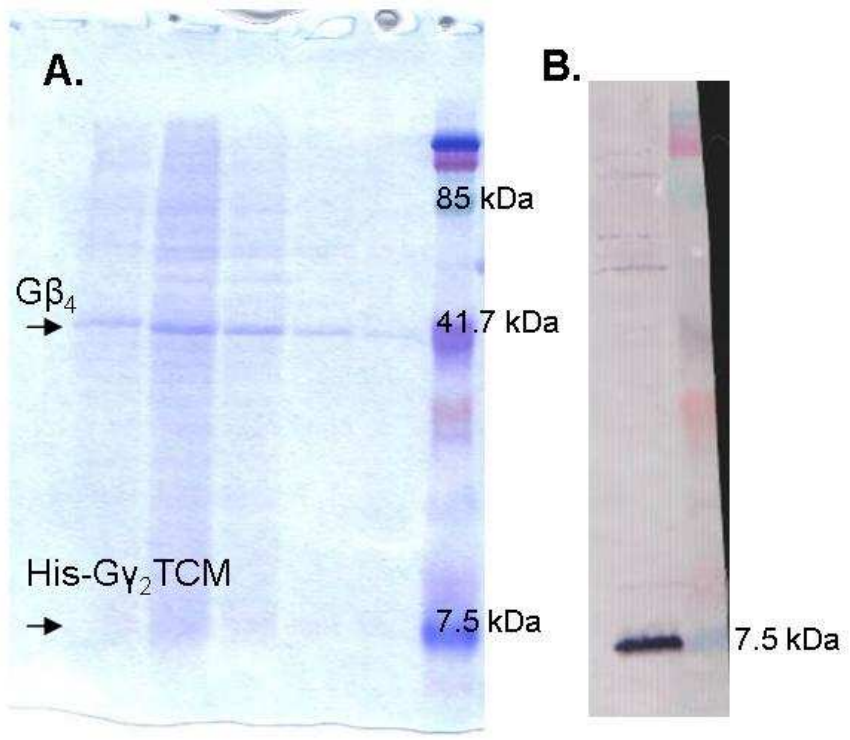

Figure 4.7: Expression and Purification of $G\beta_4\gamma_2$-TCM. (A) 1 L of *Sf*9 cells at a density of 2 x10^6 cells/mL were infected with recombinant $G\beta_4$ and His-tagged $G\gamma_2$-TCM baculoviruses with an MOI of ~2. The $G\beta_4\gamma_2$-TCM dimer was purified using Ni-NTA beads and eluted from the column with an excess of imidazole. **(B)** Expression of His-tagged $G\gamma_2$-TCM was confirmed by western blot using alkaline phosphate conjugated monoclonal anti poly-His antibody (1:5000).

The ability of $G\gamma_2$-TCM to bind to FlAsH was then compared to that of the TCM peptide. The fluorescence from FlAsH increased with the increasing concentration of $G\gamma_2$-TCM indicating that FlAsH was binding. However, the performance of the fusion protein was significantly poorer compared to the TCM peptide which produced much higher amounts of fluorescence from FlAsH (**Figure 4.8**). It therefore appeared that labelling low concentrations of fusion proteins was inefficient since overnight incubation was required and background fluorescence from unbound FlAsH was present. Labelling was subsequently carried out using a higher concentration of protein (μM) overnight and buffer exchange or washing was used to remove any unbound FlAsH. This method successfully produced labelled protein although the efficiency of labelling was

difficult to determine since unbound FlAsH has different spectral properties to TCM bound FlAsH and it was also unknown if the TCM peptide would produce the same amount of fluorescence upon binding FlAsH as a TCM within a fusion protein. This information will be required when trying to optimize labelling conditions and subsequent TR-FRET assays. The removal of non-labelled proteins could produce better signals. It would also be desirable to determine if FlAsH was specifically bound to the TCM and not other single or dithiols that may have resulted in the lower increases in fluorescence compared to the TCM peptide.

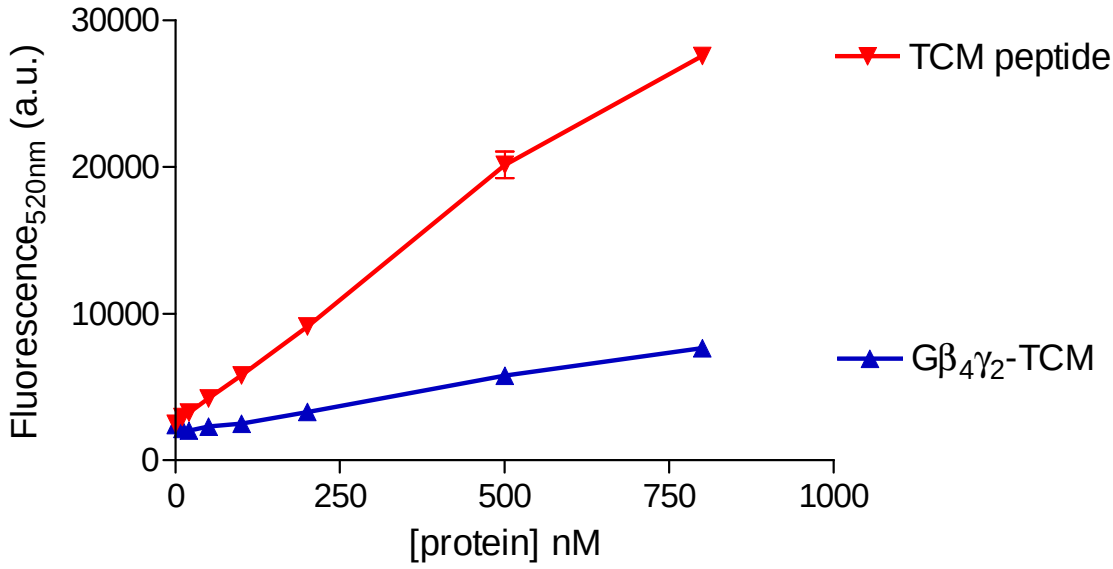

Figure 4.8: Comparison of FlAsH labelling efficiency of Gβ$_4$γ$_2$-TCM with the TCM peptide. 0 – 800 nM of the indicated protein was mixed with 4 µM FlAsH in Tb binding buffer and 1 mM TCEP and then incubated overnight at 4ºC. FlAsH fluorescence was then measured using the following parameters: λ_{ex} 485 nm, λ_{em} 520 nm. Data shown are mean ± SEM (n=3).

To show that the functionality of Gβ$_4$γ$_2$-TCM:FlAsH was also maintained in signalling from a GPCR, the fusion protein was reconstituted with Gα$_{i1}$ and either the M$_2$-muscarinic receptor or the α$_{2A}$-adrenergic receptor. In the absence of Gβγ, ligand mediated stimulation of [^{35}S]GTPγS binding was relatively low. The presence of Gβ$_4$γ$_2$ or Gβ$_4$γ$_2$-TCM significantly increased the signal possibly due to the presence of Gβγ resulting in more efficient coupling of the G-proteins to the

receptors. The results also showed that labelling with FlAsH did not have an adverse affect on protein function as measured by the [^{35}S]GTPγS binding assay following agonist activation (**Figure 4.9**). These results show that $G\beta_4\gamma_2$-TCM:FlAsH is functional in receiving signals from the receptor and interacting with the Gα-subunit to promote GTP binding as a result of agonist stimulation.

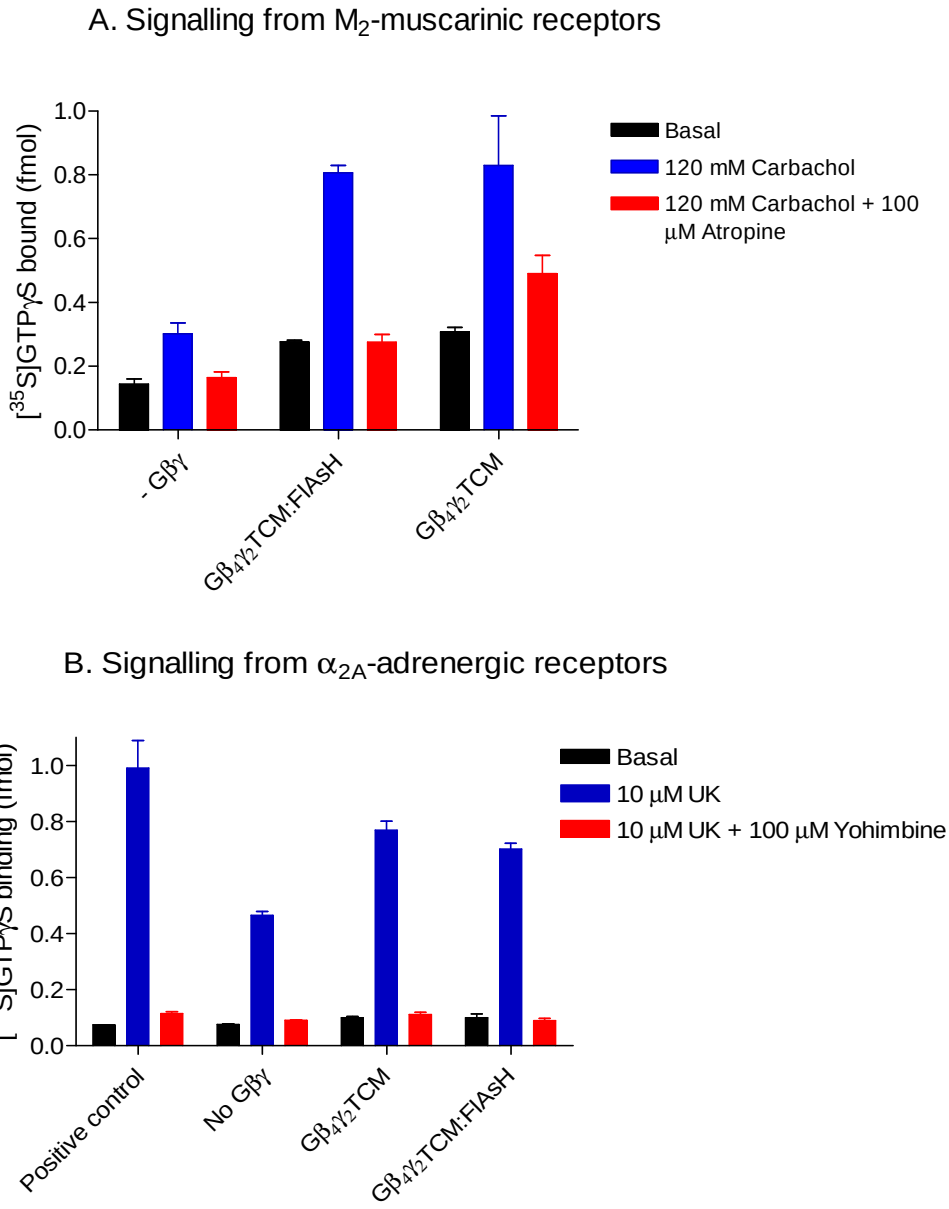

Figure 4.9: $G\beta_4\gamma_2$-TCM:FlAsH can receive signals from GPCRs in a reconstituted system. (A) 0.1 mg/mL of recombinant M_2-muscarinic receptors in *Sf*9 membranes or **(B)** 0.1 mg/mL of recombinant α_{2A}-adrenergic receptors were reconstituted with 20 nM purified $G\alpha_{i1}$ ± $G\beta_4\gamma_2$-TCM:FlAsH or $G\beta_4\gamma_2$-TCM. [^{35}S]GTPγS (0.2 nM) binding was stimulated by the agonists UK (10 µM) or carbachol (120 mM) and the effect blocked by the antagonists yohimbine (100 µM) or atropine (100 µM) for the α_{2A}-adrenergic or the M_2-muscarinic receptors, respectively. The

reactions were incubated for 90 min at 27ºC with shaking and triplicate 25 µL samples were filtered through GFC filters and washed with 3 x 4 mL of cold TMN buffer to remove unbound [^{35}S]GTPγS. Data shown are triplicate samples (mean ± SEM) of single representative experiments.

His-tagged $G\gamma_2$ with a TCM at the N-terminus (TCM-$G\gamma_2$) was also co-expressed with $G\beta_4$ and with $G\alpha_{i1}$ in *Sf*9 cells. The heterotrimer was purified using Ni-NTA beads and the TCMs labelled with FlAsH on the column overnight. This allowed unbound FlAsH and possibly non-specifically bound FlAsH to be washed from the column before the proteins were eluted. The non His-tagged $G\alpha_{i1}$ was eluted using aluminium fluoride and the His-tagged $G\beta_4$TCM-γ_2 dimer eluted from the column using an excess of imidazole (**Appendix 8.7**). Since $G\alpha_{i1}$ was present during FlAsH labelling, a comparison was made between the labelling of GβTCM-γ_2 and $G\alpha_{i1}$. Significantly higher levels of fluorescence were generated by $G\beta_4$TCM-γ_2 indicating that FlAsH was binding with some specificity to the protein containing a TCM since the fluorescence from $G\alpha_{i1}$ was lower (**Appendix 8.7**). However, it is also possible that more non-specific binding sites exist on Gβγ and a direct comparison is required to confirm labelling specificity. Time constraints prevented the full characterization of this TCM fusion protein with regard to function in receptor-mediated signalling in a reconstituted system with a GPCR. However, fusions to the N-terminus of $G\gamma_2$ with larger fluorescent proteins such as CFP, have not impaired the ability to form a heterotrimer, couple to a GPCR, or to interact with downstream effectors (Ruiz-Velasco, Ikeda 2001).

In summary, His-tagged $G\gamma_2$-TCM and TCM-$G\gamma_2$ were constructed and co-expressed with other G-protein subunits in *Sf*9 cells. The Gβγ dimers could then be purified using Ni-NTA chromatography and the TCMs labelled with FlAsH. Unbound FlAsH could be removed and FlAsH binding appeared to be occurring with some specificity since FlAsH labelling of $G\alpha_{i1}$ was minimal compared to that of $G\beta_4$TCM-γ_2. $G\gamma_2$-TCM was also shown to be functional when reconstituted into a signalling system with a GPCR.

4.3.4. Construction and characterization of TCM-$G\alpha_{i1}$

TCM-$G\alpha_{i1}$ was constructed using PCR with the forward primer encoding the TCM. This fragment was then ligated in pFastBac™1 and recombinant baculovirus generated. TCM-$G\alpha_{i1}$ was co-expressed with His-tagged $G\beta_4\gamma_2$ in *Sf*9 cells and the heterotrimer purified together using Ni-NTA beads. TCM-$G\alpha_{i1}$ was then eluted separately from $G\beta_4\gamma_2$ using aluminium fluoride although some TCM-$G\alpha_{i1}$ remained bound to His-tagged $G\beta_4\gamma_2$ (**Figure 4.10**). The TCM-$G\alpha_{i1}$ obtained was highly pure and it may be possible to increase the yield of TCM-$G\alpha_{i1}$ by infecting with this baculovirus separately from $G\beta\gamma$ and combining for purification or by optimising the virus titre for infection. Alternatively, it may prove that the affinity of TCM-$G\alpha_{i1}$ for $G\beta\gamma$ has been decreased resulting in a low yield of TCM-$G\alpha_{i1}$ after the washing procedures during purification.

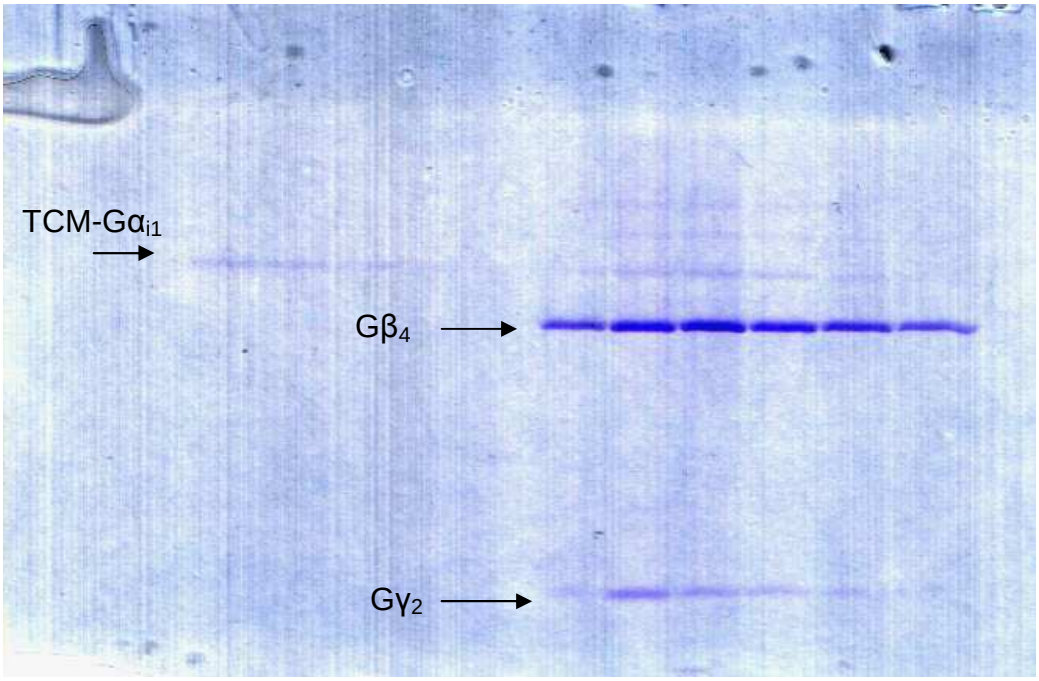

Figure 4.10: Polyacrylamide gel showing purified TCM-$G\alpha_{i1}$ captured using co-purified His-tagged $G\beta\gamma$. 1.8 L of *Sf*9 cells were infected with TCM-$G\alpha_{i1}$, $G\beta_4$, and His-$G\gamma_2$ baculoviruses at a MOI of 2 for 72 hr. The heterotrimeric G-protein was purified using Ni-NTA beads and the non His-tagged TCM-$G\alpha_{i1}$ was eluted from His-tagged $G\beta_4\gamma_2$ using AlF_4^-. The His-tagged $G\beta\gamma$ dimer was then eluted from the Ni-NTA column using an excess of imidazole.

TCM-$G\alpha_{i1}$ was reconstituted with the M_2-muscarinic receptor or the α_{2A}-adrenergic receptor into functional signalling systems with $G\beta\gamma$. The presence of TCM-$G\alpha_{i1}$ increased agonist stimulated

[^{35}S]GTPγS binding compared to when no Gα was present and this was blocked by the presence of the respective antagonists for both the M_2-muscarinic receptor and the α_{2A}-adrenergic receptor. However, in both cases the amount of stimulation decreased compared to that achieved by using $G\alpha_{i1}$ (**Figure 4.11**) and this may further indicate that the affinity of TCM-$G\alpha_{i1}$ for Gβγ has been reduced by the TCM fusion. Nevertheless, the results indicated that TCM-$G\alpha_{i1}$ remained functional in receiving signals from the receptor and in this case, the N-terminal fusion appeared to be reasonably well tolerated.

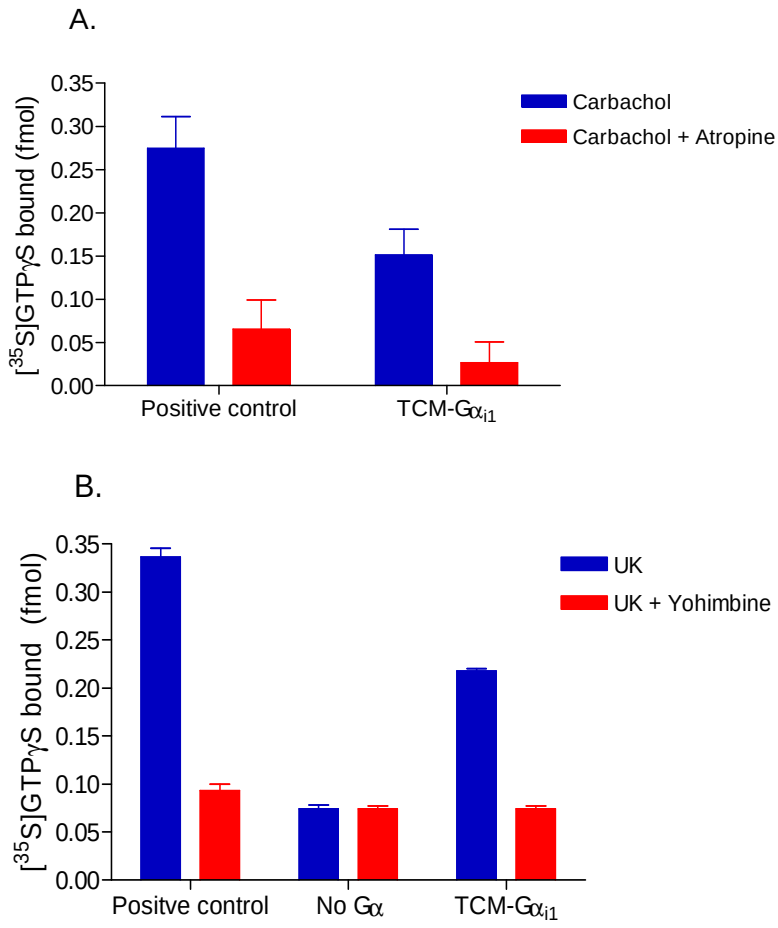

Figure 4.11: TCM-$G\alpha_{i1}$ can receive signals from the M_2-muscarinic receptor and the α_{2A}-adrenergic receptor. (A) 0.1 mg/mL of recombinant M_2-muscarinic receptors in *Sf*9 membranes were reconstituted with 20 nM purified G-proteins (positive control: $G\alpha_{i1}\beta_1\gamma_2$, TCM-Gα: TCM-$G\alpha_{i1}\beta_1\gamma_2$). [^{35}S]GTPγS (0.2 nM) binding was stimulated by the agonist carbachol (120 mM) and the effect blocked by the antagonist atropine (100 µM). The reactions were incubated for 90 min at 27ºC with shaking and triplicate 25 µL samples were filtered through GFC filters and washed with 3 x 4 mL of cold TMN buffer. Data shown are triplicate samples (mean ± SEM) of a single representative experiment from which basal levels of [^{35}S]GTPγS binding have been deducted. (B) 0.1 mg/mL of recombinant α_{2A}-adrenergic receptors in *Sf*9 membranes were reconstituted

with 20 nM purified G-proteins (positive control: $G\alpha_{i1}\beta_1\gamma_2$, No Gα: $G\beta_1\gamma_2$, TCM-Gα: TCM-$G\alpha_{i1}\beta_1\gamma_2$). [^{35}S]GTPγS (0.2 nM) binding was stimulated by the agonist UK (10 μM) and the effect blocked by the antagonist yohimbine (100 μM). The reactions were incubated for 90 min at 27 ºC with shaking and triplicate 25 μL samples were filtered through GFC filters and washed with 3 x 4 mL of cold TMN buffer. Data shown are triplicate samples (mean ± SEM) of a single representative experiment.

Purified TCM-$G\alpha_{i1}$ was then assessed for its ability to bind FlAsH and was compared to FlAsH binding to the TCM peptide alone. The TCM of $G\alpha_{i1}$ was in the format of a slightly longer peptide (Phe-Leu-Asn-**Cys-Cys-Pro-Gly-Cys-Cys-**Met-Glu-Pro-Gly-Gly-Gly) that had been reported to improve FlAsH binding and fluorescence in mammalian cells (Martin *et al*. 2005). However, FlAsH binding to 500 nM TCM-$G\alpha_{i1}$ did not increase above the background fluorescence of FlAsH alone, as occurs with the TCM peptide (**Figure 4.12)**. This indicates that under these conditions, FlAsH was not binding to TCM-$G\alpha_{i1}$ perhaps due to the fusion protein construction interfering with accessibility of FlAsH to the TCM. Alternatively, since traditional prompt fluorescence measurements were being used, scattering and autofluorescence when the fusion protein was present may have prevented the detection of FlAsH binding to the TCM and the subsequent increase in fluorescence at the concentrations used. Labelling of the more concentrated stock of TCM-$G\alpha_{i1}$ was later carried out but time constraints prevented its characterization.

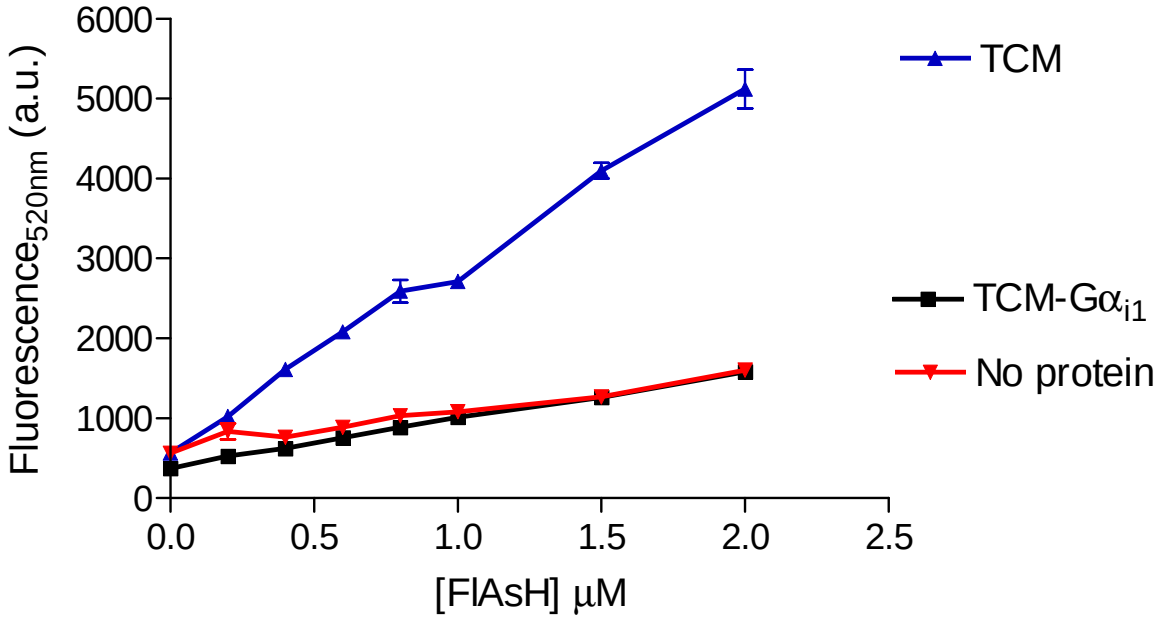

Figure 4.12: Comparison of FlAsH binding to TCM-Gα$_{i1}$ and the TCM peptide. 500 nM protein was mixed with 0-2 µM FlAsH in a final volume of 100 µL in Tb binding buffer containing 1 mM TCEP. After incubation overnight at 4ºC, FlAsH fluorescence was measured using the following parameters: λ_{ex} 485 nm, λ_{em} 520 nm. Data shown are mean ± SEM (n=3).

In summary, TCM-Gα$_{i1}$ was encoded in a recombinant baculovirus and expressed in *Sf*9 cells with Gβγ. TCM-Gα$_{i1}$ was then purified separately from Gβγ using aluminium fluoride and was shown to be functional receiving signals from agonist-activated GPCRs. However, FlAsH binding to the TCM of TCM-Gα$_{i1}$ was not apparent at the concentrations used and alternative FlAsH labelling conditions or fusion constructs need to be investigated further.

4.3.5. Construction and Characterization of His-TCM-Gα$_{i1}$

His-tagged TCM-Gα$_{i1}$ (His-TCM-Gα$_{i1}$) was constructed from the same PCR product as TCM-Gα$_{i1}$ but a His-tag was incorporated onto the N-terminus before recombinant baculovirus was generated. His-TCM-Gα$_{i1}$ was expressed in *Sf*9 cells and purified using Ni-NTA beads and eluted from the column with an excess of imidazole (**Figure 4.13**). The yield of a His-tagged protein is generally greater than non His-tagged proteins eluted from the column using aluminium fluoride (for example TCM-Gα$_{i1}$). Contaminating proteins are also more commonly present with His-

tagged protein, although for the purposes of the following experiments, the degree of purification from IMAC alone was sufficient.

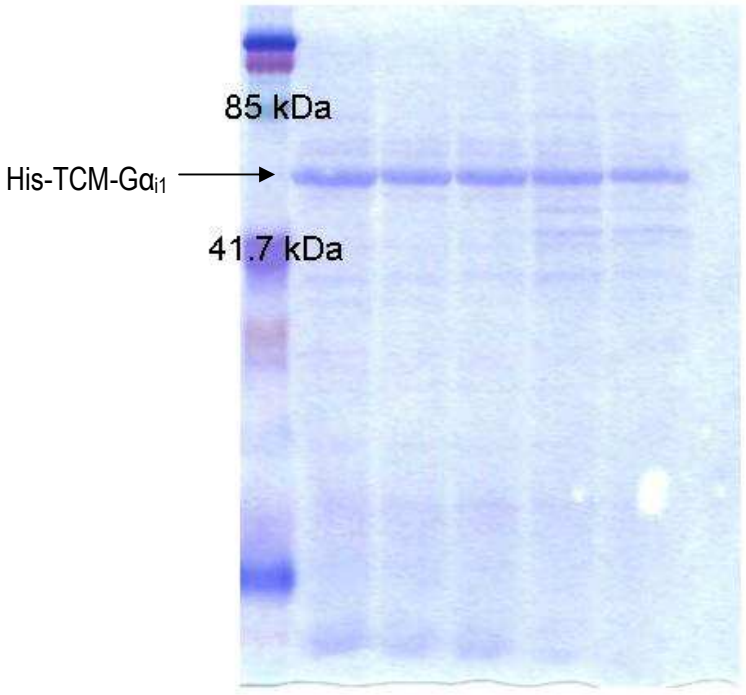

Figure 4.13: Purification of His-TCM-Gα$_{i1}$. 1 L of *Sf*9 cells was infected with recombinant His-TCM-Gα$_{i1}$ baculovirus at an MOI of 2 for 72 hr. His-TCM-Gα$_{i1}$ was purified using Ni-NTA beads and eluted from the column using an excess of imidazole.

FlAsH binding to His-TCM-Gα$_{i1}$ was subsequently investigated and while His-TCM-Gα$_{i1}$ performed better than other TCM fusion proteins discussed so far, the performance remained inferior to that of the TCM peptide, again indicating that the fusion protein format had some effect on the ability to bind FlAsH or in detecting the resulting fluorescence (**Figure 4.14**). However, FlAsH fluorescence with the His-TCM-Gα$_{i1}$ construct increased up to 4-fold when low µM concentrations of FlAsH and protein were used (**Figure 4.15**). Subsequently, His-TCM-Gα$_{i1}$ was labelled with FlAsH on the Ni-NTA column after purification but prior to elution so that non-bound FlAsH could be removed by washing the column.

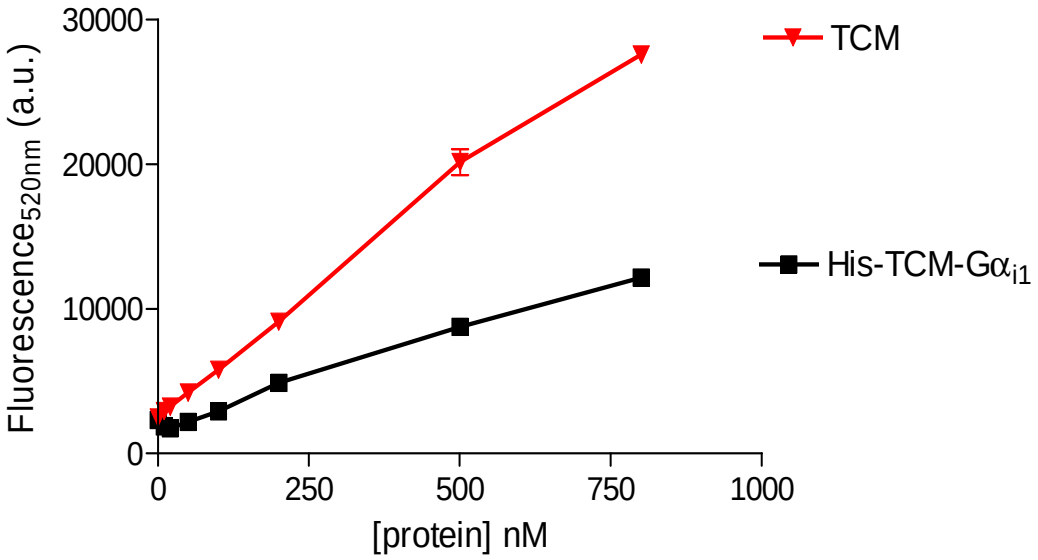

Figure 4.14: His-TCM-Gα$_{i1}$ binding to FlAsH compared to the TCM peptide. Increasing concentrations of TCM peptide or purified His-TCM-Gα$_{i1}$ (0-800nM) were mixed with 4 µM FlAsH and incubated overnight at 4ºC. FlAsH fluorescence was then measured using the following parameters: λ$_{ex}$ 485 nm, λ$_{em}$ 520 nm. Data shown are mean ± SEM (n=3).

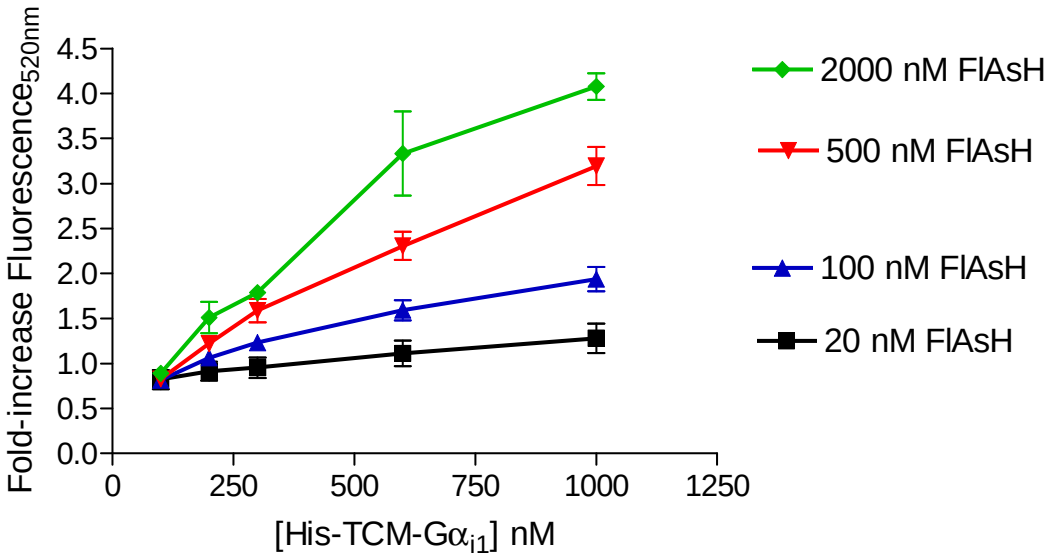

Figure 4.15: FlAsH binding increases with protein and FlAsH concentration. 100-1000 nM His-TCM-Gα$_{i1}$ was mixed with 20-2000 nM FlAsH in a final volume of 100 µL in Tb binding buffer and incubated overnight at 4°C. FlAsH fluorescence was then measured using the following parameters: λ$_{ex}$ 485 nm, λ$_{em}$ 520 nm. Data shown is mean ± SEM (n=3) of the fold increase over background from FlAsH alone in solution.

To investigate if the functional integrity of His-TCM-Gα had been maintained, it was reconstituted into a receptor signalling system with Gβγ and the M_2-muscarinic receptor. However, upon reconstitution of His-TCM-$G\alpha_{i1}$ either with or without FlAsH, it was found that [^{35}S]GTPγS-binding to the G-protein subunit was no longer stimulated by agonist binding to the M_2-muscarinic receptor (**Figure 4.16**) or the α_{2A}-adrenergic receptor (data not shown). His-TCM-$G\alpha_{i1}$ was not co-purified with Gβγ where an interaction could have been observed, so this lack of signalling function could be due to the inability to form a heterotrimer with Gβγ. However, even when Gβγ is absent, usually a small amount of signalling can be detected when a functional Gα-subunit is present.

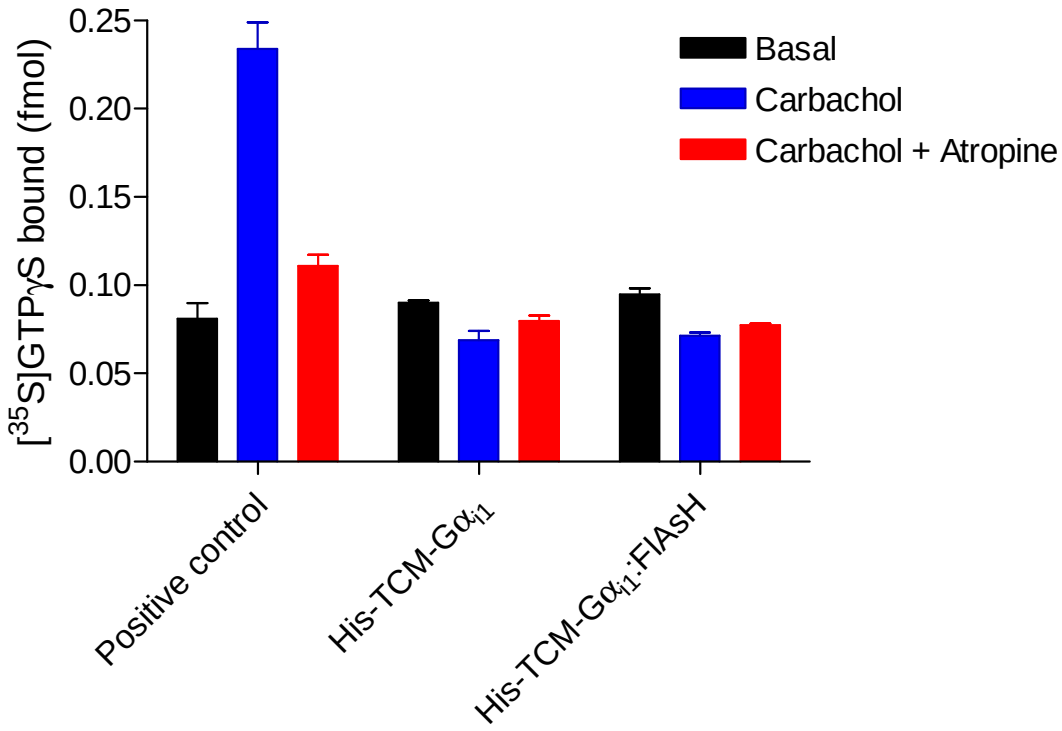

Figure 4.16: His-TCM-$G\alpha_{i1}$ is non-functional in receiving signals from the M_2-muscarinic receptor. 20 nM of $G\alpha_{i1}$ (positive control) or His-TCM-$G\alpha_{i1}$ were reconstituted with 0.01 mg/mL of M_2-muscarinic receptor and 20 nM $G\beta_4\gamma_2$. [^{35}S]GTPγS (0.2 nM) binding was stimulated by the agonist carbachol (120 mM) and the effect blocked by the antagonist atropine (100 µM). The reactions were incubated for 90 min at 27ºC with shaking and triplicate 25 µL samples were filtered through GFC filters and washed with 3 x 4 mL of cold TMN buffer. Data shown are triplicate samples (mean ± SEM) of a single representative experiment.

The failure of His-TCM-Gα_{i1} in responding to signals from GPCRs was further investigated by determining if His-TCM-Gα_{i1} could bind [^{35}S]GTPγS. Interestingly, although His-TCM-Gα_{i1} appeared unable to receive signals from GPCRs, the [^{35}S]GTPγS binding ability appeared increased compared to Gα_{i1} and TCM-Gα_{i1} (**Figure 4.17**). This was in contrast to the His-LBT2-Gα_{i1} fusion protein that was unable to respond to signals from GPCRs and appeared to have decreased [^{35}S]GTPγS binding ability. These results indicate that the interaction of His-TCM-Gα_{i1} with the receptor may be impaired, possibly due to the interaction with Gβγ also being impaired and it would seem that the type of fusion or length of extension to the N-terminus of Gα could affect different aspects of subunit function.

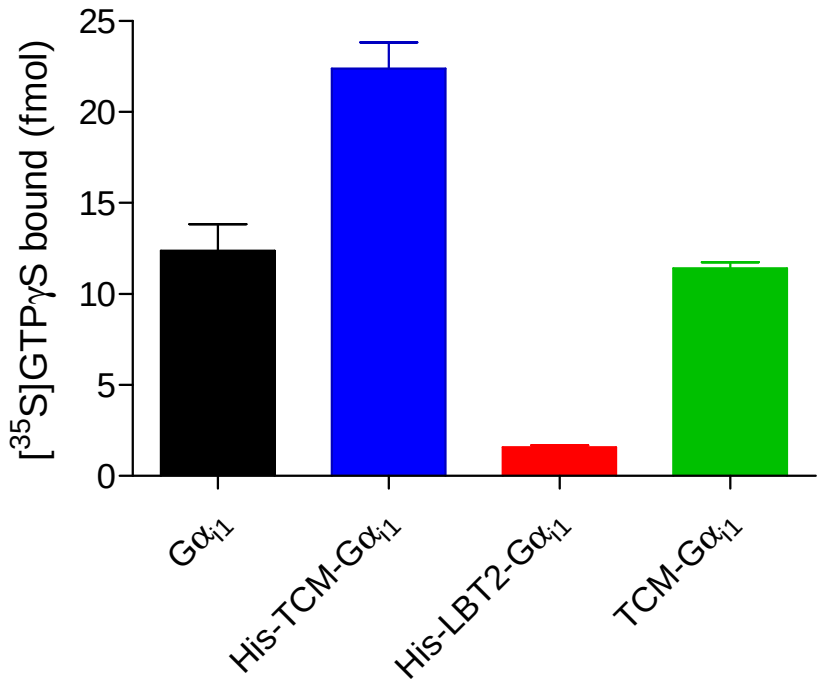

Figure 4.17: His-TCM-Gα_{i1} binds to [^{35}S]GTPγS. 40 nM of Gα was mixed with 1 nM [^{35}S]GTPγS and incubated in a shaking water bath for 90 min at 27ºC and triplicate 25 µL samples were filtered through GFC filters and washed with 3 x 4 mL of cold TMN buffer. Data shown are triplicate samples (n=6, mean ± SEM) of 2 experiments.

In summary, His-TCM-Gα_{i1} was expressed in *Sf*9 cells and a higher yield of purified protein obtained compared to TCM-Gα_{i1}. FlAsH binding to His-TCM-Gα_{i1} was also more successful. However, the functional integrity of the Gα-subunit of His-TCM-Gα_{i1} was not preserved. Although,

the GTP binding ability of the subunit appeared maintained, the ability to couple to and receive signals from a GPCR appeared to be abolished.

4.4. Further discussion and conclusions

The advantages of FlAsH-labelling include the use of a smaller binding domain, only 6 amino acids in length, compared to the widely used fluorescent proteins such as green fluorescent protein (GFP) and its variants which are 220 amino acids in length and often larger than the protein being investigated. A small motif such as the TCM is less likely to be disruptive to protein function and this has been shown in a study monitoring the activation of the A_{2A}-adenosine receptor (Hoffmann *et al*. 2005). CFP/YFP FRET was used to monitor receptor activation via conformational changes induced by agonist binding. However, the inclusion of the CFP rendered the receptor unable to activate its downstream effector, adenylyl cyclase. Replacement of CFP with a TCM (and labelling with FlAsH) restored receptor function while also enabling receptor conformations to be monitored using FRET. This chapter examined the feasibility of fusing TCMs to G-protein subunits in four different constructs and labelling with FlAsH. Although the TCMs used were small tags of between 6-15 amino acids, in some cases basic protein function was still disturbed (**Table 4.1**).

Construct	FlAsH binding	Functionality
$G\beta_4\gamma_2$-TCM	Poorer than TCM peptide. Possible to label in solution .	Yes
$G\beta_4$TCM-γ_2	Poor compared to TCM Labelled on column	Not tested
TCM-$G\alpha_{i1}$	No Labelling detected in solution	Yes
His-TCM-$G\alpha_{i1}$	Poor compared to TCM. Possible to label on column.	Binds GTP but does not receive signals from GPCRs

Table 4.1: Summary of FlAsH binding and signalling properties of G-protein subunit constructs fused to TCMs.

$G\alpha_{i1}$ had proved problematic when trying to maintain the integrity of the protein with regard to signalling function when LBTs were fused to the N-terminus, the same site to which TCMs were fused. Likewise, His-TCM-$G\alpha_{i1}$ was not capable of binding GTP in response to GPCR activation.

This was similar to His-LBT2-Gα_{i1}, however, comparison of the GTP binding ability showed marked differences with the GTP binding ability of His-TCM-Gα_{i1} being maintained, and possibly increased, while this function was abolished with the His-LBT2-Gα_{i1} fusion construct. The N-terminal extension was slightly longer in His-LBT2-Gα_{i1} and that may have resulted in the different functional ability observed. Furthermore, the structure of the extension itself may have contributed to a structural anomally that produced this loss of functionality. Interestingly, TCM-Gα_{i1} could bind GTP and respond to signals from GPCRs although its N-terminal extension was a mere 6 amino acids shorter due to the absence of the His-tag and of course, a His-tag alone is well tolerated indicating that the length of the extension could indicate how well the fusion will be tolerated. As discussed previously, a more appropriate fusion site could also be investigated. Gα_{i1} has successfully been tagged with YFP within the α-helical domain of the subunit (Bunemann, Frank & Lohse 2003) and TCMs have previously been successfully introduced within α-helical domains of other proteins.

TCM fusion to Gγ subunits appeared to be more readily tolerated and Gγ_2-TCM was able to function in a reconstituted signal transduction system. Fusions of larger GFP mutants to the N-terminus of Gγ_2 have been reported to be successful without impairing heterotrimer formation, coupling to receptors or interactions with downstream effectors (Ruiz-Velasco, Ikeda 2001). However, fusions to the C-terminus have previously resulted in defective membrane targeting presumably due to the lipid modification at the C-terminus being abolished due to the fusion, and altered interactions with downstream effectors were also reported (Bunemann, Frank & Lohse 2003). In this study, it could also be assumed that the post- translational modification of Gγ_2-TCM was absent although this did not appear to impair the purification of Gγ_2-TCM from the membrane fraction of *Sf*9 cells with Gβ_4, nor the ability to increase [^{35}S]GTPγS binding to Gα upon agonist stimulation of a GPCR in an *in vitro* reconstituted system. It remains to be seen if downstream

interactions are effected by the smaller TCM motif compared to GFP variants. It would be of interest to investigate whether $G\gamma_2$ fused to a fluorescent protein at its C-terminus was non-functional in the systems used here to determine if the smaller TCM has less impact on protein function.

Compared to the TCM peptide, all of the fusion constructs appeared to have a decreased ability to bind to FlAsH resulting in a decreased level of fluorescence output. This could indicate that the fusion was having some effect on the tag which may have lowered the affinity or accessibility of FlAsH to the TCM. Alternatively, the presence of the larger fusion protein, and possibly contaminating proteins, increased the incidence of light scatter making the fluorescence from FlAsH binding less distinguishable from when the TCM peptide was used alone. Furthermore, with regard to labelling of the fusion proteins with FlAsH, there was no apparent benefit to using the optimized TCM that was fused to the Gα subunits in this *in vitro* system. However, while the specificity of FlAsH binding to TCMs has been questioned (Hearps *et al*. 2007; Stroffekova, Proenza & Beam 2001), in this study little non-specific binding to proteins without a TCM was detected, although the *in vitro* nature of this study lends itself to thorough washing procedures that may have reduced the extent of this problem. Due to the apparent poor performance of FlAsH binding to the TCM in the context of a fusion protein, it was found to be convenient and more successful to pre-label the proteins with FlAsH so that once thawed from storage they were immediately ready to be used in assays. To confirm labelling specificity and efficiency, an alternate method such as mass spectrometry would be required and could be useful for optimizing FRET assays. Likewise, it could also prove useful to remove any unlabelled proteins.

Improvements are still being made to the biarsenical dyes and the TCMs, and recent developments have seen alternative motifs developed that improve binding affinities or brightness

of the complex and these are discussed with regard to improving FlAsH labelling (as an acceptor for terbium in TR-FRET) in the following chapter. Overall, it appears that fusing a TCM to a G-protein subunit and labelling with FlAsH is feasible although care needs to be taken in maintaining the integrity of the protein of interest even though the motif is significantly smaller than commonly used fluorescent proteins. The performance of the TCM binding to FlAsH when fused to a protein appeared poorer than expected, however, by pre-labelling with FlAsH, proteins could be adequately labelled for TR-FRET applications and this will be investigated further in the following chapter.

5. TCM and LBT fusion proteins as TR-FRET partners in a G-protein subunit interaction assay

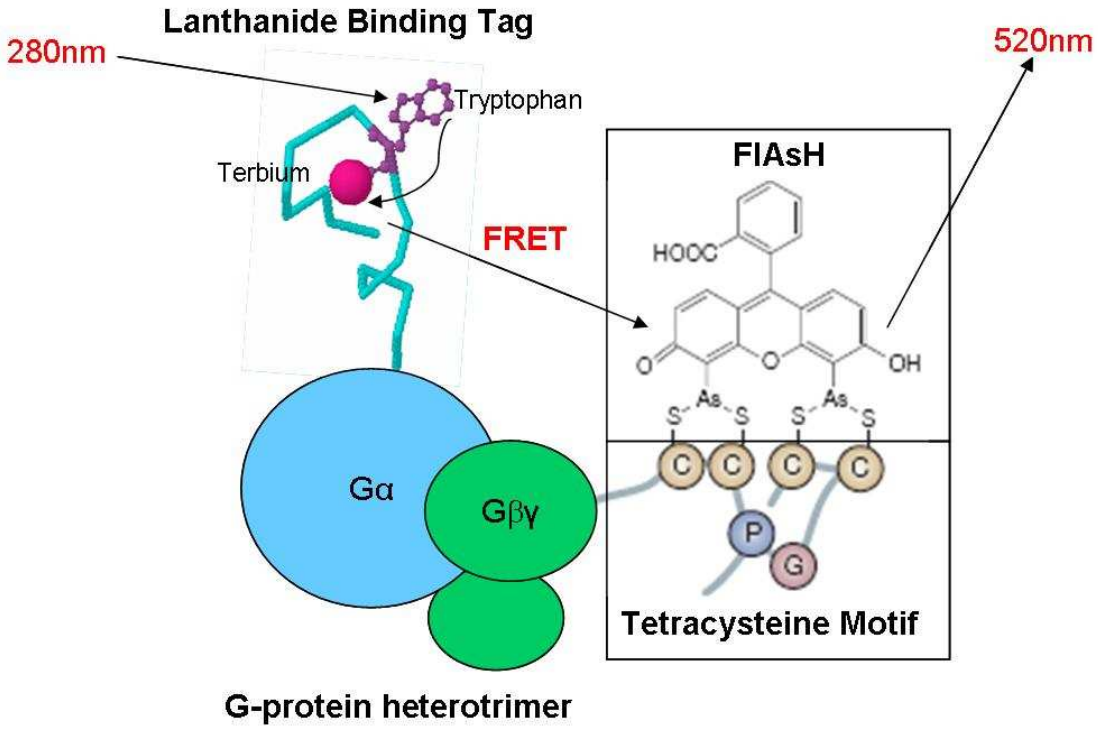

5.1. Introduction

FRET studies have usually made use of green fluorescent protein variants CFP and YFP to site-specifically label interacting proteins. While these assays have shed light on many biochemical interactions, their use in high throughput screens has been hampered due to the small changes in the FRET signal due to non-ideal spectral overlap and interference from background fluorescence. The development of LBTs has generated a method for site-specifically labelling a protein with a much smaller fluor, for use in TR-FRET. Compared to FRET, TR-FRET has the benefit of a lower background signal since autofluorescence and scattering can be effectively removed using time-gating. At the commencement of this project, proteins fused to a LBT had so far included only ubiquitin (76 amino acids) to which terbium binding was demonstrated (Franz, Nitz & Imperiali 2003). Later, SH2 domains (100 amino acids) (Sculimbrene, Imperiali 2006) and GST (220 amino acids) (Goda *et al*. 2007) fusions were also demonstrated although the latter study did not examine TR-FRET interactions. Using TR-FRET, the SH2 domain tagged with a LBT and labelled with terbium, could be seen to interact with synthesized peptide ligands labelled with BODIPY but LBTs had yet to be exploited with a similar site-specific labelling technique such as that of FlAsH:TCM.

In this chapter, the utility of the fusion proteins as TR-FRET partners is examined first in combination with Alexa546 or CS124-DTPA-EMCH:Tb to confirm their use with known TR-FRET partners. The ability of terbium-labelled LBTs to transfer energy to FlAsH-labelled TCMs, when fused to respective G-protein subunits, is then examined in this chapter towards the development of a cell-free, generic, G-protein signalling assay platform (**Figure 5.1**).

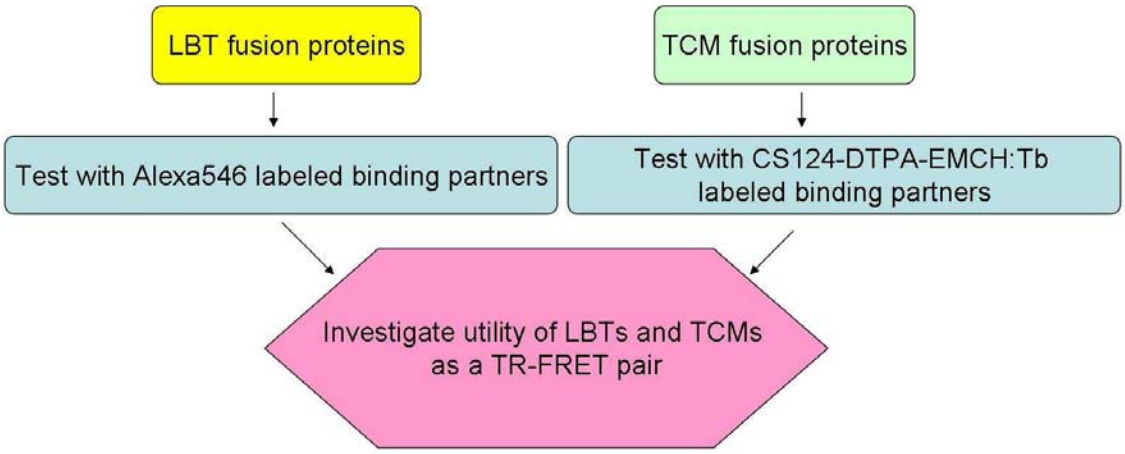

Figure 5.1: Flow diagram of investigation of fusion proteins as TR-FRET partners.

5.2. Methods

5.2.1. Protein production and labelling

LBT and TCM fusion proteins were generated as previously described in chapters 3 and 4, respectively. LBTs were labelled with terbium during the TR-FRET assay while FlAsH labelling, unless otherwise stated, was carried out on purified protein and unbound FlAsH removed prior to -80ºC storage.

5.2.2. TR-FRET assays

TR-FRET assays were carried out in black 96-well plates. As per other TR-FRET assays described earlier, 20x working solutions of proteins were applied separately to the wells with any other indicated components and reactions were commenced upon the addition of Tb binding buffer to make the final assay volume up to 100 µL, which resulted in the mixing of the assay components. After the required incubation period, TR-FRET measurements were taken using a Victor3 multilabel plate reader using the indicated TR-FRET settings

5.2.3. Data analysis

Data was analysed using Prism™ 4.00 (GraphPad software Inc., San Diego CA, USA). Data is presented as mean ± SEM where n is equal or greater than 3. If error bars are not visible they are behind the symbols. Apparent *K*d values were generated by fitting a one-site binding curve of the equation Y= Bmax . X / (*K*d + X).

5.3. Results and Discussion

5.3.1. LBT2-Gα_{S25} TR-FRET with Gβγ:Alexa

Although it was not possible to purify LBT2-Gα_{S25} during the course of this study, terbium binding to LBT2-Gα_{S25} in membrane preparations had been demonstrated as described earlier. The potential of LBT2-Gα_{S25} to be used in TR-FRET assays was then investigated. The addition of purified, Alexa546 labelled Gβγ (Gβγ:Alexa) to Tb:LBT2-Gα_{S25} increased the emission of Alexa at 572 nm by ~2-fold and was accompanied by a slight decrease in terbium luminescence at 545 nm, which could indicate an association between Gβγ:Alexa and Tb:LBT2-Gα_{S25} (**Figure 5.2**). This was further supported since the addition of unlabelled Gα_{i1} decreased the emission of Alexa suggesting that the unlabelled protein was competing for binding with labelled proteins reducing the fluorescent signal. Protease treatment with proteinase K (PK) should cleave the LBT and both proteins at a number of sites. The treatment resulted in a reduction of both Alexa546 fluorescence and terbium luminescence. The terbium luminescence is expected to decrease due to the destruction of the LBT as has been previously shown. Although the protease would cut Gβγ:Alexa, it should not intrinsically affect the Alexa fluorescence, therefore the decrease in fluorescence at 572 nm could be attributed to a decrease in TR-FRET due to either the lack of terbium labelled proteins or protein interactions.

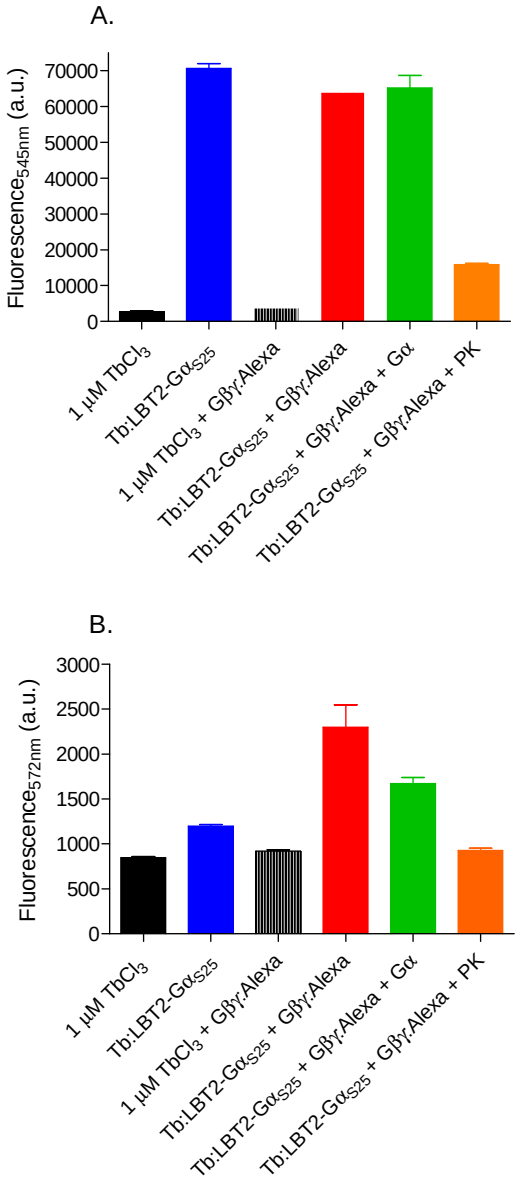

Figure 5.2: Association of Tb:LBT2:Gα_{S25} with Gβγ:Alexa measured using TR-FRET. 2 µg of LBT2:Gα_{S25} preparation was mixed with 1 µM $TbCl_3$ and 50 nM Gβγ:Alexa. As controls, unlabelled Gα_{i1} (2.47 µM) or proteinase K (PK) (0.2 mg/mL) was added. The final volume was made up to 100 µL with Tb binding buffer and after a 10 min incubation, the terbium and Alexa emissions were measured using a Victor3 plate reader set for time-resolved fluorescence with the following parameters: λ_{ex} 280 nm, λ_{em} 545 nm and 572 nm, 50 µs delay and 900 µs counting duration. Data shown are mean ± SEM (n=3). **(A)** Shows the data obtained at 545 nm and **(B)** the data obtained at 572 nm.

LBT2-Gα_{S25} has been shown to be a potential TR-FRET partner although improvements in the signal:noise ratio may be possible if unbound or non-specifically bound terbium could be removed or reduced. Washing procedures may achieve this, although, the nature of the membrane

preparations in which LBT2-$G\alpha_{S25}$ is present makes this difficult and it is unknown whether the affinity between terbium and the LBT would be enough to withstand washing.

Although His-LBT2-$G\alpha_{i1}$ was observed to bind terbium with high affinity, no TR-FRET signal could be generated with Gβγ:Alexa using nM concentrations of protein. This could have been a result of the lower luminescence intensity generated by terbium-binding and/or the integrity of the Gα subunit being disrupted by the LBT, which resulted in the loss of GTP binding and signalling capability.

5.3.2. Investigation of the LBT1-$G\beta_4\gamma_2$ interaction with Gα:Alexa using TR-FRET

Although the affinity for terbium and amount of luminescence from LBT1-$G\beta_4\gamma_2$ was lower than that of the LBT2 peptide, the ability to observe an interaction between LBT1-$G\beta_4\gamma_2$ and $G\alpha_{i1}$ subunits labelled with Alexa546 (Gα:Alexa) using TR-FRET was investigated. However, while a signal above the background of Tb:LBT1-$G\beta_4\gamma_2$ was observed, a similar response from Gα:Alexa mixed with $TbCl_3$ was also apparent suggesting that this was probably not a signal from the specific interaction of Gαβγ (**Figure 5.3**). Further investigation showed that at higher concentrations of $TbCl_3$, luminescence increased in the presence of $G\alpha_{i1}$ indicating that non-specific terbium binding was interfering with the generation of a measurable TR-FRET signal. $G\alpha_{i1}$ contains a Mg^{2+} binding site, which have been observed to bind terbium with lower affinity in other proteins (Girardet, Dupont & Lacapere 1989). However, the presence of an excess of magnesium chloride failed to compete with terbium for binding (data not shown). Using a lower concentration of terbium could reduce non-specific binding but this requires the LBT to have a higher affinity for terbium. Alternatively, washing to remove non-specifically bound Tb^{3+} could again have benefits, although, due to the decreased affinity for terbium, this may not be feasible.

This has demonstrated the importance of maintaining a high affinity between the LBT and terbium to generate a TR-FRET signal that is produced due to a specific protein interaction.

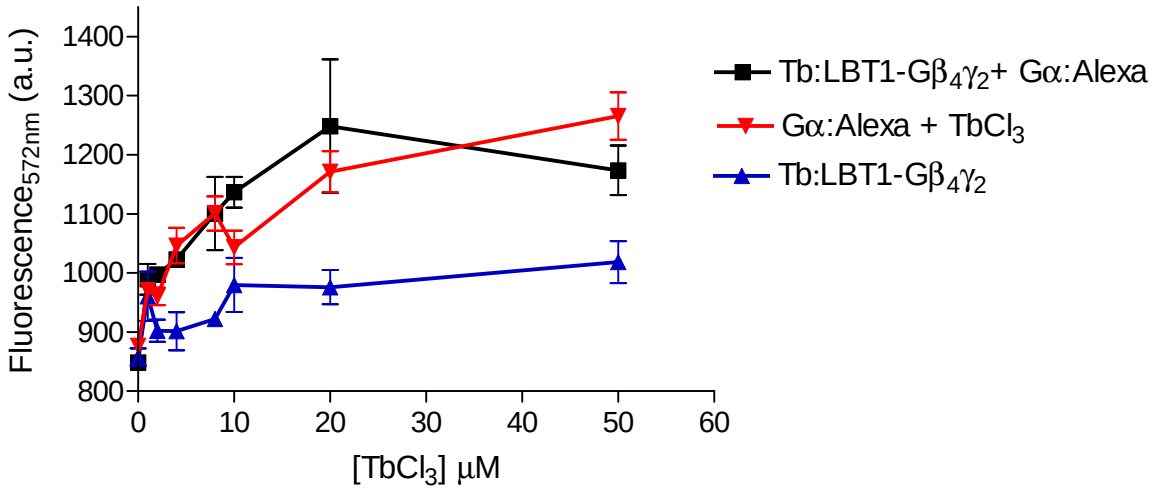

Figure 5.3: Association of LBT1-Gβ$_4$γ$_2$ with Gα$_{i1}$-Alexa. 100 nM LBT1-Gβ$_4$γ$_2$ was mixed with 20 nM Gα$_{i1}$:Alexa and varying concentrations of $TbCl_3$ as indicated. The final volume was made up to 100 µL with Tb binding buffer and after a 10 min incubation, TR-FRET was measured using a Victor3 plate reader set for time-resolved fluorescence with the following parameters: λ_{ex} 280 nm, λ_{em} 572 nm, 50 µs delay and 900 µs counting duration. Data shown are mean ± SEM (n=3).

5.3.3. Interaction of Gβ$_4$γ$_2$-TCM:FlAsH with Gα$_{i1}$:Tb

Pre-labelled Gβ$_4$γ$_2$-TCM:FlAsH was then investigated concerning its ability to act as a TR-FRET acceptor binding partner for Gα$_{i1}$ labelled with CS124-DTPA-EMCH:Tb (Gα:Tb). When 15 nM Gβ$_4$γ$_2$-TCM:FlAsH was added to 10 nM Gα:Tb the TR-FRET signal increased 3-fold above background fluorescence from Gα:Tb. This signal could be reduced to near background levels by the presence of unlabelled Gα showing that the TR-FRET signal was due to a specific interaction (**Figure 5.4**A). The interaction between Gβ$_4$γ$_2$-TCM:FlAsH and Gα:Tb had an apparent *K*d of 3.6 nM indicating that a high affinity interaction was occurring (typical of a Gαβγ interaction) and that Gβ$_4$γ$_2$-TCM:FlAsH could be used as a TR-FRET acceptor binding partner (**Figure 5.4**B). Although good fold-increases in fluorescence (signal:noise) could be obtained, fluorescence counts were lower than those obtained when using the CS124-DTPA-EMCH:Tb:Alexa546 TR-FRET pair. This could be explained in part by FlAsH excitation occurring via the first emission

peak of terbium, which is significantly less intense than the second emission peak that excites Alexa546.

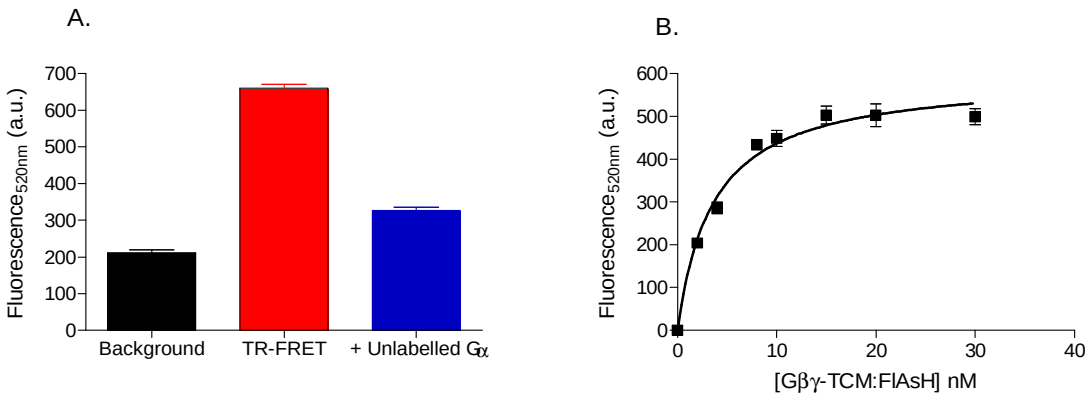

Figure 5.4: $G\beta_4\gamma_2$-TCM:FlAsH association with $G\alpha_{i1}$:Tb. (A) When 10 nM of Gα:Tb and 10 nM of $G\beta_4\gamma_2$-TCM:FlAsH were mixed together, there was a >3-fold increase in signal that could be reduced by the addition of 1.3 µM unlabelled Gα. **(B)** A $G\beta_4\gamma_2$-TCM:FlAsH dose curve gave an apparent *K*d of 3.6 ± 0.5 nM. 10 nM $G\alpha_{i1}$:Tb was mixed with 0-30 nM of $G\beta_4\gamma_2$-TCM:FlAsH. Both experiments were in a final volume of 100 µL in a black 96-well plate. After a 5 min incubation, a Victor3 multilabel plate reader was used to measure TR-FRET with the following parameters: λ_{ex} 340 nm, λ_{em} 520 nm, 50 µs delay and 900 µs counting duration. Data shown are mean ± SEM (n=3).

5.3.4. Investigation of TR-FRET using GβTCM-γ_2

$G\beta_4$TCM-γ_2 had also been pre-labelled with FlAsH before adding to TR-FRET assays with $G\alpha_{i1}$:Tb and increases up to 5-fold above background were generated (**Figure 5.5**A). Doses of $G\beta_4$TCM-γ_2:FlAsH against $G\alpha_{i1}$:Tb, increased fluorescence until saturation was reached, however, the results indicated a lower than expected affinity between Gαβγ with a *K*d of 21.5 ± 3.2 nM generated, approximately 10x greater than has been previously measured using TR-FRET (Leifert *et al*. 2006) (**Figure 5.5**B). This decrease in apparent affinity could be caused by a low FlAsH-labelling efficiency resulting in a higher concentration of protein being required to generate a signal. Similarly, it is possible that some unlabelled Gα contamination remains in the $G\beta_4$TCM-γ_2 preparation due to incomplete separation by aluminium fluoride. However, while this may affect the maximum TR-FRET signal generated, it would be unlikely that this would affect the

affinity. It would more likely make the indicated concentrations inaccurate and calculated apparent dissociation constant misleading. Accuracy could be improved by further purification to remove contaminating proteins as well as unlabelled binding partners. $G\beta_4TCM\text{-}\gamma_2$ was co-purified with $G\alpha_{i1}$ showing that the fusion protein does not appear to abolish Gα binding. However, it is possible that the fusion site has some effect on the binding affinity of Gβγ to Gα.

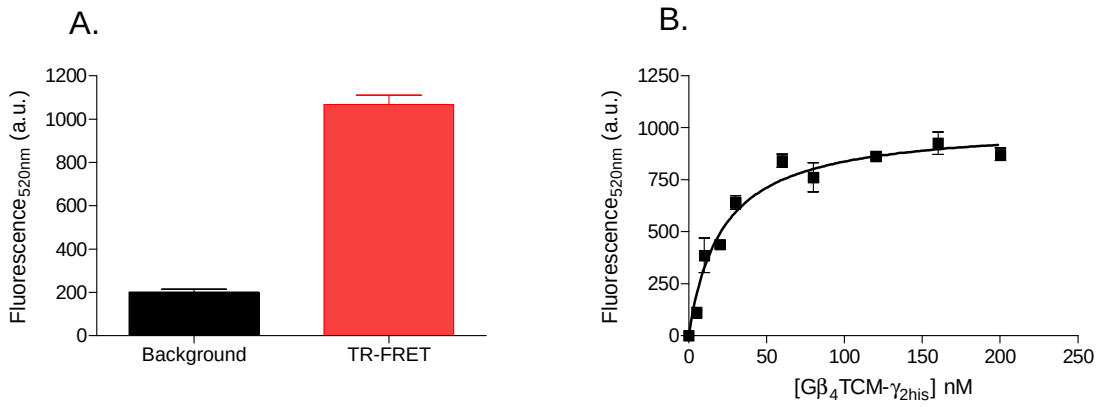

Figure 5.5: TR-FRET between $G\beta_4TCM\text{-}\gamma_2$ and $G\alpha_{i1}$:Tb. (A) 10 nM $G\alpha_{i1}$:Tb ± 50 nM $G\beta_4TCM\text{-}\gamma_2$ was mixed together in a final volume of 100 µL in TMN buffer. **(B)** 10 nM $G\alpha_{i1}$:Tb and increasing concentrations of $G\beta_4TCM\text{-}\gamma_2$ (0-200 nM) were mixed together in a final volume of 100 µL in TMN buffer. For both experiments, the background luminescence from 10 nM $G\alpha_{i1}$:Tb has been deducted. A Victor3 multilabel plate reader was used to measure TR-FRET with the following parameters: λ_{ex} 340 nm, λ_{em} 520 nm, 50 µs delay and 900 µs counting duration. Data shown are mean ± SEM (n=3).

Binding of $G\beta_4TCM\text{-}\gamma_2$ to $G\alpha_{i1}$:Tb occurred over a matter of minutes and was not as stable as normally observed with a maximum signal being generated before a gradual decrease in fluorescence occurred. This could be due to the lower affinity between the subunits indicated previously. Although fluorescence is decreasing, the addition of unlabelled Gβγ decreased the TR-FRET signal to near background levels at a relatively greater rate, while the addition of an equivalent volume of buffer did not have the same effect, with fluorescence reaching a steady state level, which was approximately 2x above background. This indicated that unlabelled Gβγ could compete for binding resulting in a decrease in TR-FRET (**Figure 5.6**).

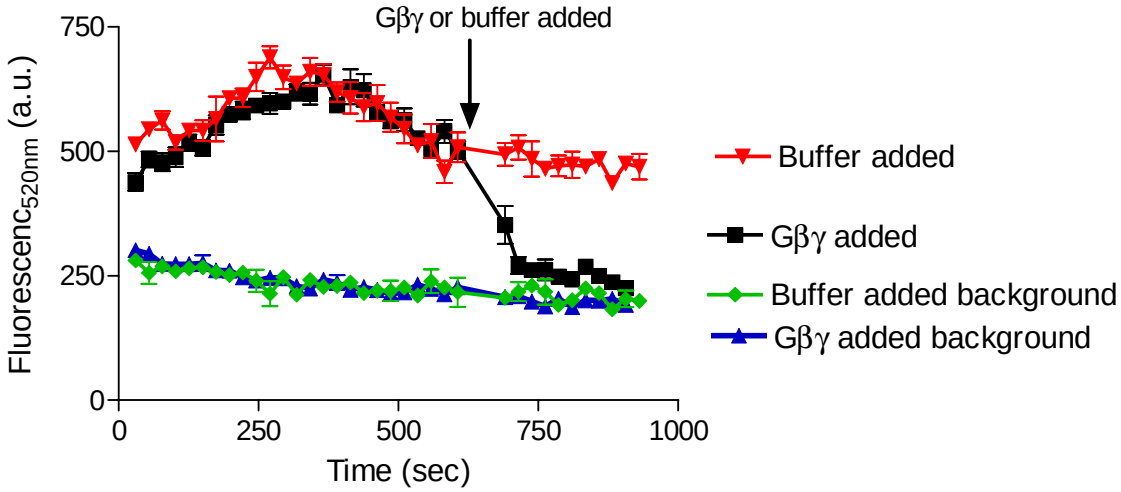

Figure 5.6: Time course of Gβ$_4$TCM-γ$_2$ binding Gα$_{i1}$:Tb and competitive binding of Gβγ. 10 nM Gα$_{i1}$:Tb was mixed with 30 nM Gβ$_4$TCM-γ$_2$ prelabelled with FlAsH. Background measurements were determined in the absence of Gβ$_4$TCM-γ$_2$. TR-FRET was measured with the following parameters: λ$_{ex}$ 340 nm, λ$_{em}$ 520 nm, 50 µs delay and 900 µs counting duration. At approximately 600 s, an excess of Gβγ (1 µM) was added or an equivalent volume of buffer and measurements resumed. Data shown are mean ± SEM (n=3).

5.3.5. TR-FRET between His-TCM-Gα$_{i1}$:FlAsH and Gβγ:Tb

Although His-TCM-Gα$_{i1}$:FlAsH had been determined to be non-functional in receiving signals from a GPCR, the addition of Gβγ:Tb produced a TR-FRET signal (**Figure 5.7**). However, the results showed that His-TCM-Gα$_{i1}$:FlAsH may have a lower affinity for Gβγ and the error bars indicated a higher degree of variation than normally seen in TR-FRET assays. This could indicate that His-TCM-Gα$_{i1}$:FlAsH was unstable in this format and these factors could both contribute to the lack of signalling in [^{35}S]GTPγS signalling assays.

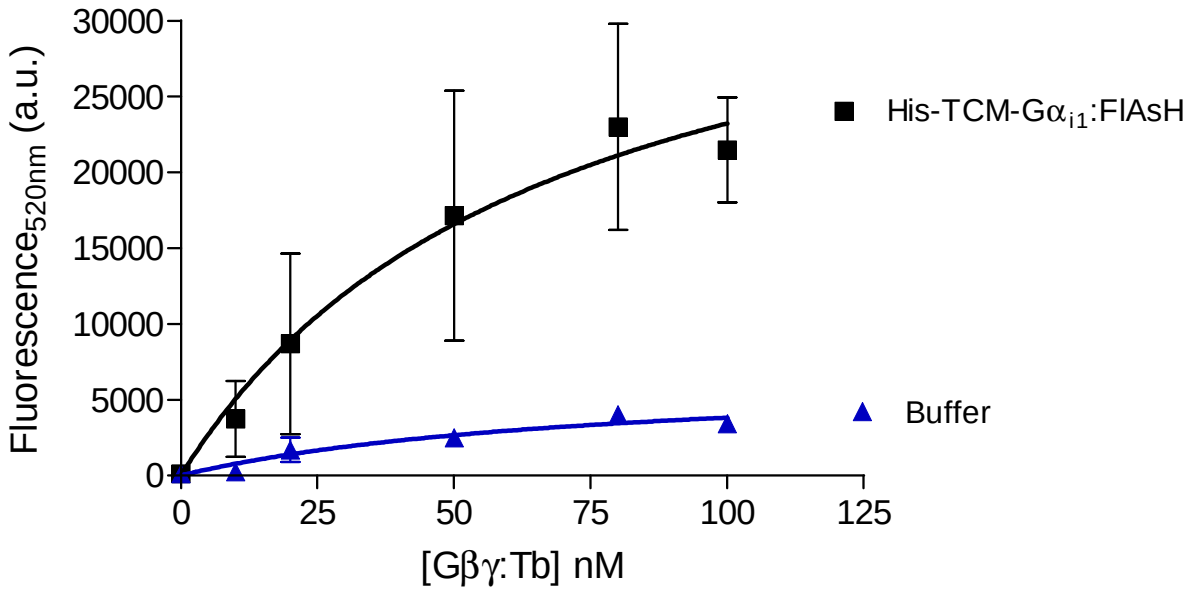

Figure 5.7: Association of His-TCM-Gα$_{i1}$:FlAsH with Gβγ:Tb. Concentrations ranging from 0-100 nM of Gβγ:Tb were mixed with 100 nM His-TCM-Gα:FlAsH or an equivalent volume of buffer in a final volume of 100 µL using Tb binding buffer. A Victor3 multilabel plate reader was used to measure TR-FRET with the following parameters: λ_{ex} 340 nm, λ_{em} 520 nm, 50 µs delay and 900 µs counting duration. Data shown are mean ± SEM (n=3).

5.3.6. Spectral overlap of LBT2:Tb and TCM:FlAsH

The excitation and emission spectra determined from LBT2:Tb and TCM:FlAsH (discussed in chapters 3 and 4, respectively), show that TCM:FlAsH should be a suitable acceptor fluor for LBT2:Tb (**Figure 5.8**). Upon excitation of LBT2:Tb at 280 nm, the first emission peak and part of the second emission peak should excite TCM:FlAsH, the emission of which can be measured where the terbium emission is minimal. Available filters for the Victor3 multilabel plate reader dictated that excitation would be carried out at 280nm and the emission of TCM:FlAsH measured at 520 nm. From these spectra, it can be observed that the excitation wavelengths of the donor LBT2:Tb are clearly distanced from that of TCM:FlAsH, reducing direct excitation of the acceptor as often happens when using GFP variants. There is also good overlap between the emission spectra of LBT2:Tb and the excitation spectra of TCM:FlAsH for TR-FRET.

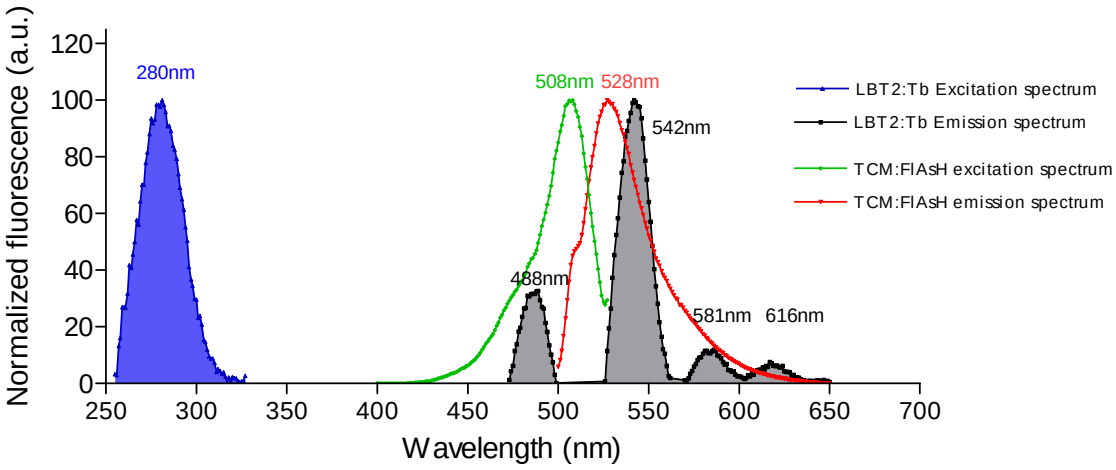

Figure 5.8. Overlay of normalized LBT2:Tb and TCM:FlAsH spectra for TR:FRET measurements.

5.3.7. TR-FRET between TCM:FlAsH and LBT:Tb

As proof-of-concept for the utility of a terbium labelled LBT and a TCM labelled with FlAsH as a TR-FRET donor/acceptor pair, LBT1-Gβ_4 was co-expressed with Gγ_2-TCM in *Sf*9 cells in an attempt to produce a protein that was interacting stably. Both of these fusion proteins had been shown to function in forming a G-protein heterotrimer and receiving signals from a GPCR (see chapters 3 and 4). The Gβγ dimer was partially purified using IMAC with Coomassie-stained polyacrylamide gels of the elutions showing the presence of some contaminating proteins. Labelling of Gγ_2-TCM with FlAsH was carried out on the IMAC column overnight, before unbound FlAsH was washed from the column and labelled proteins eluted. This preparation was then examined for FlAsH labelling. FlAsH fluorescence at 520 nm increased with protein concentration after excitation at 485 nm. An increasing concentration of $TbCl_3$ had no effect on Gγ_2-TCM:FlAsH fluorescence upon direct excitation of the FlAsH (**Appendix 8.8**). Likewise, when an increasing concentration of $TbCl_3$ was added, fluorescence at 545 nm increased following excitation at 280 nm and a 50 µs delay (**Appendix 8.8**). These results indicated that labelling with FlAsH and terbium had occurred and the ability of terbium to excite FlAsH within the Gβγ dimer was then investigated. TR-FRET occurring in the Gβγ dimer was examined by exciting the terbium in the

LBT at 280 nm and measuring the emission of FlAsH at 520 nm in the presence of increasing concentrations of $TbCl_3$. The fluorescence at 520 nm increased with increasing $TbCl_3$ concentrations and protein concentration suggesting the occurrence of TR-FRET (**Figure 5.9**).

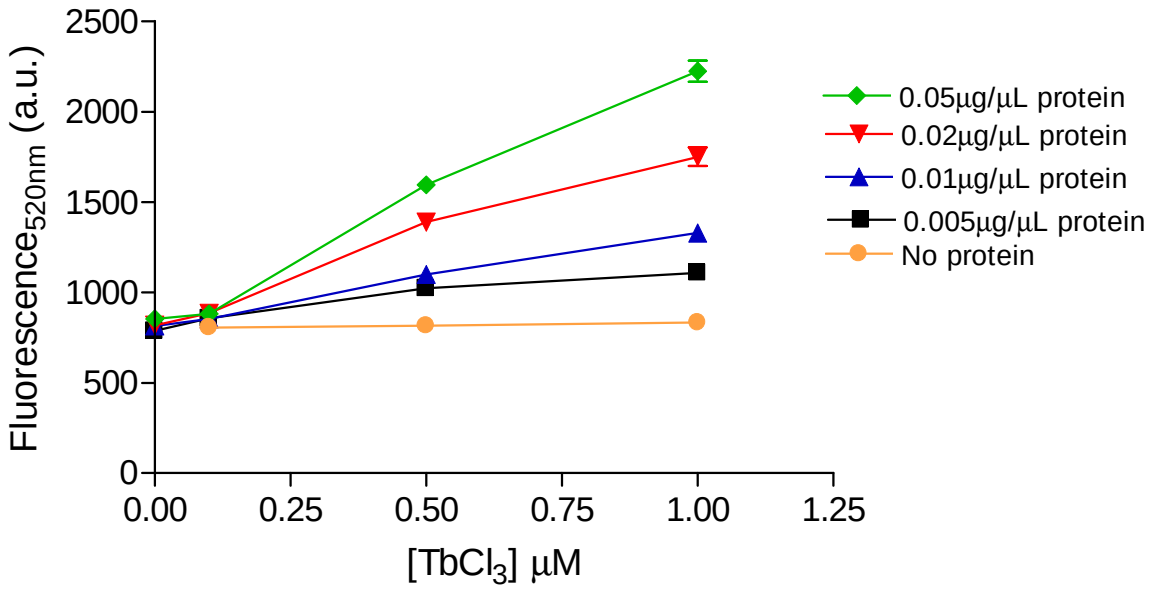

Figure 5.9: TR-FRET between LBT1-Gβ$_4$ and Gγ$_2$-TCM. Various concentrations of LBT1-Gβ$_4$γ$_2$-TCM dimer preparation pre-labelled with FlAsH were mixed with various concentrations of $TbCl_3$. A Victor3 multilabel plate reader was used to measure TR-FRET with the following parameters: λ_{ex} 280 nm, λ_{em} 520 nm, 50 µs delay and 900 µs counting duration. Data shown are mean ± SEM (n=3).

To confirm that this signal was TR-FRET, protease treatment was used to reduce the signal showing that the increase was due to a specific protein interaction (**Figure 5.10**). Gadolinium was also used to reduce the TR-FRET signal by reducing terbium-binding through competitive displacement (**Appendix 8.8**). These results were the first indication that LBT:Tb and TCM:FlAsH could be utilized as a TR-FRET pair.

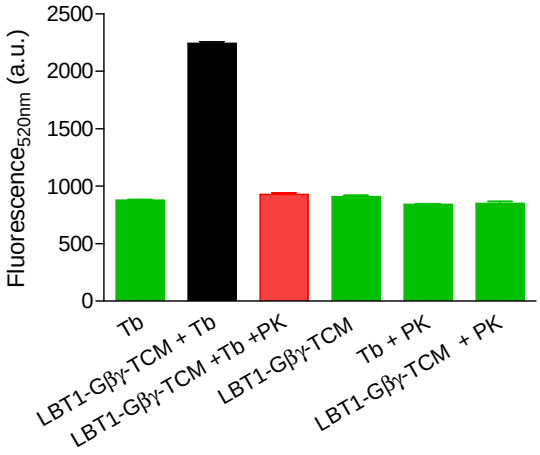

Figure 5.10: Protease treatment reduced TR-FRET signal between LBT1-Gβ$_4$ and Gγ$_2$-TCM. 5 ng/µL of LBT1-Gβ$_4$γ$_2$-TCM dimer preparation pre-labelled with FlAsH was mixed with 1 µM of $TbCl_3$, +/- 0.2 mg/mL Proteinase K (PK). A Victor3 multilabel plate reader was used to measure TR-FRET with the following parameters: λ_{ex} 280 nm, λ_{em} 520 nm, 50 µs delay and 900 µs counting duration. Data shown are mean ± SEM (n=3).

5.3.8. TR-FRET between LBT2-Gα$_{S25}$ and Gβ$_4$γ$_2$-TCM

LBT2-Gα$_{S25}$ was previously shown to bind terbium in membrane preparations (Chapter 3) and interact with Gβγ:Alexa subunits. Similarly, Gβ$_4$γ$_2$-TCM was labelled with FlAsH and shown to be a functional TR-FRET partner with Gα:Tb. The ability of LBT2-Gα$_{S25}$ to generate a TR-FRET signal upon interaction with Gβ$_4$γ$_2$-TCM:FlAsH was then investigated. Existing Gβ$_4$γ$_2$-TCM:FlAsH was mixed with LBT2-Gα$_{S25}$ and an excess of $TbCl_3$. A Gβ$_4$γ$_2$-TCM:FlAsH concentration response curve showed saturation of LBT2-Gα$_{S25}$ with Gβ$_4$γ$_2$-TCM:FlAsH and generated an apparent *K*d of 2.3 ± 0.5 nM which shows a high affinity interaction similar to that generated in our G-protein subunit interaction assays using conjugated small molecule fluors (Leifert *et al*. 2006) and those of others (Sarvazyan, Remmers & Neubig 1998) (**Figure 5.11**).

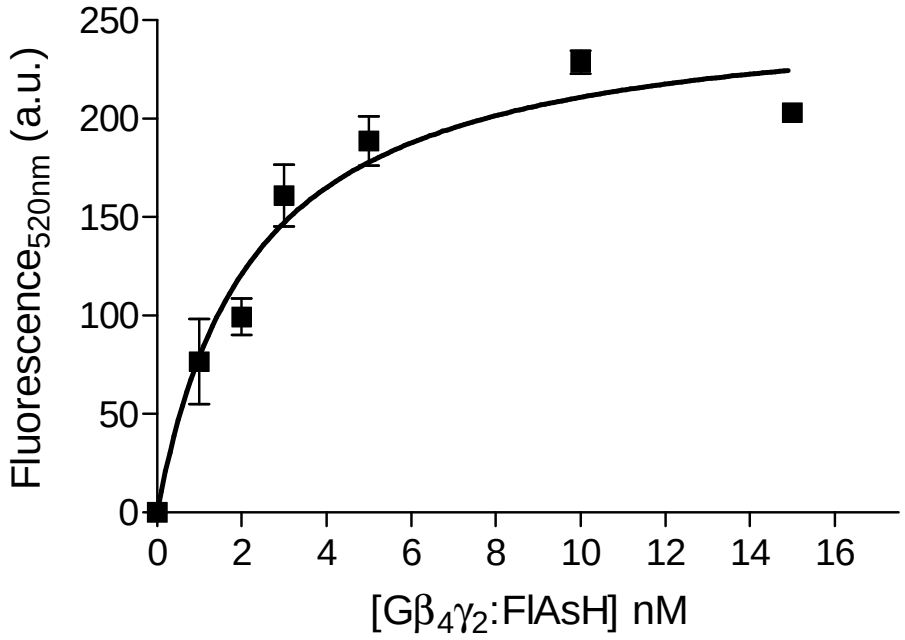

Figure 5.11: TR-FRET concentration response curve of Gβ$_4$γ$_2$-TCM:FlAsH against LBT2-Gα$_{S25}$. 0.01 mg/mL LBT2-Gα$_{S25}$ membrane preparation was mixed with 0-15 nM purified Gβ$_4$γ$_2$-TCM:FlAsH and 1 µM $TbCl_3$. After 10 min incubation, a Victor3 multilabel plate reader was used to measure TR-FRET with the following parameters: λ_{ex} 280 nm, λ_{em} 520 nm, 150 µs delay and 900 µs counting duration. Data shown are mean ± SEM (n=3).

Likewise, concentration response curves of LBT2-Gα$_{S25}$ could be generated showing that the presence of Gβ$_4$γ$_2$-TCM:FlAsH increased the fluorescence value at 520 nm above the background level in the absence of Gβ$_4$γ$_2$-TCM:FlAsH. The presence of unlabelled Gα$_{i1}$ partially inhibited this signal suggesting that a specific interaction between Gβ$_4$γ$_2$-TCM:FlAsH and LBT2-Gα$_{S25}$ was responsible for the increase in emission at 520 nm (**Figure 5.12**). The signal may have been able to be further reduced with a greater concentration of unlabelled protein since the amount of LBT2-Gα$_{S25}$ present in the membrane preparation was not quantitatively known.

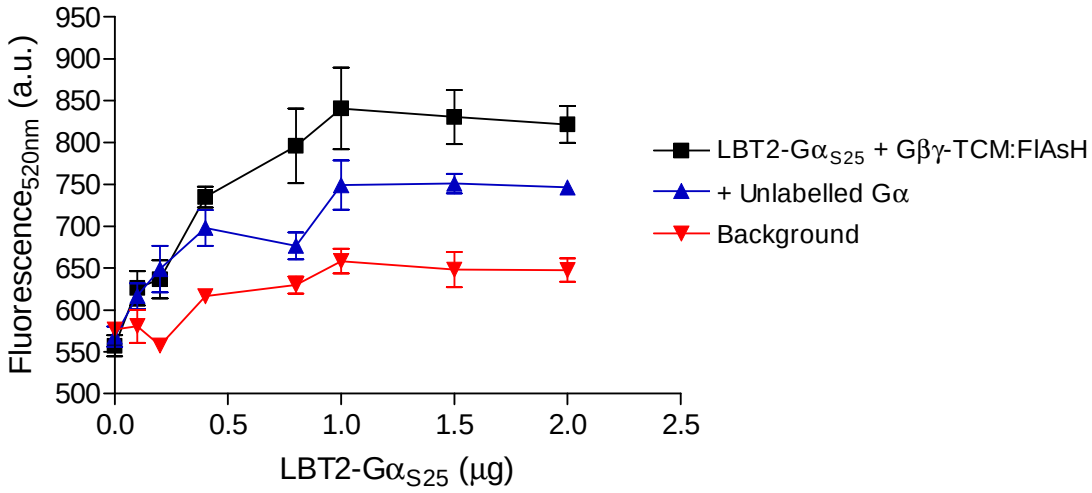

Figure 5.12: LBT2-Gα$_{S25}$ concentration response curves against Gβ$_4$γ$_2$-TCM:FlAsH. 20 nM Gβ$_4$γ$_2$-TCM:FlAsH was mixed with 0-2 µg LBT2-Gα$_{S25}$ preparation, 1 µM $TbCl_3$ ± 80 nM unlabelled Gα. The final assay volume was made up to 100 µL using Tb binding buffer. The background fluorescence was measured in the absence of Gβ$_4$γ$_2$-TCM:FlAsH. After 10 min of incubation, a Victor3 multilabel plate reader was used to measure TR-FRET with the following parameters: λ_{ex} 280 nm, λ_{em} 520 nm, 150 µs delay and 900 µs counting duration. Data shown are mean ± SEM (n=3).

The other lanthanide binding tagged Gα subunit His-LBT2-Gα$_{i1}$ was also examined for a TR-FRET signal upon interaction with Gβγ-TCM. However, no signals were detected. This could have resulted for a number of reasons including the low amount of fluorescence generated by terbium binding to this fusion protein rendering the system too insensitive at the concentrations of protein used or problems with the functionality of the subunit since signalling was not observed. Other effects of the fusion may have resulted in poor affinity for the Gβγ dimer.

5.4. Further Discussion and Conclusions

Pathological conditions exist where multiple receptors converge on a single G-protein signal pathway. For example, cardiac hypertrophy is in part responsible for the chronic stimulation of the Gq pathway (Akhter *et al*. 1998) by several receptors, and G-protein mutations (and altered functions) have been implicated in disease states such as Albright Hereditary Osteodystrophy, cancer and bipolar affective disorders (reviewed in (Di Cesare Mannelli *et al*. 200)). Gi proteins have been implicated in headaches and fibromyalgia (Galeotti *et al*. 2001a, Galeotti *et al*. 2001b). Novel therapeutics could be targeted at the interfaces of G-protein interactions as an alternative target to the GPCR that could produce effects that are not achievable at the receptor level alone (Freissmuth *et al*. 1999; Holler, Freissmuth & Nanoff 1999). Recently, a study using BIM-46174, an inhibitor of the heterotrimeric G-protein complex has been investigated for anti cancer activity and was found to be antiproliferative in preclinical studies (Prevost *et al*. 2006). The ability of a compound to modulate G-proteins in a cellular system fails to demonstrate a direct interaction with the G-protein since a receptor-mediated interaction cannot be excluded. This indicates that cell-free assays for G-protein subunit interactions per se could be useful for screening, and to evaluate efficacy and potency in the drug discovery arena. This chapter examined a possible approach to establishing a second-generation TR-FRET assay platform specific for G-protein subunit interactions using small, genetically-encoded tags for site-specific fluorescent labelling.

The previously established first generation TR-FRET assay using CS124-DTPA-EMCH:Tb as the donor and Alexa546 as the acceptor generated binding partners useful for concluding whether the new fusion protein constructs could be potential TR-FRET partners, and a number of combinations were tested (**Table 5.1**). TR-FRET signals between LBT2-Gα_{S25} and G$\beta\gamma$:Alexa could be generated which were approximately 2-fold above background, and these signals could be reduced by protease treatment or addition of unlabelled Gα. While LBT1-Gβ_4 was shown to be

functional, this construct appeared to be a non-viable TR-FRET partner for Gα:Alexa due to the lower affinity between terbium and the LBT. His-Gγ_2-TCM co-expressed with Gβ_4 (G$\beta_4\gamma_2$-TCM) yielded good TR-FRET signals with Gα:Tb once pre-labelling with FlAsH was carried out. Signals were 3-fold above background and could be reduced, close to background levels by the addition of an excess of unlabelled Gα. Furthermore, a *K*d of 3.6 nM was generated, close to the expected affinity making G$\beta_4\gamma_2$-TCM appear a good candidate for use in the second generation TR-FRET assay. A Gγ_2 construct with a TCM on the N-terminus was also expressed and, while a signal 5-fold over background could be generated with Gα:Tb, the affinity between the subunits was lower than found previously (*K*d 21.5 nM). Since the functionality of this construct in receptor initiated signalling had not yet been determined, in the interests of time the first Gγ_2-TCM construct was pursued. It would, however, be of interest to determine if this loss of affinity had an effect on signalling in a reconstituted system. Preliminary experiments showed His-TCM-Gα_{i1} to interact with Gβγ:Tb. However, due to the lack of signalling ability when reconstituted with GPCRs and the limited supply of Gβγ:Tb, this construct was not pursued further. TCM-Gα_{i1} appeared to be a better option since the ability to signal from GPCRs was more consistent compared to His-TCM-Gα_{i1}. However, FlAsH labelling of this construct proved more difficult than anticipated although not all conditions were exhausted in the duration of this study and this aspect warrants further investigation. With some constructs already successfully used as TR-FRET partners, the utility of both genetic modifications in a TR-FRET assay was then investigated.

Donor	Acceptor	TR-FRET	Comment
Lanthanide binding tags as donors			
Tb:LBT2-Gα_{S25}	G$\beta\gamma$:Alexa	Yes	
Tb:LBT1-G$\beta_4\gamma_2$	Gα:Alexa	No	Affinity of LBT1 for terbium may be too low for a specific TR-FRET signal.
Tb:His-LBT2-Gα_{i1}	G$\beta_4\gamma_2$:Alexa	No	Terbium luminescence may not be high enough.
Tetracysteine motifs as Acceptors			
Gα:Tb	G$\beta_4\gamma_2$-TCM:FlAsH	Yes	*K*d 3.6 nM
Gα:Tb	Gβ_4TCM-γ_2:FlAsH	Yes	*K*d 21.5 nM
G$\beta\gamma$:Tb	His-TCM-Gα_{i1}:FlAsH	Yes	Affinity between subunits appeared to be decreased
LBTs and TCMs as a TR-FRET pair			
Tb:LBT1-Gβ_4	Gγ_2-TCM:FlAsH	Yes	
Tb:LBT2-Gα_{S25}	G$\beta_4\gamma_2$-TCM:FlAsH	Yes	*K*d 2.3 nM

Table 5.1: TR-FRET partner combinations investigated.

The strong, stable interaction of G$\beta\gamma$ was firstly used as proof-of-concept that the TR-FRET phenomenon could be observed using terbium chelated in a LBT as a donor, and FlAsH bound to a TCM as the acceptor. Indeed, a TR-FRET signal was observed using the dimer LBT1-G$\beta_4\gamma_2$-TCM, however, establishing that this TR-FRET signal was specific to a protein interaction was difficult due to the strong interaction between Gβ and Gγ and the decrease in labelling caused by protease treatment. Although LBT1-Gβ_4 was found to be a non-viable TR-FRET partner for Gα:Alexa, the stronger, more stable interaction with Gγ together with the lower amount of non-specific terbium-binding to this subunit compared to Gα, may have made TR-FRET measurable for this interaction. Tagging proteins that do not interact, preferably mutant G-proteins, would further validate TR-FRET assays and determine the limits before bystander FRET from random collisions is observed. His-LBT2-Gα_{i1} was not a successful TR-FRET partner for G$\beta\gamma$:Alexa and likewise, no TR-FRET signal could be generated with G$\beta_4\gamma_2$-TCM:FlAsH. If the terbium luminescence was not strong enough to generate a TR-FRET signal with Alexa-labelled proteins, it would have been unlikely that FlAsH-labelled proteins would have been successful since the

emission from terbium that excites FlAsH is of a lower intensity than that which excites Alexa. TR-FRET between the terbium-bound LBT of LBT2-$G\alpha_{S25}$ with the FlAsH-bound TCM of $G\beta_4\gamma_2$-TCM gave only a small 25% increase in signal although a reduction was induced by the addition of unlabelled Gα indicating the likelihood of some specificity. Furthermore, although only a small signal window was available, an apparent *K*d of 2.3 nM was generated indicating that the expected high affinity interaction was occurring and could be measured, even in the presence of the many contaminating proteins and lipids. We had previously used aluminium fluoride to specifically dissociate the G-protein subunits. However, this was no longer feasible since $AlCl_3$ used to generate aluminium fluoride was found to compete with terbium for binding to the LBT resulting in reduced terbium labelling, making TR-FRET measurements of subunit dissociation uncertain. The small signal window may be increased by using a ratio of acceptor emission:donor emission to take into account a decrease in donor emission as well as the increase in acceptor emission upon TR-FRET. Unfortunately, an appropriate filter to measure donor fluorescence was not available on the Victor3 multilabel plate reader used here. Alternatively, measuring the lifetime of the terbium may also validate the assay since the lifetime should be reduced when an interaction that results in TR-FRET occurs. However, the Victor3 multilabel plate reader used in the studies undertaken was not capable of such measurements.

Since the development of the first reactive biarsenical dyes that included FlAsH, ReAsH, and CHoXasH (Adams *et al*. 2002), several more derivatives have been developed and recently reviewed (Soh 2008) and these could offer better properties as an acceptor for terbium. In particular, fluorinated FlAsH derivatives (Spagnuolo, Vermeij & Jares-Erijman 2006) have shown higher absorbance, larger Stokes shift, higher quantum yield, higher photostability and reduced pH dependence. However, the associated spectral shifts are likely to counteract these benefits when used as an acceptor for terbium. Carboxy-FlAsH (CrAsH), a less hydrophobic version of

FlAsH has also been synthesized and this compound exhibits lower non-specific binding to hydrophobic proteins and membranes, which could reduce background signals (Cao *et al*. 2006). Variations in colour of biarsenical dyes have been somewhat limited by the structural requirements of the rigid display of arsenic atoms, and rhodamine biarsenics were found to be non-fluorescent (Adams *et al*. 2002). This has been improved upon by the development of a moiety called SplAsH (spirolactam Arsenical Hairpin binder) that can be attached to a variety of fluorophores including MANT, Dansyl, X-rhodamine and Alexa594 (Bhunia, Miller 2007). This may offer an opportunity to use the second, larger emission peak of terbium to excite a biarsenical acceptor that could produce a stronger signal. However, unlike FlAsH, which is non-fluorescent until bound to the TCM, SplAsH dyes are fluorescent in the absence of a TCM, which would make the washing procedures used in this study for labelling a requirement. With regard to the LBT, efforts have been made to improve the luminescent emissions that would increase the amount of energy available to be transferred to the acceptor. These efforts have included improving the antenna molecule for better sensitization of the terbium (Reynolds, Sculimbrene & Imperiali 2008) and the concatenation of LBTs that has increased the luminescence up to 3-fold (Martin *et al*. 2007). Further improvements to the affinity of terbium for the LBT would also decrease background signals from non-specific terbium interactions and possibly increase signals due to a more stable interaction between terbium and the LBT.

A recent study has emerged using a LBT that recognizes the utility of small genetically encoded tags and has used LBT1 in combination with a His-tag to label *Shaker* potassium channels expressed in *Xenopus laevis* oocytes. Ni^{2+} or Cu^{2+} bound to the histidine tag was used as the acceptor for LBT:Tb and distances within the membrane protein measured using lifetime measurements (Sandtner, Bezanilla & Correa 2007). This could present an interesting alternative to the TCM used in this study.

In conclusion, LBTs and TCMs bound to terbium and FlAsH respectively, have been found to be a viable donor and acceptor pair for TR-FRET studies and could be utilized in assays to measure G-protein interactions.

6. Exploring the use of LBTs fused to G-protein Coupled Receptors

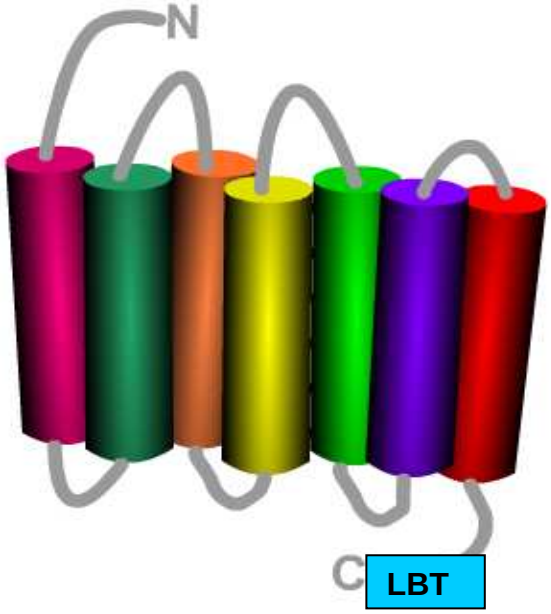

6.1. Introduction

The site-specific labelling of G-proteins for GPCR assay platforms as has so far been discussed, offers a generic signal that could be applied to a range of GPCRs without modification of the receptor. However, the tagging of receptors offers alternative platforms and the opportunity to further exploit the benefits of labelling with a LBT.

While it is of course well established that receptors associate with G-proteins, our understanding of whether G-proteins are pre-coupled to receptors or are recruited after GPCR activation is relatively limited and current studies do not concur (Gales *et al*. 2005; Hein *et al*. 2005; Nobles, Benians & Tinker 2005). Fluorescent tagging of GPCRs has allowed this aspect of GPCR signalling to be investigated and this in itself represents an interesting functional assay platform. GPCRs can often couple to different classes of G-proteins and novel therapeutics could target the receptor interaction with a certain G-protein while leaving other G-protein pathways activated by the receptor unaffected, a property that cannot be achieved using receptor antagonists (Manetti *et al*. 2005). This chapter examines the fusion of LBTs to the M_2-muscarinic receptor (M2R) and the β_2-adrenergic receptor (β2AR). The functional integrity of the receptors is investigated using ligand-binding and [^{35}S]GTPγS signalling assays. The terbium-binding ability is also assessed and the utilization of these receptors in examining associations with G-proteins is investigated.

6.2. Methods

6.2.1. Construction and expression of β2AR-LBT2

The coding sequence for LBT2 was fused to the 3' end of the human β2AR receptor gene by PCR. A *Bam*H1 restriction site was introduced to the 5' end of the recombinant gene using the forward primer 5' GC GGA TCC ATG GGG CAA CCC GGG AAC 3' and the LBT2 and *Hind*III site to the 3' end using the reverse primer 5' GC AAG CTT TCA AGC ACA TTC GTC ACC TTC GTA CCA ACC GTC ATT ATT CCA GTC AAC ACA AGC CAG CAG TGA GTC ATT TGT AC 3'. Template DNA was obtained from β2AR baculovirus from Dr. Roger Sunahara (University of Michigan, USA). The resulting PCR product was then ligated into pGEM®-T Easy (Promega) and digested from this vector using the restriction enzymes *Bam*H1 and *Hind*III and ligated into pFastBac™1 (Invitrogen). The recombinant pFastBac™1 was then transformed into DH10Bac™ *E. coli* and recombinant bacmid generated as per Invitrogen's guidelines as has previously been described. Purified recombinant bacmid was then transfected into *Sf*9 cells using Cellfectin® (Invitrogen) and the resulting baculovirus then underwent successive rounds of amplification at an MOI of 0.1 described in detail in chapter 3. A larger scale infection of 1-2 L of cells was then performed using an MOI of 1 from which membrane preparations were made. *Sf*9 cell culture, amplifications and infections were carried out as has previously been described.

6.2.2. Construction of β2AR-TCM-LBT2

To construct β2AR with a TCM within the third intracellular loop and LBT2 at the C-terminus, a unique endogenous *Bgl*II restriction enzyme site located within the third intracellular loop of β2AR was utilized. A PCR product was generated using the same forward primer that was used to construct β2AR-LBT2 which introduced a 5' *BamH*1 site and the reverse primer 5' GC AGA TCT ACA GCA TCC TGG ACA GCA GCG GAG TCC ATG CCC CG 3' that annealed upstream of the *Bgl*II site to produce a PCR product consisting of β2AR that terminated with a 3' TCM and *Bgl*II

site. β2AR-LBT2 (cloned into pGEM®-T Easy) was then digested with *BamH*1 and *Bgl*II and the similarly digested PCR product ligated in. The resulting full length β2AR-TCM-LBT2 sequence was then digested out of pGEM®-T Easy using *BamH*1 and *Hind*III and ligated into pFastBac™1 for subsequent generation of recombinant baculovirus.

6.2.3. Construction and expression of M2-LBT1

M2R was fused to LBT1 at its C-terminus to generate the M2-LBT1 construct, which was made in much the same manner as β2AR-LBT2. PCR was used to generate a coding sequence that placed LBT1 at the 3' end of M2R. Template DNA was generously obtained as baculovirus from Dr. Andrejs Kremlins and Prof. Alfred Gilman (University of Texas Southwestern Medical Centre, USA). A *Kpn*1 restriction site was introduced at the 5' end of the gene using the forward primer 5' G CGC GGT ACC ATG AAT AAC TCA ACA AAC TCC 3' while LBT1 and a *Hind*III site were introduced at the 3' end of the gene using the reverse primer 5' AAG CTT TTA AGC AAG AAG TTC GTC ACC TTC GTA CCA ACC GTC ATT ATT AGT ATC AAT ATA CCT TGT AGC GCC TAT GTT C 3'. The generation of recombinant bacmid and transfection of *Sf*9 cells then followed as has been previously described to generate recombinant baculovirus. M2-LBT1 baculovirus underwent successive rounds of amplification before M2-LBT1 was expressed in *Sf*9 cells as has been described earlier.

6.2.4. Construction of M2-TCM-LBT1

To construct M2R with a TCM within the third intracellular loop and LBT1 on the C-terminus (M2-TCM-LBT1), the unique endogenous restriction enzyme site of *Xma*I which resides within the third intracellular loop was exploited. A PCR product was generated using the forward primer used to construct M2-LBT1 and a reverse primer 5' CCC GGG AGC AAC ATC CTG GGC AAC AGA TGC ATG TTT GCT TAG AGT T 3' that annealed upstream of an *Xma*I site to introduce the TCM. This product was then ligated into M2-LBT1 cloned into pFastBac™1 digested with *Kpn*I

and *Xma*I to produce full length M2-TCM-LBT1. The design of the primers by Amanda Aloia (CSIRO) was such that 54 amino acids were deleted from the large third intracellular loop of M2R (226-379 inclusively) that are largely non-conserved between muscarinic receptors.

6.2.5. Sequencing

Sequencing of the constructs was carried out as previously described and the results can be found in **Appendix 8.9.**

6.2.6. Production of receptor membrane preparations

Membrane preparation of M2-LBT1 and β2AR-LBT2 were prepared as has been previously described for the other GPCRs used in this study in chapter 3.

6.2.7. [^{3}H]Ligand-binding assays

To determine the level of expression and ligand-binding activity of the receptor, [^{3}H]CGP-12177 (Perkin Elmer) or [^{3}H]scopolamine (Perkin Elmer) were used to probe the β2AR-LBT2 or M2-LBT1 receptors, respectively. Various concentrations of [^{3}H]ligand were added to 0.02-0.03 µg/mL (total protein) of receptor containing membrane preparation. To determine the amount of non-specific binding, the antagonists propranolol, or atropine for β2AR-LBT2 or M2-LBT1, respectively, were added to compete for binding with the [^{3}H]ligand. The final membrane protein concentration in the assay was such that less than 10% of the total [^{3}H]ligand was receptor bound. After a 90 min incubation period at 27ºC, three 100 µL samples were then filtered through GFC filters on a vacuum manifold and the filters washed 3x with 4 mL of TMN buffer to remove non-bound ligand. 100 µL samples of each concentration of [^{3}H]ligand was also applied to dry filters without washing to determine the total counts for each concentration of ligand used. Filters were then dried and Ultima Gold™ scintillant cocktail (Perkin Elmer) added in pico pro vials for scintillation counting using a count time of 1 min in a Wallac 1410 liquid scintillation counter.

6.2.8. [^{35}S]GTPγS signalling assays

Membrane preparations of M2-LBT1 and β2AR-LBT2 were reconstituted with purified G-protein subunits and the appropriate agonists added to stimulate [^{35}S]GTPγS binding. These assays were conducted as previously described in chapter 3.

6.2.9. Labelling LBTs with terbium

Labelling LBTs with terbium was performed as previously described. Briefly, a 100 mM terbium chloride hexahydrate stock solution was made in 1 mM HCl and then diluted to the required 20x working concentration using Tb binding buffer. $TbCl_3$, receptor preparation and any additional components were added to black 96-well plates and were mixed upon the addition of Tb binding buffer to bring the volume of the assay to 100 µL. The plate could then be shaken at 500 rpm at room temperature for the desired time before the measurement of luminescence. A Victor3 multilabel plate counter (Perkin Elmer) fitted with a 1500 V Xenon Flash light source was then used to conduct time-resolved fluorescence measurements using the following instrument settings: excitation at 280 nm, emission at 545 nm, 50 µs delay and 900 µs counting duration.

6.2.10. TR-FRET assay between M2-LBT1 or β2AR-LBT2 and $G\alpha_{i1}$:Alexa

Terbium-binding to M2-LBT1 and association with $G\alpha_{i1}$:Alexa occurred concurrently. 20x working dilutions of each and any other indicated components were applied to the sides of a well and the reaction commenced by component mixing upon the addition of Tb binding buffer to a final volume of 100 µL. The plate could then be shaken at 500 rpm at room temperature for the desired time before initiating measurements. TR-FRET was measured using a Victor3 multilabel plate counter (Perkin Elmer) fitted with a 1500 V Xenon Flash light source was then used to conduct time-resolved fluorescence measurements using the following instrument settings: excitation at 280 nm, emission at 572 and 545 nm, 50 µs delay and 900 µs counting duration.

6.2.11. Data Analysis

Data was analysed using Prism™ 4.00 (GraphPad software Inc., San Diego CA, USA). Data is presented as mean ± SEM where n is equal or greater than 3. If error bars are not visible they are behind the symbols. Apparent *K*d and Bmax values were generated by fitting a one-site binding curve of the equation Y= Bmax . X / (*K*d + X).

6.3. Results and Discussion

6.3.1. Expression and characterization of M2-LBT1

Recombinant M2-LBT1 baculovirus was constructed and used to express M2-LBT1 in insect (*Sf*9) cells. Successful expression was confirmed by specific [^{3}H]scopolamine binding to generate a Bmax value of 2.2 pmol/mg and an apparent *K*d of 0.57 nM (**Figure 6.1**). High expression levels for a GPCR of 20-30 pmol/mg has previously been reported from M2R expressed in *Sf*9 cells (Parker *et al*. 1991) as have lower expression levels of 4 and 3 pmol/mg (Rinken *et al*. 1994; Weill *et al*. 1997), with the latter 2 studies using [^{3}H]scopolamine to measure the expression level. Although an adequate amount of expression was obtained, it may be that the infection could probably be further optimized for a greater amount of expression. The ligand binding properties of the receptor could also be further characterized with regard to rank order potencies of a set of other ligands to confirm the integrity of the binding site.

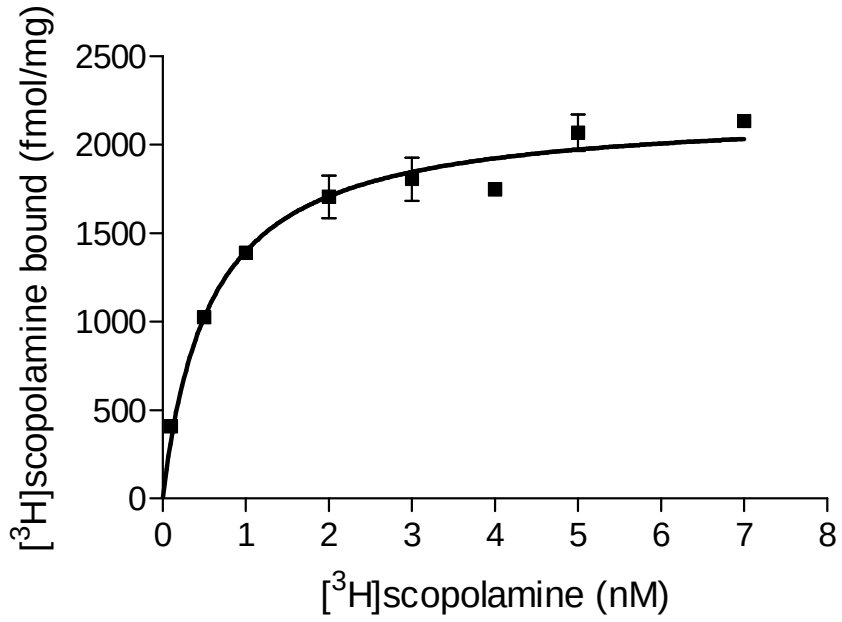

Figure 6.1: Specific [^{3}H]scopolamine binding to M2-LBT1. 0.025 mg/mL receptor membrane preparation was incubated for 90 min with 100-7000 pM of [^{3}H]scopolamine, +/- 100 µM atropine to determine non-specific binding, which has been deducted. Data shown are triplicate samples (mean ± SEM) of a single representative experiment.

The M2-LBT1 receptor was also tested for functional signalling through G-proteins upon stimulation by the agonist acetylcholine. The presence of acetylcholine increased [^{35}S]GTPγS binding approximately 3-fold above basal levels. This signal was then shown to be specific since in the presence of the antagonist, atropine, acetylcholine stimulation of [^{35}S]GTPγS binding was completely inhibited (**Figure 6.2**). Again, time permitting, the receptor could have been further characterized in comparison to wild type M2R with regard to efficacy using doses of various ligands to confirm the integrity of the receptor when fused to the LBT.

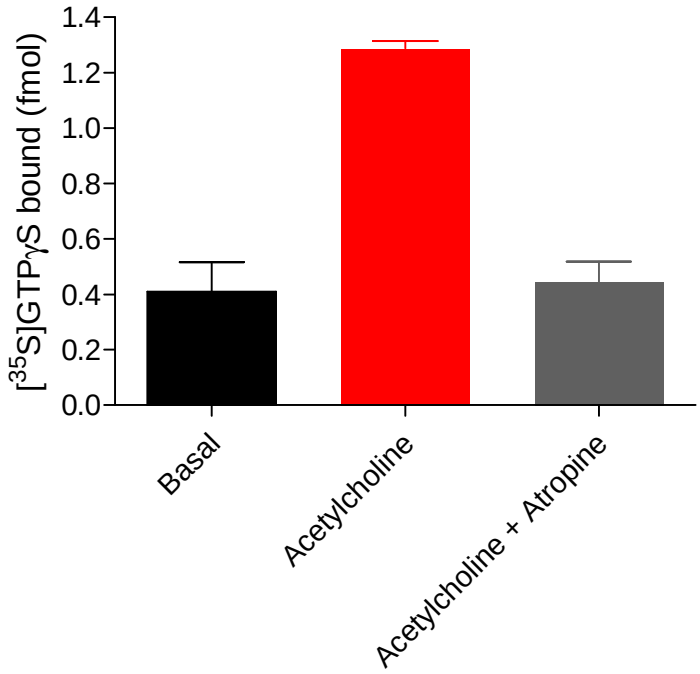

Figure 6.2: M2-LBT1 signals to G-proteins, stimulating [^{35}S]GTPγS binding. 0.01 mg/mL of M2-LBT1 receptor preparation was reconstituted with 20 nM G-proteins, 5 µM GDP, 10 µM AMP-PNP and 0.25 nM [^{35}S]GTPγS. The receptor was stimulated using 5 mM acetylcholine and 100 µM of the antagonist atropine used to compete with acetylcholine. The reactions were incubated for 90 min at 27 ºC with shaking and triplicate 25 µL samples were filtered through GFC filters and washed with 3 x 4 mL of cold TMN buffer. Data shown are triplicate samples (mean ± SEM) of a single representative experiment.

These data confirmed that membrane preparations of M2-LBT1 could specifically bind to the radiolabelled antagonist [^{3}H]scopolamine and signal through G-proteins when stimulated with acetylcholine. The receptor preparations were then assessed for their ability to bind terbium

indicated by an increase in terbium emission measured at 545 nm. The addition of increasing amounts of M2-LBT1 membrane preparation to 1 µM $TbCl_3$ increased the luminescence at 545 nm to saturation. Preparations that contained M2-LBT1 generated significantly greater amounts of luminescence (4-fold) than preparations of M2R (without the LBT) indicating that terbium was binding to the LBT (**Figure 6.3**). However, some non-specific terbium binding was also apparent as shown by the relatively small increase in luminescence in the presence of M2R membrane preparations.

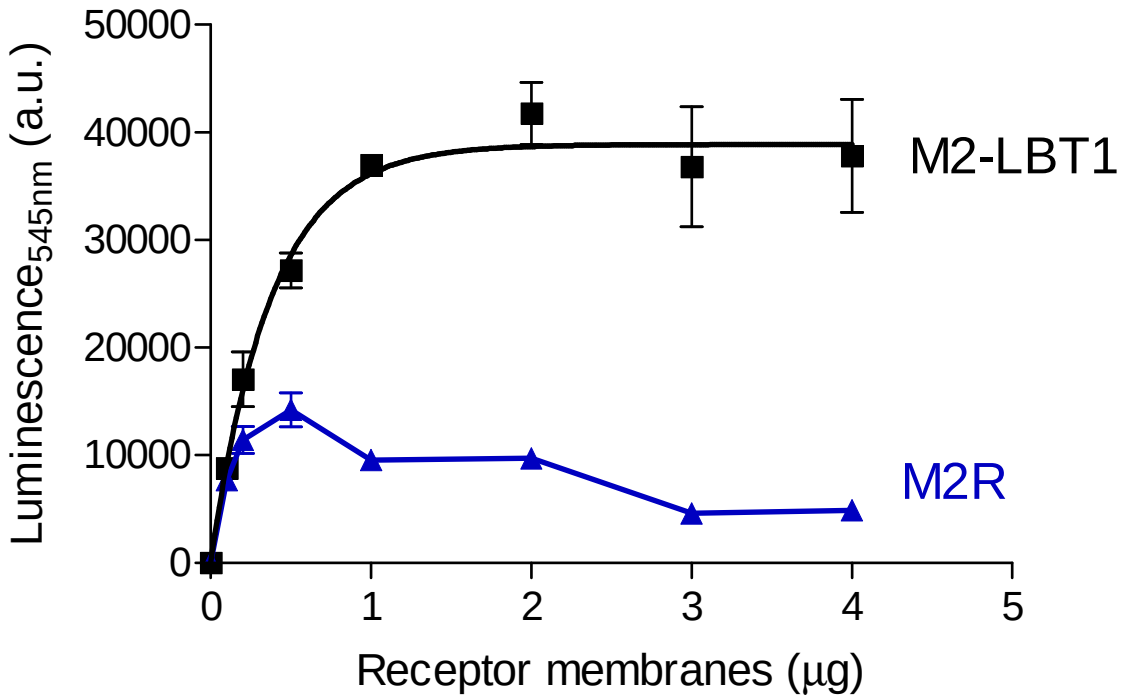

Figure 6.3: Terbium luminescence was significantly greater with M2-LBT1 preparations compared to M2R. Terbium binding was carried out by mixing 0.025 mg/mL of receptor preparations with 1 µM $TbCl_3$. The final volume was made up to 100 µL with Tb binding buffer and after 40 min incubation, the terbium emission was measured using a Victor3 plate reader set for time-resolved fluorescence with the following parameters: λ_{ex} 280 nm, λ_{em} 545 nm, 50 µs delay and 900 µs counting duration. Background from 1 µM $TbCl_3$ has been deducted. Data shown are mean ± SEM (n=3).

Furthermore, the presence of a 100-fold excess of $GdCl_3$ decreased the luminescence at 545 nm by competing for the terbium-binding sites, and treatment with proteinase K also reduced

luminescence at 545 nm indicating that terbium binding sites were perturbed or eliminated (**Figure 6.4**). Again, $GdCl_3$ reduced the Tb emissions below that following treatment with proteinase K as has previously been discussed for membrane preparations containing LBT2-$G\alpha_{S25}$.

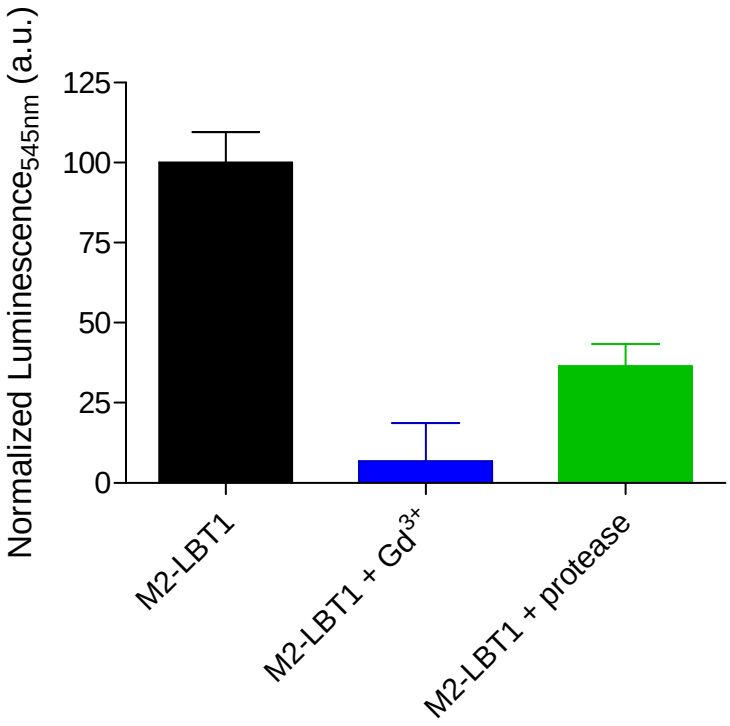

Figure 6.4: The presence of gadolinium and treatment with a protease reduced terbium binding to M2-LBT1. 0.025 mg/mL receptor preparation was mixed with 100 µM $GdCl_3$ or 0.2 mg/mL proteinase K and 1 µM $TbCl_3$. The final volume was made up to 100 µL with Tb binding buffer and after 40 min incubation, the terbium emission was measured using a Victor3 plate reader set for time-resolved fluorescence with the following parameters: λ_{ex} 280 nm, λ_{em} 545 nm, 50 µs delay and 900 µs counting duration. Data shown are mean ± SEM (n=3)

Since M2-LBT1 had been shown to be capable of interacting with G-proteins and appeared able to be labelled with terbium, the association of the receptor with G-protein subunits was investigated using TR-FRET with Alexa546 labelled $G\alpha_{i1}$-subunits (Gα:Alexa). Mixing of M2-LBT1:Tb with Gα:Alexa increased the acceptor emission significantly upon excitation of the donor. While this produced only a small increase, when M2-LBT1 membranes were substituted for membranes of *Sf*9 cells that had not been infected, there was no significant increase in

acceptor emission. These results suggested that M2-LBT1 was associating with Gα:Alexa to produce TR-FRET (**Figure 6.5A**). Unlabelled $G\alpha_{i1}$ was then included to compete with labelled proteins for binding to the receptor and this was indicated by a decrease in fluorescence (**Figure 6.5**B) and suggested that the TR-FRET signal was specifically due to interactions between M2-LBT1 and Gα:Alexa. The effect of the presence of ligands (including agonists and antagonists) and also Gβγ were investigated but failed to result in reproducible significant changes in TR-FRET. The method developed here is currently limited by a small signal window and efforts to further decrease the background signal perhaps by removing unbound and non-specifically bound terbium may prove useful in optimizing the format as discussed earlier. Other improvements might be made by either increasing the expression level of M2-LBT1 such that less membrane preparation needs to be included in the assay for a sufficient number of receptors, or enhancing the purification of the receptors from membrane preparations which may be responsible for scattering or absorbing light.

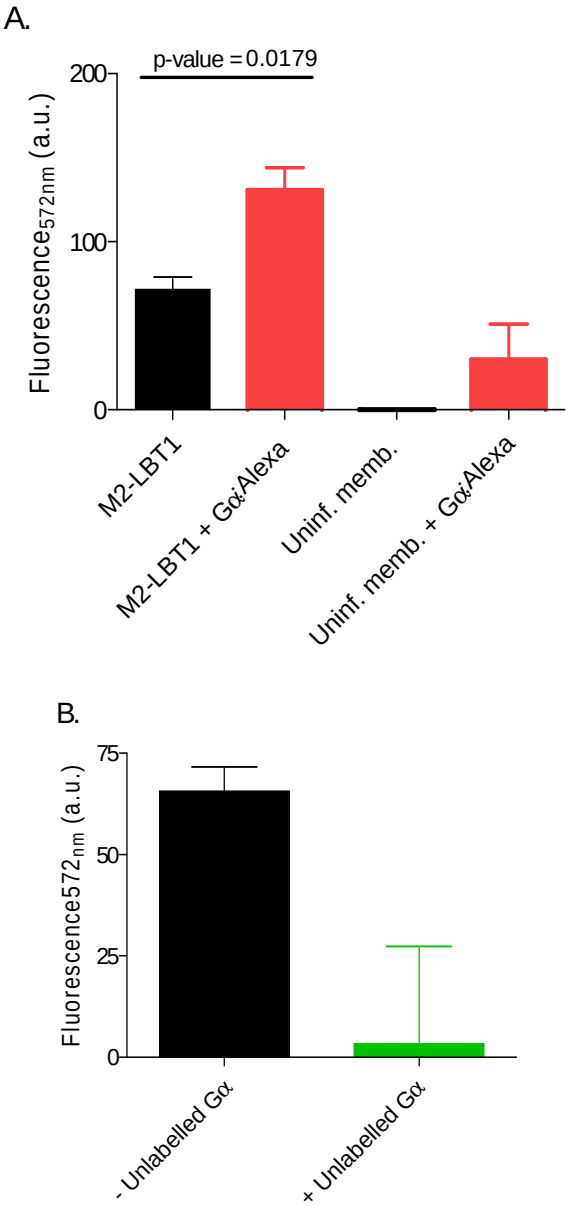

Figure 6.5: Interactions between M2-LBT1 and Gα:Alexa measured with TR-FRET. 4.6 mg/mL receptor preparation was mixed with 20 nM purified Gα:Alexa and 1 µM $TbCl_3$. After 1 hr incubation at room temperature with shaking, TR-FRET was measured using the following instrument parameters; λ_{ex} 280 nm, λ_{em} 545 nm, 50 µs delay and 900 µs counting duration. Data shown are mean ± SEM (n=3). **(A)** Comparison of the TR-FRET signal in the presence of M2-LBT1 to when these membranes are substituted for uninfected membranes. Background from uninfected membranes mixed with $TbCl_3$ has been deducted. In the presence of M2-LBT1 and Gα:Alexa, emission from the acceptor was siginificantly higher than the background produced by M2-LBT1 (student's T-test; p-value = 0.0179) **(B)** Effect of the presence of 600 nM unlabelled $G\alpha_{i1}$ on the TR-FRET signal. Backgrounds of M2-LBT1 and $TbCl_3$ ± unlabelled Gα have been deducted.

Relatively few publications examining the molecular interaction of GPCRs with G-proteins exist and at the time of writing, no study characterizing the coupling of M2R with G-proteins could be

located. Studies of receptor and G-protein coupling have mostly been performed in cells and have been contradictory with regard to whether receptors and G-proteins are pre-coupled or if G-proteins are subsequently recruited due to agonist binding. With regard to the β2AR, BRET studies have indicated that the receptor and G-protein interaction existed before agonist binding and persisted during signal transduction although it was thought that the constitutive activity of the receptor determined the level of precoupling (Gales *et al*. 2005). This conclusion appeared appropriate since in a study using α_{2A}-adrenergic receptors labelled with YFP, and CFP-labelled G_i-proteins there was no evidence of pre-coupling in HEK293 cells which was consistent with the lack of constitutive activity displayed by this receptor (Hein *et al*. 2005). This study also indicated that G-proteins were not associated with the receptor during much of the G-protein signalling cycle. However, in yet another study, basal interactions between α_{2A}-adrenergic receptors and M_4-muscarinic receptors with $G\alpha_o$ family G-proteins, were not abolished by the presence of an inverse agonist that reduced constitutive activity of the receptor. This suggested that pre-coupling of the receptor with G-proteins was not due to constitutive activity of the receptor (Nobles, Benians & Tinker 2005). Other levels of complexity in the interaction have also been suggested since the cytosolic surface of a single receptor is too small to contact all of the potential points of interaction that have been located on the heterotrimeric G-proteins. This has lead to GPCR dimers or oligomers being suggested as necessary for G-protein binding (evidence for this has been reviewed in (Oldham, Hamm 2008)).

6.3.2. Expression and characterization of the β_2-adrenergic receptor fused to LBT2

β_2AR was fused to LBT2 at its C-terminus (β_2AR-LBT2) and this recombinant fusion protein was expressed in *Sf*9 cells. The presence of the receptor in subsequent membrane preparations was confirmed by specific radiolabelled antagonist binding ([^{3}H]CGP-12177) (**Figure 6.6**). The resulting binding curve showed that a high affinity for the ligand was maintained (Apparent *K*d 1.2

nM) and a high level of expression was achieved (Bmax of 91 pmol/mg). The β_2AR has been widely expressed in *Sf*9 cells (reviewed in (Sarramegna *et al*. 2003)) and expression levels have ranged from 5-40 pmol/mg indicating that the expression level achieved here is unusually high.

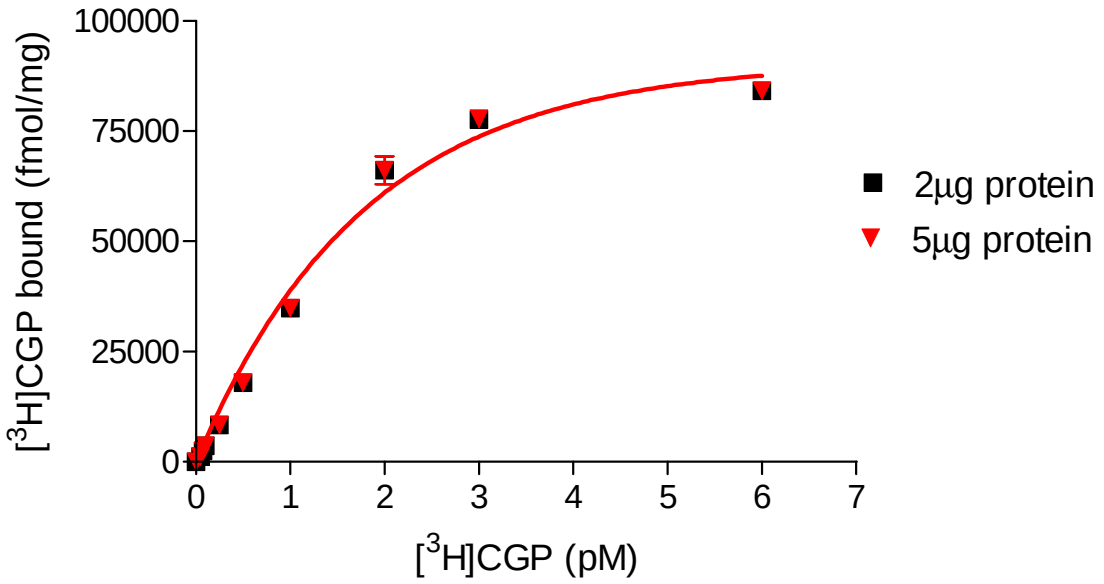

Figure 6.6: Specific [^{3}H]CGP ligand binding to β2AR-LBT2. 0.02 or 0.05 µg/µL of receptor membrane preparation was mixed with 0-6 nM of [^{3}H]CGP-12177 +/- 100 µM propranolol to determine non-specific binding, which has been deducted. Data shown are triplicate samples (mean ± SEM) of single representative experiments.

The β2AR-LBT2 fusion protein was also shown to be capable of signalling through G-proteins. The receptor was reconstituted with G-protein subunits and [^{35}S]GTPγS-binding to the Gα subunit stimulated using the receptor agonist isoproterenol. [^{35}S]GTPγS bound to Gα was captured onto GFC filters and measured. The presence of agonist increased [^{35}S]GTPγS-binding to above that of basal both in the presence and absence of terbium, and the reduction of this signal in the presence of antagonist showed that this was a receptor-mediated, specific response (**Figure 6.7**). Although the agonist stimulated [^{35}S]GTPγS-binding was not as large as normally generated using $G\alpha_{i1}$, this could reflect less optimal coupling of the receptors with G-proteins since the β2AR is normally associated with G_s G-protein coupling although reports of G_i coupling exist (Kilts *et al*. 2000). As per the M2-LBT1 receptor, had time permitted, β2AR-LBT2 could be further

characterized with regard to rank order affinities and potencies of various ligands compared to wild type β2AR, to further confirm that the LBT fusion had no effect on the function of the receptor.

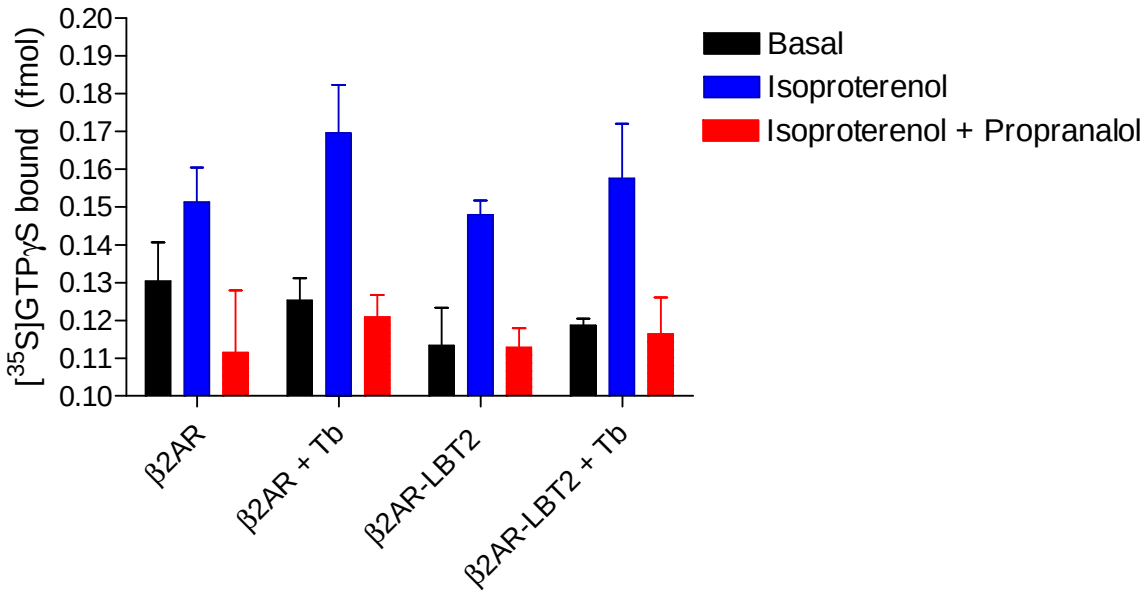

Figure 6.7: β2AR-LBT2 can signal to G-proteins. 0.1 mg/mL of receptor preparations were reconstituted with 20 nM purified G-proteins ($G\alpha_{i1}\beta_4\gamma_2$), 5 μM GDP, 10 μM AMP-PNP and 0.5 nM [^{35}S]GTPγS. The agonist isoproterenol (10 μM) was used to stimulate [^{35}S]GTPγS-binding and the antagonist propranolol (100 μM) used to show signalling specificity by competing with isoproterenol for binding to the receptor. The reactions were incubated for 90 min at 27ºC with shaking and triplicate 25 μL samples were filtered through GFC filters and washed with 3 x 4 mL of cold TMN buffer. Data shown are triplicate samples (mean ± SEM) of a single representative experiment.

The ability of β2AR-LBT2 to bind terbium in comparison to preparations of β2AR was then investigated. A concentration response curve of membrane preparations against 1 μM $TbCl_3$ showed much higher (~ 5-fold) luminescence at 545 nm in the presence of β2AR-LBT2 compared to β2AR (**Figure 6.8**). This indicated that terbium was binding to the LBT fused to β2AR.

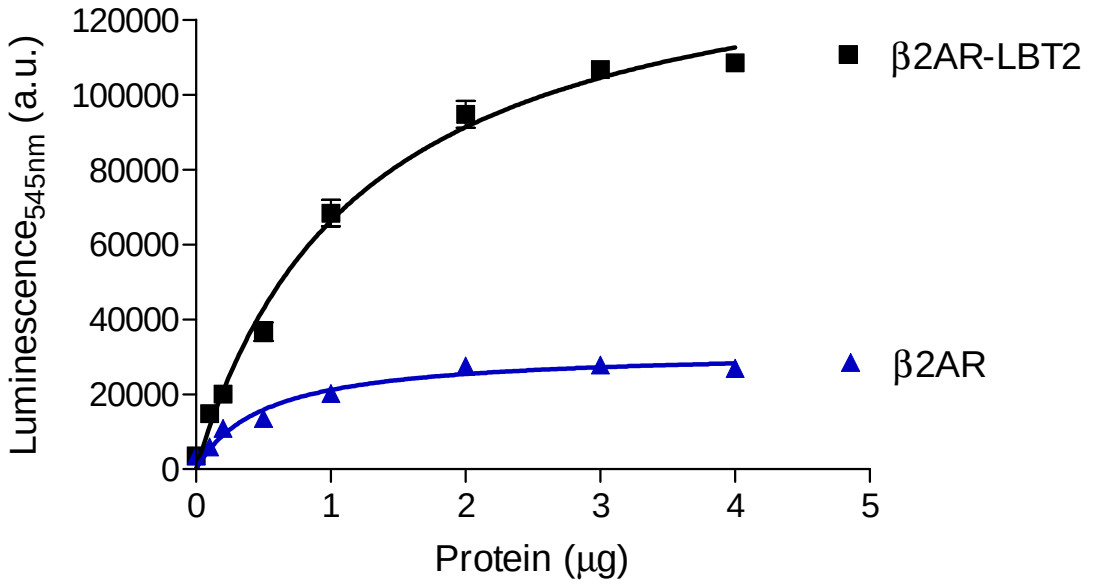

Figure 6.8: Terbium binding to β2AR-LBT2 compared to β2AR. 1 µM $TbCl_3$ was mixed with 0-4 µg of β_2AR-LBT2 (■) or β_2AR (▲) in a final volume of 100 µL using Tb binding buffer. After a 40 min incubation, the terbium emission was measured using a Victor3 plate reader set for time-resolved fluorescence with the following parameters: λ_{ex} 280 nm, λ_{em} 545 nm, 50 µs delay and 900 µs counting duration. Data shown are mean ± SEM (n=3).

BRET has previously been used to demonstrate β2AR coupling to G-protein (G_s) subunits (Gales *et al*. 2005). The study by Gales *et al*. used *R*luc fused to the C-terminus of β2AR and GFP10 inserted within $G\alpha_s$, or fused to the N-terminus of $G\beta_1$ or $G\gamma_2$. Interactions with the receptor were measured in human embryonic kidney (HEK) cells expressing, as required, the receptor, one of the GFP10 G-protein subunits and the remaining unlabelled G-protein subunits. Pre-coupling between the receptor and the GFP10 labelled G-protein subunits constructs was found. However, while an agonist stimulated further coupling between GFP10 fusions to Gβ or Gγ and the receptor, there was no increase with $G\alpha_s$. The presence of the heterotrimer increased agonist stimulated G-protein engagement by the receptor although again, less robustly when GFP10-$G\alpha_s$ was used. $G\alpha_i$ was also found to couple less efficiently with β2AR than $G\alpha_s$. In the present study, pre-coupling of the receptor to the G-protein in the absence of a ligand could not be detected as a TR-FRET signal. When β2AR-LBT2:Tb was mixed with $G\alpha_{i1}$:Alexa using various concentrations, there was no increase in the TR-FRET signal compared to when β_2AR-LBT2:Tb alone was

present. This appeared to indicate that the receptor and G-protein were not pre-coupled. However, the system may not have been sensitive enough to detect the interaction and more success may be achievable using Gβγ:Alexa, a higher concentration of Gα:Alexa and/or the G-protein heterotrimer. Furthermore, the ratio of G-protein to receptor has been indicated to determine the degree of precoupling and this could be investigated further. The use of isoproterenol to stimulate further coupling was also inconclusive since the agonist appeared to quench the luminescence emission at 545 nm.

6.4. Further discussion and conclusions

This chapter described the construction of two GPCRs fused to LBTs at their C-termini. These fusion proteins were successfully expressed in *Sf*9 cells, could bind to ligands and signalled through G-proteins. Membrane preparations containing these receptors also demonstrated significantly higher terbium-binding properties compared to wild-type receptor preparations. The interaction of these receptors with G-proteins (labelled with Alexa546) was then examined using TR-FRET and preliminary results indicated pre-coupling of the M_2-muscarinic receptor with $G\alpha_{i1}$ whereas there was no indication of an interaction between the β_2-adrenergic receptor with $G\alpha_{i1}$. Further optimization of the assay is required and there is potential to increase the signal window through optimization of receptor and G-protein subunit concentrations and improvements to the preparation of receptors and labelled proteins. The system could also be further characterized with regard to dose responses, consideration of kinetics and the effects of ligands, and further validated through the use of GPCR mutants that do not couple to G-proteins.

This study has so far investigated using the G-protein subunit interaction as a potential platform for monitoring receptor-mediated G-protein activation and detecting inhibitors or activators of this interaction within the drug discovery arena. An alternate platform could be to detect novel compounds that interact at the interface of the G-protein and the receptor. This could have the potential to identify compounds producing effects not obtainable using receptor ligands. By controlling what could be specific G-protein pathways from a receptor, different responses or reduced side effects may be achieved. With regard to using G-protein interactions with the receptor as a method for determining ligand-binding to a GPCR, this platform could be feasible but would be less generic in nature compared to using the G-protein subunit interaction alone as the assay format. This would require the tagging of the receptors under investigation, possibly leading to altered function, whereas monitoring the G-protein subunit interaction could potentially

be applied to a wider variety of receptors without modification of the receptor. While other studies have shown ligand-induced changes in G-protein coupling, this could not currently be established in the cell-free TR-FRET assay developed in this study.

So far, this study has exploited TR-FRET to monitor binding events between separate proteins. However, site-specific labelling within the same protein could be used to detect changes in conformation within that protein. In the case of GPCRs, changes in conformation, particularly involving the third intracellular loop and the C-terminus have been reported for some receptors including the M_3-muscarinic receptor (Han *et al*. 2005), the β_2-adrenergic receptor (Granier *et al*. 2007; Nakanishi *et al*. 2006), the α_{2A}-adrenergic receptor (Vilardaga *et al*. 2005) and the A_{2A}-adenosine receptor (Hoffmann *et al*. 2005), although it has not been conclusively established whether this conformational change is common to all GPCRs. Studies measuring these conformational changes have also shown the advantages of using smaller fluorescent tags as opposed to fluorescent proteins since the substitution of a fluorescent protein within the third intracellular loop of the A_{2A}-adenosine receptor with a TCM restored the signalling function of the receptor to wild-type (Hoffmann *et al*. 2005). With a LBT already fused to the C-terminus of two receptors, a TCM was then introduced into the third intracellular loop. However, these constructs only reached the generation of recombinant bacmid before time constraints intervened in their expression and characterization.

Further modifications of the LBT receptors may increase their utility. For example, an additional His-tag could facilitate receptor purification, which may aid in increasing the TR-FRET signal and the terbium-binding properties of LBT and the X-ray scattering properties of terbium could be exploited during crystallization studies in determining phases of diffracted X-rays. Atomic structures of GPCRs have been notoriously difficult to obtain due to the purification of the

receptors and the formation of crystals for X-ray diffraction, and modifications to the GPCR have often been necessary to facilitate both of these processes. Structure determination from X-ray diffraction of crystals requires data from the amplitudes and phases of the diffracted X-rays. Determining phases uses techniques that require the incorporation of heavy atoms into the protein structure and often selenium is used. The powerful X-ray scattering properties of terbium could lend LBTs to aid in determining the phases with terbium expected to have 4 times the phasing power of selenium (Silvaggi *et al*. 2007).

Purification and His-tagging could also facilitate surface display and orientation of receptors, which could be useful in developing arrays that may provide increased accessibility for G-protein interactions to improve the signal generation in TR-FRET assays.

7. General discussion, future directions and conclusion

This study has developed the use of TR-FRET for investigating interactions of G-protein subunits with each other or with receptors as potential platforms for identifying novel therapeutics and/or as a tool for characterizing novel interactions such as that between Gα and CrV2 (**Figure 7.1**). Our first-generation assay using Alexa546 and CS124-DTPA-EMCH:Tb as the acceptor and donor respectively, was exploited to show a specific, high affinity interaction between Gα and CrV2 that warrants further investigation for its implications on immune regulation in invertebrates. Attention then turned to utilizing site-specific labelling strategies to improve both the donor and acceptor labelling of proteins for TR-FRET applications, which had not previously been demonstrated using two genetically encodable small peptide fusions in a second-generation TR-FRET platform. LBTs and TCMs were fused to various G-protein subunits and the integrity of the tags and G-protein subunits examined. The fusion proteins could be integrated into the first-generation assay platform to show their utility as TR-FRET partners and both terbium labelled LBTs and FlAsH labelled TCMs were successful in generating TR-FRET signals with Alexa546 or CS124-DTPA-EMCH:Tb labelled binding partners, respectively. To our knowledge, these pairs of fluors have not previously been used in TR-FRET studies. TCM:FlAsH and CS124-DTPA-EMCH:Tb were particularly successful with the generation of signal levels up to 5-fold above background. Since FlAsH is excited by the first peak of terbium emissions this could give rise to the possibiity of multiplexing with another fluor such as Alexa546 that receives energy transferred from the second emission peak of terbium to measure separate interactions using the one donor. It was then demonstrated that LBT:Tb and TCM:FlAsH labelled proteins could be used as a donor and acceptor pair in TR-FRET where an interaction between labelled Gα and Gβγ subunits was observed. LBTs were also fused to GPCRs to investigate other potential assay platforms such as the interaction with the G-protein, which was demonstrated using an LBT fused to the M_2-muscarinic receptor and Alexa546 labelled Gα-subunits. The possible exploitation of these constructs in other applications such as X-ray crystallography was also discussed.

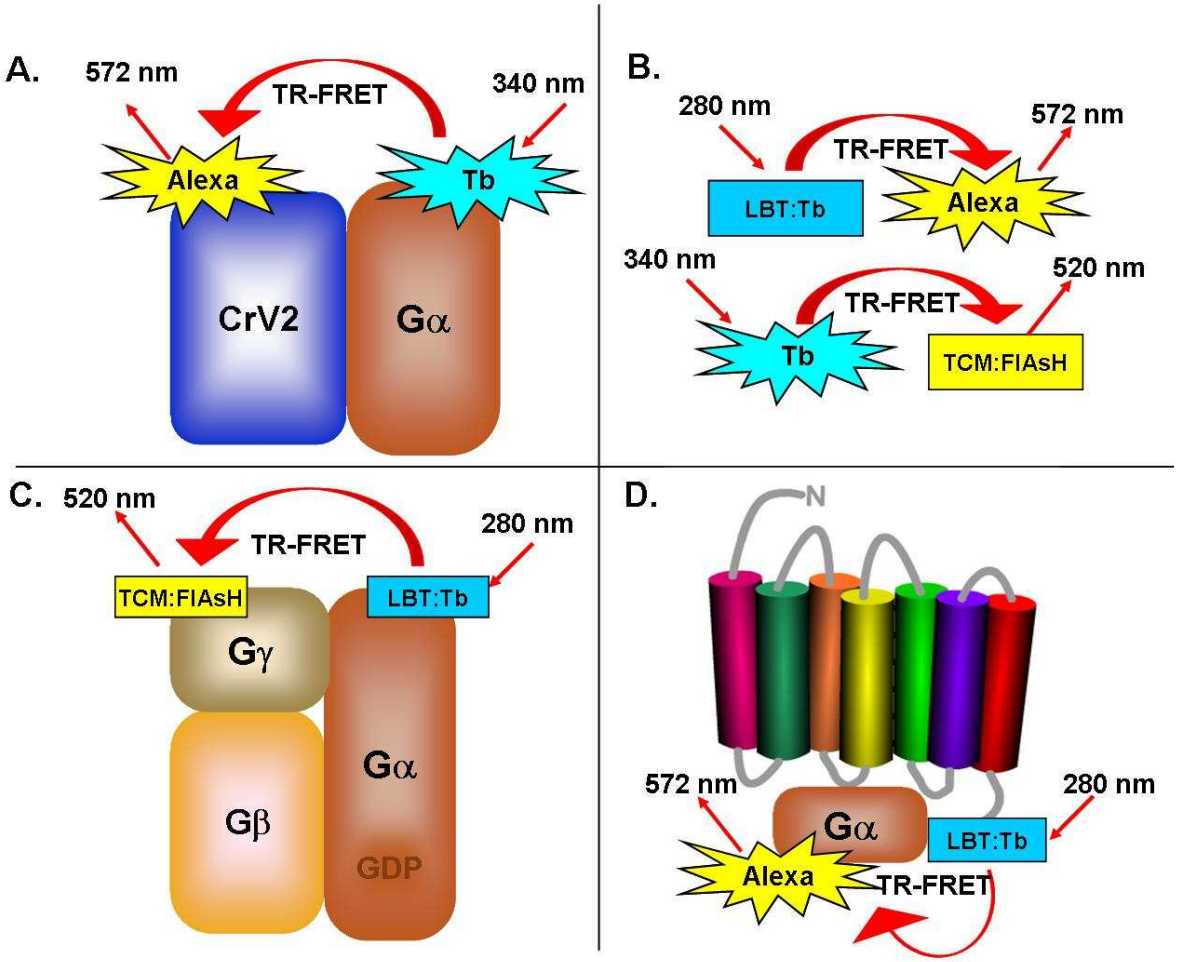

Figure 7.1: Schematic of TR-FRET platforms investigated during this study. (A) First generation assay used to show an interaction between Gα and CrV2 with proteins labelled with CS124-DTPA-EMCH:Tb or Alexa546, respectively. **(B)** LBT fusion proteins labelled with terbium were investigated as TR-FRET partners with Alexa546-labelled binding partners and tetracysteine motif fusion proteins labelled with FlAsH were investigated as TR-FRET partners with CS124-DTPA-EMCH:Tb-labelled binding partners. **(C)** Second generation TR-FRET assay using LBT fusion proteins labelled with terbium and TCM fusion proteins labelled with FlAsH. **(D)** GPCRs were fused to a LBT at the C-terminus of the receptor and the association with Alexa546 labelled Gα-subunits investigated using TR-FRET.

It was generally found that the performance of both the LBT and the TCM in the context of a fusion protein was inferior to that of the tags as peptides alone. This could be due to the fusion disturbing the binding properties of the tag. However, the introduction of the larger fusion protein could change the properties of the assay since other moieties are introduced that can absorb excitation light (e.g. other tryptophan residues), and/or produce scattering of light. This suggests that a direct comparison between the tag as a peptide and when fused to a significantly larger

protein is not feasible in some aspects. The properties of the fluorescent tags within fusion proteins could be further characterized with regard to their quantum yield to establish the distances over which TR-FRET will occur (R_o). Measurement of these parameters could also allow the generation of more specific information regarding the distances involved with the conformational changes occurring. Although these tags were considerably smaller than more common fluorescent fusion proteins, it remained that the fusion site needs to be carefully considered since even small extensions were sometimes found to be detrimental to protein function. In this study, preservation of protein function was determined by reconstituting the G-protein subunits with a GPCR and measuring agonist induced [^{35}S]GTPγS binding. This could be examined further by carrying out dose-responses of agonists to investigate whether the efficacy of GPCR signalling to the G-protein subunits was maintained. Functional Gα and Gβγ subunits were shown to be necessary for maximal [^{35}S]GTPγS binding, but this assay cannot rule out interactions with effectors downstream being affected by the fusion of LBTs or TCMs. This may or may not be important depending on the application of the construct and assay.

Nevertheless, a TR-FRET signal could be generated via labelling interacting proteins with LBTs and TCMs. Compared to the fluorescent labels used in the first-generation TR-FRET assay, the LBT and TCM strategy of labelling proteins produced a smaller TR-FRET signal that, at the present time, would require further refinement for high throughput applications but could be a useful tool in biochemical studies of G-proteins or for studies of other protein interactions. It should also be noted that TR-FRET using LBT2-Gα_{S25} and G$\beta\gamma_2$-TCM was measured in the presence of membranes and many other contaminating proteins unlike previous assays, which used purified protein preparations. This could have contributed to higher background signals or scattering of the acceptor emission, and the LBT:Tb/TCM:FlAsH TR-FRET pair could prove to be more robust in a purified system. However, future refinements to both the LBT and TCM

strategies could also provide a larger signal window by improving luminescence, affinity and spectral properties as has been discussed in the previous chapters. Although efforts to show that specific protein interactions were producing the TR-FRET signals such as protease treatment, generation of saturation curves and addition of unlabelled binding partners, the TR-FRET platforms shown here should be further validated. Mutants that no longer bind, but contain the fluorescent moieties could be used to characterize conditions under which bystander FRET occurs from random collisions and begins to interfere in the specific TR-FRET signal. The addition of such mutated proteins could also aid in validating that the addition of unlabelled binding partners are truly competing for binding and not merely inhibiting collisions or increasing scattering. Alternatively, with appropriate instrumentation, TR-FRET could be detected by measuring changes in the donor lifetime, which would also further validate the TR-FRET signals generated in this study. In analyzing data to determine the apparent *K*d values for protein interactions and terbium binding, it was not possible to determine whether ligand depletion was occurring in the homogenous assay platform and analysis was not conducted for this instance. It is therefore possible that the *K*d values found here could be an over-estimation resulting in an under-estimation of the affinity (Carter *et al*. 2007). Avoiding depletion in the experiment is difficult since it would be necessary to use a lower concentration of terbium labelled protein which would decrease the signal, or alternatively, to conduct the assay in a larger volume which would require much larger quantities of protein. It is possible to account for depletion in the analysis of radioligand binding data (Carter *et al*. 2007), however, the homogenous fluorescent assay platforms used in this study do not lend themselves to such analysis.

Monitoring the G-protein subunit interaction offers a fluorescent TR-FRET platform that itself could be useful for identifying novel therapeutics capable of producing different effects from receptor ligands. In addition, it could be expanded upon by the introduction of a receptor into the

system to modulate the G-protein interaction. Such a platform would be generic in that a range of receptors could be applied without requiring engineering of the receptor. The use of promiscuous G-proteins such as $G\alpha_{S25}$ could further increase the range of GPCRs able to be applied. The introduction of a receptor to modulate the G-protein interaction in either the first or second-generation assay platforms would greatly increase the applications of the assay. However, our efforts to do so have been unsuccessful thus far. The problem could lie in the lower expression level of receptor, with it being likely that enrichment or purification of receptors may produce an observable signal. Furthermore, Kelly Bailey (CSIRO) has also shown that Gα bound to GTPγS can remain bound to Gβγ in the absence of receptor and this may contribute to a background signal that makes receptor activation indistinguishable. The assay platform itself may also be problematic since receptor activation is expected to induce dissociation of the G-protein subunits *in vitro* resulting in a decrease in TR-FRET. This decrease in TR-FRET would be observed as a decrease in acceptor emission and increase in terbium emission. Some luminescence from terbium can be detected in the acceptor channel as background and the increase in terbium emission caused by a decrease in TR-FRET could therefore mask the change in acceptor emission. Alternative TR-FRET platforms could be investigated such as fluorescent GTPγS, for example BODIPY-GTPγS binding to terbium-labelled Gα subunits. However, while BODIPY-GTP binding to Gα:Tb could be detected and competed off using unlabelled GTPγS, agonist-mediated binding could not be seen in an assay platform analogous to the [^{35}S]GTPγS-binding system. The problems arising when a receptor preparation is introduced into the assay platform warrant further investigation and improvements to the TR-FRET signal generated by the G-protein subunits may be useful.

In the future, the LBT/TCM system could lend itself to TR-FRET studies in cells to produce a significantly better signal:noise ratio than that achieved using the traditional CFP and YFP FRET

pair. This would also extend the utility of TR-FRET in studying intracellular targets rather than being limited to cell surface proteins due to the use of antibodies to label proteins with an appropriate donor. While cell-based studies using TCMs labelled with the membrane permeable FlAsH have become relatively established, the use of LBTs in cellular studies are few, and could be regarded as preliminary. A study by Goda *et al*. (2007) has developed a method of cellular delivery of exogenous LBT fusion proteins into HeLa or NIH3T3 cells that were then imaged using fluorescent microscopy. This study also reported that there was no obvious growth arrest indicating an absence of toxic effects with 1 μM $TbCl_3$. This work could be built upon firstly by exploiting the long-lived luminescence of terbium by employing a time-gated measurement such as has been demonstrated by Hanaoka *et al*. (2007). It may also be possible to recombinantly express the fusion proteins so that the proteins localize in a normal manner *in situ* if a method of terbium transportation into the cells can be developed perhaps by using ionophores (Wang, Taylor & Pfeiffer 1998). Multiple photon excitation of the tryptophans that act as antennas to, in turn, excite terbium could also overcome the problems associated with direct UV excitation (Lippitz *et al*. 2002; Majoul *et al*. 2002; Svoboda, Yasuda 2006).

In conclusion, this study has focussed on developing TR-FRET platforms for the investigation of G-protein subunit interactions. This has lead to the discovery of a putative Gα subunit interaction with CrV2 that had not previously been reported. If this interaction can be confirmed *in vivo*, this would demonstrate the utility of the assay in screening for receptor-independent G-protein interactors. Furthermore, the utility of LBTs and TCMs has also been the focus of the study in terms of developing a novel, site-specific labelling strategy for TR-FRET assays which could have many potential applications.

8. Appendices

8.1. Comparison of *Drosophila* $G\alpha_o$ and rat $G\alpha_{i1}$ amino acid sequences

Analysis conducted using protein BLAST program at http://blast.ncbi.nlm.nih.gov/Blast.cgi

69.6% identity in 355 residues overlap; Score: 1293.0; Gap frequency: 0.6%

```
RatGα_i1          1 MGCTLSAEDKAAVERSKMIDRNLREDGEKAAREVKLLLLGAGESGKSTIVKQMKIIHEAG
Drosophila Gα_o   1 MGCTTSAEERAAIQRSKQIEKNLKEDGIQAAKDIKLLLLGAGESGKSTIVKQMKIIHESG
                    **** ***  **  *** *  ** ***  **   ********************** *

Rat              61 YSEEECKQYKAVVYSNTIQSIIAIIRAMGRLKIDFGDAARADDARQLF-VLAGAAEEGFM
Drosophila       61 FTAEDFKQYRPVVYSNTIQSLVAILRAMPTLSIQYSNNERESDAKMVFDVCQRMHDTEPF
                       *  ***  *********  ** ***  * *      *  **   * *

Rat             120 TAELAGVIKRLWKDSGVQACFNRSREYQLNDSAAYYLNDLDRIAQPNYIPTQQDVLRTRV
Drosophila      121 SEELLAAMKRLWQDAGVQECFSRSNEYQLNDSAKYFLDDLDRLGAKDYQPTEQDILRTRV
                      **    **** * *** ** ** ******** * * ****     * ** ** *****

Rat             180 KTTGIVETHFTFKDLHFKMFDVGGQRSERKKWIHCFEGVTAIIFCVALSDYDLVLAEDEE
Drosophila      181 KTTGIVEVHFSFKNLNFKLFDVGGQRSERKKWIHCFEDVTAIIFCVAMSEYDQVLHEDET
                    ******* ** ** * ** ***************** ******** * ** ** ***

Rat             240 MNRMHESMKLFDSICNNKWFTDTSIILFLNKKDLFEEKIKKSPLTICYPEYAGSNTYEEA
Drosophila      241 TNRMQESLKLFDSICNNKWFTDTSIILFLNKKDLFEEKIRKSPLTICFPEYTGGQEYGEA
                     *** ** ******************************** ******* *** *   * **

Rat             300 AAYIQCQFEDLNKRKDTKEIYTHFTCATDTKNVQFVFDAVTDVIIKNNLKDCGLF
Drosophila      301 AAYIQAQFEAKNK-STSKEIYCHMTCATDTNNIQFVFDAVTDVIIANNLRGCGLY
                    ***** ***  **    **** * ****** * ************ ***  ***
```

8.2. Effect of CrV2 on GTP-binding to $G\alpha_{i1}$

To further establish the function of CrV2 in relation to binding to Gα subunits, increasing concentrations of CrV2 were added to $G\alpha_{i1}$ in the presence of [^{35}S]GTPγS. $G\alpha_{i1}$ was seen to bind [^{35}S]GTPγS and this was not significantly influenced by the presence of CrV2, which alone did not bind [^{35}S]GTPγS (**Figure 8.1**). This implies that CrV2 does not act as a guanine nucleotide exchange factor. However, a time course of [^{35}S]GTPγS binding would be appropriate to confirm CrV2 has no effect on the kinetics of [^{35}S]GTPγS binding.

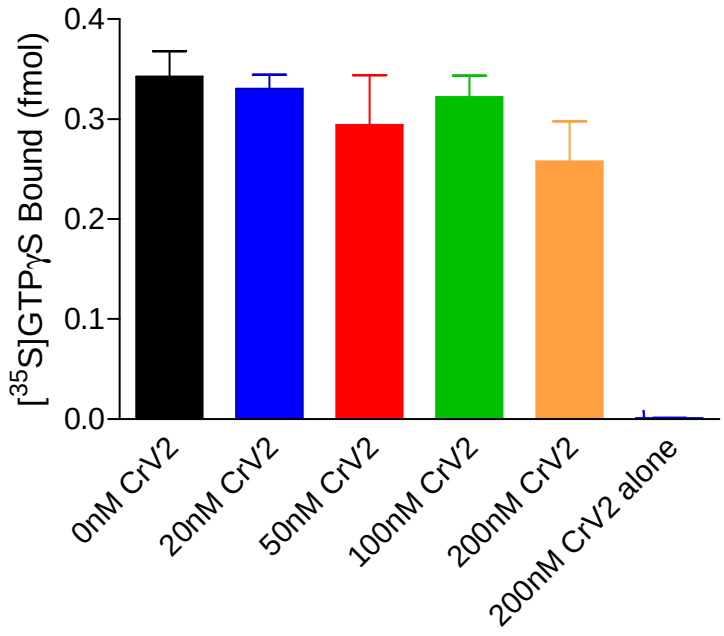

Figure 8.1: Effect of CrV2 on GTP-binding to $G\alpha_{i1}$. 40 nM of purified $G\alpha_{i1}$ was mixed with increasing concentrations of CrV2 (0-200 nM) and 0.4 nM [^{35}S]GTPγS. After a 100 min incubation period in a shaking water bath at 27ºC, triplicate 25µL samples were filtered through GFC filters on a vacuum manifold and unbound [^{35}S]GTPγS removed by washing 3x with 4 ml of TMN buffer. The amount of [^{35}S]GTPγS bound was determined by scintillation counting. Data shown are mean ± SEM (n=3) of filter triplicates of a single representative experiment.

8.3. Lanthanide binding tag fusion protein sequences

Histidine tags are indicated in red
Lanthanide binding tags are indicated in blue

8.3.1. His-LBT2-$G\alpha_{S25}$

Nucleotide Sequence

ATGAGAGGATCG**CATCACCATCACCATCAC**GGATCCGCATGCGAGCTCGGTACC**GCTTG**
TGTTGACTGGAATAATGACGGTTGGTACGAAGGTGACGAATGTGCTATGGCCCGCTCGC
TGACCTGGCGCTGCTGCCCCTGGTGCCTGACGGAGGATGAGAAGGCCGCCGCCCGGGTG
GACCAGGAGATCAACAGGATCCTCTTGGAGCAGAAGAAGCAGGACCGCGGGGAGCTGAA
GCTGCTGCTTTTGGGCCCAGGCGAGAGCGGGAAGAGCACCTTCATCAAGCAGATGCGGA
TCATCCACGGCGCCGGCTACTCGGAGGAGGAGCGCAAGGGCTTCCGGCCCCTGGTCTAC
CAGAACATCTTCGTGTCCATGCGGGCCATGATCGAGGCCATGGAGCGGCTGCAGATTCC
ATTCAGCAGGCCCGAGAGCAAGCACCACGCTAGCCTGGTCATGAGCCAGGACCCCTATA
AAGTGACCACGTTTGAGAAGCGCTACGCTGCGGCCATGCAGTGGCTGTGGAGGGATGCC
GGCATCCGGGCCTGCTATGAGCGTCGGCGGGAATTCCACCTGCTCGATTCAGCCGTGTA
CTACCTGTCCCACCTGGAGCGCATCACCGAGGAGGGCTACGTCCCCACAGCTCAGGACG
TGCTCCGCAGCCGCATGCCCACCACTGGCATCAACGAGTACTGCTTCTCCGTGCAGAAA
ACCAACCTGCGGATCGTGGACGTCGGGGGCCAGAAGTCAGAGCGTAAGAAATGGATCCA
TTGTTTCGAGAACGTGATCGCCCTCATCTACCTGGCCTCACTGAGTGAATACGACCAGT
GCCTGGAGGAGAACAACCAGGAGAACCGCATGAAGGAGAGCCTCGCATTGTTTGGGACT
ATCCTGGAACTACCCTGGTTCAAAAGCACATCCGTCATCCTCTTTCTCAACAAAACCGA
CATCCTGGAGGAGAAAATCCCCACCTCCCACCTGGCTACCTATTTCCCCAGTTTCCAGG
GCCCTAAGCAGGATGCTGAGGCAGCCAAGAGGTTCATCCTGGACATGTACACGAGGATG
TACACCGGGTGCGTGGACGGCCCCGAGGGCAGCAAGAAGGGCGCACGATCCCGACGCCT
TTTCAGCCATTACACATGTGCCACAGACACTGAGAACATCCGCCGTGTCTTCAACGACT
GCCGTGACATCATCCAGCGCATGCATCTTCGCCAATACGAGCTGCTCTAA

Amino Acid Sequence

MRGS**HHHHHH**GSACELGT**ACVDWNNDGWYEGDECA**MARSLTWRCCPWCLTEDEKAAARV
DQEINRILLEQKKQDRGELKLLLLGPGESGKSTFIKQMRIIHGAGYSEEERKGFRPLVY
QNIFVSMRAMIEAMERLQIPFSRPESKHHASLVMSQDPYKVTTFEKRYAAAMQWLWRDA
GIRACYERRREFHLLDSAVYYLSHLERITEEGYVPTAQDVLRSRMPTTGINEYCFSVQK
TNLRIVDVGGQKSERKKWIHCFENVIALIYLASLSEYDQCLEENNQENRMKESLALFGT
ILELPWFKSTSVILFLNKTDILEEKIPTSHLATYFPSFQGPKQDAEAAKRFILDMYTRM
YTGCVDGPEGSKKGARSRRLFSHYTCATDTENIRRVFNDCRDIIQRMHLRQYELL

8.3.2. His-LBT2-$G\alpha_{i1}$

Nucleotide sequence:

ATGAGAGGATCG**CATCACCATCACCATCAC**GGATCCGCATGCGAGCTCGGTACC**GCTTG**
TGTTGACTGGAATAATGACGGTTGGTACGAAGGTGACGAATGTGCTATGGGCTGCACAC

TGAGCGCTGAGGACAAGGCGGCCGTGGAGCGCAGCAAGATGATCGACCGCAACCTCCGG
GAGGACGGAGAGAAGGCAGCGCGCGAGGTCAAGCTGCTGCTGCTGGGTGCTGGTGAATC
CGGGAAGAGCACAATTGTGAAGCAGATGAAAATTATCCACGAGGCTGGCTACTCAGAGG
AAGAGTGTAAGCAGTACAAAGCAGTGGTCTACAGCAACACCATCCAGTCCATCATTGCC
ATCATTAGAGCTATGGGGAGATTGAAAATCGACTTTGGAGACGCTGCTCGTGCGGATGA
TGCTCGCCAACTCTTCGTGCTTGCTGGGGCTGCAGAGGAAGGCTTTATGACCGCGGAGC
TCGCCGGCGTCATAAAGAGACTGTGGAAGGACAGCGGTGTGCAAGCCTGCTTCaACAGA
TCCCGGGAGTACCAGCTGAACGATTCGGCGGCGTACTACCTGAATGACTTGGACAGAAT
AGCACAACCaAATTACATCCCAACCCAGCAGGATGTTCTCAGAACTAGAGTGAAAACGA
CGGGAATTGTGGAAACCCACTTTACTTTCaAAGATCTTCATTTTAAAATGTTTGACGTG
GGAGGCCaGAGATCAGAGCGGAAGAAGTGGATTCACTGCTTTGAAGGCGTGACTGCCAT
CATCTTCTGTGTGGCCCTGAGTGACTATGACCTGGTTCTTGCTGAGGATGAAGAAATGA
ACCGGATGCACGAAAGCATGAAGCTGTTCGATAGCATATGTAACAACAAGTGGTTTACG
GACACATCCATCATCCTTTTCCTGAACAAGAAGGACCTCTTCGAAGAGAAGATCAAAAA
GAGTCCCCTCACGATATGCTATCCAGAATATGCAGGCTCAAACACATATGAAGAGGCGG
CTGCGTATATCCAGTGTCAGTTTGAAGACCTCAATAAAAGGAAGGACACAAAGGAAATT
TACACCCACTTCACTTGCGCCACGGATACGAAGAATGTGCAGTTTGTGTTCGATGCTGT
AACGGACGTCATCATAAAGAATAACCTAAAAGATTGTGGTCTCTTTTAAAAGCTT

Amino acid sequence:

MRGS**HHHHHH**GSACELGT**ACVDWNNDGWYEGDECA**MGCTLSAEDKAAVERSKMIDRNLR
EDGEKAAREVKLLLLGAGESGKSTIVKQMKIIHEAGYSEEECKQYKAVVYSNTIQSIIA
IIRAMGRLKIDFGDAARADDARQLFVLAGAAEEGFMTAELAGVIKRLWKDSGVQACFNR
SREYQLNDSAAYYLNDLDRIAQPNYIPTQQDVLRTRVKTTGIVETHFTFKDLHFKMFDV
GGQRSERKKWIHCFEGVTAIIFCVALSDYDLVLAEDEEMNRMHESMKLFDSICNNKWFT
DTSIILFLNKKDLFEEKIKKSPLTICYPEYAGSNTYEEAAAYIQCQFEDLNKRKDTKEI
YTHFTCATDTKNVQFVFDAVTDVIIKNNLKDCGLF

8.3.3. LBT1-Gβ_4

Nucleotide Sequence:

ATG**TATATTGATACTAATAACGACGGTTGGTACGAAGGTGACGAACTTCTTGCT**ATGAG
CGAGCTGGAGCAGCTGAGGCAGGAGGCTGAACAGCTTCGGAATCAGATCCAGGATGCTC
GGAAGGCCTGCAACGATGCCACGCTGGTTCAGATCACGTCTAATATGGACTCCGTGGGC
CGAATACAAATGCGAACAAGGCGCACGCTGCGTGGCCACCTCGCTAAGATCTACGCCAT
GCACTGGGGATATGATTCCAGGCTACTAGTCAGTGCTTCGCAAGATGGAAAATTAATTA
TTTGGGATAGCTATACGACAAATAAGATGCACGCCATCCCTCTGAGGTCCTCCTGGGTG
ATGACCTGTGCCTACGCCCCGTCCGGGAACTACGTTGCCTGTGGAGGCTTGGATAACAT
CTGCTCCATATACAACCTAAAGACCCGAGAGGGGAATGTGCGGGTGAGCCGAGAATTGC
CAGGACACACGGGCTACTTGTCCTGCTGCCGATTCTTAGATGATGGACAAATCATTACA
AGTTCGGGAGACACGACTTGTGCTTTGTGGGACATTGAGACCGGACAGCAGACTACGAC
CTTCACAGGACACTCGGGTGACGTGATGAGCCTCTCACTGAGTCCTGACTTGAAGACCT
TTGTGTCTGGTGCTTGCGATGCATCCTCAAAGCTGTGGGATATCCGAGATGGGATGTGT
AGACAGTCTTTCACCGGACACATCTCAGACATCAACGCTGTCAGTTTCTTCCCGAGTGG
ATATGCCTTTGCCACTGGTTCTGATGATGCCACATGCCGACTCTTTGACCTCCGTGCAG
ACCAGGAGCTCCTGCTATACTCTCATGACAATATCATCTGTGGCATTACTTCTGTGGCC
TTCTCAAAGAGTGGGCGCCTCCTGTTAGCCGGCTATGACGACTTCAACTGCAGTGTGTG
GGACGCTCTGAAAGGGGGCCGGTCAGGTGTCCTTGCTGGTCATGACAACCGTGTTAGCT

GCTTAGGTGTGACTGATGACGGCATGGCTGTGGCCACTGGCTCCTGGGACAGTTTTCTT
AAAATCTGGAATTGA

Amino acid sequence:

MYIDTNNDGWYEGDELLAMSELEQLRQEAEQLRNQIQDARKACNDATLVQITSNMDSV
GRIQMRTRRTLRGHLAKIYAMHWGYDSRLLVSASQDGKLIIWDSYTTNKMHAIPLRSSW
VMTCAYAPSGNYVACGGLDNICSIYNLKTREGNVRVSRELPGHTGYLSCCRFLDDGQII
TSSGDTTCALWDIETGQQTTTFTGHSGDVMSLSLSPDLKTFVSGACDASSKLWDIRDGM
CRQSFTGHISDINAVSFFPSGYAFATGSDDATCRLFDLRADQELLLYSHDNIICGITSV
AFSKSGRLLLAGYDDFNCSVWDALKGGRSGVLAGHDNRVSCLGVTDDGMAVATGSWDSF
LKIWN

Mutations:
Lysine should be Arginine (indicated in orange)

8.3.4. $G\alpha_{i1}$-LBT2

Nucleotide Sequence:

AGTGGCTGCACGCTGAGCGCTGAGGACAAGGCGGCCGTGGAGCGCAGCAAGATGATCGA
CCGCAACCTCCGGGAGGACGGAGAGAAGGCAGCGCGCGAGGTCAAGCTGCTGCTGCTGG
GTGCTGGTGAATCCGGGAAGAGCACAATTGTGAAGCAGATGAAAATTATCCACGAGGCT
GGCTACTCAGAGGAAGAGTGTAAGCAGTACAAAGCAGTGGTCTACAGCAACACCATCCA
GTCCATCATTGCCATCATTAGAGCTATGGGGAGATTGAAAATCGACTTTGGAGACGCTG
CTCGTGCGGATGATGCTCGCCAACTCTTCGTGCTTGCTGGGGCTGCAGAGGAAGGCTTT
ATGACCGCGGAGCTCGCCGGCGTCATAAAGAGACTGTGGAAGGACAGCGGTGTGCAAGC
CTGCTTCAACAGATCCCGGGAGTACCAGCTGAACGATTCGGCGGCGTACTACCTGAATG
ACTTGGACAGAATAGCACAACCAAATTACATCCCAACCCAGCAGGATGTTCTCAGAACT
AGAGTGAAAACGACGGGAATTGTGGAAACCCACTTTACTTTCAAAGATCTTCATTTTAA
AATGTTTGACGTGGGAGGCCAGAGATCAGAGCGGAAGAAGTGGATTCACTGCTTTGAAG
GCGTGACTGCCATCATCTTCTGTGTGGCCCTGAGTGACTATGACCTGGTTCTTGCTGAG
GATGAAGAAATGAACCGGATGCACGAAAGCATGAAGCTGTTCGATAGCATATGTAACAA
CAAGTGGTTTACGGACACATCCATCATCCTTTTCCTGAACAAGAAGGACCTCTTCGAAG
AGAAGATCAAAAAGAGTCCCCTCACGATATGCTATCCAGAATATGCAGGCTCAAACACA
TATGAAGAGGCGGCTGCGTATATCCAGTGTCAGTTTGAAGACCTCAATAAAAGGAAGGA
CACAAAGGAAATTTACACCCACTTCACTTGCGCCACGGATACGAAGAATGTGCAGTTTG
TGTTCGATGCTGTAACGGACGTCATCATAAAGAATAACCTAAAAGATTGTGGTCTCTTC
CTCGAGGCTTGTGTTGACTGGAATAATGACGGTTGGTACGAAGGTGACGAATGTGCTTA
G

Amino Acid Sequence:

MGCTLSAEXKAAVERSKMIDRNLREDGEKAAREVKLLLLGAGESGKSTIVKQMKIIHEA
GYSEEECKQYKAVVYSNTIQSIIAIIRAMGRLKIDFGDAARADDARQLFVLAGAAEEGF
MTAELAGVIKRLWKDSGVQACFNRSREYQLNDSAAYYLNDLDRIAQPNYIPTQQDVLRT
RVKTTGIVETHFTFKDLHFKMFDVGGQRSERKKWIHCFEGVTAIIFCVALSDYDLVLAE
DEEMNRMHESMKLFDSICNNKWFTDTSIILFLNKKDLFEEKIKKSPLTICYPEYAGSNT

YEEAAAYIQCQFEDLNKRKDTKEIYTHFTCATDTKNVQFVFDAVTDVIIKNNLKDCGLF
LE**ACVDWNNDGWYEGDECA**

8.4. Expression of promiscuous chimeric Gα-subunits in *E. coli*

Recombinant proteins were expressed in M15[pREP4] *E. coli* (Qiagen) and a high level of expression was achieved for most constructs as observed in cell lysates run on SDS-PAGE (**Figure 8.2**A) with the exception of LBT1-$G\alpha_{z44}$ which could not be detected. Western blotting showed that these highly induced proteins carried a histidine tag (**Figure 8.2**B) and staining of the gel in a $TbCl_3$ solution also showed this protein to fluoresce under UV light from a UV transilluminator (**Figure 8.2** C and D).

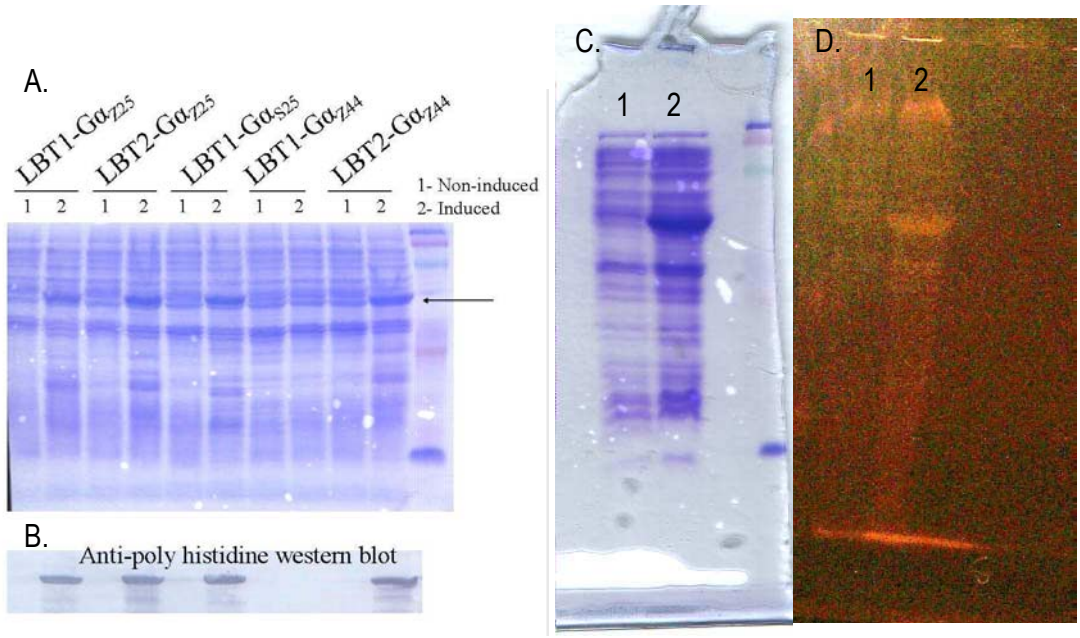

Figure 8.2: Expression of lanthanide binding tagged chimeric Gα-subunits in *E. coli*. (A) Recombinant *E. coli* lysates showing induction of expression (using IPTG) compared to lysates from non-induced recombinant *E. coli*. (B) Western blot of the lysates shown in (A) with proteins detected by anti-poly His antibodies. (C) Induced and non-induced LBT2-$G\alpha_{Z25}$ *E. coli* lysates separated on SDS-PAGE and (D) stained with $TbCl_3$ and visualized under UV light.

8.5. Other LBT fusion proteins

8.5.1. Purification of $G\alpha_{i1}$-LBT2 and terbium-binding properties

The C-terminus of $G\alpha_{i1}$ was fused to LBT2 ($G\alpha_{i1}$-LBT2) and the recombinant protein co-expressed in *Sf*9 cells with $G\beta_1$ and His-tagged $G\gamma_2$. The G-protein heterotrimer was purified using IMAC and then $G\alpha_{i1}$-LBT2 was eluted from the column using aluminium fluoride in highly pure fractions (**Figure 8.3**).

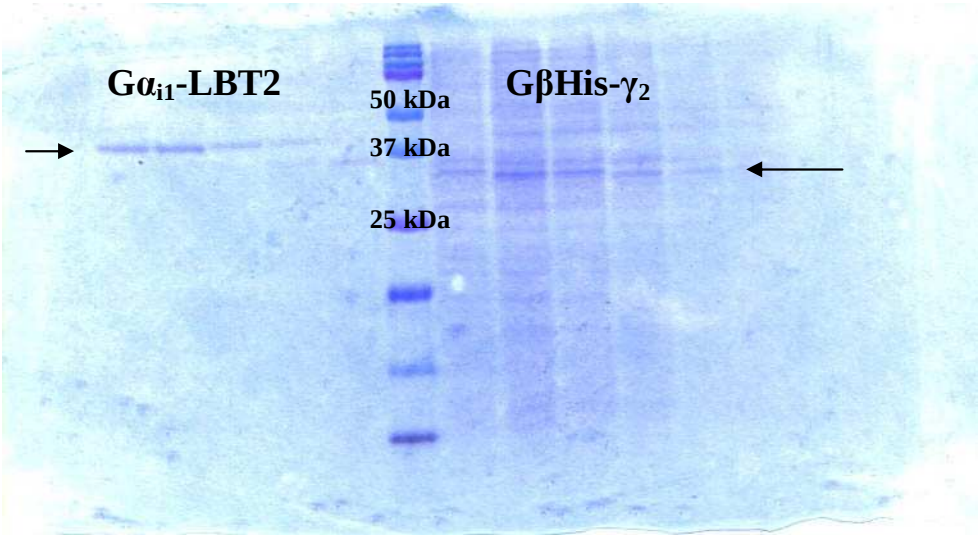

Figure 8.3: SDS-PAGE elution profile from purification of $G\alpha_{i1}$-LBT2 from His-$G\beta_1\gamma_2$ using Ni-NTA beads. 1.2 L of *Sf*9 cells at ~2 x 10^6 cells/mL were triple infected with $G\alpha_{i1}$-LBT2, $G\beta_1$ and His-$G\gamma_2$ recombinant baculoviruses. AlF_4^- was used to dissociate the G-protein heterotrimer so that $G\alpha_{i1}$-LBT2 could be purified separately from $G\beta_1$His-γ_2.

The terbium-binding ability of $G\alpha_{i1}$-LBT2 was then assessed. However, while the presence of $G\alpha_{i1}$-LBT2 increased the terbium luminescence above $TbCl_3$ alone in solution, it was not a large increase and it appeared that the affinity of the LBT for terbium had decreased with saturation not achieved at 200 nM $TbCl_3$ (**Figure 8.4**). These results indicated that the integrity of the LBT may have been affected by the fusion to $G\alpha_{i1}$ decreasing its ability to chelate terbium and generate a good luminescent signal, making it an unlikely candidate for a successful TR-FRET donor.

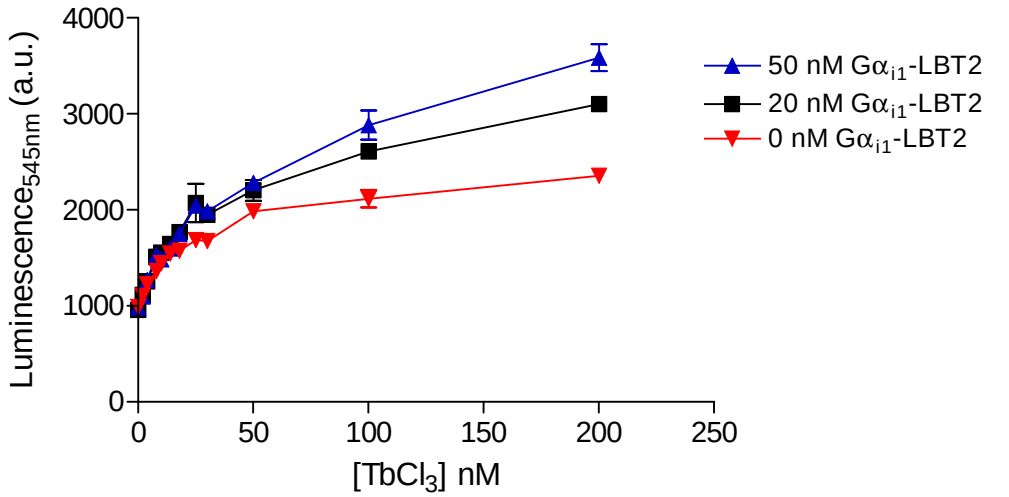

Figure 8.4: Terbium binding to $G\alpha_{i1}$-LBT2. 50 nM, 20 nM or 0 nM of purified Gαi1-LBT2 was mixed with 0-200 nM TbCl3. The final volume was made upto 100 µL with Tb binding buffer and after a 10 min incubation the terbium emission was measured using a Victor3 plate reader set for time-resolved fluorescence with the following parameters: λex 280 nm, λem 545 nm, 50 µs delay and 900 µs counting duration. Data shown are mean ± SEM (n=3).

8.5.2. Purification of $G\gamma_2$-LBT2 and terbium binding properties

The C-terminus of $G\gamma_2$ was fused to LBT2 and the N-terminus to a His-tag ($G\gamma_2$-LBT2). This recombinant protein was successfully co-expressed in *Sf*9 cells with $G\beta_1$ and the dimer purified using IMAC (**Figure 8.5**).

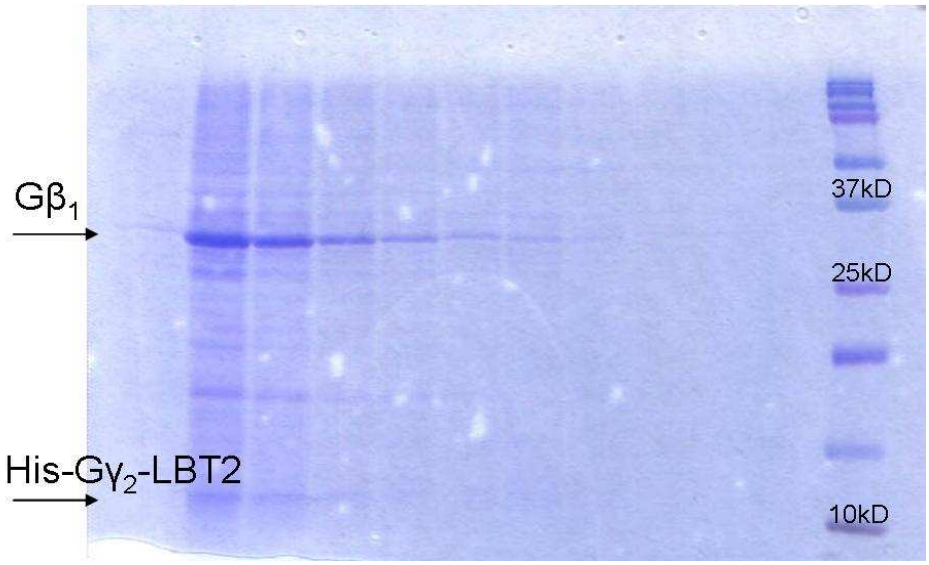

Figure 8.5: Purification of His-$G\gamma_2$-LBT2 with $G\beta_1$. 1.8 L of *Sf*9 cells at 1.5 x 10^6 cells/mL were infected at an MOI of 2. After incubation for 72 hours, cells were harvested and protein purified using Ni-NTA chromatography.

The terbium binding properties of this dimer were found to be poor at the concentration of protein used, making this construct an unlikely TR-FRET donor (**Figure 8.6**).

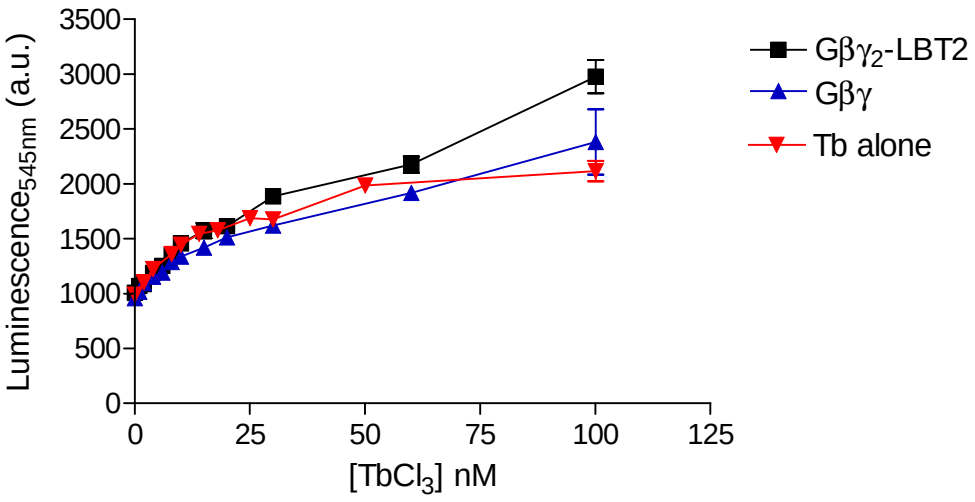

Figure 8.6: Terbium binding to Gβγ$_2$-LBT2. 20 nM of protein was mixed with the indicated concentrations of $TbCl_3$. The final volume was made up to 100 µL with Tb binding buffer and after 30 min incubation the Tb emission was measured using a Victor3 plate reader set for time-resolved fluorescence with the following parameters: λ_{ex} 280 nm, λ_{em} 545 nm, 50 µs delay and 900 µs counting duration. Data shown are mean ± SEM (n=3).

Time constraints and poor first indications of terbium labelling prevented these constructs from being further characterized.

8.6. Tetracysteine motif fusion protein sequences

Tetracysteine motifs are indicated in blue
Extra flanking regions of TCM are indicated in green
His-tags are indicated in red

8.6.1. His-TCM-Gγ2

Sequencing was performed in pGEM-T Easy before ligation into pQE30, which adds the His-tag to the N-terminus

Nucleotide Sequence:

ATG**TGCTGTCCAGGATGCTGT**GGAGGCGGCGGAGCCAGCAACAACACCGCCAGCATAGC
ACAAGCCAGGAAACTGGTAGAACAGCTGAAGATGGAAGCCAACATCGATAGGATAAAGG
TGTCCAAGGCAGCTGCAGATTTGATGGCCTACTGTGAAGCGCATGCCAAGGAAGATCCC
CTCCTGACACCTGTTCCGGCTTCAGAAAACCCATTTAGGGAGAAGAAGTTCTTCTGCGC
CATCCTTTAA

Amino acid sequence:

M**CCPGCC**GGGGASNNTASIAQARKLVEQLKMEANIDRIKVSKAAADLMAYCEAHAK
EDPLLTPVPASENPFREKKFFCAIL

8.6.2. His-Gγ$_2$-TCM

Sequencing was performed in pGEM-T Easy before ligation into pQE30, which adds the His-tag to the N-terminus

Nucleotide sequence:

ATGGCCAGCAACAACACCGCCAGCATAGCACAAGCCAGGAAACTGGTAGAACAGCTGAA
GATGGAAGCCAACATCGATAGGATAAAGGTGTCCAAGGCAGCTGCAGATTTGATGGCCT
ACTGTGAAGCGCATGCCAAGGAAGATCCCCTCCTGACACCTGTTCCGGCTTCAGAAAAC
CCATTTAGGGAGAAGAAGTTCTTCTGCGCCATCCTT**TGCTGTCCAGGATGCTGT**TAA

Amino acid sequence:

MASNNTASIAQARKLVEQLKMEANIDRIKVSKAAADLMAYCEAHAKEDPLLTPVPASEN
PFREKKFFCAIL**CCPGCC**

8.6.3. TCM-Gα$_{i1}$

Nucleotide Sequence:

GGTACCATG**TTTCTTAAT****TGTTGTCCTGGTTGTTGT****ATGGAACCT**GGTGGTGGTGGCTG
CACACTGAGCGCTGAGGACAAGGCGGCCGTGGAGCGCAGCAAGATGATCGACCGCAACC

TCCGGGAGGACGGAGAGAAGGCAGCGCGCGAGGTCAAGCTGCTGCTGCTGGGTGCTGGT
GAATCCGGGAAGAGCACAATTGTGAAGCAGATGAAAATTATCCACGAGGCTGGCTACTC
AGAGGAAGAGTGTAAGCAGTACAAAGCAGTGGTCTACAGCAACACCATCCAGTCCATCA
TTGCCATCATTAGAGCTATGGGGAGATTGAAAATCGACTTTGGAGACGCTGCTCGTGCG
GATGATGCTCGCCAACTCTTCGTGCTTGCTGGGGCTGCAGAGGAAGGCTTTATGACCGC
GGAGCTCGCCGGCGTCATAAAGAGACTGTGGAAGGACAGCGGTGTGCAAGCCTGCTTCA
ACAGATCCCGGGAGTACCAGCTGAACGATTCGGCGGCGTACTACCTGAATGACTTGGAC
AGAATAGCACAACCAAATTACATCCCAACCCAGCAGGATGTTCTCAGAACTAGAGTGAA
AACGACGGGAATTGTGGAAACCCACTTTACTTTCAAAGATCTTCATTTTAAAATGTTTG
ACGTGGGAGGCCAGAGATCAGAGCGGAAGAAGTGGATTCACTGCTTTGAAGGCGTGACT
GCCATCATCTTCTGTGTGGCCCTGAgTGACTATGACCTGGTtCTTGCTGAGGATGAAGA
AATGAAcCGGATGCACGAAAGCATGAAGCTGtTCGATAGCATATGTAACaACAaGTGGT
TTACGGACACATCCATCATCCTTTTCCTGAACAAGAAGGACCTCTTCGAAGAGAAGATC
AAAAAGAGTCCCCTCACGATATGCTATCCAGAATATGCAGGCTCAAACACATATGAAGA
GGCGGCTGCGTATATCCAGTGTCAGTTTGAAGACCTCAATAAAAGGAAGGACACAAAGG
AAATTTACACCCACTTCACTTGCGCCACGGATACGAAGAATGTGCAGTTTGTGTTCGAT
GCTGTAACGGACGTCATCATAAAGAATAACCTAAAAGATTGTGGTCTCTTTAA

Amino acid sequence:

MFLNCCPGCCMEPGGGGCTLSAEDKAAVERSKMIDRNLREDGEKAAREVKLLLLGAGE
SGKSTIVKQMKIIHEAGYSEEECKQYKAVVYSNTIQSIIAIIRAMGRLKIDFGDAARAD
DARQLFVLAGAAEEGFMTAELAGVIKRLWKDSGVQACFNRSREYQLNDSAAYYLNDLDR
IAQPNYIPTQQDVLRTRVKTTGIVETHFTFKDLHFKMFDVGGQRSERKKWIHCFEGVTA
IIFCVALSDYDLVLAEDEEMNRMHESMKLFDSICNNKWFTDTSIILFLNKKDLFEEKIK
KSPLTICYPEYAGSNTYEEAAAYIQCQFEDLNKRKDTKEIYTHFTCATDTKNVQFVFDA
VTDVIIKNNLKDCGLFKSCR

8.6.4. His-TCM-Gα$_{i1}$

Nucleotide sequence was as above for TCM-Gα$_{i1}$ and His-tag region originates from the pQE30 vector.

Amino acid sequence:

MRGSHHHHHHGSACELGTMFLNCCPGCCMEPGGGGCTLSAEDKAAVERSKMIDRNLRED
GEKAAREVKLLLLGAGESGKSTIVKQMKIIHEAGYSEEECKQYKAVVYSNTIQSIIAII
RAMGRLKIDFGDAARADDARQLFVLAGAAEEGFMTAELAGVIKRLWKDSGVQACFNRSR
EYQLNDSAAYYLNDLDRIAQPNYIPTQQDVLRTRVKTTGIVETHFTFKDLHFKMFDVGG
QRSERKKWIHCFEGVTAIIFCVALSDYDLVLAEDEEMNRMHESMKLFDSICNNKWFTDT
SIILFLNKKDLFEEKIKKSPLTICYPEYAGSNTYEEAAAYIQCQFEDLNKRKDTKEIYT
HFTCATDTKNVQFVFDAVTDVIIKNNLKDCGLFKSCR

8.7. Purification and FlAsH-labelling of GβTCM-γ_2

His-tagged TCM-Gγ_2 was co-expressed with Gβ_4 and Gα_{i1} in *Sf*9 cells. The heterotrimer was purified using Ni-NTA beads and the TCMs labelled with FlAsH on the IMAC column overnight. The non His-tagged Gα_{i1} was eluted using aluminium fluoride and the His-tagged G$\beta\gamma$ dimer eluted from the column using an excess of imidazole (
Figure 8.7).

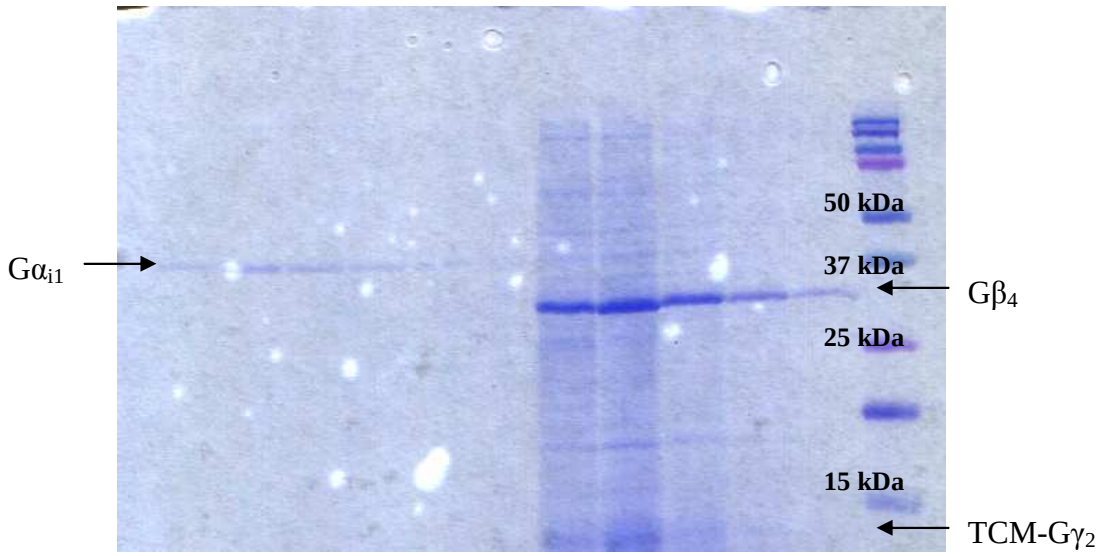

Figure 8.7: Purification of His-tagged TCM-γ_2 with Gβ_4. 1.2 L of *Sf*9 cells were triple infected with Gα_{i1}, Gβ_4 and His-TCM-Gγ_2 baculoviruses. The G-protein heterotrimer was purified using a Ni-NTA column and labelled with FlAsH overnight. The Gα subunits were then eluted separately from the G$\beta\gamma$ dimer using aluminium fluoride which was subsequently eluted using imidazole.

Since Gα_{i1} was present during FlAsH labelling, a comparison was made between the labelling of GβTCM-γ_2 and Gα_{i1}. Significantly higher amounts of fluorescence were generated by GβTCM-γ_2 indicating that FlAsH was binding with some specificity to TCMs (**Figure 8.8**).

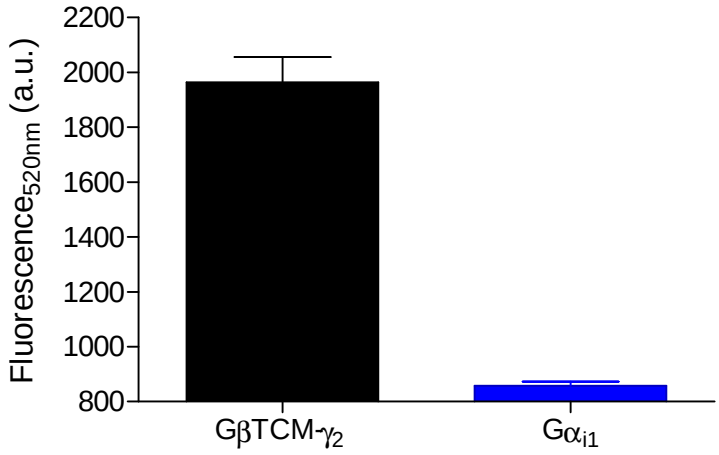

Figure 8.8: Comparison of FlAsH labelling of GβTCM-γ_{2his} and Gα_{i1}. Proteins were labelled as the heterotrimer on a Ni-NTA column overnight. Unbound FlAsH was removed by washing and the proteins eluted from the column separately. 30 nM of each protein or an equivalent volume of buffer was measured in an assay volume of 100 µL in a Victor3 multilabel plate reader using the following parameters: λ_{ex} 485 nm, λ_{em} 520 nm. Data shown are mean ± SEM (n=3).

8.8. Labelling and TR-FRET of LBT1-G$\beta_4\gamma_2$-TCM

Before TR-FRET measurements were taken of the interaction between LBT1-G$\beta_4\gamma_2$-TCM, the labelling of the TCM with FlAsH was determined (**Figure 8.9**). Increasing concentrations of protein increased the FlAsH emission (fluorescence measured at 520 nm) indicating that the protein was labelled. Increasing concentrations of $TbCl_3$ did not change the emission of FlAsH when it was directly excited at 485 nm.

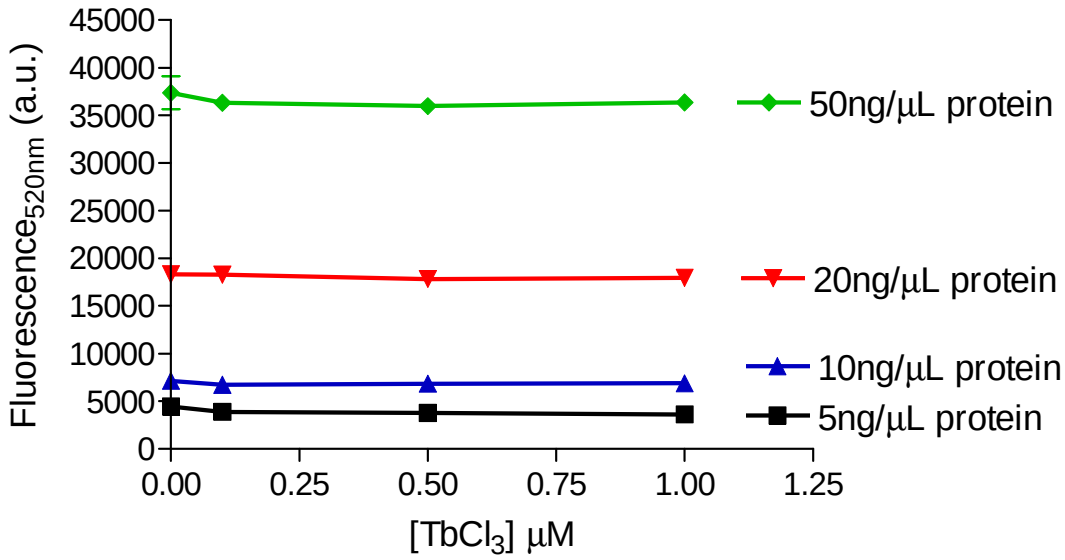

Figure 8.9: Labelling of His-Gγ_2-TCM with FlAsH and effect of an increasing concentration of $TbCl_3$ on FlAsH fluorescence. Various concentrations of LBT1-Gβ_4:His-Gγ_2-TCM dimer preparation pre-labelled with FlAsH were mixed with various concentrations of $TbCl_3$. The FlAsH was then directly excited at 485 nm and the emission measured at 520 nm. Data shown are mean ± SEM (n=3).

The ability of the LBT to be labelled with terbium was also determined (**Figure 8.10**) and increasing concentrations of both $TbCl_3$ and protein increased the terbium luminescence at 545 nm.

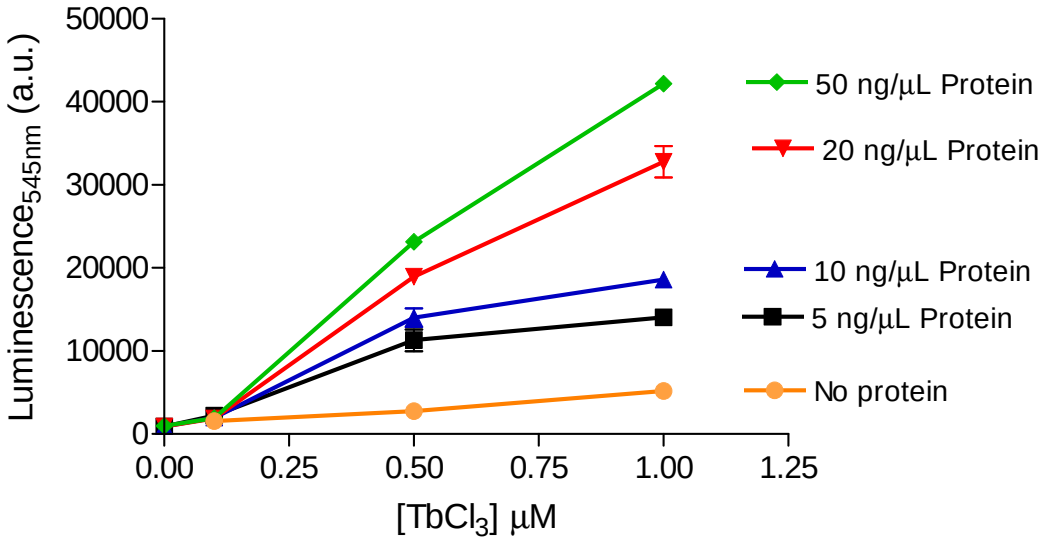

Figure 8.10: Terbium-binding to the LBT1-Gβ$_4$:His-Gγ$_2$-TCM preparation. Various concentrations of LBT1-Gβ$_4$:His-Gγ$_2$-TCM dimer preparation pre-labelled with FlAsH were mixed with various concentrations of $TbCl_3$. A Victor3 multilabel plate reader was used to measure terbium luminescence with the following parameters: λ_{ex} 280 nm, λ_{em} 545 nm, 50 µs delay and 900 µs counting duration. Data shown are mean ± SEM (n=3).

Once TR-FRET between LBT1-Gβ$_4$γ$_2$-TCM had been established, $GdCl_3$ could be added to reduce the terbium-labelling of the LBT, which resulted in a decrease in TR-FRET signal (**Figure 8.11**).

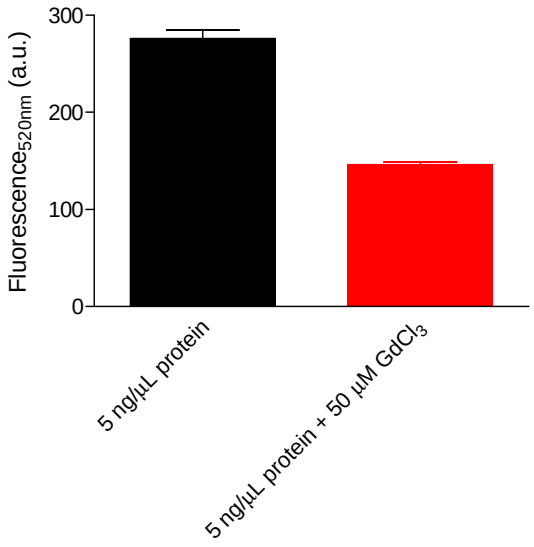

Figure 8.11: $GdCl_3$ reduces TR-FRET signal between LBT1-Gβ$_4$ and His-Gγ$_2$-TCM. 5 ng/µL of LBT1-Gβ$_4$:His-Gγ$_2$-TCM dimer preparation pre-labelled with FlAsH was mixed with 1 µM $TbCl_3$ +/- 50 µM $GdCl_3$. A Victor3 multilabel plate reader was used to measure TR-FRET with the following

parameters: λ_{ex} 280 nm, λ_{em} 520 nm, 50 µs delay and 900 µs counting duration. Background from 1 µM $TbCl_3$ +/- 50 µM $GdCl_3$ has been deducted. Data shown are mean ± SEM (n=3).

8.9. Receptor fusion protein sequences

Lanthanide binding tags are indicated in **blue**

8.9.1. M2-LBT1

Nucleotide sequence:

ATGAATAACTCAACAAACTCCTCTAACAATAGCCTGGCTCTTACAAGTCCTTATAAGAC
ATTTGAAGTGGTGTTTATTGTCCTGGTGGCTGGATCCCTCAGTTTGGTGACCATTATCG
GGAACATCCTAGTCATGGTTTCCATTAAAGTCAACCGCCACCTCCAGACCGTCAACAAT
TACTTTTTATTCAGCTTGGCCTGTGCTGACCTTATCATAGGTGTTTTCTCCATGAACTT
GTACACCCTCTACACTGTGATTGGTTACTGGCCTTTGGGACCTGTGGTGTGTGACCTTT
GGCTAGCCCTGGACTATGTGGTCAGCAATGCCTCAGTTATGAATCTGCTCATCATCAGC
TTTGACAGGTACTTCTGTGTCACAAAACCTCTGACCTACCCAGTCAAGCGGACCACAAA
AATGGCAGGTATGATGATTGCAGCTGCCTGGGTCCTCTCTTTCATCCTCTGGGCTCCAG
CCATTCTCTTCTGGCAGTTCATTGTAGGGGTGAGAACTGTGGAGGATGGGGAGTGCTAC
ATTCAGTTTTTTTCCAATGCTGCTGTCACCTTTGGTACGGCTATTGCAGCCTTCTATTT
GCCAGTGATCATCATGACTGTGCTATATTGGCACATATCCCGAGCCAGCAAGAGCAGGA
TAAAGAAGGACAAGAAGGAGCCTGTTGCCAACCAAGACCCCGTTTCTCCAAGTCTGGTA
CAAGGAAGGATAGTGAAGCCAAACAATAACAACATGCCCAGCAGTGACGATGGCCTGGA
GCACAACAAAATCCAGAATGGCAAAGCCCCCAGGGATCCTGTGACTGAAAACTGTGTTC
AGGGAGAGGAGAAGGAGAGCTCCAATGACTCCACCTCAGTCAGTGCTGTTGCCTCTAAT
ATGAGAGATGATGAAATAACCCAGGATGAAAACACAGTTTCCACTTCCCTGGGCCATTC
CAAAGATGAGAACTCTAAGCAAACATGCATCAGAATTGGCACCAAGACCCCAAAAAGTG
ACTCATGTACCCCAACTAATACCACCGTGGAGGTAGTGGGGTCTTCAGGTCAGAATGGA
GATGAAAAGCAGAATATTGTAGCCCGCAAGATTGTGAAGATGACTAAGCAGCCTGCAAA
AAAGAAGCCTCCTCCTTCCCGGGAAAAGAAAGTCACCAGGACAATCTTGGCTATTCTGT
TGGCTTTCATCATCACTTGGGCCCCATACAATGTCATGGTGCTCATTAACACCTTTTGT
GCACCTTGCATCCCCAACACTGTGTGGACAATTGGTTACTGGCTTTGTTACATCAACAG
CACTATCAACCCTGCCTGCTATGCACTTTGCAATGCCACCTTCAAGAAGACCTTTAAAC
ACCTTCTCATGTGTCATTATAAGAACATAGGCGCTACAAGG**TATATTGATACTAATAAT**
GACGGTTGGTACGAAGGAGACGAACTTCTTGCTTAA

Amino acid sequence:

MNNSTNSSNNSLALTSPYKTFEVVFIVLVAGSLSLVTIIGNILVMVSIKVNRHLQTVNNYFLFSLACADL
IIGVFSMNLYTLYTVIGYWPLGPVVCDLWLALDYVVSNASVMNLLIISFDRYFCVTKPLTYPVKRTTKMA
GMMIAAAWVLSFILWAPAILFWQFIVGVRTVEDGECYIQFFSNAAVTFGTAIAAFYLPVIIMTVLYWHIS
RASKSRIKKDKKEPVANQDPVSPSLVQGRIVKPNNNNMPSSDDGLEHNKIQNGKAPRDPVTENCVQGEEK
ESSNDSTSVSAVASNMRDDEITQDENTVSTSLGHSKDENSKQTCIRIGTKTPKSDSCTPTNTTVEVVGSS
GQNGDEKQNIVARKIVKMTKQPAKKKPPPSREKKVTRTILAILLAFIITWAPYNVMVLINTFCAPCIPNT
VWTIGYWLCYINSTINPACYALCNATFKKTFKHLLMCHYKNIGATR**YIDTNNDGWYEGDELLA**-

8.9.2. β2-LBT2

Nucelotide sequence:

ATGGGGCAACCCGGGAACGGCAGCGCCTTCTTGCTGGCACCCGATGGAAGCCATGCGCC
GGACCACGACGTCACGCAGCAAAGGGACGAGGTGTGGGTGGTGGGCATGGGCATCGTCA
TGTCTCTCATCGTCCTGGCCATCGTGTTTGGCAATGTGCTGGTCATCACAGCCATTGCC
AAGTTCGAGCGTCTGCAGACGGTCACCAACTACTTCATCACTTCACTGGCCTGTGCTGA
TCTGGTCATGGGCCTGGCAGTGGTGCCCTTTGGGGCCGCCCATATTCTTATGAAAATGT
GGACTTTTGGCAACTTCTGGTGCGAGTTTTGGACTTCCATTGATGTGCTGTGCGTCACG
GCTAGCATTGAGACCCTGTGCGTGATCGCAGTGGATCGCTACTTTGCCATTACTTCACC
TTTCAAGTACCAGAGCCTGCTGACCAAGAATAAGGCCCGGGTGATCATTCTGATGGTGT
GGATTGTGTCAGGCCTTACCTCCTTCTTGCCCATTCAGATGCACTGGTACCGGGCCACC
CACCAGGAAGCCATCAACTGCTATGCCGATGAGACCTGCTGTGACTTCTTCACGAACCA
AGCCTATGCCATTGCCTCTTCCATCGTGTCCTTCTACGTTCCCCTGGTGATCATGGTCT
TCGTCTACTCCAGGGTCTTTCAGGAGGCCAAAAGGCAGCTCCAGAAGATTGACAAATCT
GAGGGCCGCTTCCATGTCCAGAACCTTAGCCAGGTGGAGCAGGATGGGCGGACGGGGCA
TGGACTCCGCAGATCTTCCAAGTTCTGCTTGAAGGAGCACAAAGCCCTCAAGACGTTAG
GCATCATCATGGGCACTTTCACCCTCTGCTGGCTGCCCTTCTTCATCGTTAACATTGTG
CATGTGATCCAGGATAACCTCATCCGTAAGGAAGTTTACATCCTCCTAAATTGGATAGG
CTATGTCAATTCTGGTTTCAATCCCCTTATCTACTGCCGGAGCCCAGATTTCAGGATTG
CCTTCCAAGAGCTCCTGTGCCTGCGCAGGTCTTCTTTGAAGGCCTATGGGAATGGCTAC
TCCAGCAACGGCAACACAGGGGAGCAGAGTGGATATCACGTGGAACAGGAGAAAGAAAA
TAAACTGCTGTGTGAAGACCTCCCAGGCACGGAAGACTTTGTGGGCCATCAAGGTACTG
TGCCTAGCGATAACATTGATTCACAAGGGAGGAATTGTAGTACAAATGACTCACTGCTG
GCTTGTGTTGACTGGAATAATGACGGTTGGTACGAAGGTGACGAATGTGCTTGA

Amino acid sequence:

MGQPGNGSAFLLAP**D**GSHAPDHDVTQQRDEVWVVGMGIVMSLIVLAIVFGNVLVITAIAKFERLQTVTNY
FITSLACADLVMGLAVVPFGAAHILMKMWTFGNFWCEFWTSIDVLCVTASIETLCVIAVDRYFAITSPFK
YQSLLTKNKARVIILMVWIVSGLTSFLPIQMHWYRATHQEAINCYA**D**ETCCDFFTNQAYAIASSIVSFYV
PLVIMVFVYSRVFQEAKRQLQKIDKSEGRFHVQNLSQVEQDGRTGHGLRRSSKFCLKEHKALKTLGIIMG
TFTLCWLPFFIVNIVHVIQDNLIRKEVYILLNWIGYVNSGFNPLIYCRSPDFRIAFQELLCLRRSSLKAY
GNGYSSNGNTGEQSGYHVEQEKENKLLCEDLPGTEDFVGHQGTVPSDNIDSQGRNCSTNDSLL**ACVDWNN
DGWYEGDECA**

Two mutations where D should be N are indicated in **orange**.

9. References

Adams, S.R., Campbell, R.E., Gross, L.A., Martin, B.R., Walkup, G.K., Yao, Y., Llopis, J. & Tsien, R.Y. 2002, "New biarsenical ligands and tetracysteine motifs for protein labeling in vitro and in vivo: synthesis and biological applications", *Journal of the American Chemical Society,* vol. 124, no. 21, pp. 6063-6076.

Akdis, C.A. & Simons, F.E. 2006, "Histamine receptors are hot in immunopharmacology", *European Journal of Pharmacology,* vol. 533, no. 1-3, pp. 69-76.

Akhter, S.A., Luttrell, L.M., Rockman, H.A., Iaccarino, G., Lefkowitz, R.J. & Koch, W.J. 1998, "Targeting the receptor-Gq interface to inhibit in vivo pressure overload myocardial hypertrophy", *Science,* vol. 280, no. 5363, pp. 574-577.

Andresen, M., Schmitz-Salue, R. & Jakobs, S. 2004, "Short tetracysteine tags to beta-tubulin demonstrate the significance of small labels for live cell imaging", *Molecular Biology of the Cell,* vol. 15, no. 12, pp. 5616-5622.

Angers, S., Salahpour, A., Joly, E., Hilairet, S., Chelsky, D., Dennis, M. & Bouvier, M. 2000, "Detection of beta 2-adrenergic receptor dimerization in living cells using bioluminescence resonance energy transfer (BRET)", *Proceedings of the National Academy of Sciences of the United States of America,* vol. 97, no. 7, pp. 3684-3689.

Banks, P. & Harvey, M. 2002, "Considerations for using fluorescence polarization in the screening of G protein-coupled receptors", *Journal of Biomolecular Screening,* vol. 7, no. 2, pp. 111-117.

Beckage, N.E. & Gelman, D.B. 2004, "Wasp parasitoid disruption of host development: implications for new biologically based strategies for insect control", *Annual Review of Entomology,* vol. 49, pp. 299-330.

Berman, D.M., Kozasa, T. & Gilman, A.G. 1996, "The GTPase-activating protein RGS4 stabilizes the transition state for nucleotide hydrolysis", *Journal of Biological Chemistry,* vol. 271, no. 44, pp. 27209-27212.

Bhunia, A.K. & Miller, S.C. 2007, "Labeling tetracysteine-tagged proteins with a SplAsH of color: a modular approach to bis-arsenical fluorophores", *Chembiochem,* vol. 8, no. 14, pp. 1642-1645.

Birnbaumer, L. 2007, "Expansion of signal transduction by G proteins. The second 15 years or so: from 3 to 16 alpha subunits plus betagamma dimers", *Biochimica et biophysica acta,* vol. 1768, no. 4, pp. 772-793.

Blackmer, T., Larsen, E.C., Bartleson, C., Kowalchyk, J.A., Yoon, E.J., Preininger, A.M., Alford, S., Hamm, H.E. & Martin, T.F. 2005, "G protein betagamma directly regulates SNARE protein fusion machinery for secretory granule exocytosis", *Nature Neuroscience,* vol. 8, no. 4, pp. 421-425.

Blomberg, K., Hurskainen, P. & Hemmila, I. 1999, "Terbium and rhodamine as labels in a homogeneous time-resolved fluorometric energy transfer assay of the beta subunit of human chorionic gonadotropin in serum", *Clinical Chemistry,* vol. 45, no. 6 Pt 1, pp. 855-861.

Bradford, M.M. 1976, "A rapid and sensitive method for the quantitation of microgram quantities of protein utilizing the principle of protein-dye binding", *Analytical Biochemistry,* vol. 72, pp. 248-254.

Bunemann, M., Frank, M. & Lohse, M.J. 2003, "Gi protein activation in intact cells involves subunit rearrangement rather than dissociation", *Proceedings of the National Academy of Sciences of the United States of America,* vol. 100, no. 26, pp. 16077-16082.

Bylund, D.B. & Toews, M.L. 1993, "Radioligand binding methods: practical guide and tips", *The American Journal of Physiology,* vol. 265, no. 5 Pt 1, pp. L421-9.

Cao, H., Chen, B., Squier, T.C. & Mayer, M.U. 2006, "CrAsH: a biarsenical multi-use affinity probe with low non-specific fluorescence", *Chemical Communications*, vol. (24), no. 24, pp. 2601-2603.

Caulfield, M.P. & Birdsall, N.J. 1998, "International Union of Pharmacology. XVII. Classification of muscarinic acetylcholine receptors", *Pharmacological Reviews,* vol. 50, no. 2, pp. 279-290.

Chen, I., Howarth, M., Lin, W. & Ting, A.Y. 2005, "Site-specific labeling of cell surface proteins with biophysical probes using biotin ligase", *Nature Methods,* vol. 2, no. 2, pp. 99-104.

Chen, I. & Ting, A.Y. 2005, "Site-specific labeling of proteins with small molecules in live cells", *Current Opinion in Biotechnology,* vol. 16, no. 1, pp. 35-40.

Cherezov, V., Rosenbaum, D.M., Hanson, M.A., Rasmussen, S.G., Thian, F.S., Kobilka, T.S., Choi, H.J., Kuhn, P., Weis, W.I., Kobilka, B.K. & Stevens, R.C. 2007, "High-resolution crystal structure of an engineered human beta2-adrenergic G protein-coupled receptor", *Science,* vol. 318, no. 5854, pp. 1258-1265.

Cherfils, J. & Chabre, M. 2003, "Activation of G-protein Galpha subunits by receptors through Galpha-Gbeta and Galpha-Ggamma interactions", *Trends in Biochemical Sciences,* vol. 28, no. 1, pp. 13-17.

Chin, J.W., Cropp, T.A., Anderson, J.C., Mukherji, M., Zhang, Z. & Schultz, P.G. 2003, "An expanded eukaryotic genetic code", *Science,* vol. 301, no. 5635, pp. 964-967.

Civantos Calzada, B. & Aleixandre de Artiñano, A. 2001, "Alpha-adrenoceptor subtypes", *Pharmacological Research,* vol. 44, no. 3, pp. 195-208.

Clapham, D.E. & Neer, E.J. 1997, "G protein beta gamma subunits", *Annual Review of Pharmacology and Toxicology,* vol. 37, pp. 167-203.

Clapp, A.R., Medintz, I.L. & Mattoussi, H. 2005, "Forster resonance energy transfer investigations using quantum-dot fluorophores", *Chemphyschem,* vol 7, no. 1, pp 47-57.

Cooper, T.H., Leifert, W.R., Glatz, R.V. & McMurchie, E.J. 2008, "Expression and characterisation of functional lanthanide binding tags fused to a Gα-protein and muscarinic (M2) receptor", *Journal of Bionanoscience,* .2, pp27-34.

Daly, C.J. & McGrath, J.C. 2003, "Fluorescent ligands, antibodies, and proteins for the study of receptors", *Pharmacology & therapeutics,* vol. 100, no. 2, pp. 101-118.

de Jong, L.A., Uges, D.R., Franke, J.P. & Bischoff, R. 2005, "Receptor-ligand binding assays: Technologies and Applications", *Journal of Chromatography B,* vol. 829, pp. 1-25.

Denker, B.M., Schmidt, C.J. & Neer, E.J. 1992, "Promotion of the GTP-liganded state of the Go alpha protein by deletion of the C terminus", *Journal of Biological Chemistry,* vol. 267, no. 14, pp. 9998-10002.

Di Cesare Mannelli, L., Pacini, A., Toscano, A., Fortini, M., Berti, D., Ghelardini, C., Galeotti, N., Baglioni, P. & Bartolini, A. 200, "Gi/o proteins: Expression for direct activation enquiry", *Protein Expression and Purification,* vol. 47, no. 1, pp. 303-310.

Duvernay, M.T., Filipeanu, C.M. & Wu, G. 2005, "The regulatory mechanisms of export trafficking of G protein-coupled receptors", *Cellular Signalling,* vol. 17, no. 12, pp. 1457-1465.

Eglen, R.M. 2005, "An Overview of High Throughput Screening at G Protein Coupled Receptors", *Frontiers in Drug Design & Discovery,* vol. 1, pp. 97-111(15).

Escriba, P.V., Wedegaertner, P.B., Goni, F.M. & Vogler, O. 2007, "Lipid-protein interactions in GPCR-associated signaling", *Biochimica et biophysica acta,* vol. 1768, no. 4, pp. 836-852.

Farfel, Z., Bourne, H.R. & Iiri, T. 1999, "The expanding spectrum of G protein diseases", *The New England Journal of Medicine,* vol. 340, no. 13, pp. 1012-1020.

Ferrer, M., Kolodin, G.D., Zuck, P., Peltier, R., Berry, K., Mandala, S.M., Rosen, H., Ota, H., Ozaki, S., Inglese, J. & Strulovici, B. 2003, "A fully automated [35S]GTPgammaS scintillation proximity assay for the high-throughput screening of Gi-linked G protein-coupled receptors", *Assay and Drug Development Technologies,* vol. 1, no. 2, pp. 261-273.

Frang, H., Mukkala, V.M., Syysto, R., Ollikka, P., Hurskainen, P., Scheinin, M. & Hemmila, I. 2003, "Nonradioactive GTP binding assay to monitor activation of g protein-coupled receptors", *Assay and Drug Development Technologies*, vol. 1, no. 2, pp. 275-280.

Franz, K.J., Nitz, M. & Imperiali, B. 2003, "Lanthanide-binding tags as versatile protein coexpression probes", *Chembiochem,* vol. 4, no. 4, pp. 265-271.

Fredriksson, R., Lagerstrom, M.C., Lundin, L.G. & Schioth, H.B. 2003, "The G-protein-coupled receptors in the human genome form five main families. Phylogenetic analysis, paralogon groups, and fingerprints", *Molecular Pharmacology,* vol. 63, no. 6, pp. 1256-1272.

Freissmuth, M., Waldhoer, M., Bofill-Cardona, E. & Nanoff, C. 1999, "G protein antagonists", *Trends in Pharmacological Sciences,* vol. 20, no. 6, pp. 237-245.

Galeotti, N., Ghelardini, C., Zoppi, M., Bene, E.D., Raimondi, L., Beneforti, E. & Bartolini, A. 2001a, "A reduced functionality of Gi proteins as a possible cause of fibromyalgia", *The Journal of Rheumatology,* vol. 28, no. 10, pp. 2298-2304.

Galeotti, N., Ghelardini, C., Zoppi, M., Del Bene, E., Raimondi, L., Beneforti, E. & Bartolini, A. 2001b, "Hypofunctionality of Gi proteins as aetiopathogenic mechanism for migraine and cluster headache", *Cephalalgia,* vol. 21, no. 1, pp. 38-45.

Gales, C., Rebois, R.V., Hogue, M., Trieu, P., Breit, A., Hebert, T.E. & Bouvier, M. 2005, "Real-time monitoring of receptor and G-protein interactions in living cells", *Nature Methods,* vol. 2, no. 3, pp. 177-184.

Gautam, N., Downes, G.B., Yan, K. & Kisselev, O. 1998, "The G-protein betagamma complex", *Cellular Signalling,* vol. 10, no. 7, pp. 447-455.

George, N., Pick, H., Vogel, H., Johnsson, N. & Johnsson, K. 2004, "Specific labeling of cell surface proteins with chemically diverse compounds", *Journal of the American Chemical Society,* vol. 126, no. 29, pp. 8896-8897.

Ghosh, S., Parvez, M.K., Banerjee, K., Sarin, S.K. & Hasnain, S.E. 2002, "Baculovirus as mammalian cell expression vector for gene therapy: an emerging strategy", *Molecular Therapy,* vol. 6, no. 1, pp. 5-11.

Giepmans, B., Adams, S., Ellisman, M. & Tsien, R., 2006, "The fluorescent toolbox for assessing protein location and function", *Science*, vol. 312, pp. 217-224.

Girardet, J.L., Dupont, Y. & Lacapere, J.J. 1989, "Evidence of a calcium-induced structural change in the ATP-binding site of the sarcoplasmic-reticulum Ca2+-ATPase using terbium formycin triphosphate as an analogue of Mg-ATP", *European Journal of Biochemistry / FEBS,* vol. 184, no. 1, pp. 131-140.

Glatz, R., Schmidt, O. & Asgari, S. 2004, "Isolation and characterization of a Cotesia rubecula bracovirus gene expressed in the lepidopteran Pieris rapae", *The Journal of General Virology,* vol. 85, no. 10, pp. 2873-2882.

Goda, N., Tenno, T., Inomata, K., Iwaya, N., Sasaki, Y., Shirakawa, M. & Hiroaki, H. 2007, "LBT/PTD dual tagged vector for purification, cellular protein delivery and visualization in living cells", *Biochimica et Biophysica Acta,* vol. 1773, no. 2, pp. 141-146.

Gomez-Hens, A. & Aguilar-Caballos, M.P. 2002, "Terbium-sensitized luminescence: a selective and versatile analytical approach", *Trends in Analytical Chemistry,* vol. 21, no. 2, pp. 131-141.

Graber, S.G., Figler, R.A. & Garrison, J.C. 1992, "Expression and purification of functional G protein alpha subunits using a baculovirus expression system", *The Journal of Biological Chemistry,* vol. 267, no. 2, pp. 1271-1278.

Granier, S., Kim, S., Shafer, A.M., Ratnala, V.R., Fung, J.J., Zare, R.N. & Kobilka, B. 2007, "Structure and conformational changes in the C-terminal domain of the beta2-adrenoceptor: insights from fluorescence resonance energy transfer studies", *The Journal of Biological Chemistry,* vol. 282, no. 18, pp. 13895-13905.

Griffin, B.A., Adams, S.R., Jones, J. & Tsien, R.Y. 2000, "Fluorescent labeling of recombinant proteins in living cells with FlAsH", *Methods in Enzymology,* vol. 327, pp. 565-578.

Griffin, B.A., Adams, S.R. & Tsien, R.Y. 1998, "Specific covalent labeling of recombinant protein molecules inside live cells", *Science,* vol. 281, no. 5374, pp. 269-272.

Guignet, E.G., Hovius, R. & Vogel, H. 2004, "Reversible site-selective labeling of membrane proteins in live cells", *Nature Biotechnology,* vol. 22, no. 4, pp. 440-444.

Han, S.J., Hamdan, F.F., Kim, S.K., Jacobson, K.A., Brichta, L., Bloodworth, L.M., Li, J.H. & Wess, J. 2005, "Pronounced conformational changes following agonist activation of the M(3) muscarinic acetylcholine receptor", *The Journal of Biological Chemistry,* vol. 280, no. 26, pp. 24870-24879.

Hanaoka, K., Kikuchi, K., Kobayashi, S. & Nagano, T. 2007, "Time-Resolved Long-Lived Luminescence Imaging Method Employing Luminescent Lanthanide Probes with a New Microscopy System", *Journal of the American Chemical Society,* vol. 129, no. 44, pp. 13502-13509.

Handl, H.L. & Gillies, R.J. 2005, "Lanthanide-based luminescent assays for ligand-receptor interactions", *Life Sciences,* vol. 77, no. 4, pp. 361-371.

Harris, D.A. & Walter, N.G. 2003, "Probing RNA structure and metal-binding sites using Terbium(III) footprinting", *Current Protocols in Nucleic Acid Chemistry,* , pp. 6.8.1-6.8.8.

Harrison, C. & Traynor, J.R. 2003, "The [^{35}S]GTPgammaS binding assay: approaches and applications in pharmacology", *Life Sciences,* vol. 74, no. 4, pp. 489-508.

Hazari, A., Lowes, V., Chan, J.H., Wong, C.S., Ho, M.K. & Wong, Y.H. 2004, "Replacement of the alpha5 helix of Galpha16 with Galphas-specific sequences enhances promiscuity of Galpha16 toward Gs-coupled receptors", *Cellular Signalling,* vol. 16, no. 1, pp. 51-62.

Hearps, A.C., Pryor, M.J., Kuusisto, H.V., Rawlinson, S.M., Piller, S.C. & Jans, D.A. 2007, "The biarsenical dye Lumio exhibits a reduced ability to specifically detect tetracysteine-containing proteins within live cells", *Journal of Fluorescence,* vol. 17, no. 6, pp. 593-597.

Hein, P., Frank, M., Hoffmann, C., Lohse, M.J. & Bunemann, M. 2005, "Dynamics of receptor/G protein coupling in living cells", *The EMBO journal,* vol. 24, pp. 4106-4114.

Hemmila, I. & Laitala, V. 2005, "Progress in lanthanides as luminescent probes", *Journal of Fluorescence,* vol. 15, no. 4, pp. 529-542.

Heyduk, T. 2002, "Measuring protein conformational changes by FRET/LRET", *Current Opinion in Biotechnology,* vol. 13, no. 4, pp. 292-296.

Higashijima, T., Ferguson, K.M., Sternweis, P.C., Smigel, M.D. & Gilman, A.G. 1987, "Effects of Mg2+ and the beta gamma-subunit complex on the interactions of guanine nucleotides with G proteins", *Journal of Biological Chemistry,* vol. 262, no. 2, pp. 762-766.

Higashijima, T., Uzu, S., Nakajima, T. & Ross, E.M. 1988, "Mastoparan, a peptide toxin from wasp venom, mimics receptors by activating GTP-binding regulatory proteins (G proteins)", *Journal of Biological Chemistry,* vol. 263, no. 14, pp. 6491-6494.

Hild, W.A., Breunig, M. & Goepferich, A. 2008, "Quantum dots - nano-sized probes for the exploration of cellular and intracellular targeting", *European Journal of Pharmaceutics and Biopharmaceutics,* vol. 68, no. 2, pp. 153-168.

Hill, S.J., Ganellin, C.R., Timmerman, H., Schwartz, J.C., Shankley, N.P., Young, J.M., Schunack, W., Levi, R. & Haas, H.L. 1997, "International Union of Pharmacology. XIII. Classification of histamine receptors", *Pharmacological Reviews,* vol. 49, no. 3, pp. 253-278.

Hoffmann, C., Gaietta, G., Bunemann, M., Adams, S.R., Oberdorff-Maass, S., Behr, B., Vilardaga, J.P., Tsien, R.Y., Ellisman, M.H. & Lohse, M.J. 2005, "A FlAsH-based FRET approach to determine G protein-coupled receptor activation in living cells", *Nature Methods,* vol. 2, no. 3, pp. 171-176.

Holler, C., Freissmuth, M. & Nanoff, C. 1999, "G proteins as drug targets", *Cellular and Molecular Life Sciences,* vol. 55, no. 2, pp. 257-270.

Iniguez-Lluhi, J.A., Simon, M.I., Robishaw, J.D. & Gilman, A.G. 1992, "G protein beta gamma subunits synthesized in Sf9 cells. Functional characterization and the significance of prenylation of gamma", *Journal of Biological Chemistry,* vol. 267, no. 32, pp. 23409-23417.

Ishii, M. & Kurachi, Y. 2006, "Muscarinic acetylcholine receptors", *Current Pharmaceutical Design,* vol. 12, no. 28, pp. 3573-3581.

Ja, W.W. & Roberts, R.W. 2005, "G-protein-directed ligand discovery with peptide combinatorial libraries", *Trends in Biochemical Sciences,* vol. 30, no. 6, pp. 318-324.

Jamieson, T., Bakhshi, R., Petrova, D., Pocock, R., Imani, M. & Seifalian, A.M. 2007, "Biological applications of quantum dots", *Biomaterials,* vol. 28, no. 31, pp. 4717-4732.

Janetopoulos, C. & Devreotes, P. 2002, "Monitoring receptor-mediated activation of heterotrimeric G-proteins by fluorescence resonance energy transfer", *Methods,* vol. 27, no. 4, pp. 366-373.

Janetopoulos, C., Jin, T. & Devreotes, P. 2001, "Receptor-mediated activation of heterotrimeric G-proteins in living cells", *Science,* vol. 291, no. 5512, pp. 2408-2411.

Jensen, A.A. & Spalding, T.A. 2004, "Allosteric modulation of G-protein coupled receptors", *European Journal of Pharmaceutical Sciences,* vol. 21, no. 4, pp. 407-420.

Jones, J.W., Greene, T.A., Grygon, C.A., Doranz, B.J. & Brown, M.P. 2008, "Cell-free assay of g-protein-coupled receptors using fluorescence polarization", *Journal of Biomolecular Screening,* vol. 13, no. 5, pp. 424-429.

Kapanidis, A.N., Ebright, Y.W. & Ebright, R.H. 2001, "Site-specific incorporation of fluorescent probes into protein: hexahistidine-tag-mediated fluorescent labeling with (Ni(2+):nitrilotriacetic Acid (n)-fluorochrome conjugates", *Journal of the American Chemical Society,* vol. 123, no. 48, pp. 12123-12125.

Keppler, A., Kindermann, M., Gendreizig, S., Pick, H., Vogel, H. & Johnsson, K. 2004, "Labeling of fusion proteins of O6-alkylguanine-DNA alkyltransferase with small molecules in vivo and in vitro", *Methods,* vol. 32, no. 4, pp. 437-444.

Kilts, J.D., Gerhardt, M.A., Richardson, M.D., Sreeram, G., Mackensen, G.B., Grocott, H.P., White, W.D., Davis, R.D., Newman, M.F., Reves, J.G., Schwinn, D.A. & Kwatra, M.M. 2000, "Beta(2)-adrenergic and several other G protein-coupled receptors in human atrial membranes activate both G(s) and G(i)", *Circulation Research.,* vol. 87, no. 8, pp. 705-709.

Klabunde, T. & Hessler, G. 2002, "Drug design strategies for targeting G-protein-coupled receptors", *Chembiochem,* vol. 3, no. 10, pp. 928-944.

Knight, P.J. & Grigliatti, T.A. 2004, "Diversity of G proteins in Lepidopteran cell lines: partial sequences of six G protein alpha subunits", *Archives of Insect Biochemistry and Physiology,* vol. 57, no. 3, pp. 142-150.

Kobilka, B.K. 2007, "G protein coupled receptor structure and activation", *Biochimica et Biophysica Acta,* vol. 1768, no. 4, pp. 794-807.

Kokko, L., Lovgren, T. & Soukka, T. 2007, "Europium(III)-chelates embedded in nanoparticles are protected from interfering compounds present in assay media", *Analytica Chimica Acta,* vol. 585, no. 1, pp. 17-23.

Kost, T.A., Condreay, J.P. & Jarvis, D.L. 2005, "Baculovirus as versatile vectors for protein expression in insect and mammalian cells", *Nature Biotechnology,* vol. 23, no. 5, pp. 567-575.

Kozasa, T., Hepler, J.R., Smrcka, A.V., Simon, M.I., Rhee, S.G., Sternweis, P.C. & Gilman, A.G. 1993, "Purification and characterization of recombinant G16 alpha from Sf9 cells: activation of purified phospholipase C isozymes by G-protein alpha subunits", *Proceedings of the National Academy of Sciences of the United States of America,* vol. 90, no. 19, pp. 9176-9180.

Krasel, C., Vilardaga, J.P., Bunemann, M. & Lohse, M.J. 2004, "Kinetics of G-protein-coupled receptor signalling and desensitization", *Biochemical Society Transactions,* vol. 32, no. 6, pp. 1029-1031.

Kroemer, J.A. & Webb, B.A. 2004, "Polydnavirus genes and genomes: emerging gene families and new insights into polydnavirus replication", *Annual Review of Entomology,* vol. 49, pp. 431-456.

Kurata, S., Ariki, S. & Kawabata, S. 2006, "Recognition of pathogens and activation of immune responses in Drosophila and horseshoe crab innate immunity", *Immunobiology,* vol. 211, no. 4, pp. 237-249.

Lang, J., Nishimoto, I., Okamoto, T., Regazzi, R., Kiraly, C., Weller, U. & Wollheim, C.B. 1995, "Direct control of exocytosis by receptor-mediated activation of the heterotrimeric GTPases Gi and G(o) or by the expression of their active G alpha subunits", *The EMBO Journal,* vol. 14, no. 15, pp. 3635-3644.

Langhorst, M.F., Genisyuerek, S. & Stuermer, C.A. 2006, "Accumulation of FlAsH/Lumio Green in active mitochondria can be reversed by beta-mercaptoethanol for specific staining of tetracysteine-tagged proteins", *Histochemistry and Cell Biology,* vol. 125, no. 6, pp. 743-747.

Lecca, D. & Abbracchio, M.P. 2008, "Deorphanisation of G protein-coupled receptors: A tool to provide new insights in nervous system pathophysiology and new targets for psycho-active drugs", *Neurochemistry International,* vol. 52, no. 3, pp. 339-351.

Lee, P.H. & Bevis, D.J. 2000, "Development of a homogeneous high throughput fluorescence polarization assay for G protein-coupled receptor binding", *Journal of Biomolecular Screening,* vol. 5, no. 6, pp. 415-419.

Lefkowitz, R.J., Haber, E. & O'Hara, D. 1972, "Identification of the cardiac beta-adrenergic receptor protein: solubilization and purification by affinity chromatography", *Proceeding of*

the National Academy of Sciences of the United States of America, vol. 69, no. 10, pp. 2828-2832.

Leifert, W.R., Aloia, A.L., Bucco, O., Glatz, R.V. & McMurchie, E.J. 2005, "G-protein-coupled receptors in drug discovery: nanosizing using cell-free technologies and molecular biology approaches", *Journal of Biomolecular Screening,* vol. 10, no. 8, pp. 765-779.

Leifert, W.R., Bailey, K., Cooper, T.H., Aloia, A.L., Glatz, R.V. & McMurchie, E.J. 2006, "Measurement of heterotrimeric G-protein and regulators of G-protein signaling interactions by time-resolved fluorescence resonance energy transfer", *Analytical Biochemistry,* vol. 355, no. 2, pp. 201-212.

Li, M. & Selvin, P.R. 1997, "Amine-reactive forms of a luminescent diethylenetriaminepentaacetic acid chelate of terbium and europium: attachment to DNA and energy transfer measurements", *Bioconjugate Chemistry,* vol. 8, no. 2, pp. 127-132.

Lippitz, M., Erker, W., Decker, H., van Holde, K.E. & Basche, T. 2002, "Two-photon excitation microscopy of tryptophan-containing proteins", *Proceedings of the National Academy of Sciences of the United States of America,* vol. 99, no. 5, pp. 2772-2777.

Liu, A.M., Ho, M.K., Wong, C.S., Chan, J.H., Pau, A.H. & Wong, Y.H. 2003, "Galpha(16/z) chimeras efficiently link a wide range of G protein-coupled receptors to calcium mobilization", *Journal of Biomolecular Screening,* vol. 8, no. 1, pp. 39-49.

Liu, J., Maurel, D., Etzol, S., Brabet, I., Ansanay, H., Pin, J.P. & Rondard, P. 2004, "Molecular determinants involved in the allosteric control of agonist affinity in the GABAB receptor by the GABAB2 subunit", *The Journal of Biological Chemistry,* vol. 279, no. 16, pp. 15824-15830.

Luckow, V.A., Lee, S.C., Barry, G.F. & Olins, P.O. 1993, "Efficient generation of infectious recombinant baculoviruses by site-specific transposon-mediated insertion of foreign genes into a baculovirus genome propagated in Escherichia coli", *Journal of Virology,* vol. 67, no. 8, pp. 4566-4579.

Lundstrom, K. 2005, "Structural genomics of GPCRs", *Trends in Biotechnology,* vol. 23, no. 2, pp. 103-108.

Luttrell, L.M. 2008, "Reviews in molecular biology and biotechnology: Transmembrane signaling by G protein-coupled receptors", *Molecular Biotechnology,* vol. 39, no. 3, 239-264.

Majoul, I., Straub, M., Duden, R., Hell, S.W. & Soling, H.D. 2002, "Fluorescence resonance energy transfer analysis of protein-protein interactions in single living cells by multifocal multiphoton microscopy", *Journal of Biotechnology,* vol. 82, no. 3, pp. 267-277.

Manetti, D., Di Cesare Mannelli, L., Dei, S., Galeotti, N., Ghelardini, C., Romanelli, M.N., Scapecchi, S., Teodori, E., Pacini, A., Bartolini, A. & Gualtieri, F. 2005, "Design, synthesis, and preliminary pharmacological evaluation of a set of small molecules that directly activate Gi proteins", *Journal of Medicinal Chemistry,* vol. 48, no. 20, pp. 6491-6503.

Marinissen, M.J. & Gutkind, J.S. 2001, "G-protein-coupled receptors and signaling networks: emerging paradigms", *Trends in Pharmacological Sciences,* vol. 22, no. 7, pp. 368-376.

Marks, K.M., Braun, P.D. & Nolan, G.P. 2004, "A general approach for chemical labeling and rapid, spatially controlled protein inactivation", *Proceedings of the National Academy of Sciences of the United States of America,* vol. 101, no. 27, pp. 9982-9987.

Marks, K.M., Rosinov, M. & Nolan, G.P. 2004, "In vivo targeting of organic calcium sensors via genetically selected peptides", *Chemistry & Biology,* vol. 11, no. 3, pp. 347-356.

Martin, B.R., Giepmans, B.N., Adams, S.R. & Tsien, R.Y. 2005, "Mammalian cell-based optimization of the biarsenical-binding tetracysteine motif for improved fluorescence and affinity", *Nature Biotechnology,* vol. 23, no. 10, pp. 1308-1314.

Martin, L.J., Hahnke, M.J., Nitz, M., Wohnert, J., Silvaggi, N.R., Allen, K.N., Schwalbe, H. & Imperiali, B. 2007, "Double-lanthanide-binding tags: design, photophysical properties, and NMR applications", *Journal of the American Chemical Society,* vol. 129, no. 22, pp. 7106-7113.

McCudden, C.R., Hains, M.D., Kimple, R.J., Siderovski, D.P. & Willard, F.S. 2005, "G-protein signaling: back to the future", *Cellular and Molecular Life Sciences,* vol. 62, no. 5, pp. 551-577.

McCusker, E. & Robinson, A.S. 2008, "Refolding of G protein alpha subunits from inclusion bodies expressed in Escherichia coli", *Protein Expression and Purification,* vol. 58, no. 2, pp. 342-355.

McCusker, E.C., Bane, S.E., O'Malley, M.A. & Robinson, A.S. 2007, "Heterologous GPCR expression: a bottleneck to obtaining crystal structures", *Biotechnology Progress,* vol. 23, no. 3, pp. 540-547.

McEwen, D.P., Gee, K.R., Kang, H.C. & Neubig, R.R. 2001, "Fluorescent BODIPY-GTP analogs: real-time measurement of nucleotide binding to G proteins", *Analytical Biochemistry,* vol. 291, no. 1, pp. 109-117.

McVey, M., Ramsay, D., Kellett, E., Rees, S., Wilson, S., Pope, A.J. & Milligan, G. 2001, "Monitoring receptor oligomerization using time-resolved fluorescence resonance energy transfer and bioluminescence resonance energy transfer. The human delta -opioid receptor displays constitutive oligomerization at the cell surface, which is not regulated by receptor occupancy", *Journal of Biological Chemistry,* vol. 276, no. 17, pp. 14092-14099.

Mercier, J.F., Salahpour, A., Angers, S., Breit, A. & Bouvier, M. 2002, "Quantitative assessment of beta 1- and beta 2-adrenergic receptor homo- and heterodimerization by bioluminescence resonance energy transfer", *Journal of Biological Chemistry,* vol. 277, no. 47, pp. 44925-44931.

Michalet, X., Pinaud, F.F., Bentolila, L.A., Tsay, J.M., Doose, S., Li, J.J., Sundaresan, G., Wu, A.M., Gambhir, S.S. & Weiss, S. 2005, "Quantum dots for live cells, in vivo imaging, and diagnostics", *Science,* vol. 307, no. 5709, pp. 538-544.

Miller, L.W., Sable, J., Goelet, P., Sheetz, M.P. & Cornish, V.W. 2004, "Methotrexate conjugates: a molecular in vivo protein tag", *Angewandte Chemie (International ed. in English),* vol. 43, no. 13, pp. 1672-1675.

Milligan, G. 2004, "Applications of bioluminescence- and fluorescence resonance energy transfer to drug discovery at G protein-coupled receptors", *European Journal of Pharmaceutical Sciences,* vol. 21, no. 4, pp. 397-405.

Milligan, G. 2003, "Principles: extending the utility of [35S]GTP gamma S binding assays", *Trends in Pharmacological Sciences,* vol. 24, no. 2, pp. 87-90.

Milligan, G. 2000, "Insights into ligand pharmacology using receptor-G-protein fusion proteins", *Trends in Pharmacological Sciences.,* vol. 21, no. 1, pp. 24-28.

Milligan, G. & Bouvier, M. 2005, "Methods to monitor the quaternary structure of G protein-coupled receptors", *FEBS Journal,* vol. 272, no. 12, pp. 2914-2925.

Milligan, G. & Kostenis, E. 2006, "Heterotrimeric G-proteins: a short history", *British Journal of Pharmacology,* vol. 147 Suppl 1, pp. S46-55.

Milligan, G. & Rees, S. 1999, "Chimaeric G alpha proteins: their potential use in drug discovery", *Trends in Pharmacological Sciences,* vol. 20, no. 3, pp. 118-124.

Milligan, G. & Smith, N.J. 2007, "Allosteric modulation of heterodimeric G-protein-coupled receptors", *Trends in Pharmacological Sciences,* vol. 28, no. 12, pp. 615-620.

Milligan, G. & White, J.H. 2001, "Protein-protein interactions at G-protein-coupled receptors", *Trends in Pharmacological Sciences,* vol. 22, no. 10, pp. 513-518.

Miyawaki, A., Nagai, T. & Mizuno, H. 2003, "Mechanisms of protein fluorophore formation and engineering", *Current Opinion in Chemical Biology,* vol. 7, no. 5, pp. 557-562.

Miyawaki, A., Sawano, A. & Kogure, T. 2003, "Lighting up cells: labelling proteins with fluorophores", *Nature Cell Biology,* vol. Suppl, pp. S1-7.

Mody, S.M., Ho, M.K., Joshi, S.A. & Wong, Y.H. 2000, "Incorporation of Galpha(z)-specific sequence at the carboxyl terminus increases the promiscuity of galpha(16) toward G(i)-coupled receptors", *Molecular Pharmacology,* vol. 57, no. 1, pp. 13-23.

Moore, K. & Rees, S. 2001, "Cell-based versus isolated target screening: how lucky do you feel?", *Journal of Biomolecular Screening,* vol. 6, no. 2, pp. 69-74.

Myung, C.S., Lim, W.K., Defilippo, J., Yasuda, H., Neubig, R. & Garrison, J.C. 2006, "Regions in the G Protein {gamma} Subunit Important for Interaction with Receptors and Effectors", *Molecular Pharmacology,* vol. 69, no. 3, pp. 877-887.

Nakamura, T., Furunaka, H., Miyata, T., Tokunaga, F., Muta, T., Iwanaga, S., Niwa, M., Takao, T. & Shimonishi, Y. 1988, "Tachyplesin, a class of antimicrobial peptide from the hemocytes of the horseshoe crab (Tachypleus tridentatus). Isolation and chemical structure", *The Journal of Biological Chemistry,* vol. 263, no. 32, pp. 16709-16713.

Nakanishi, J., Takarada, T., Yunoki, S., Kikuchi, Y. & Maeda, M. 2006, "FRET-based monitoring of conformational change of the beta2 adrenergic receptor in living cells", *Biochemical and Biophysical Research Communications,* vol. 343, no. 4, pp. 1191-1196.

Nemoto, N., Miyamoto-Sato, E. & Yanagawa, H. 1999, "Fluorescence labeling of the C-terminus of proteins with a puromycin analogue in cell-free translation systems", *FEBS letters,* vol. 462, no. 1-2, pp. 43-46.

Neubig, R., Siderovski, D. 2002, "Regulators of G-protein signalling as new central nervous system drug targets", *Nature Reviews Drug Discovery*, vol. 1, no. 3, pp. 187-197.

Niedernberg, A., Tunaru, S., Blaukat, A., Harris, B. & Kostenis, E. 2003, "Comparative analysis of functional assays for characterization of agonist ligands at G protein-coupled receptors", *Journal of Biomolecular Screening,* vol. 8, no. 5, pp. 500-510.

Nitz, M., Franz, K.J., Maglathlin, R.L. & Imperiali, B. 2003, "A powerful combinatorial screen to identify high-affinity terbium(III)-binding peptides", *Chembiochem,* vol. 4, no. 4, pp. 272-276.

Nobles, M., Benians, A. & Tinker, A. 2005, "Heterotrimeric G proteins precouple with G protein-coupled receptors in living cells", *Proceedings of the National Academy of Sciences of the United States of America,* vol. 102, no. 51, pp. 18706-18711.

Offermanns, S. 2003, "G-proteins as transducers in transmembrane signalling", *Progress in Biophysics and Molecular Biology,* vol. 83, no. 2, pp. 101-130.

Oldham, W.M. & Hamm, H.E. 2008, "Heterotrimeric G protein activation by G-protein-coupled receptors", *Nature Reviews. Molecular cell biology,* vol. 9, no. 1, pp. 60-71.

Osmond, R.I., Sheehan, A., Borowicz, R., Barnett, E., Harvey, G., Turner, C., Brown, A., Crouch, M.F. & Dyer, A.R. 2005, "GPCR screening via ERK 1/2: a novel platform for screening G protein-coupled receptors", *Journal of Biomolecular Screening,* vol. 10, no. 7, pp. 730-737.

Ozaki, A., Ariki, S. & Kawabata, S. 2005, "An antimicrobial peptide tachyplesin acts as a secondary secretagogue and amplifies lipopolysaccharide-induced hemocyte exocytosis", *The FEBS Journal,* vol. 272, no. 15, pp. 3863-3871.

Palczewski, K., Kumasaka, T., Hori, T., Behnke, C.A., Motoshima, H., Fox, B.A., Le Trong, I., Teller, D.C., Okada, T., Stenkamp, R.E., Yamamoto, M. & Miyano, M. 2000, "Crystal structure of rhodopsin: A G protein-coupled receptor", *Science,* vol. 289, no. 5480, pp. 739-745.

Park, J.H., Scheerer, P., Hofmann, K.P., Choe, H.W. & Ernst, O.P. 2008, "Crystal structure of the ligand-free G-protein-coupled receptor opsin", *Nature,* vol. 454, pp. 183-188.

Parker, D. & Williams, J.A.G. 1996, "Getting excited about lanthanide complexation chemistry", *Journal of the Chemical Society, Dalton Transactions,* vol. 18, pp. 3613-3628.

Parker, E.M., Kameyama, K., Higashijima, T. & Ross, E.M. 1991, "Reconstitutively active G protein-coupled receptors purified from baculovirus-infected insect cells", *Journal of Biological Chemistry,* vol. 266, no. 1, pp. 519-527.

Pfleger, K.D. & Eidne, K.A. 2005, "Monitoring the formation of dynamic G-protein-coupled receptor-protein complexes in living cells", *The Biochemical Journal,* vol. 385, no. 3, pp. 625-637.

Philipp, M. & Hein, L. 2004, "Adrenergic receptor knockout mice: distinct functions of 9 receptor subtypes", *Pharmacology &Therapeutics,* vol. 101, no. 1, pp. 65-74.

Pinxteren, J.A., O'Sullivan, A.J., Tatham, P.E. & Gomperts, B.D. 1998, "Regulation of exocytosis from rat peritoneal mast cells by G protein beta gamma-subunits", *The EMBO Journal,* vol. 17, no. 21, pp. 6210-6218.

Prevost, G.P., Lonchampt, M.O., Holbeck, S., Attoub, S., Zaharevitz, D., Alley, M., Wright, J., Brezak, M.C., Coulomb, H., Savola, A., Huchet, M., Chaumeron, S., Nguyen, Q.D., Forgez, P., Bruyneel, E., Bracke, M., Ferrandis, E., Roubert, P., Demarquay, D., Gespach, C. & Kasprzyk, P.G. 2006, "Anticancer activity of BIM-46174, a new inhibitor of the heterotrimeric Galpha/Gbetagamma protein complex", *Cancer Research,* vol. 66, no. 18, pp. 9227-9234.

Qanbar, R. & Bouvier, M. 2003, "Role of palmitoylation/depalmitoylation reactions in G-protein-coupled receptor function", *Pharmacology & Therapeutics,* vol. 97, no. 1, pp. 1-33.

Raftos, D.A., Fabbro, M. & Nair, S.V. 2004, "Exocytosis of a complement component C3-like protein by tunicate hemocytes", *Developmental and Comparative Immunology,* vol. 28, no. 3, pp. 181-190.

Ramsay, D., Kellett, E., McVey, M., Rees, S. & Milligan, G. 2002, "Homo- and hetero-oligomeric interactions between G-protein-coupled receptors in living cells monitored by two variants of bioluminescence resonance energy transfer (BRET): hetero-oligomers between receptor subtypes form more efficiently than between less closely related sequences", *The Biochemical Journal,* vol. 365, no. 2, pp. 429-440.

Rasmussen, S.G., Choi, H.J., Rosenbaum, D.M., Kobilka, T.S., Thian, F.S., Edwards, P.C., Burghammer, M., Ratnala, V.R., Sanishvili, R., Fischetti, R.F., Schertler, G.F., Weis, W.I. & Kobilka, B.K. 2007, "Crystal structure of the human beta(2) adrenergic G-protein-coupled receptor", *Nature,* vol. 450, pp. 383-387.

Remmers, A.E. 1998, "Detection and quantitation of heterotrimeric G proteins by fluorescence resonance energy transfer", *Analytical Biochemistry,* vol. 257, no. 1, pp. 89-94.

Reynolds, A.M., Sculimbrene, B.R. & Imperiali, B. 2008, "Lanthanide-binding tags with unnatural amino acids: sensitizing Tb3+ and Eu3+ luminescence at longer wavelengths", *Bioconjugate Chemistry,* vol. 19, no. 3, pp. 588-591.

Rinken, A., Kameyama, K., Haga, T. & Engstrom, L. 1994, "Solubilization of muscarinic receptor subtypes from baculovirus infected Sf9 insect cells", *Biochemical Pharmacology,* vol. 48, no. 6, pp. 1245-1251.

Rosenbaum, D.M., Cherezov, V., Hanson, M.A., Rasmussen, S.G., Thian, F.S., Kobilka, T.S., Choi, H.J., Yao, X.J., Weis, W.I., Stevens, R.C. & Kobilka, B.K. 2007, "GPCR engineering yields high-resolution structural insights into beta2-adrenergic receptor function", *Science,* vol. 318, no. 5854, pp. 1266-1273.

Rozinov, M.N. & Nolan, G.P. 1998, "Evolution of peptides that modulate the spectral qualities of bound, small-molecule fluorophores", *Chemistry & Biology,* vol. 5, no. 12, pp. 713-728.

Ruiz-Velasco, V. & Ikeda, S.R. 2001, "Functional expression and FRET analysis of green fluorescent proteins fused to G-protein subunits in rat sympathetic neurons", *The Journal of Physiology,* vol. 537, no. 3, pp. 679-692.

Sandtner, W., Bezanilla, F. & Correa, A.M. 2007, "In vivo measurement of intramolecular distances using genetically encoded reporters", *Biophysical Journal,* vol. 93, no. 9, pp. L45-7.

Sarramegn, V., Muller, I., Milon, A. & Talmont, F. 2006, "Recombinant G protein-coupled receptors from expression to renaturation: a challenge towards structure", *Cellular and Molecular Life Sciences,* vol. 63, no. 10, pp. 1149-1164.

Sarramegna, V., Talmont, F., Demange, P. & Milon, A. 2003, "Heterologous expression of G-protein-coupled receptors: comparison of expression systems fron the standpoint of large-scale production and purification", *Cellular and Molecular Life Sciences,* vol. 60, no. 8, pp. 1529-1546.

Sarvazyan, N.A., Remmers, A.E. & Neubig, R.R. 1998, "Determinants of gi1alpha and beta gamma binding. Measuring high affinity interactions in a lipid environment using flow cytometry", *Journal of Biological Chemistry,* vol. 273, no. 14, pp. 7934-7940.

Sculimbrene, B.R. & Imperiali, B. 2006, "Lanthanide-binding tags as luminescent probes for studying protein interactions", *Journal of the American Chemical Society,* vol. 128, no. 22, pp. 7346-7352.

Seifert, R., Hageluken, A., Hoer, A., Hoer, D., Grunbaum, L., Offermanns, S., Schwaner, I., Zingel, V., Schunack, W. & Schultz, G. 1994, "The H1 receptor agonist 2-(3-chlorophenyl)histamine activates Gi proteins in HL-60 cells through a mechanism that is independent of known histamine receptor subtypes", *Molecular Pharmacology,* vol. 45, pp. 578-586.

Selvin, P.R. 1996, "Lanthanide-based resonance energy transfer", *IEEE Journal of Selected Topics in Quantum Electronics,* vol. 2, pp. 1077-1087.

Selvin, P.R. 2002, "Principles and biophysical applications of lanthanide-based probes", *Annual Review of Biophysics and Biomolecular Structure,* vol. 31, pp. 275-302.

Selvin, P.R. 2000, "The renaissance of fluorescence resonance energy transfer", *Nature Structural Biology,* vol. 7, no. 9, pp. 730-734.

Selvin, P.R. 1995, "Fluorescence resonance energy transfer", *Methods in Enzymology,* vol. 246, pp. 300-334.

Selvin, P.R. & Hearst, J.E. 1994, "Luminescence energy transfer using a terbium chelate: improvements on fluorescence energy transfer", *Proceedings of the National Academy of Sciences of the United States of America,* vol. 91, no. 21, pp. 10024-10028.

Silvaggi, N.R., Martin, L.J., Schwalbe, H., Imperiali, B. & Allen, K.N. 2007, "Double-lanthanide-binding tags for macromolecular crystallographic structure determination", *Journal of the American Chemical Society,* vol. 129, no. 22, pp. 7114-7120.

Smrcka, A.V. 2008, "G protein betagamma subunits: Central mediators of G protein-coupled receptor signaling", *Cellular and Molecular Life Sciences,* vol. 65, no. 14, pp. 2191-214

Soh, N. 2008, "Selective Chemical Labeling of Proteins with Small Fluorescent Molecules Based on Metal-Chelation Methodology", *Sensors,* vol. 8, pp. 1004-1024.

Spagnuolo, C.C., Vermeij, R.J. & Jares-Erijman, E.A. 2006, "Improved photostable FRET-competent biarsenical-tetracysteine probes based on fluorinated fluoresceins", *Journal of the American Chemical Society,* vol. 128, no. 37, pp. 12040-12041.

Srinivasan, R., Yao, S.Q. & Yeo, D.S. 2004, "Chemical approaches for live cell bioimaging", *Combinatorial Chemistry & High Throughput Screening,* vol. 7, no. 6, pp. 597-604.

Stroffekova, K., Proenza, C. & Beam, K.G. 2001, "The protein-labeling reagent FLASH-EDT2 binds not only to CCXXCC motifs but also non-specifically to endogenous cysteine-rich proteins", *Pflugers Archiv : European Journal of Physiology,* vol. 442, no. 6, pp. 859-866.

Sutherland, A.J. 2002, "Quantum dots as luminescent probes in biological systems", *Current Opinion in Solid State and Materials Science,* vol. 6, no. 4, pp. 365-370.

Svoboda, K. & Yasuda, R. 2006, "Principles of two-photon excitation microscopy and its applications to neuroscience", *Neuron,* vol. 50, no. 6, pp. 823-839.

Thomsen, W., Frazer, J. & Unett, D. 2005, "Functional assays for screening GPCR targets", *Current Opinion in Biotechnology,* vol. 16, no. 6, pp. 655-665.

Torrecilla, I. & Tobin, A.B. 2006, "Co-ordinated covalent modification of G-protein coupled receptors", *Current Pharmaceutical Design,* vol. 12, no. 14, pp. 1797-1808.

Tsien, R.Y. 2005, "Building and breeding molecules to spy on cells and tumors", *FEBS Letters,* vol. 579, no. 4, pp. 927-932.

Tsien, R.Y. 1998, "The green fluorescent protein", *Annual Review of Biochemistry,* vol. 67, pp. 509-544.

van Rijn, R.M., Chazot, P.L., Shenton, F.C., Sansuk, K., Bakker, R.A. & Leurs, R. 2006, "Oligomerization of recombinant and endogenously expressed human histamine H(4) receptors", *Molecular Pharmacology,* vol. 70, no. 2, pp. 604-615.

Vazquez-Ibar, J.L., Weinglass, A.B. & Kaback, H.R. 2002, "Engineering a terbium-binding site into an integral membrane protein for luminescence energy transfer", *Proceedings of the National Academy of Sciences of the United States of America,* vol. 99, no. 6, pp. 3487-3492.

Verkhusha, V.V. & Lukyanov, K.A. 2004, "The molecular properties and applications of Anthozoa fluorescent proteins and chromoproteins", *Nature Biotechnology,* vol. 22, no. 3, pp. 289-296.

Vilardaga, J.P., Steinmeyer, R., Harms, G.S. & Lohse, M.J. 2005, "Molecular basis of inverse agonism in a G protein-coupled receptor", *Nature Chemical Biology,* vol. 1, no. 1, pp. 25-28.

Waggoner, A. 1995, "Covalent labeling of proteins and nucleic acids with fluorophores", *Methods in Enzymology,* vol. 246, pp. 362-373.

Wall, M.A., Posner, B.A. & Sprang, S.R. 1998, "Structural basis of activity and subunit recognition in G protein heterotrimers", *Structure,* vol. 6, no. 9, pp. 1169-1183.

Wang, E., Taylor, R.W. & Pfeiffer, D.R. 1998, "Mechanism and specificity of lanthanide series cation transport by ionophores A23187, 4-BrA23187, and ionomycin", *Biophysical Journal,* vol. 75, no. 3, pp. 1244-1254.

Wang, F., Tan, W.B., Zhang, Y., Fan, X. & Wang, M. 2006, "Luminescent nanomaterials for biological labelling", *Nanotechnology,* vol. 17, no. 1, pp. R1-R13.

Warne, T., Serrano-Vega, M.J., Baker, J.G., Moukhametzianov, R., Edwards, P.C., Henderson, R., Leslie, A.G.W., Tate, C.G. & Schertler, G.F.X. 2008, "Structure of a [bgr]1-adrenergic G-protein-coupled receptor", *Nature,* vol. 454, pp. 486-491.

Wedegaertner, P.B., Wilson, P.T. & Bourne, H.R. 1995, "Lipid modifications of trimeric G proteins", *Journal of Biological Chemistry,* vol. 270, no. 2, pp. 503-506.

Weill, C., Autelitano, F., Guenet, C., Heitz, F., Goeldner, M. & Ilien, B. 1997, "Pharmacological and structural integrity of muscarinic M2 acetylcholine receptors produced in Sf9 insect cells", *European Journal of Pharmacology,* vol. 333, no. 2-3, pp. 269-278.

Wess, J., Eglen, R.M. & Gautam, D. 2007, "Muscarinic acetylcholine receptors: mutant mice provide new insights for drug development", *Nature Reviews. Drug Discovery,* vol. 6, no. 9, pp. 721-733.

Wilkins, A.L., Ye, Y., Yang, W., Lee, H.W., Liu, Z.R. & Yang, J.J. 2002, "Metal-binding studies for a de novo designed calcium-binding protein", *Protein Engineering,* vol. 15, no. 7, pp. 571-574.

Wolff, M., Wiedenmann, J., Nienhaus, G.U., Valler, M. & Heilker, R. 2006, "Novel fluorescent proteins for high-content screening", *Drug Discovery Today,* vol. 11, no. 23-24, pp. 1054-1060.

Wong, C.S., Ho, M.K. & Wong, Y.H. 2003, "The beta6/alpha5 regions of Galphai2 and GalphaoA increase the promiscuity of Galpha16 but are insufficient for pertussis toxin-catalyzed ADP-ribosylation", *European Journal of Pharmacology,* vol. 473, no. 2-3, pp. 105-115.

Ye, Y., Lee, H.W., Yang, W., Shealy, S.J., Wilkins, A.L., Liu, Z.R., Torshin, I., Harrison, R., Wohlhueter, R. & Yang, J.J. 2001, "Metal binding affinity and structural properties of an isolated EF-loop in a scaffold protein", *Protein Engineering,* vol. 14, no. 12, pp. 1001-1013.

Ye, Z., Tan, M., Wang, G. & Yuan, J. 2005, "Development of functionalized terbium fluorescent nanoparticles for antibody labeling and time-resolved fluoroimmunoassay application", *Talanta,* vol. 65, no. 1, pp. 206-210.

Yin, J., Liu, F., Li, X. & Walsh, C.T. 2004, "Labeling proteins with small molecules by site-specific posttranslational modification", *Journal of the American Chemical Society,* vol. 126, no. 25, pp. 7754-7755.

Yu, N., Atienza, J.M., Bernard, J., Blanc, S., Zhu, J., Wang, X., Xu, X. & Abassi, Y.A. 2006, "Real-time monitoring of morphological changes in living cells by electronic cell sensor arrays: an

approach to study g protein-coupled receptors", *Analytical Chemistry,* vol. 78, no. 1, pp. 35-43.

Zhang, H., Yasrebi-Nejad, H. & Lang, J. 1998, "G-protein betagamma-binding domains regulate insulin exocytosis in clonal pancreatic beta-cells", *FEBS Letters,* vol. 424, no. 3, pp. 202-206.

Zhang, J., Campbell, R.E., Ting, A.Y. & Tsien, R.Y. 2002, "Creating new fluorescent probes for cell biology", *Nature Reviews. Molecular Cell Biology,* vol. 3, no. 12, pp. 906-918.

Zhang, Z., Smith, B.A., Wang, L., Brock, A., Cho, C. & Schultz, P.G. 2003, "A new strategy for the site-specific modification of proteins in vivo", *Biochemistry,* vol. 42, no. 22, pp. 6735-6746.